DIAPHRAGM-ACTION OF ASBESTOS-CEMENT DECKS

Noor El-Din Mohamed El-Hakim

A Thesis
in
The Faculty
of
Engineering

Presented in Partial Fulfillment of the Requirements
for the
DEGREE OF DOCTOR OF PHILOSOPHY
at
Concordia University
Montreal, Quebec, Canada

November 1980

ABSTRACT

ABSTRACT

DIAPHRAGM-ACTION OF ASBESTOS-CEMENT DECKS

Noor El-Din Mohamed El-Hakim, Ph.D.
Concordia University, 1980

This study represents the first attempt (in North America) at evaluating the in-plane shear behaviour of asbestos-cement decking systems which are widely used in the construction of industrial buildings. Properly designed and constructed, these decks can effectively be used as structural elements to transfer lateral forces caused by wind. The study covers both the experimental and theoretical investigation of the diaphragmic capabilities of two asbestos-cement decking systems, the cavity and "T" decks, currently manufactured by Atlas Asbestos Company, Quebec, Canada.

Preliminary design information on the diaphragm action of the two decking systems as presently used is established by full-scale testing. The cantilever test frame (10 ft x 10 ft) and the test procedure are in accordance with ASTM E455-76 and the American Iron and Steel Institute (AISI) recommendations. A total of thirteen tests were performed with the fastener pattern as the main varying parameter. Test data obtained includes: load-deformation curves, ultimate shear strengths, shear stiffnesses, maximum deflections, and failure modes. In general, the two decking systems were found to be very flexible (especially the cavity decking) in comparison with welded light-gage steel diaphragms of the same size. Nevertheless, use of the deck's limited shear resistance may still effect some reduction in building costs. On the other hand, the two decking systems possess sufficiently high shear strength to meet the normal requirements of diaphragm design based on strength alone.

Small sample tests were also conducted to determine the mechanical properties of asbestos-cement sheeting, and the strength and stiffness of fasteners.

The finite element method is applied to the analysis of the tested diaphragms. Based on the direct stiffness method, an efficient special purpose computer program requiring minimal input data was developed. With the proposed idealization of the two decking systems, the finite element technique is shown to yield results in good agreement with experimental data. A parametric study is also conducted to establish the relative importance of different diaphragm design parameters and their influence on diaphragm behaviour.

For routine design, a simplified method of analysis is developed based on a simple deformation mode observed in tests and on an assumed distribution of internal fastener forces as revealed by finite element analyses. This results in a set of general and simple analytical expressions, suitable for hand calculations.

Guidelines for the design and construction of asbestos-cement diaphragms are outlined and illustrated by a practical design example.

ACKNOWLEDGEMENTS

ACKNOWLEDGEMENTS

The author wishes to express his sincere gratitude to Professors P.P. Fazio and H.K. Ha, under whose supervision this work was carried out. Dr. Fazio is due credit for proposing this investigation. His provocative questions, advice and counsel were invaluable in directing and shaping the program of investigation. Dr. Ha's constructive guidance, cooperation and encouragement through out all stages of this work are greatly appreciated.

The financial support of the National Sciences and Engineering Research Council of Canada, and La Formation de Chercheurs et d'Action Concertee du Quebec is gratefully acknowledged. Acknowledgement is also extended to Atlas Asbestos Company, Montreal, Quebec, for supplying the materials and fabrication of the specimens. Special thanks to Mr. Guy Blain for his interest and helpful comments.

Thanks are also due to the technical staff and friends at the Center for Building Studies for their help and cooperation in the experimental work. Special thanks to a colleague and friend, Dr. O. Moselhi for his many helpful discussions and proofreading of the manuscript.

The author is grateful to Miss Joan Armour who has done such an excellent job of typing this dissertation.

Last, but not least, the author would like to thank his wife, Mahasen, who bore with him through all the tribulations of this work, and without whose encouragement and support he could not have completed it.

TO my Mother, to whom I owe my life.

TO my wife, for all her love and sacrifices.

TO my daughter, Heba, for just being beautiful.

TABLE OF CONTENTS

TABLE OF CONTENTS

IV LOAD-DEFORMATION CHARACTERISTICS OF DIAPHRAGM CONNECTIONS

V FINITE ELEMENT ANALYSIS AND CORRELATION WITH EXPERIMENTAL RESULTS

LIST OF FIGURES

LIST OF FIGURES

LIST OF TABLES

LIST OF TABLES

NOTATIONS

NOTATIONS

a	Length of diaphragm in direction perpendicular to corrugations
A	Cross-sectional area of perimeter test frame members perpendicular to load direction, also cross-sectional area of a beam element
b	Depth of diaphragm in direction parallel to corrugations
C, C'	Diaphragm flexibility when load is applied in direction parallel and perpendicular to corrugations, respectively
D, D'	Tip deflections when load is applied in direction parallel and perpendicular to corrugations, respectively
D_1	Deflection component due to vertical deformations of connections
D_2	Deflection component due to horizontal deformations of end connections
D_3	Deflection component due to shear strains in sheetings and profile distortions
D_a	Deflection component due to axial strains in perimeter members
D_e	Vertical separation between the end member and the panels at the diaphragm corners
D_s	Vertical separation between the end member and the panels at the seam lines
E	Modulus of elasticity of steel (29.5×10^6 psi)
E_L or E_{yy}	Asbestos-cement elastic modulus in the direction of fibers (longitudinal direction - L)
E_T or E_{xx}	Asbestos-cement elastic modulus in the orthogonal direction (transverse direction - T)
E_x	Asbestos-cement elastic modulus in the x-direction (at 45° to the fibers direction)
E_w	Modulus of elasticity of wall material
f_c	Allwable flexural compressive strength of wall material
F	Diaphragm flexibility factor measured in micro-inches per pound
F_d, F_{du}	Force and strength, respectively, of a side fastener

F_e, F_{eu}	Vertical component of force and strength, respectively, of an end or sheet-to-purlin fastener
F_{eh}	Horizontal component of force in end fastener
F_p, F_{pu}	Force and strength, respectively, of a sheet-to-purlin fastener
F_v	Vertical component of force in end or purlin connections
F_s, F_{su}	Force and strength, respectively, of a seam fastener
F_{u_L}	Ultimate load of connection in the longitudinal direction
F_{u_T}	Ultimate load of connection in the transverse direction
G'	Diaphragm shear modulus
G_{LT} or G_{xy}	Asbestos-cement shear modulus
h_w	Height of building wall between horizontal supports
I	Moment of inertia of beam element about its axis of bending
K	Diaphragm stiffness
k_d	Stiffness of a side fastener
k_e	Stiffness of an end fastener
k_p	Stiffness of a sheet-to-purlin fastener
k_s	Stiffness of a seam fastener
k_x or k_T	Stiffness of a connection in the transverse direction
k_y of k_L	Stiffness of a connection in the longitudinal direction
L	length of beam element
M	Number of purlins
n_d	Number of side fasteners per side
n_e	Number of end fasteners per panel end
n_p	Number of purlins
n_s	Number of seam fasteners per seam line
N	Number of panels or sheets in diaphragm
q	Shear flow in diaphragm

Q, Q'	Forces applied in directions parallel and perpendicular to corrugations, respectively
Q	Applied jack load in diaphragm full-scale testing
Q_{ult}	Ultimate applied load (or failure load) in diaphragm full-scale testing
S, S'	Stiffness of diaphragm when load is applied in directions parallel and perpendicular to corrugations, respectively
S_{desg}	Diaphragm allowable design shear
S_u	Diaphragm ultimate shear strength
t	Thickness of sheeting
t_w	Thickness of building walls
w	Width of a panel
x_o, x_i	Distances defined in Fig. 6.4
γ	Shear strain or shear angle
Δ_i	Measured deflection at gage i [Fig. 3.2]
Δ_b	Cantilever test frame bending deflection
Δ_{max}	Maximum permissible deflection of building wall
Δ_{NET}	Net tip deflection in direction of applied load of tested diaphragm, after correction for support movements
Δ_s	Shear deflection of tested diaphragm
Δ_s'	Shear deflection of tested diaphragm at 40% of the ultimate load
ε_L, ε_T	Longitudinal and transverse strain, respectively
ν_{LT}	Asbestos-cement Poisson's ratio relating strains in the longitudinal direction (L) to stresses in the transverse direction (T)
ν_{TL}	Asbestos-cement Poisson's ratio relating strains in the transverse direction (T) to stresses in the longitudinal direction (L)
σ_L, σ_T	Longitudinal and transverse stress, respectively
σ_{uL}, σ_{uT}	Ultimate tensile strength of asbestos-cement specimens in the longitudinal and transverse directions, respectively
τ_{LT}	Shear stress

$\{\varepsilon\}$	Strain vector
$\{\sigma\}$	Stress vector
$[K]$	Stiffness matrix
$\{P\}$	Load vector
$\{U\}$	Displacement vector
$\{Q\}$	Elasticity matrix

CHAPTER I

INTRODUCTION

CHAPTER I

INTRODUCTION

1.1 INTRODUCTION

In industrial buildings, asbestos-cement cladding (roof decking and wall sheathing) has long been noted for its durability, fire-resistance, noncorrosiveness and relative economy. The two decking systems: Cavity and "T" decks (Fig. 1.1), manufactured by Atlas Asbestos Company, have been widely used in Canada and the U.S. as roofing components for paper mills (see map, Fig. 1.2), tobacco factories, warehouses, laundries, hangars, etc..., where high humidity conditions prevail or where fire is a hazard.

Until now, it is customary to treat these claddings as non-structural components in the design of steel framed structures. They are being used to merely enclose the space and transmit loads normal to their plane by virtue of their flexural rigidity. Because of the lack of design information on the in-plane behaviour of the two decking systems, designers hesitate to take advantage of the stiffening effect offered by the sheeting. The availability of such data would permit the effective use of asbestos-cement decks as main resisting elements against lateral shear forces caused by wind.

This thesis is the outgrowth of a study requested by Atlas Asbestos Company on the diaphragmic action of the two asbestos-cement decking systems.

1.2 DIAPHRAGM ACTION

A diaphragm, like a plate, is basically a two-dimensional structural element capable of resisting and transmitting in-plane forces. The in-plane behaviour of a diaphragm (or often termed stressed-skin form of construction) and its associated stiffening effect is refered to as "diaphragm action".

Diaphragm action has long been recognized and widely used in many fields of construction, particularly those associated with the transport industry (aircrafts, cars and ships). In the building industry, reinforced concrete floors are also designed to act as diaphragms for transmitting lateral loads. Shear walls, deep girders, and diaphragms of shells are various forms of effective shear resisting elements.

Roof decking, wall sheathing and light cladding materials in steel framed structures, on the other hand, have been designed for many years to carry their own weight and resist transversal loads only. Although practical experience demonstrated that a framed structure becomes noticably stiffer when the cladding or decking is added, designers viewed these components as an additional margin of safety in cases of extreme loading or as a lateral support for the framing members. With experimental evidence, it then became apparent that these components could very well serve the role of transmitting in-plane forces. By virtue of its inherent in-plane shear stiffness and strength, the cladding also acts as bracing against lateral loads (due to wind).

The in-plane action of a decking is illustrated in Fig. 1.3, which shows the conventional steel framing of a one-storey structure with roof panels in place. If the panels are merely fastened to the frame, but not interconnected, they offer little resistance to lateral loads shown, and special bracing or other measures must be provided. However, with the panels interconnected along the seams, the diaphragm so obtained together with the longitudinal framing members BF and FG acts in a manner similar to a plate girder supported at BC and FG by the end gables ABCD and EFGH (schematically indicated by the cross-bracing). Being present in any event as part of the roof, and thus available with little or no extra cost, the diaphragms can be designed to replace part or all of the conventional bracing systems, resulting in a more economical design. This in-plane shear behaviour has been widely known as shear diaphragm action.

Although recognized, such use of the shear diaphragm action has been largely neglected in building design until recently. The cause has been the lack of quantitative design data as well as the lack of a rational theory to describe and predict this behaviour. Today, the substantial amount of experimental and theoretical research done on light-gauge steel diaphragms over a span of 25 years, has led into a considerable progress in developing methods to predict and evaluate the behaviour of diaphragm assemblies. With such accumulated experience, the field of shear diaphragms has grown substantially, extending its applications into branches covering many related aspects of building structural design.

1.3 DIAPHRAGM COMPONENTS AND DESIGN PARAMETERS

A typical isolated diaphragm (see Fig. 1.4) is constructed of three types of components. These are: the corrugated panels; the fasteners, and a perimeter frame which encloses the panels. The marginal or perimeter frame serves two important functions: to provide resistance against bending due to the lateral shear load and at the same time to transfer shear forces to all the panels through the end and side fasteners, thus providing a state of "pure shear" in the panels. The end fasteners attach the panels' corrugated ends to the frame, and they are required in order to prevent excessive distortion of the corrugation profile which could result in a considerably flexible diaphragm. In some cases, the side fasteners are eliminated, in which the shear forces are transfered to the panels mainly through the end fasteners. The sheet-to-sheet, or seam, fasteners transfer forces from one sheet to the next.

The two most important behavioural parameters for design of shear diaphragms are, the diaphragm shear stiffness (or conversely the flexibility) and the ultimate shear strength. The diaphragm shear stiffness, commonly denoted as G', is a measure of the relationship between in-plane load and shear deflection in the direction of that load. The diaphragm strength, S_u, on the other hand, designates the ultimate lateral in-plane force (required to produce failure of the assembly) divided by the length of the diaphragm in the direction of the applied load.

1.4 REVIEW OF PREVIOUS STUDIES

Extensive survey of literature reveals that very little research has been carried out on the stiffening effect of asbestos-cement sheeting or its behaviour as shear diaphragms. The work of Bryan, Kallaur an Akhtar [1] at the University of Manchester, 1970, is the earliest known attempt to study the shear resistance of conventional corrugated asbestos sheets. It was found that, although the material has ample strength for use as a shear membrane, its potential is not realised with the use of hookbolts to connect the sheets to the steel roof. It was then recommended that the stiffening effect offered by the sheeting should not be used in design. The use of hookbolts resulted in a very flexible membrane, even when the sheet overlaps (seams) were fastened together. In addition, Bryan et.al. pointed out that the effect of creep rupture and weathering could later lead to unpredictable difficulties.

Although the outcome of this first attempt was on the negative side, it was found from bending tests on zed purlins used in conjunction with asbestos-cement sheets in accordance with usual practice [1, 2], that the lateral support offered by the sheeting is adequate to prevent lateral instability in zed purlins even up to the verge of plastic collapse.

A year later, 1971, Bryan, Balmain and Oliver [3] reported on testing of an asbestos-cement sheeted house (≃ 23x23x15 ft), where the roofing, cladding, lining panels and partitions were made of asbestos-cement and the structural skeleton was made from light gauge steel. Test results confirmed that the cladding shares in load bearing as well as in providing shear resistance. The roof truss and interior floor beam deflections were noticably reduced with the addition of claddings. This reduction was due largely to the effect of the roof lining which, because of the more secure method of fixing, was more effective than the sheeting as a shear membrane in taking the load back to the gable ends.

Other site tests to evaluate the effects of asbestos-cement sheeting on the behaviour of a single-storey precast barn frame were described in a report by the Cement and Concrete Association, England [4]. It was concluded in the report that conventionally sheeted structures have a considerable reserve of strength and that deflections under normal service conditions are much reduced.

Up to the present time (1979), diaphragm action has only been taken advantage of when steel sheeting or decking is used. This has been the outcome of hundreds of full-scale diaphragm tests, in which the performance of specific combinations of light-gauge steel panels, marginal framing members, purlins, and connections have been studied. Testing has resulted in a considerable amount of design information and disclosed several variables influencing the performance of diaphragms. In addition, research in the field has produced a number of analytical methods and semi-empirical formulas to predict the behaviour of light-gauge steel diaphragms.

The present work covers several aspects on both the theoretical and experimental investigation of the diaphragmic capabilities of the two asbestos-cement decking systems (cavity and "T" decks). Thus, if seems to be appropriate to review the relevant literature on metal diaphragms for each topic when it is first discussed.

1.5 OBJECTIVES AND PROGRAM OF RESEARCH

Unlike metal sheeting, the inherent shear stiffness and strength of asbestos-cement panels have never been actually utilized, and their stiffening effect has not been introduced in design. Since the publication of the early investigations by Bryan and others from England, the technology of construction of asbestos-cement decks has considerably improved. Present practice employs a variety of more effective connections between the various components (between sheeting overlaps and sheeting to supporting steel structure). Furthermore, the sheeting is often covered with rigid insulation and built-up roofing which provides a weathering skin to protect the deck from weather.

The prime concern of the present research work is to determine quantitatively if the asbestos-cement decking systems (Cavity and "T" deck) as being used in present day could effectively work as shear diaphragms, and if so, could the load sharing and ultimate strength behaviour be predicted analytically? In addition, suggestions and recommendations are to be made for improving current practice concerning the use of the two systems as stiffening elements.

The research program comprises both experimental and theoretical investigation.

The experimental part includes the development, design and fabrication of a full-scale test frame. This part is aimed at establishing preliminary design information on the diaphragmic action of the two currently used asbestos-cement decking systems. The test results are also meant to provide a basis for verification of the analytical techniques. The experimental program includes also small-scale tests, conducted to provide the stiffness and strength characteristics of the diaphragm components. This information is needed as input data for the theoretical analysis. These tests are aimed at:

(a) establishing the mechanical properties of the asbestos-cement material of the two decking systems.

(b) evaluation of the load-displacement response of the two decks' different fasterners.

The theoretical study is directed toward the development of methods of analysis for asbestos-cement shear diaphragms. The theoretical investigation covers the following:

(a) application of the finite element method to predict the elastic response of the two decking systems.

(b) development of simple closed-form expressions for the diaphragm deflections and fastener forces.

1.6 ORGANIZATION OF THE THESIS

Chapter II of the thesis deals with the experimental determination of the elastic properties of asbestos-cement material as used in the decking systems manufactured by Atlas.

Chapter III presents an evaluation of the structural behaviour of the two decking systems by full-scale testing. Description of the test frame and the experimental procedure are also presented. Information obtained from the tests include: load deflection curves, ultimate shear strengths, shear stiffnesses, maximum deflections and failure modes.

Chapter IV is concerned with the experimental evaluation of the load-displacement response of the fasteners used in the installation of the two deckings. The stiffness and the strength of the connections as well as their failure modes are determined.

In Chapter V the finite element method is applied to the analysis of asbestos-cement shear diaphragms. A parametric study is conducted to establish the relative importance of different diaphragm design parameters and their influence on diaphragm behaviour.

Development of a simple analytical method for the analysis of shear diaphragms is presented in Chapter VI. The analysis is based on a simple deformation mode observed in tests and on an assumed distribution of internal fastener forces as revealed by finite element analyses.

Asbestos-cement diaphragm design and construction guidelines are outlined in Chapter VII. A practical design example is also presented.

Finally, a summary of the work, conclusions and recommendations for further research are presented in Chapter VIII.

A refined version of the simplified method of diaphragm analysis of Chapter VI is presented in Appendix A.

A detailed derivation of some deflection components contributing to the diaphragms' shear flexibility is presented in Appendix B.

Appendix C is a User's Guide for the developed special-purpose finite element computer program for the linear elastic analysis of regular shear diaphragms.

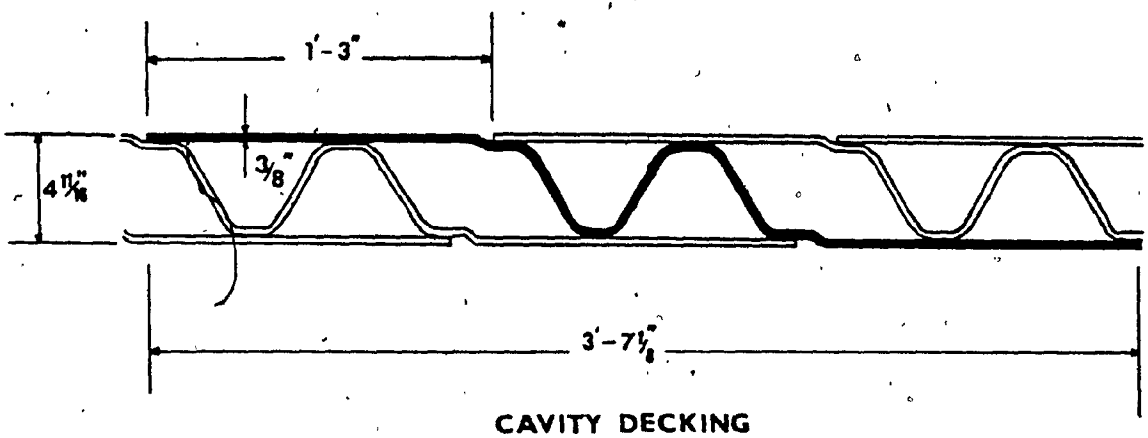

CAVITY DECKING

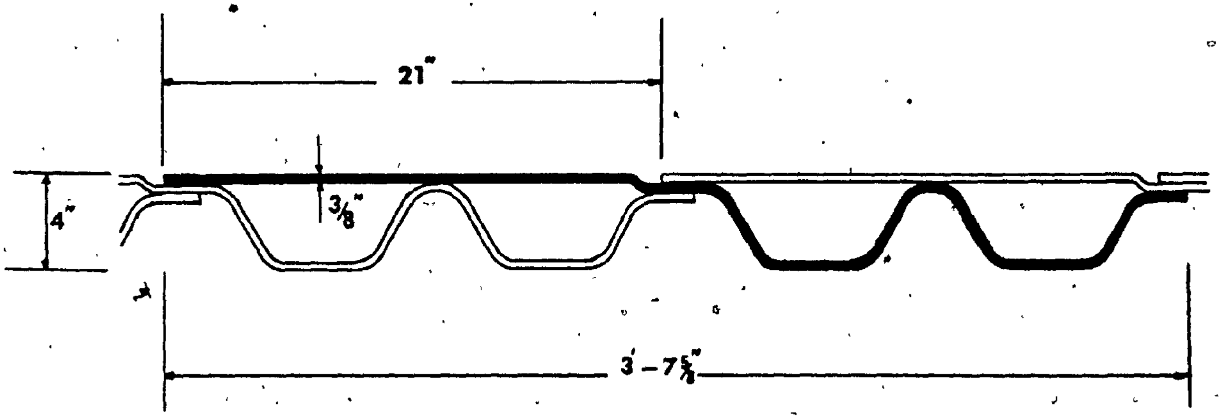

"T" DECK

FIG. 1.1 ASBESTOS-CEMENT ROOF DECKING SYSTEMS

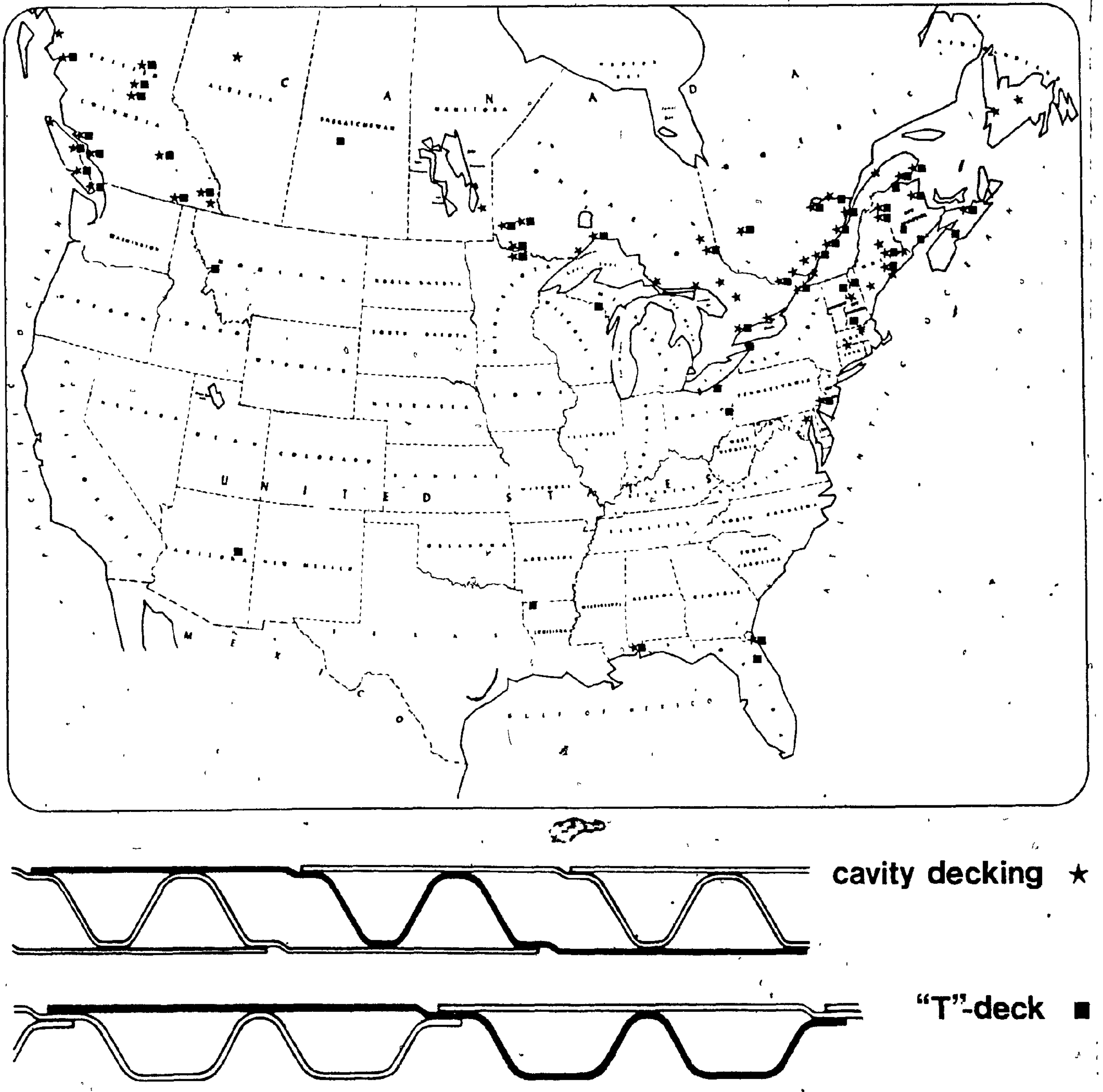

FIG. 1.2 PULP AND PAPER MILLS IN THE U.S. AND CANADA WITH ASBESTOS-CEMENT ROOF DECKS

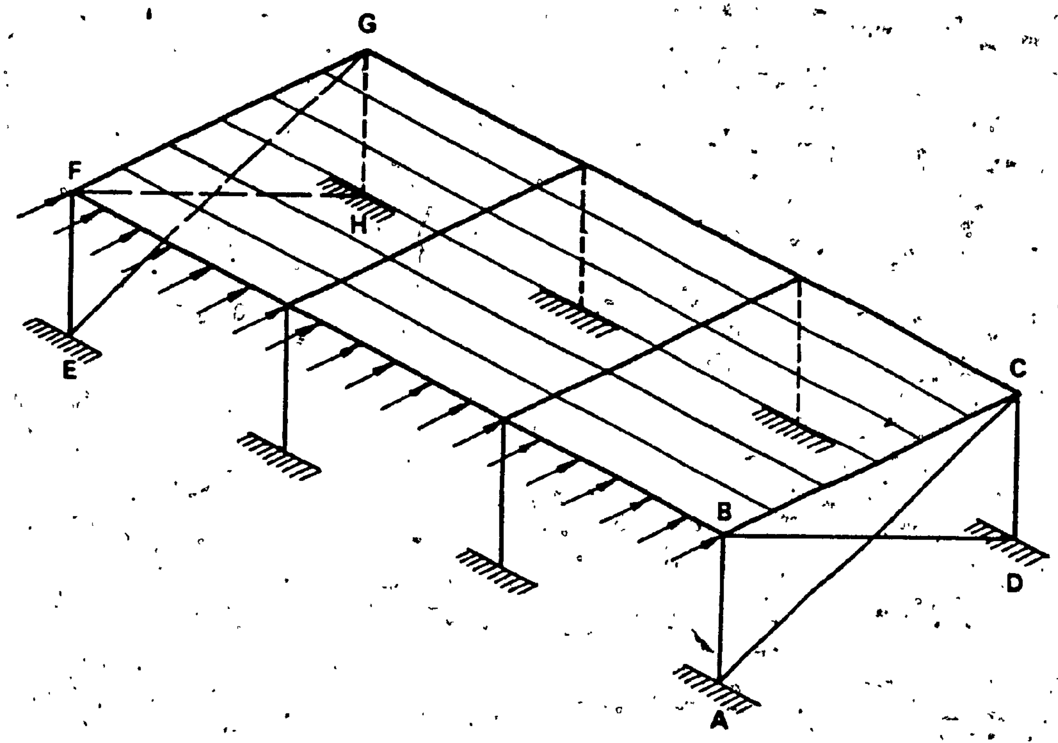

FIG. 1.3 ROOF DECKING CAN EFFECTIVELY RESIST IN-PLANE SHEAR BY VIRTUE OF DIAPHRAGM ACTION

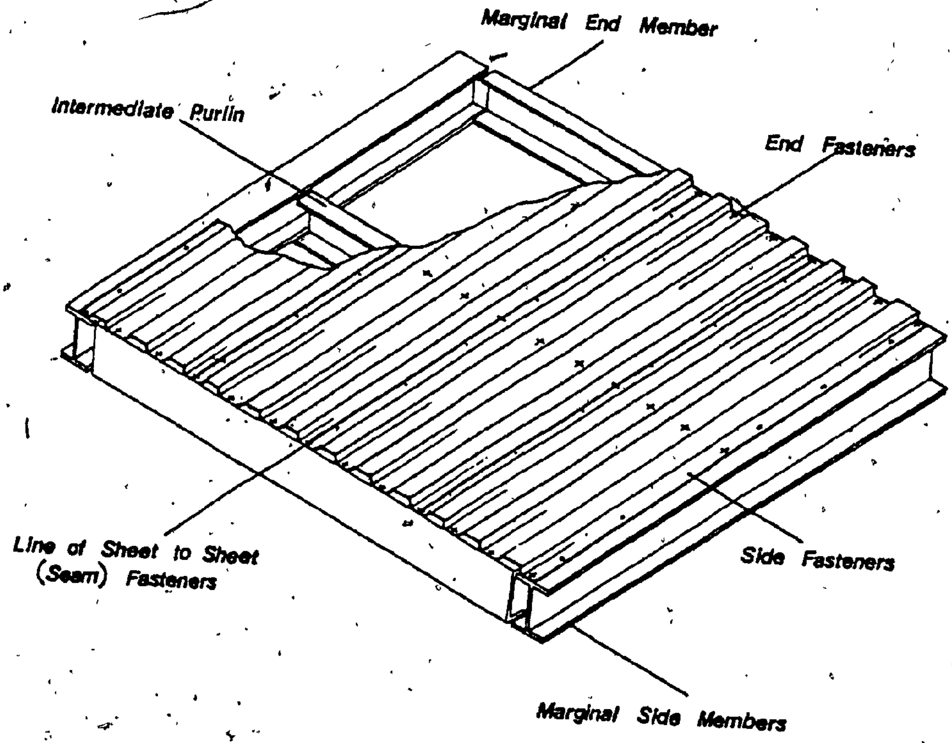

FIG. 1.4 GENERAL ARRANGEMENT OF A TYPICAL ISOLATED DIAPHRAGM

CHAPTER II

MECHANICAL PROPERTIES OF ASBESTOS-CEMENT

CHAPTER II

MECHANICAL PROPERTIES OF ASBESTOS-CEMENT

2.1 GENERAL

Asbestos-cement is a form of composite material. The word "composite" signifies that two or more materials are combined in such a manner that their best qualities are exploited; and often the resulting material exhibits certain properties that none of the consituents possess.

Composite materials have a long history of usage. Asbestos-cement is probably the oldest material ever produced in an industrial way [5], since the first patent in this field goes back to 1900 (Hatscheck, Austrian Patent No. 5970, 1900). It consists essentially of asbestos and Portland cement mixed in water in the proportion of 15-20% of asbestos fibre to 80-85% of cement.

Asbestos-cement products are produced in various shapes among which pipes, flat, corrugated or profiled sheets are the most important. It is employed in large quantities for roofs and walls of industrial buildings in all parts of the world. The popularity of asbestos-cement as a building material is a consequence of its many desirable physical and chemical properties in conjunction with low material costs. Asbestos-cement is:

(1) fire-resistant. It will not burn or support combustion. Thus, it is widely specified for construction where fire hazards are present.

(2) light in weight. Though dense and hard, it is relatively light in comparison with most alternative materials.

(3) damp proof and non-corrodible. It will not rot, rust or corrode. Therefore, it is ideally suited for construction of buildings

where high humidity conditions prevail (e.g., pulp and paper mills, laundries,....etc.)

(4) vermin-proof. It effectively hampers entry to buildings by rodents and insects.

(5) effective for sound insulation

Although asbestos-cement has been in use for nearly seventy years, knowledge of the engineering properties of the material is very limited. It is likely that if asbestos-cement were better understood as an engineering material, more innovation in the use of the material might be possible. Unfortunately, research has not kept pace with the practical developments of the material. This can be attributed to the fact that the production process and fibre mixture are changing from time to time and from one country to another. The mechanical properties of the material basically depend on the manufacturing practice and fibre mixture. For example, the tensile strength of asbestos-cement may vary from 30 to 400 kg/cm^2 (420 to 6000 psi) depending on the composition [6].

This chapter concentrates on the experimental determination of the elastic constants and tensile strengths of the material of the two decking systems manufactured by Atlas.

2.2 MANUFACTURING METHODS

Common techniques of asbestos-cement manufacture follows from the laminated process invented by Hatschek and adopted by Eternit in Europe nearly seventy years ago. Although many changes involving modifications and innovations in the mechanical plants have taken place, the greatest change has been in the improved methods for the fabrication of the many new industrial products that are now in general use.

The three basic methods of manufacture in use are: the wet transfer roller or Hatschek process, the semi-dry or Magnani process and the dry or Manville process. In the following the three methods are briefly described [7, 8, 9].

2.2.1 The Wet or Hatschek Process:

This is the most widely used method of manufacture, and can be adapted to make a great variety of products. The process developed from the one used to make paperboard.

Before mixing asbestos and Portland cement in water, the fibre (usually a milled grade) is normally subjected to further treatment depending on its nature and quality of milling and on whether it contains impurities of any kind. It is often essential to fully fibrize the asbestos to remove dust and grit in order that a truly homogeneous pulp can be made. The process begins with the preparation of a dilute suspension of asbestos fibre and cement in water. This contains about 6% by weight of solids. After agitation the suspended solids are picked up as a thin film on the surface of a rotating drum of wire mesh, and transferred from this to an endless conveyor band of permeable felt. This passes over a vacuum box to remove excess water from the film, which is transferred to a steel assimilation drum, on which it is compacted and further dewatered by a pressure roller and is plied to the required thickness. When the accumulated layers of the 0.6 to 1.4 mm thick film reach the required total thickness, the deposit on the assimilation drum is cut and peeled off to an endless rubber conveyor belt. This "wet flat" is pliable and has considerable tear strength, and can be moulded, either by mechanical means or by hand, to form flat or profiled sheets or quite complex shapes.

2.2.2 The Semi-Dry or Magnani Process:

For the manufacture of corrugated sheet this process has the advantage that it can provide a greater thickness of material at the peaks and throughs of the corrugations, and so increase the bending strength.

The mix, which has a solids to water ratio of about 0.5 and is heated to facilitate the dewatering process, is pumped on to a fabric belt and spread and levelled by reciprocating rollers. Both the belt and the rollers may be shaped to form corrugated or profiled sheet. Vacuum boxes under the belt move with it to suck excess water from the hot mix, and dewatered sheet or profiled material is transferred to pallets to mature.

2.2.3 The Manville Extrusion Process:

Quite complex and sharp edged profiles can be formed by this process. The materials; asbestos fibres, cement, fine silica and a plasticiser such as polyethylene oxide, are fed from a hopper into a mixer, with just sufficient water to produce a stiff mix. This is transferred to the extruder, where a worm drive forces it through a steel die of the desired profile. The resulting extrusion is cut to lengths which are moved by a take-off belt to ballets on rollers. After drying, the extruded sections are autoclaved and finally cut to the required lengths.

2.3 REVIEW OF PREVIOUS MATERIAL TESTING

The literature on the mechanical properties of asbestos-cement is surprisingly limited. A few material-testing studies have been reported and these are reviewed in the following.

In the course of investigation into the stiffening effect of asbestos-cement sheeting when used in the roofs of buildings, Kallaur [10] carried out a series of tests to determine the mechanical properties of new and old (25 years) asbestos-cement sheets. It was emphasized that the results obtained were not quite typical of standard production material, as the specimens were cut from sheets produced at a reduced machine speed, and also because the specimens were older than usual when tested. The obtained strengths were believed to be higher than those of the normal product. Straight-sided specimens (12" x $1\frac{1}{2}$") were used for uniaxial tension tests to evaluate Young's moduli, Poisson's ratios (width increased to $2\frac{1}{2}$"), and the ultimate tensile strength in the two directions. The shear modulus of the material was measured by torsion of thin rectangular strip (22" x $1\frac{1}{2}$"). For comparison purposes the results obtained by Kallaur are given in Table 2.1.

H.G. Allen [11] presented a paper describing tensile tests performed on seven varieties of asbestos-cement boards to study the effect of the void content and the fibre content on the modulus of elasticity and the ultimate strength of the material in the two directions. Also, in this work, straight-sided specimens (1" wide) were loaded in an Instron machine and axial strains were measured by an extensometer with a gauge length of 3". Stress-strain curves showed that materials with a low fibre content were very brittle while those with a higher fibre content had a relatively high ultimate strain. The stress-strain curves of the in-between types of material were intermediate in character. It was evident that there is no simple relationship between fibre content and the measured Young's moduli, the ultimate strength or the strain at failure of the material (Table 2.2).

2.4 THEORETICAL BASIS FOR EXPERIMENTAL EVALUATION OF MECHANICAL PROPERTIES

The manufacturing process of asbestos-cement sheets imparts a certain degree of orientation to the fibres, and the mechanical properties of the sheeting strongly depends on this orientation. Based on this fact, asbestos-cement can be classified as a natural orthotropic composite.

If a homogeneous orthotropic medium is subjected to a plane stress state, only four independent elastic constants are required in the stress-strain relationships:

$$\begin{Bmatrix} \sigma_L \\ \sigma_T \\ \tau_{LT} \end{Bmatrix} = \begin{bmatrix} \frac{E_L}{1-\nu_{LT}\nu_{TL}} & \frac{\nu_{LT} E_T}{1-\nu_{LT}\nu_{TL}} & 0 \\ & \frac{E_T}{1-\nu_{LT}\nu_{TL}} & 0 \\ \text{SYMMETRIC} & & G_{LT} \end{bmatrix} \begin{Bmatrix} \varepsilon_L \\ \varepsilon_T \\ \gamma_{LT} \end{Bmatrix} \quad (2.1)$$

or $$\{\sigma\} = [Q]\{\varepsilon\}$$

in which:

E_L - the elastic modulus in the direction of fibres (L).

E_T = the elastic modulus in the orthogonal direction (T).

ν_{LT} - the Poisson's ratio relating strains in the T direction to stresses in the L direction

ν_{TL} - the Poisson's ratio relating strains in the L direction to stresses in the T direction.

and G_{LT} - the shear modulus

In the two decking systems under investigation, the longitudinal direction "L" is parallel to the corrugations, where "T" signifies the transverse direction (perpendicular to corrugations). Accordingly, the four elastic constants are designated: E_L, E_T, ν_{LT} and G_{LT}. The fifth elastic constant, ν_{TL}, is dependent on the other constants, and may be determined from the symmetry condition of the elasticity matrix [Q]:

$$\nu_{TL} E_L = \nu_{LT} E_T \qquad (2.2)$$

The Young's moduli and Poisson's ratios can be easily determined by direct uniaxial tension tests. However, a rigorous determination of the shear modulus of an anisotropic medium is more complex. The problem results from the difficulty in producing a stress field of pure shear. Many test techniques have been reported to determine the shear modulus of composite materials showing pronounced orthotropy [12,13,14].

For fibre composites, a method which has been used [12] is to test in pure tension a specimen for which the principle directions of material properties "L" and "T" are inclined at 45° with respect to the direction (x) of the load as shown in Fig. 2.1. It can be proved that:

$$\frac{1}{E_x} = \frac{1}{4}\left[\frac{1-2\nu_{LT}}{E_L} + \frac{1}{E_T} + \frac{1}{G_{LT}}\right] \qquad (2.3)$$

in which: $E_x = \dfrac{\sigma_x}{\varepsilon_x}$

Thus, by evaluating E_x from the tensile test and in conjunction with the known values E_L, ν_{LT} and E_T, the shear modulus, G_{LT}, can be determined from Eq. 2.3 as:

$$\frac{1}{G_{LT}} = \frac{4}{E_x} - \frac{1}{E_T} - \left(\frac{1-2\nu_{LT}}{E_L}\right) \qquad (2.4)$$

Although this approach seems attractive, the restraint induced at the gripped ends of the test specimen may raise doubts about the validity of the measurements. The above analytical relations, Eqs. 2.3 and 2.4, are theoretically valid if the tensile test is conducted in a manner which insures that the stress is applied uniformly across the specimen ends allowing them to deform freely in the manner shown in Fig. 2.2a. In the case of clamped ends, the specimen would be restrained from shearing deformation so it would twist in the fashion shown in Fig. 2.2b. This can affect the axial strain distribution and would result in an erroneous evaluation of the modulus E_x [12]. However, if a long and slender specimen is used, disturbances at its ends would be reduced, and the boundary conditions at the specimen end grips would be of little consequence. At the center of such specimen, the deformation is very similar to the shearing and extension of the unrestrained specimen of Fig. 2.2a.

The mechanical properties of asbestos-cement are also affected by the residual humidity of the sheet. It has been observed [5,10] that the properties in humid state (24 hours immersion in water) are considerably lower than those measured in dry conditions. In this work, the material has been tested in both conditions.

2.5 TEST SPECIMENS

Asbestos-cement has been previously tested using straight-sided specimens [10,11], as many other composites [15]. However, it is believed that a more conventional specimen configuration (the dog-bone) might yield more reliable results. In general, a tensile test specimen should be symmetrical with respect to a longitudinal axis throughout its length in order to avoid bending during application of load. The central portion of the length is usually (but not always) of smaller cross section than the end portions in order to cause failure to occur at a section where the stresses are not affected by the gripping device.

Since there is no ASTM test method and procedure for the determination of the elastic constants of asbestos-cement and its tensile properties, it was thus decided that specimens of various sizes and shapes should be tested to evaluate any possible size or shape effects. Three specimen configurations having the dimensions shown in Fig. 2.3 were selected [15,16,17] for tension tests. In addition, straight-sided specimens of the same outer dimensions were also tested, Fig. 2.4. The specimens were cut from the flat portions of randomly selected units of both Cavity and "T" decks, typical of Atlas' standard production.

The specimens were grouped into three sets, each set included:

(1) Specimens cut in the longitudinal direction "L" (parallel to corrugations), to determine E_L, ν_{LT} and the ultimate tensile strength σ_{UL}.

(2) Specimens cut in the transverse direction "T", to determine E_T, ν_{TL} and σ_{UT}.

(3) Specimens cut at 45° to the longitudinal direction, to determine E_X and subsequently G_{LT}, the shear modulus.

2.6 TEST TECHNIQUES AND PROCEDURE

All static tensile tests were conducted on the Instron Universal Testing Machine Model 1125, under room temperature and normal laboratory conditions. Prior to testing, each specimen was carefully checked for alignment and dimensional accuracy.

Two reliable devices to measure axial strains of the tensile specimens were used, each in conjunction with a procedure of loading and recording. These are described in the following.

2.6.1 Strain Gauge Extensometers

Two Instron strain gauge extensometers (Models G-51-14MA and G-51-11MA) of medium and high magnification ranges with initial gauge lengths of 50 and 25 mm, respectively, were used. The appearance of the extensometer and its application to the test specimen is shown in Fig. 2.5.

The applied load was increased continuously until failure of the specimen occured within its gauge length. Load/strain curve was plotted automatically from zero to failure on a strip chart recorder.

2.6.2 Electrical-Resistance Strain Gauge

The surface of the test specimen was first sanded smooth and then was cleaned and washed thoroughly to remove any dirt particles or grease that could interfere with the quality of the bond.

One strain gauge (Type EA-06-250BG-120, manufactured by Micro-Measurement) was bonded on one prepared surface of the test specimen using Micro-Measurement M-Bond AE-10, room temperature curing epoxy adhesive (an ideal material for precoating concrete). To enable the determination of Poisson's ratios, three-element strain gauge rosettes (of Type EA-13-125RA-120) were used. The two active gauge elements were oriented at 0° and 90° to the specimen principal axes and connected one at a time into a "Quarter Wheatstone Bridge" arrangement together with a dummy identical gauge which was mounted on an unstrained specimen for temperature compensation.

Loading was applied in equal increments (0.1 kN) to facilitate periodic recording of strain gauge data. Test results were obtained from the Instron strip chart recorder (load) and from a Vishay Instruments Inc. P-350A strain indicator (strains). When rosettes were used, a SB-1 switch and balance unit was connected to the strain indicator to facilitate simultaneous recording of longitudinal and transverse strains of each element active in a quarter bridge arrangement. The test set-up is shown in Fig. 2.6.

Tension tests were conducted at different strain rates (cross-head speeds: 0.05-0.1-0.2 mm/min).

2.7 TEST RESULTS AND DISCUSSIONS

The average test results obtained for the material elastic constants, tensile strengths, in the longitudinal and transverse directions, and the shear modulus are listed in Table 2.3, for both the dry and wet conditions. Average stress-strain curves are depicted in Figures 2.7 to 2.9. Although the average strain values were used to construct the curves in these figures, it should be emphasized that the strains obtained by each of the two strain measurement devices (i.e.; Instron extensometers and electrical resistance strain gauges) were very close.

From the average stress-strain curves and the calculated values of the elastic properties of the asbestos used in the present study, the following observations can be made:

(1) The elastic modulus in the longitudinal direction (E_L) is slightly higher than the modulus in the transverse direction (E_T), in both the dry and wet conditions by 32% and 21%, respectively. Both are slightly lower in the wet condition.

(2) The longitudinal tensile strength (σ_{UL}) is markedly greater than the transverse strength (σ_{UT}) in both conditions by 72% (dry) and 87% (wet). It is known that the fibres are concentrated in the longitudinal direction and it is clear that the fibres have an important influence on strength. The asbestos fibres are analogous in their action to the

steel reinforcement in normal reinforced concrete, but with the advantage that the asbestos fibres are intimately mixed with the cement, thus providing a uniform mass of constant strength throughout the body of the material, avoiding any pronounced difference in stress and any possibility of lack of bond between the cement and asbestos [8].

(3) The stress-strain curves are virtually linear up to 50% of the ultimate tensile strength in the longitudinal direction, and up to 70% of strength in the transverse direction. The nonlinear behaviour being more pronounced in the longitudinal direction than in the transverse.

(4) Recorded strains showed that there is a tendency for the Poisson's ratios (ν_{LT} and ν_{TL}) to increase with increasing load. This behaviour was clear in all specimens. The average values reported herein can be seen to accurately satisfy the reciprocality relation of Eq. 2.2: $\nu_{TL} E_L = \nu_{LT} E_T$.

(5) Specimens tested at higher rates of loading showed an increase in tensile strength. This was expected, as it is known that time-dependent deformations (creep) assume greater effects at lower strain rates.

Finally, it is interesting to compare the current material testing results, Table 2.3, with those obtained by Kallaur [10], Table 2.1. It can be seen that there is slight differences between the values for the elastic constants and Poisson's ratios. However, the ultimate tensile strengths as obtained by Kallaur are quite higher. These discrepancies may be attributed to the reasons cited earlier in Section 2.3.

TABLE 2.1

MATERIAL PROPERTIES OF CORRUGATED ASBESTOS-CEMENT SHEETS

(KALLAUR - REF. [1] & [10])

Property	Grain Direction	Condition	Average Result (psi) New Sheeting	Average Result (psi) Old Sheeting
E_L	L	Dry	1.91×10^6	2.64×10^6
		Wet	1.93×10^6	2.02×10^6
E_T	T	Dry	1.57×10^6	-
		Wet	1.52×10^6	-
ν_{LT}	L	Dry	0.26	
ν_{TL}	T	Dry	0.18	
G_{LT}	-	Dry	0.98×10^6	1.30×10^6
σ_{Lult}	L	Dry	2915	2485
		Wet	2507	2000
σ_{Tult}	T	Dry	1687	
		Wet	1327	

TABLE 2.2

TENSILE PROPERTIES OF SEVEN ASBESTOS-CEMENTS

(ALLEN - REF. [11])

Type	v_f^*	Mean Values (psi)			
		E_L	E_T	σ_{Lult}	σ_{Tult}
1	0.0570	$2.45\mathrm{x}10^6$	$2.40\mathrm{x}10^6$	2581	2175
2	0.0291	$2.51\mathrm{x}10^6$	$2.54\mathrm{x}10^6$	2117	1566
3	0.0510	$2.33\mathrm{x}10^6$	$1.96\mathrm{x}10^6$	2943	1783
4	0.0732	$2.14\mathrm{x}10^6$	$2.00\mathrm{x}10^6$	3683	2668
5	0.1485	$1.23\mathrm{x}10^6$	$1.28\mathrm{x}10^6$	3088	2682
6	0.0602	$2.96\mathrm{x}10^6$	$2.72\mathrm{x}10^6$	2102	1638
7	0.04716	$1.90\mathrm{x}10^6$	-	2334	-

$$* \; v_F = \text{fibre content by volume}$$

$$= \frac{\text{volume of fibre}}{\text{total volume of composite}}$$

TABLE 2.3

AVERAGE TEST RESULTS OF ASBESTOS-CEMENT ELASTIC CONSTANTS AND MECHANICAL PROPERTIES

(PRESENT STUDY)

Property	Grain Direction	Condition	No. of Specimens	Average Result (psi)
E_L	L	Dry	18	2.25×10^6
		Wet	6	2.00×10^6
E_T	T	Dry	18	1.70×10^6
		Wet	6	1.65×10^6
$E_{45°}$	45°	Dry	10	2.04×10^6
ν_{LT}	L	Dry	4	0.20
ν_{TL}	T	Dry	4	0.15
G^*_{LT}	-	Dry	10	0.90×10^6
σ_{Lult}	L	Dry	25	2150
		Wet	12	1700
σ_{Tult}	T	Dry	25	1250
		Wet	12	910

* Calculated according to Eq. 2.4

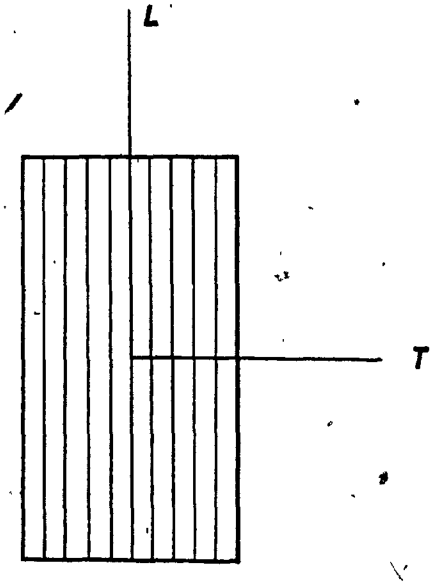

PRINCIPAL MATERIAL DIRECTIONS

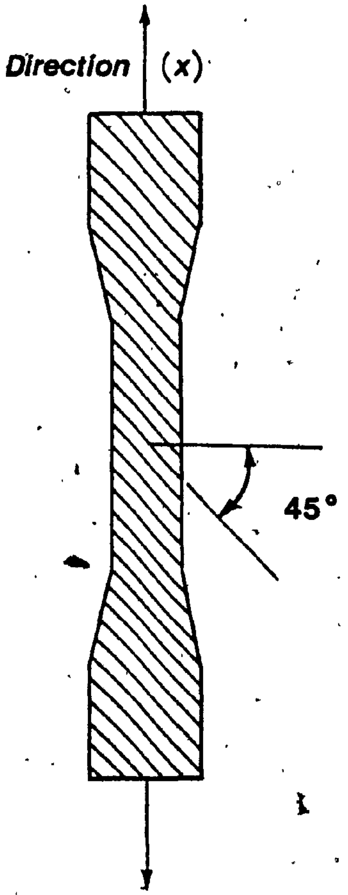

TEST SPECIMEN

FIG. 2.1 DETERMINATION OF G_{LT} FOR ORTHOTROPIC MATERIAL

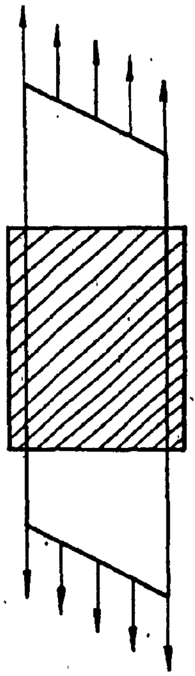

(a) PROPER UNIAXIAL TEST (No End Effect)

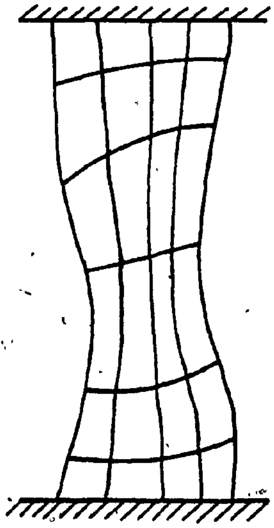

(b) IMPROPER UNIAXIAL TEST (Restrained Ends)

FIG. 2.2 DEFORMATION OF A UNIDRIECTIONALLY REINFORCED LAMINA LOADED AT 45° TO THE FIBERS [REF. 12]

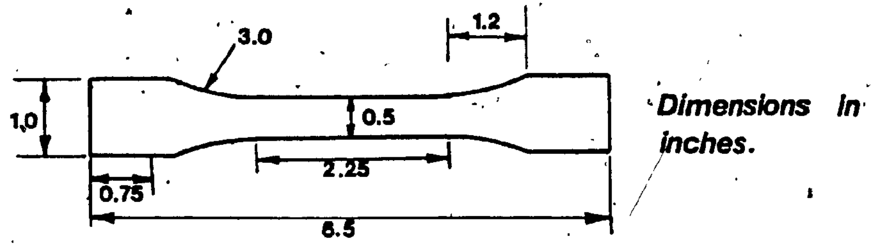

Ref. **15**

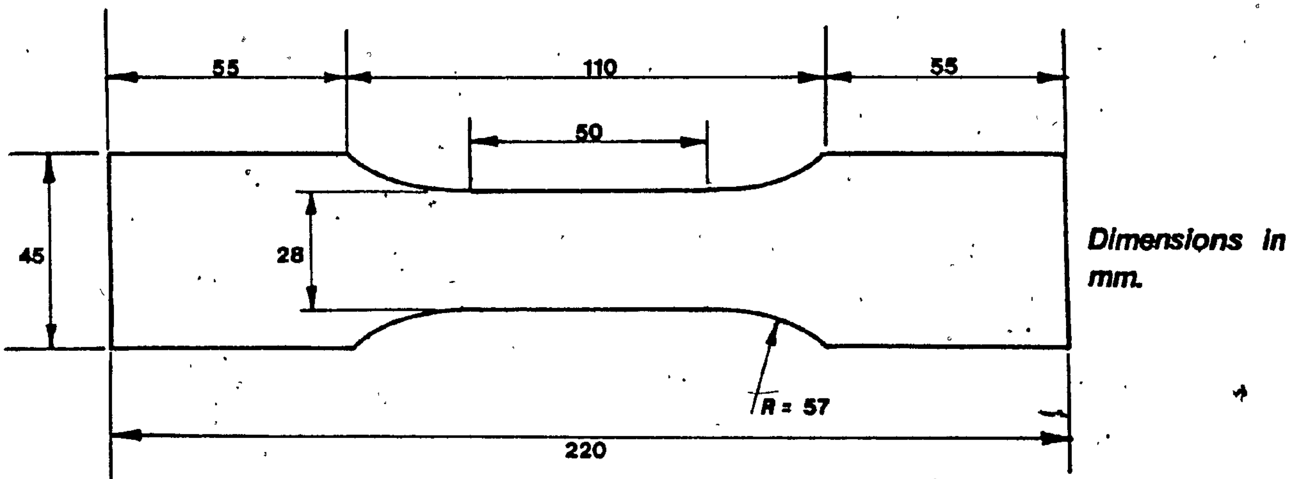

Ref. **16**

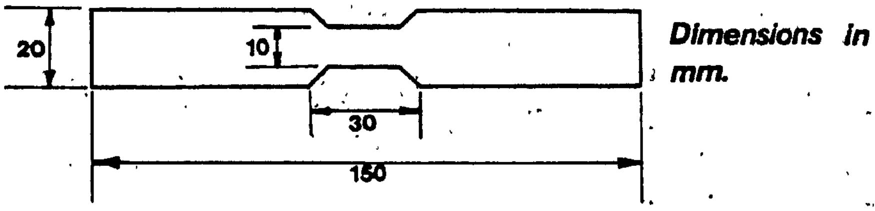

Ref. **17**

FIG. 2.3 TENSILE TEST SPECIMENS

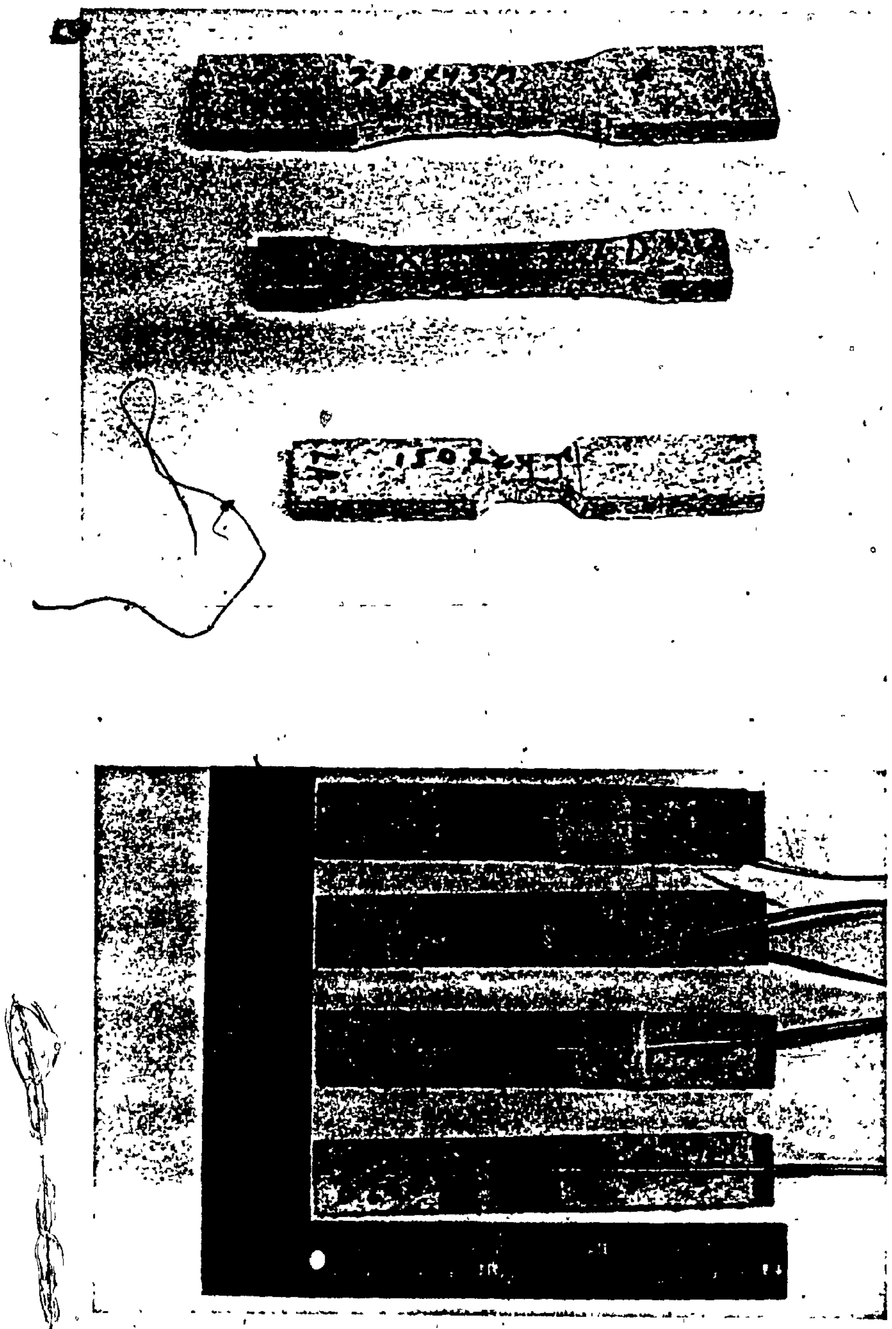

FIG. 2.4 VIEW OF CONFIGURATED AND STRAIGHT-SIDED TENSILE TEST SPECIMENS

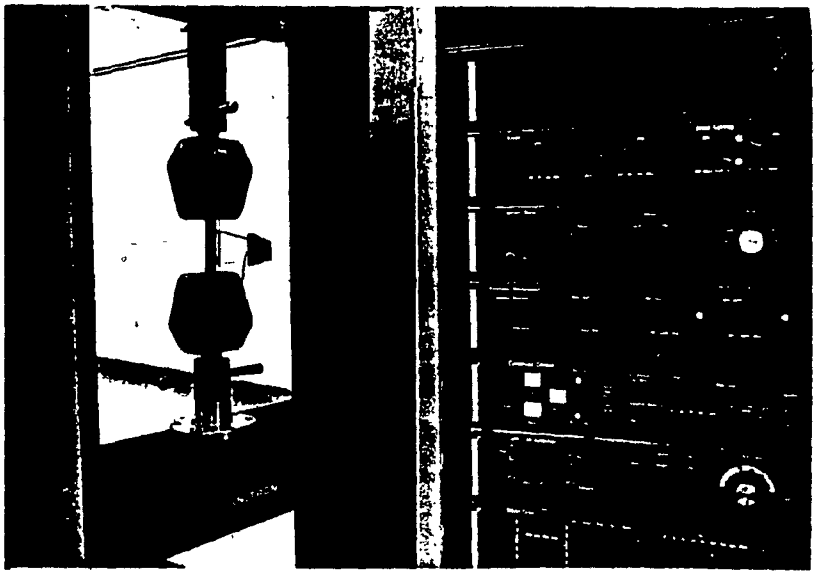

FIG. 2.5 AXIAL TENSILE STRAINS MEASUREMENT USING STRAIN GAUGE EXTENSOMETER

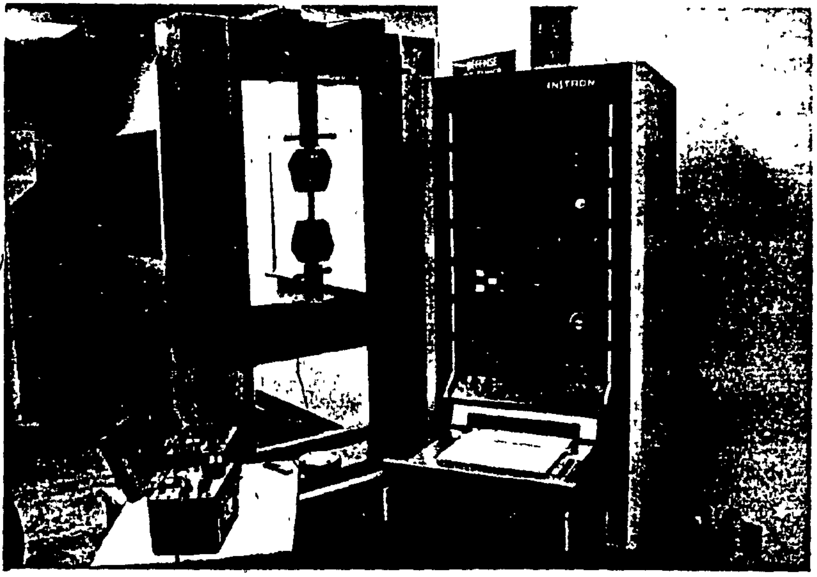

FIG. 2.6 AXIAL TENSILE STRAINS MEASUREMENT USING ELECTRICAL-RESISTANCE STRAIN GAUGES

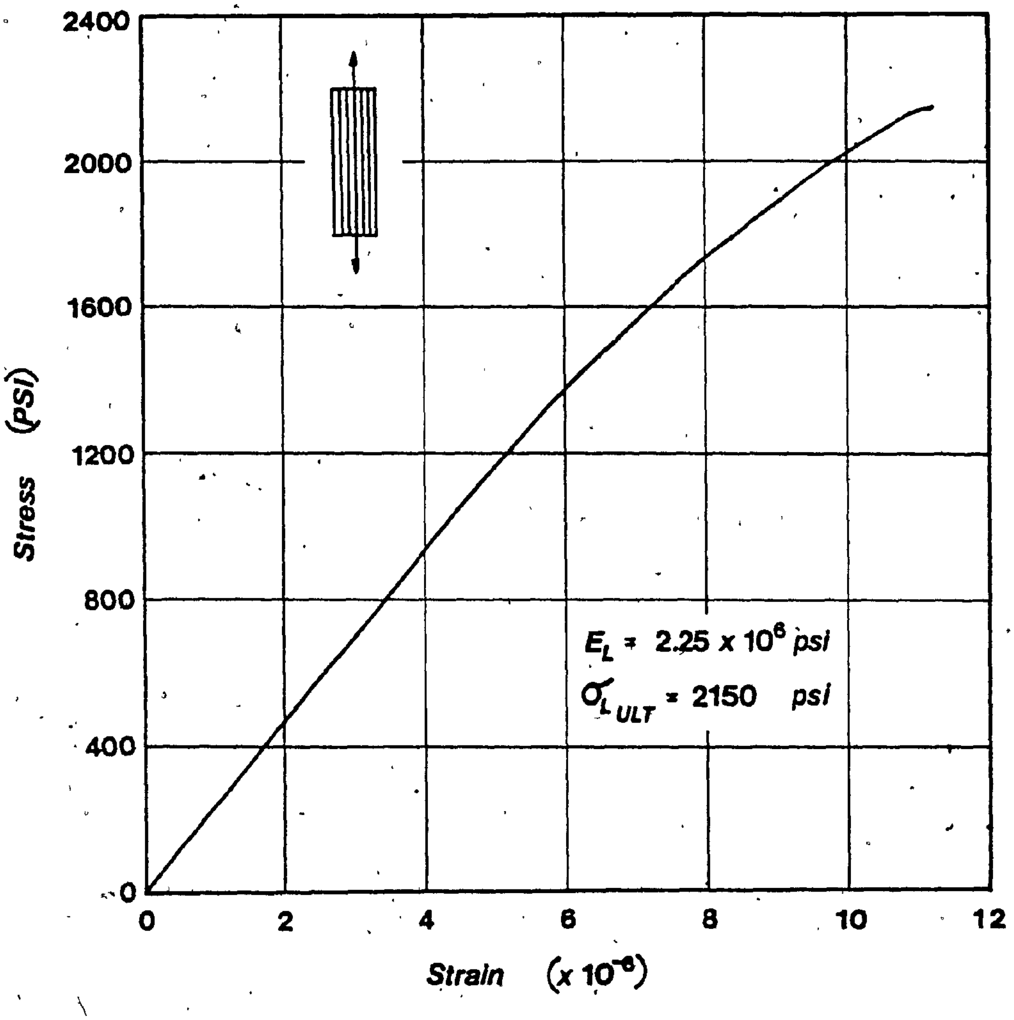

FIG. 2.7 AVERAGE STRESS-STRAIN CURVE FOR ASBESTOS-CEMENT IN TENSION ALONG THE FIBERS

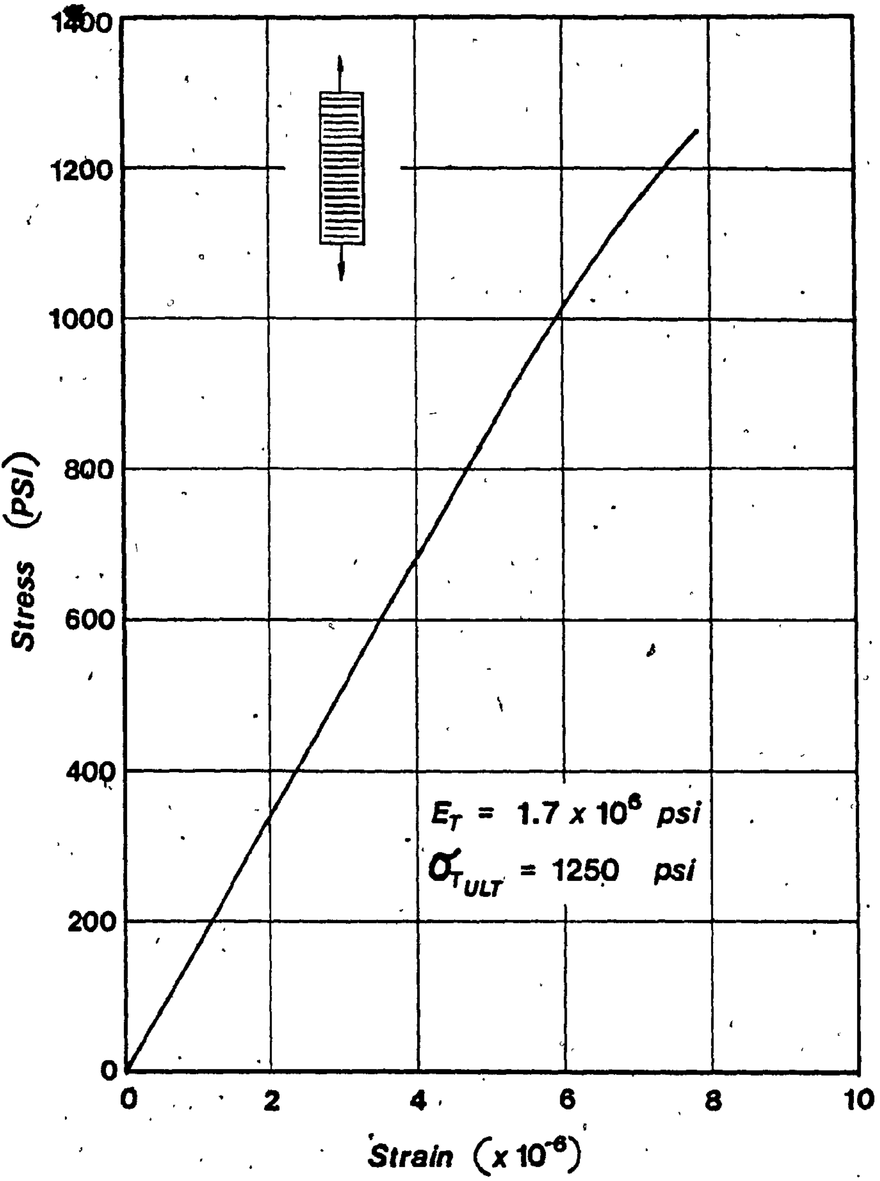

FIG. 2.8 AVERAGE STRESS-STRAIN CURVE FOR ASBESTOS-CEMENT IN TENSTION TRANSVERSE TO FIBERS

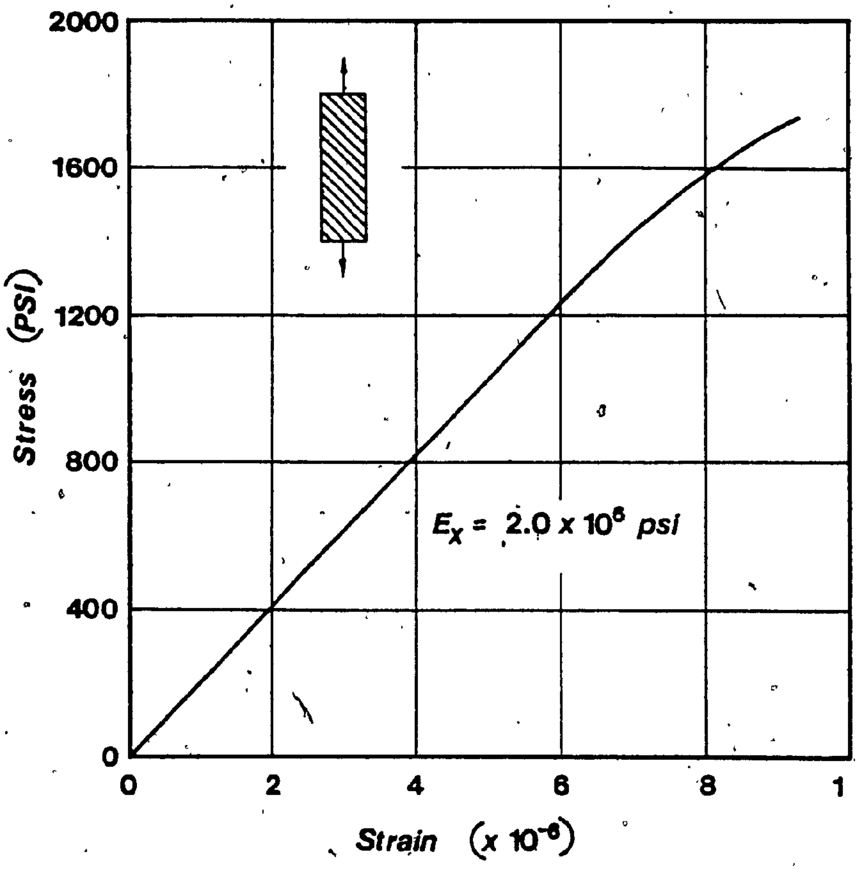

FIG. 2.9 AVERAGE STRESS-STRAIN CURVE FOR ASBESTOS-CEMENT IN TENSION ALONG AXIS-X (45° TO FIBRES)

CHAPTER III

FULL-SCALE DIAPHRAGM TESTING

CHAPTER III

FULL-SCALE DIAPHRAGM TESTS

3.1 INTRODUCTION

Testing of full-scale diaphragms is of major interest to the present study. This interest arises not only from the fact that the present asbestos-cement diaphragm testing is the first of its kind in North America but also from the desire to provide a basis for developing analytical prediction techniques. Previous experience related to metal diaphragms confirms that full-scale testing of diaphragm assemblies is the most reliable means for obtaining diaphragm performance data by which the merits of the different analytical techniques can be judged.

Planning of the present full-scale tests was based on previous research and reported experience related to metal diaphragms. A broad review of these studies is presented in the following section.

3.2 REVIEW OF PREVIOUS FULL-SCALE TESTING OF METAL DIAPHRAGMS

The first published work on shear diaphragms of light-gauge steel deck in North America was by A.H. Nilson of Cornell University [18,19,20]. He conducted a total of 46 full-scale diaphragm tests (from 1956 to 1960), and was the first to show that a shear diaphragm, loaded as a cantilever in its own plane, has approximately the same load-deformation characteristics and ultimate strength as those of a three-bay diaphragm with third-point loading (Fig. 3.1). This cantilever arrangement has greatly simplified the test procedure and resulted in a more economical and practical method of testing which has been adopted as a standard procedure [21] by most subsequent researchers. Nilson's tests disclosed many factors which influenced the performance of diaphragms. He considered the effects of end closures and marginal beams, and observed that the flexibility of diaphragms increase with diaphragm span and with the depth of the panel's open profile. Moreover, he separated the total shear deflection into components due to: (1) flexural stress, (2) shear stress, (3) seam slip and (4) slip at marginal beams.

In 1960, another program of research was initiated at the University of Manchester, England, under the direction of E.R. Bryan, on the stiffening effect of light cladding on steel building frameworks. In the course of this work, full-scale and semi full-scale tests were conducted on sheeted portal frames [22,23,24]. Measured stresses and deflections of the sheeted frame were found to be considerably less than those in the bare frame. For the theoretical analysis, shear rigidity and strength of the sheeting were established by tests using a technique similar to that described by Nilson. Close agreement was obtained between the calculated and measured bending moments in the frame. Reductions of 34% to 60% of the bare frame moments were achieved, depending on the position of the frame in the shed. Similarly, the calculated collapse load agreed well with the measured value, which was 42% above that for the bare frame. It was concluded that a material savings of 20% could be realized in the design of frames.

Luttrell [25 to 28] and Apparao [29], in extending the work begun by Nilson, investigated in detail the many parameters influencing the behaviour of the complex diaphragm installation and explored the contribution of each variable to the overall load-displacement response. Some 70 full-scale diaphragms and several small ones were tested. Luttrell investigated the influence of perimeter member stiffness and found it had only a moderate effect on the diaphragm behaviour. Other findings include: (i) the diaphragm stiffness and strength can be greatly increased by adding sidelap fasteners between purlins; (ii) stiffness increases faster than strength with increasing cover width; (iii) strength varies approximately linearly with thickness; (iv) additional end fasteners increase the stiffness by reducing warping of the profile, but have only moderate effect on the ultimate strength; and (v) an increase in material yield strength of 40% results in about 10% increase in diaphragm strength and stiffness. Additional tests on diaphragms subjected to simulated dynamic load (reversed and pulsating loading) were also carried out. It was observed that the static strength of decks fastened to the frame with screws was reduced 30% by pulsating load. Welded diaphragms experienced no such loss of strength. On the other hand, Apparao observed that shear stiffness is mainly dependent on the diaphragm length and on the type and spacing of fasteners.

The work at Cornell has resulted in a valuable design manual which includes standard test procedure, charts, guidelines and recommendations for design. This was prepared and published by AISI [21]. Since then, numerous diaphragm tests have been sponsored by the manufacturers of the sheeting units [30,31,32,33].

Work in this field was continued with more depth and interest by the group at the University of Manchester. Bryan and El-Dakhakhni [34, 35,36] reported a comprehensive series of tests which resulted in detailed practical information on the effects of purlins, purlin-rafter connections, sheet fasteners, sheet profiles and width, and the influence of insulation board. The work in Britain has now reached the stage where it has been incorporated into the Codes of Practice [37,38,39], and used extensively in the design of buildings [40,41,42].

3.3 TESTING APPARATUS

The cantilever test frame method, schematically shown in Fig. 3.2, as prescribed by ASTM E455-76 [43] and the American Iron and Steel Institute [21] was used throughout the test program. In the following, description of the testing apparatus and its loading and deflection measurement instrumentation is presented.

3.3.1 Description of Test Frame

The dimensions of the test frame were so chosen that it can accomodate, in either direction, the largest decking units manufactured by Atlas Asbestos Co. The frame, square in shape (10.0 ft by 10.0 ft) and constructed with W10X21 steel beams was supported by a rigid base frame (Fig. 3.3) which was designed to provide the action and reaction to and from the test frame. All corner connections of the test frame were pinned to ensure that the resistance of the bare frame is minimal. These pinned connections were made as follows. Half inch thick steel plates ($13\frac{3}{4}$" x 5") were welded to the tops and bottoms of members AB and DC. One inch diameter holes were drilled through the plates and the adjacent frame members (flanges and webs) to receive 7/8" diameter bolts which thus made nearly frictionless pin connections. The holes were located at the intersection of the centerlines of each two members. At corner A, the frame was connected to a W21X55 steel beam (3.0' long) in such a manner as to prevent virtually any movement at that point in any direction. The W21X55 beam, resting on the laboratory floor was in turn rigidly connected to the supporting base frame. At corner B, the frame was restricted against movement in the BC direction, but movement in the BA direction was permitted by means of a double-pinned connection, which transfered its single reaction to the base frame through similar W21X55 steel beam. Rollers ($1\frac{1}{8}$" diameter) were placed between the test frame and the base frame to reduce friction forces. Two end load plates (8" x 11" x $\frac{1}{2}$") were welded to the ends of member CD. Construction details of the test frame are illustrated in Figures 3.4 to 3.6.

In the construction and assembly of the test frame, great care was taken to ensure that the frame is dimensionally accurate, in a level position, and that corner connections are tight with no play, but would still pivot smoothly and allow the frame to deflect freely when no decks are in place. Prior to each test, it was made sure that the resistance of the frame alone to shear deformations is negligible, thus all shear loads would be transfered through the deck fixed on the top flanges.

3.3.2 Instrumentation for Load and Deflection Measurement

Shear load was applied to the frame at corner C by means of a 10 ton (100 kN) hydraulic ram in line with the centerline of member CD. The force in the ram reacted against the supporting structure through an Instron load cell (100 kN capacity) as shown in Fig. 3.7. The output of the load cell (test load) was monitored with an Instron load cell amplifier unit which was connected to a digital voltmeter (Fig. 3.8). The voltmeter was calibrated prior to each test to read the force transmitted to the frame through the load cell, represented by millivolts. It is worthwhile to note that the load cell amplifier enabled the voltmeter to record applied loads as small as 0.04 lbs.

Deflections at the test frame corners, in the plane of the diaphragm, were measured with 8 dial gauges located as shown in Fig. 3.2, enabling the determination of the net deflection to the nearest thousandth of an inch.

3.4 DETAILS OF TEST DIAPHRAGMS

A total of 13 diaphragm tests were conducted; 8 of Cavity decking (series "C"), and 5 of "T" deck (series "T"). Installation of the diaphragms in the test frame and their construction details are described below.

3.4.1 Cavity Decking

The test frame was capable of accomodating 9 units of cavity decking system. The deck was laid in accordance with Atlas' instructions [44] as follows:

(1) The deck was started with a full width uncut overlapping unit and two reduced width supporting units (first and second starters) as illustrated in Fig. 3.9a. The first and second starters were both cut from a full width unit and were aligned and bolted up to the test frame, thus ready to receive the first full width unit for further laying of full units.

(2) At a distance of 5/8" from the underlapping edge (bottom seam) holes were drilled with a 1/4" bit through both layers of the underlap. The underlap was then secured with $1\frac{1}{2}$" x $\frac{3}{16}$" diameter flat head stainless steel bolts and cadmium plated pal-nuts (Fig. 3.9b)

(3) At a distance of 5/8" from the overlapping edge (top seam) holes were drilled using a 3/16" bit, through both layers of the top seam. Only the holes in the top thickness were enlarged to 1/4" diameter, countersunk to suit and secure with $1\frac{1}{4}$" No. 12 flat head "A" type self-tapping screws (Fig. 3.9c)

Each unit of the cavity decking diaphragms was connected to the end framing members (perpendicular to the corrugation generator) with one self-tapping screw (#14 x1" type "B") per end, except for test C-7, where two screws were used (Fig. 3.10). Side connections were provided for all tests (except for C-1), using the same type of self-tapping screws.

In test C-8, a center purlin (C6x8.2 steel channel) was connected to the frame between member AB and CD using bolted clip angle connections, such that all top flanges were at the same level (Fig. 3.11). The deck units were also connected to the purlins with one self-tapping screw per unit.

Relevant characteristics of the 8 tests are given in Table 3.1. It can be noticed that the main parameter varied in the tests is the fasteners spacing or the number of the side and seam connections.

3.4.2 "T" Deck:

Six units of "T" deck were assembled to form one full deck. The deck was laid as follows [44]:

(1) For starting, 21" width of the flat part of the first unit was cut, where the remaining corrugated section was aligned and secured to the supporting steel members. The next full width unit was laid to overlap the starter and aligned with the cut edge at the extremity of the roof and both secured with self-tapping screws to the shear connectors (C3x6 channel steel section, 6" long each), Fig. 3.12a.

(2) At a distance $21\frac{1}{2}$" from the overlapping edge of the first full unit (i.e., approximately at the center of the unit) holes were drilled using a 3/16" bit through both thicknesses of the underlap (bottom seam). The holes in the top thickness were enlarged to

1/4" diameter, countersunk to suit and secure with $1\frac{1}{4}$" No. 12 flat head "A" type self-tapping screws (Fig. 3.12b).

(3) The next full unit was then laid and its underlap was fixed as in (2). At 1" clear from the overlapping edge of this unit, holes were drilled using a 3/16" bit through both thicknesses of the overlap (top seam). Similarly, the holes in the top thickness were enlarged to 1/4" diameter, countersunk to suit and secure same type of screws as in (2), Fig. 3.12c.

The "T" deck units of all test diaphragms were connected to the end members at every corrugation using self-tapping screws (#14x1" type "B"), Fig. 3.12d. Side connections were provided for all tests (except for T-1) with shear connectors, cut from a channel steel section C3X6, each 6" long, and connected to the top flanges of the side members using self-tapping screws (#14x1" type "B").

Relevant characteristics of the 5 diaphragms are given in Table 3.2.

3.5 TESTING PROCEDURE

The test procedure was in accordance with ASTM E455-76 and AISI standards. All diaphragms in the present test program were statically loaded to failure. Only in two tests (c-3 and C-4) the diaphragms were subjected to cyclic loading, then loaded to failure. This is to investigate the effect of such repeated loading ~~on~~ the general shear behaviour. In repeated loading, the load is applied in one direction to some percentage of the expected ultimate load (usually to 0.4 Q_{ult}) for a number of times to simulate repetitive wind loads.

With a deck installed and ready for testing, a relatively small load (1 to 2 kN) was first applied then released to induce fitting adjustment, and all the dial gauges set at zero references. Loads were then gradually applied in increments of 0.5-1.0 kN. Load and deflection readings were recorded after each increment. Recordings were made after the diaphragm was allowed to stabilize (for 1 to 2 minutes), especially at higher loads. Loading was continued until the deck was no longer capable of sustaining the applied load.

In all tests, corner D of the test frame started lifting off the roller supports at a load of 7 to 10 kN. The same phenomenon occured in Nilson's and Bryan's tests on steel diaphragms. This is attributed to the fact that the jack force was applied at the mid-depth of member CD, while the resistive force offered by the sheeting fasteners is developed along the surface of the top flange. Small moments could develop due to this eccentricity, however, it has been found [20,21,45] that their effect on the overall shear behaviour and deflection measurements is small and can be neglected for simplicity. In all subsequent tests to the first, this corner was then held down by means of a sliding clamp which still allowed the diaphragm to move laterally in its own plane.

3.6 TEST RESULTS AND DISCUSSIONS

In the presentation and discussion of the test results, it is convenient to consider separately the two different types of decks tested. Information obtained from the test results are load-deflection curves, ultimate shear strengths, shear stiffnesses, maximum deflections and failure modes. General observations are made from both a constructional and behavioural viewpoint on the ability of the two systems to effectively function as shear resisting elements.

3.6.1 Evaluation of the Shear Parameters:

The important parameters which characterize a diaphragm are its shear stiffness (or conversely the flexibility) and shear strength. These quantities can be computed from the load-deflection curve obtained from a diaphragm test (Fig. 3.13).

3.6.1.1 Shear Stiffness:

The shear stiffness G' (lb/in) is conventionally defined as the secant modulus of the load-shear deformation curve at 40% of the ultimate load [21,27,28,32]:

$$G' = \frac{0.4\ Q_{ult}/b}{\Delta'_s/a} \tag{3.1}$$

in which

a, b = the dimensions of the diaphragm perpendicular and parallel to the load direction, respectively.

Δ'_s = the shear deflection at 40% of the ultimate load

Q_{ult} = the ultimate load

Evaluation of G' requires accurate measurement of the actual shear deflection (Δ_s). First, the deflection effect of small unavoidable rigid body movements of the cantilever support points and corners must be eliminated. The effect of such movements on the deflection at the jack in the direction of the applied load is easily determined using the known aspect ratio of the diaphragm in conjunction with recorded dial gauge readings of such support and corner movements. Noting the geometry and dial gauge locations in Fig. 3.2, the net measured deflection, Δ_{NET}, in the load direction is given as:

$$\Delta_{NET} = \frac{1}{2}(\Delta_1 + \Delta_4 - \Delta_5 - \Delta_8) + \frac{a}{b}\left[\frac{1}{2}(\Delta_3 + \Delta_7 + \Delta_2 + \Delta_6)\right] \tag{3.2}$$

where Δ_i is the measured deflection at gauge i.

To finally arrive at the actual shear deflection, Δ_s, it is necessary to subtract the deflection component due to axial strains in the test frame's perimeter members, from the net deflection, Δ_{NET}. An estimate of this cantilever bending deflection, Δ_b, as a function of the properties of the edge frame members, is given as [21,27,30,43]:

$$\Delta_b = \frac{Q\, a^3}{3EI} \tag{3.3}$$

in which

Q = jack load. lbs

E = modulus of elasticity of steel (29.5×10^6 psi)

I = $Ab^2/2$

A = cross-sectional area of perimeter frame members perpendicular to load direction (members AD and BC)

Thus, the net shear deflection, Δ'_s, in Eq. 3.1 is given as:

$$\Delta'_s = \Delta_{NET} - \Delta_b \text{ (at } 0.4\, Q_{ult}) \tag{3.4}$$

In the present test program, the above correction is not necessary, for the bending deflection, Δ_b, is negligible in comparison with Δ_{NET} for all levels of Q.

It is important here to emphasize that the diaphragm shear modulus, G', as expressed by Eq. 3.1, is invariant with respect to loading configuration, where the diaphragm panels may be laid parallel or perpendicular to the loading direction [20,27]. This property has been verified by Cornell University Laboratory tests in 1955 as reported by Nilson in Ref. 20. A simple analytical proof of the independence of G' of load direction can be obtained by studying the shear load-shear deformation relations in the two cases as shown in Fig. 3.14. For case 1, Fig. 3.14a, where the panels are laid parallel to the load direction, G'_1 can be expressed as:

$$G'_1 = \frac{q_1}{\gamma_1} \qquad (3.5)$$

in which

$q_1 = \frac{Q_1}{b}$ the shear flow

and $\gamma_1 = \frac{\Delta_1}{a}$ the shear angle

Similarly, for case 2, Fig. 3.14b, where the panels are laid perpendicular to the load direction:

$$G'_2 = \frac{q_2}{\gamma_2} \qquad (3.6)$$

in which

$q_2 = \frac{Q_2}{a}$ and $\gamma_2 = \frac{\Delta_2}{b}$

Let Q_1 and Q_2 be such that $\gamma_1 = \gamma_2$. Since the shear distortion (γ) is the same in both cases, the work done by Q_1 and Q_2 must be identical:

$$\frac{1}{2} Q_1 \Delta_1 = \frac{1}{2} Q_2 \Delta_2 \qquad (3.7)$$

From the definitions of the equal shear distortions γ_1 and γ_2, Eq. 3.7 is reduced to:

$$Q_1 a \gamma = Q_2 b \gamma$$

or $$\frac{Q_1}{b} = \frac{Q_2}{a} \qquad (3.8)$$

i.e. $q_1 = q_2$ for the same γ

Thus,

$$G'_1 = G'_2 \qquad (3.9)$$

Another measure of the diaphragm rigidity, commonly used by researchers from England (Bryan, et al) is the diaphragm shear flexibility (c), defined as the shear deflection per unit shear load:

$$c = \frac{\Delta}{Q} \tag{3.10}$$

It can easily be deducted from the above equations that flexibilities of diaphragms of cases 1 and 2 are related by the equation:

$$c_1 = c_2 \left(\frac{a}{b}\right)^2 \tag{3.11}$$

In the current test program, because the aspect ratio (a/b) is equal to one (a=b=10.0 ft), the diaphragm shear flexibility is directly equal to the inverse of the shear modulus. Also in this case, the shear flexibility, is the same whether the panels are laid parallel or perpendicular to the load direction.

3.6.1.2 <u>Shear Strength</u>:

The ultimate shear strength S_u (lb/ft) of the deck is defined as

$$S_u = \frac{Q_{ult}}{b}$$

in which

Q_{ult} = the force required to produce failure of the deck.

The ultimate shear load, Q_{ult}, was the highest recorded load in the tests. Continued application of the load after that would result in very large deformations.

3.6.2 <u>Cavity Decking Diaphragms</u>:

The behaviour of all the tested cavity decking diaphragms followed a general pattern. The seam fasteners on the bottom face of the deck (bolts and nuts) were less effective (much smaller stiffness and strength, see Chapter IV) than the other connections in the deck. Although early failures at these fasteners were observed at loads of 50 to 60% of Q_{ult}, this did not precipitate collapse of the diaphragms. The forces in the bottom seams were transfered to the top seams which are considerably stiffer. At high loads, slipping of one unit relative to another at the seams and tilting of the edges of the diaphragm units relative to the frame were observed. When a decking was dismantled after the test, severe bearing failures of the units along the bottom seams were clearly visible. Overall collapse of the diaphragm was caused by localized bearing failure (tearing) of the asbestos around the end fasteners nearest to the diaphragm corners.

Table 3.3 contains a summary of the results obtained in testing the eight cavity decking diaphragms. A detailed discussion of each test follows:

3.6.2.1 Test C-1:

A view of the testing arrangement of diaphragm C-1 is shown in Fig. 3.15. The fastener pattern of this diaphragm was similar to that in current use (as recommended by Atlas Co.) and characterized by the use of only end and seam connections. It should be noted that the exterior units were not connected at their ends because the length of the top steel plates welded to the flanges of members AD and BC did not permit these connections. Thus, the exterior units were only connected to interior units at the seams.

The ultimate load of the deck was reached after four end fasteners at the locations shown in Fig. 3.16 failed at different but close load levels by crushing of the asbestos around the fasteners. Although by the time the first three fasteners had failed, the diaphragm was still capable of sustaining additional load.

When the deck was dismantled, the shanks of the bottom seam bolts of the 4th and 5th seams were noticably bent to different degrees, more at the ends than at the middle (Fig. 3.17). Bolts of the 3rd and 6th seams were also bent, but to a lesser degree. Other seams did not show any noticable damage or large hole elongations like the above seams. The complete load-deformation curve, with the total jacking force in Kips as the ordinate and the corrected deformation in inches as the abcissa, is given in Fig. 3.18.

The results of this first test revealed a moderate capability of asbestos-cement sheeting to function as a shear diaphragm, where the values obtained for both stiffness and strength are of a comparable order to previously tested screw connected light-gauge steel diaphragms reported in the literature, [37,62].

3.6.2.2 Test C-2:

Diaphragm C-2 was idential to C-1, except that it was connected to the other side members (AB and DC) with 5 side fasteners per side. The test set-up for this diaphragm is shown in Fig. 3.19. Failure of the diaphragm was due to tearing of asbestos around the two end fasteners, Fig. 3.20. At failure, separation of the two overlapping units at the centre of panels width and along their top seam took place (Fig. 3.20). This demonstrates that these top seam connections do contribute to the capacity of the diaphragm.

In general, the deformations at the diaphragm corners as well as the net shear deflection were much smaller compared to those of Test C-1 at comparable load levels. This deck showed an increase in stiffness of 74% and in strength of 31% over those for C-1 as a result of the use of side connections. Load-deformation curve for the diaphragm C-2 is given in Fig. 3.21.

3.6.2.3 Test C-3:

In testing this diaphragm, the deck units were laid in a direction perpendicular to the load direction as shown in Fig. 3.22. This allowed all the deck units to be connected to the end members (members AB and DC in this case). The diaphragm was subjected to two cycles of loading and unloading to a load level of about 35% of the failure load. The purpose of these cycles of loading was to determine the effects of possible screw loosening, hole elongation, and other general deterioration of the decking material. Results of this test show that the deck became stiffer in the second cycle of loading and there was no noticable damage of the diaphragm. However, this cannot be generalized to the case of more load cycles or higher load level. The deck was subsequently loaded to failure.

Failure occured when the asbestos cracked at the first end fastener at corner D (Fig. 3.23a). The ultimate load was much higher than those reached in tests C-1 and C-2. In fact, when close to failure, the welds at corner B between the test frame and the base frame failed, and the reaction-transmitting beam (W21X55) twisted noticably as shown in Fig. 3.22b. For later tests, these members were stiffened by steel stiffeners welded to the webs and flanges. And, in addition, the bottom flanges of these two reaction-transmitting beams at corners A and B were welded together.

Load-deformation curves for deck C-3 are given in Figures 3.24 and 3.25. The cumulative effect of the two cycles of loading produced a permanent set of 0.12" in the shear deflection. It is evident that by increasing the number of side and seam fasteners, a considerable increase in both the strength and stiffness of the deck results.

3.6.2.4 Test C-4:

Similar to diaphragm C-3, except that the number of side and seam connections was further increased, and the deck was loaded and unloaded in five cycles to 32% of Q_{ult}, then was loaded from zero to failure. Again, there was no noticable damage of the diaphragm after five complete cycles. Failure of the deck was brought about as before by tearing of the asbestos around end fasteners at the locations shown in Fig. 3.26. Cyclic loading resulted in excessive deformations of most of the end fasteners bearing against the asbestos which was slightly crushed. Damage to the screws neoprene washers was also observed. The cumulative effect of the repeated loading resulted in a permanent set of 0.165" in the shear deflection. Load-deformation curves for diaphragm C-4 are presented in Figures 3.27 and 3.28.

3.6.2.5 Test C-5:

The fasteners pattern of this diaphragm was identical to that of Test C-4. However, load was increased gradually from zero to failure in order to compare the results with those from cyclic loading of Test C-4. Contrary to what was expected, this diaphragm failed at load slightly lower (32 kN) than the one reached in C-4 (34 kN). Also, the stiffness was 7% lower than that of C-4. The cause for higher stiffness and strength in test C-4 may be attribtured to the gradual elongation of holes around the screws under repeated loading which tend to produce uniform load distribution to the screws. Even though these differences fall within the range of test scatter, this is considered unlikely because similar tests on light-gauge steel diaphragms have resulted in similar comparisons [28].

In every other aspect, the behaviour of the deck is similar to that of C-4, for example, the sequence of end fastener failures (Fig. 3.29). Load-deformation curve for C-5 is given in Fig. 3.30.

3.6.2.6 Test C-6:

This diaphragm was constructed using only the bottom flat wings of the profile as shown in Fig. 3.31, and the fasteners distribution was identical to that of C-4 or C-5 (end, side and bottom seam fasteners only). The aim of this test was to evaluate the contribution of the bottom flat part of the profile directly connected to the perimeter members 2nd of its seam fasteners. As anticipated, this deck failed at a low load of 19.15 kN (58% of the average Q_{ult} for C-4 and C-5). The failure was along the seam lines. The failur load was very close to the recorded levels of loading corresponding to bottom seam failures (50-60% of Q_{ult}) of the previous tests.

Due to the absence of the corrugated part and of the top flat surface with its much stiffer seams, this deck also showed a reduction in stiffness (44% of the average G' of C-4 and C-5). Considerable amount of relative displacement of adjacent units was noted as shown in Fig. 3.32, which also shows sample of the seam fasteners failure. Load-deformation curve for C-6 is given in Fig. 3.33.

3.6.2.7 Test C-7:

This diaphragm was similar to C-3 except that two end fasteners per unit end were used. Test results showed that doubling the number of end fasteners did not result in any substantial gains in either the stiffness or the strength. Typical failures at the end fasteners are shown in Fig. 3.34. Separation of the units along their top seams can also be seen in this figure. The load-deformation curve for C-7 is given in Fig. 3.35.

3.6.2.8 Test C-8:

Diaphragm C-8 was identical to the diaphragm C-2 except for an intermediate purlin as previously mentioned. By comparing the results of the two tests in Table 3.3, it is seen that the presence of the purlin only increased [illegible]y the diaphragm stiffness and strength. The sequence of failure of these two diaphragms was identical, even in the separation of two units along the top seam line: starting closest to the applied load and propagating in the direction of load as shown in Fig. 3.36. Load-deformation curve for C-8 is given in Fig. 3.37.

3.6.3 "T" Deck Diaphragms:

Table 3.4 summarizes the results obtained for the five "T" deck diaphragms tested. The type of seam fasteners used in these diaphragms provided much stiffer connections than those used in the bottom seams of cavity decking; thus considerable increase in the overall stiffness of the diaphragms can be expected. This increase was also due to the fewer seam lines (5 in case of "T" deck versus 8 in case of cavity decking) through which the shear force must be transfered. On the other hand, "T" deck diaphragms were less strong due to the open profile.

Failure of all "T" deck diaphragms was observed to initiate at the corner end fasteners.. It was also observed that at high load levels, near failure, material cracking occured around the screws of interior seams and that all fasteners along these seams exhibited the same level of bearing failure. It must be emphasized that failure of the seam fasteners does not necessarily mean that the ultimate load has been reached. However, it was observed in tests that the additional increase in load after an initial failure of this type usually did not exceed 20 to 30%. A detailed discussion of the tests is presented in the following:

3.6.3.1 Test T-1:

A view of the test set-up is shown in Fig. 3.38. The fasteners pattern of this diaphragm was similar to that in current use (as recommended by Atlas Co.), and like test C-1, characterized by the use of only the end and seam connections. Failure of the diaphragm was due to cracking of asbestos at the end fasteners nearest to the corners as shown in Fig. 3.39. Failure also occured at the interior 2nd and 3rd top seam fasteners which separated from their secure positions and pulled down through the material as shown in Fig. 3.39. The load-deflection curve for Test T-1 is given in Fig. 3.40. This test shows that the deck as being used today possess significant strength and stiffness.

3.6.3.2 Test T-2:

Diaphragm T-2 was identical to T-1, except that it was connected to the other two side members (AB and DC) utilizing three shear connectors per side (Fig. 3.41). Hairline cracks at the end fasteners were noticed shortly prior to failure, and the complete failure of the deck was brought about by simultaneous failure of the screws connecting the deck to the shear connectors. Shearing of these fasteners was sudden and with little warning. Simultaneous with this failure, the hairline cracks at the end fasteners opened as shown in Fig. 3.42.

By comparing the load-deflection curves for Tests T-1 (Fig. 3.40) and T-2 (Fig. 3.43), it can be seen that the use of side connections increased the stiffness considerably (178%) and the strength only moderately (35%).

3.6.3.3 Test T-3:

For this deck assembly, the number of bottom seam connections was increased from 3 to 5, and those of the top seam from 5 to 7. In addition, four side shear connectors were also introduced. As shown in Fig. 3.44, the deck units of this diaphragm were laid in a direction perpendicular to the load direction. The deck failed at a load higher than that of T-2 because of the increased number of seam and side fasteners. However, the diaphragm stiffness, as calculated from the load-deformation curve (Fig. 3.45), is 15%

less than that obtained for test T-2. This, although unexpected, may be due to lesser degree of tightness of the shear connectors' self-tapping screws.

3.6.3.4 Tests T-4A and T-4:

Diaphragm T-4A was identical to that of test T-3, except that the number of shear connectors was increased from 4 to 5 per side. Again, the deck failed in a similar manner as in T-2 and T-3. The failure load was 5.5% lower than that reached in T-3, while the stiffness was 10% higher, but was still lower than that for T-2.

The failure mode by shearing of the shear connectors' fasteners could be attributed to the fact that these fasteners were overtorqued in undersized drilled holes. Thus, it was decided to replace the five shear connectors in another test (T-4) by direct connections at the troughs of the corrugations to the steel members AD and BC.

Failure of diaphragm T-4 was observed to initiate at the corner end fasteners, and with increasing load, a sudden splitting of the material occurred at all the end fasteners along member CD (in line with load application). This resulted in the most complex overall failure mode observed (Fig. 3.46), which is believed to be due to a build-up of profile distortion which could not be resisted by such a brittle material as asbestos-cement, thus leading to the cracks shown. The severe profile distortion of this deck could be attributed to the fact that the end and side connections were located in a plane 4" lower than the plane of shear in the continuous sheeting. This diaphragm sustained the highest shear load of all tests. Load-deformation curves for the two tests are given in Figures 3.47 and 3.48, respectively.

3.7 CONCLUSIONS

One of the main objectives of this chapter was to investigate if the two asbestos-cement decking systems can function as shear diaphragms in building construction. The test results obtained indicate that the two decks, as currently constructed (Tests C-1 and T-1), possess a moderate amount of shear strength and a low shear stiffness. However, when the decks were connected at all four edges of the steel frame (Tests C-2 and T-2) the diaphragm stiffness increased considerably (74% and 178% respectively) and its strength only moderately (31% and 35%, respectively). Also, it has been shown that by increasing the number of seam and side fasteners, both the stiffness and strength increase substantially.

In general, the two decking systems are very flexible (especially for cavity decking) in comparison with light-gage steel diaphragms of the same size. Thus, if diaphragm design is based on deflection limitations, it would become difficult to eliminate the conventional bracing systems normally used. However, in such a situation, use of the deck's shear resistance may still effect some reduction in building costs. On the other hand, the two decking systems possess sufficiently high shear strength to meet the normal requirements of diaphragm design based on strength alone.

Tests of cavity decking have clearly shown that the fasteners connecting the underlapping edges of the sheets (i.e., bottom seams) are the main source of the diaphragm's high shear flexibility (see Fig. 3.32) as they are applied into slightly oversized holes. Thus, to enhance the deck's shear stiffness, alternate types of fasteners are required.

Overall collapse of all diaphragms was observed to be caused by localized bearing failure (tearing) of the material around the end fasteners nearest to the diaphragm corners. Failure of all diaphragms can be classified as brittle, as it took place without prior warning and was accompanied by a sudden drop in the load carrying capacity.

TABLE 3.1

CHARACTERISTICS OF CAVITY DECKING DIAPHRAGM TESTS+

Diaphragm	No. of Seam Fasteners		Spacing of Seam Fasteners (in)		No. of End Fasteners	No. of Side Fasteners	Space of Side Fasteners (in)	Load Orientation Relative to Panel Corrugations
	Top	Bottom	Top	Bottom				
C-1	5	5	4 28 28 28 28 4	@ 20	7	-	-	// (parallel)
C-2	5	5	4 28 28 28 28 4	@ 20	7	5	@ 20	//
C-3	7	7	3 19 19 19 19 19 19 3	@ 15	9	7	@ 15	⊥ (perpendicular)
C-4	8	9	4 16 16 16 16 16 16 16 4	@ 12	9	9	@ 12	⊥
C-5	8	9	4 16 16 16 16 16 16 16 4	@ 12	9	9	@ 12	⊥
C-6	-	9	-	@ 12	9	9	@ 12	⊥
C-7	7	7	3 19 19 19 19 19 19 3	@ 15	16	7	@ 15	//
C-8*	5	5	4 28 28 28 28 4	@ 12	7	5	@ 12	//

+ Frame size for all diaphragms in 10 ft x 10 ft.

* With one intermediate purlin. Sheet-to-purlin fasteners are the same in type and distribution as the end fasteners.

TABLE 3.2

CHARACTERISTICS OF "T" DECK DIAPHRAGM TESTS+

Diaphragm	No. of Seam Fasteners		Spacing of Seam Fasteners (in)		No. of End Fasteners	No. of Side Fasteners	Spacing of Side Fasteners (in)	Load Orientation Relative to Panel's Corrugations
	Top	Bottom	Top	Bottom				
T-1	5	3	4 28 28 28 28 4	@ 30	10	-	-	//
T-2	5	3	4 28 28 28 28 4	@ 30	10	3	@ 30	//
T-3	7	5	3 19 19 19 19 19 19 3	@ 20	12	4	@ 24	
T-4A	7	5	3 19 19 19 19 19 19 3	@ 20	12	5	@ 20	
T-4	7	5	3 19 19 19 19 19 19 3	@ 20	12	5	@ 20	

+ Frame size for all diaphragms is 10 ft x 10 ft.

TABLE 3.3

RESULTS OF CAVITY DECKING DIAPHRAGM TESTS

Diaphragm	Shear Stiffness	Shear Flexibility	Shear Strength	Max. Net Deflection
	G'(lb/in)	c (in/Kip)	S_u (lb/ft)	(in)
C-1	2400	0.417	360	2.50
C-2	4166	0.240	472	1.70
C-3	6135	0.163	680	2.08
C-4	7690	0.130	764	1.77
C-5	7140	0.140	720	2.20
C-6	3225	0.310	430	2.20
C-7	6250	0.160	675	1.80
C-8	5000	0.20	576	1.94

TABLE 3.4

RESULTS OF "T" DECK DIAPHRAGM TESTS

Diaphragm	Shear Stiffness G' (lb/in)	Shear Flexibility c (in/Kip)	Shear Strength S_u (lb/ft)	Max. Net Deflection (in)
T-1	5990	0.167	333	1.34
T-2	16666	0.06	450	0.66
T-3	14490	0.069	652	0.85
T-4A	15870	0.063	618	0.85
T-4	16660	0.06	814	1.0

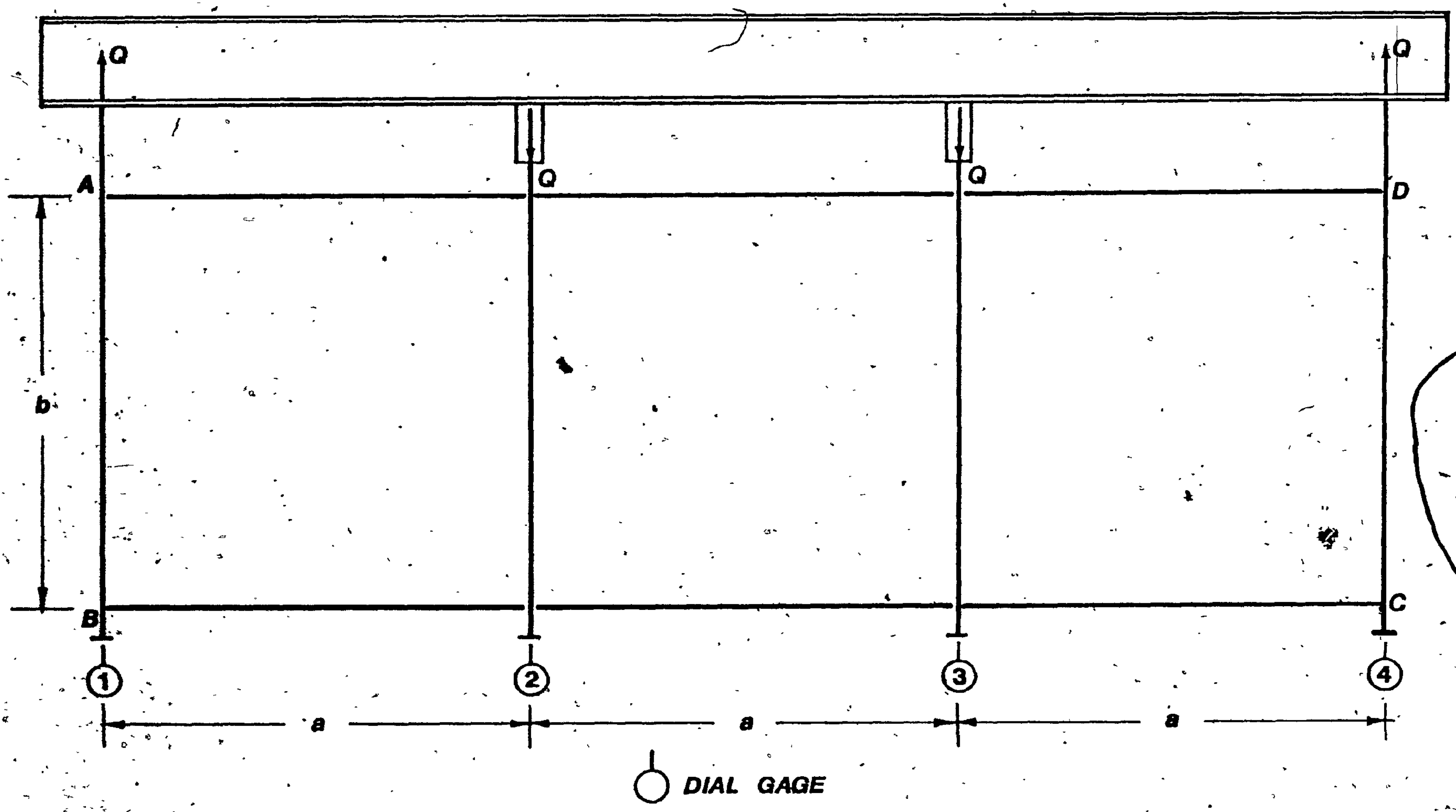

FIG. 3.1 SIMPLE BEAM TEST METHOD [REF. 21]

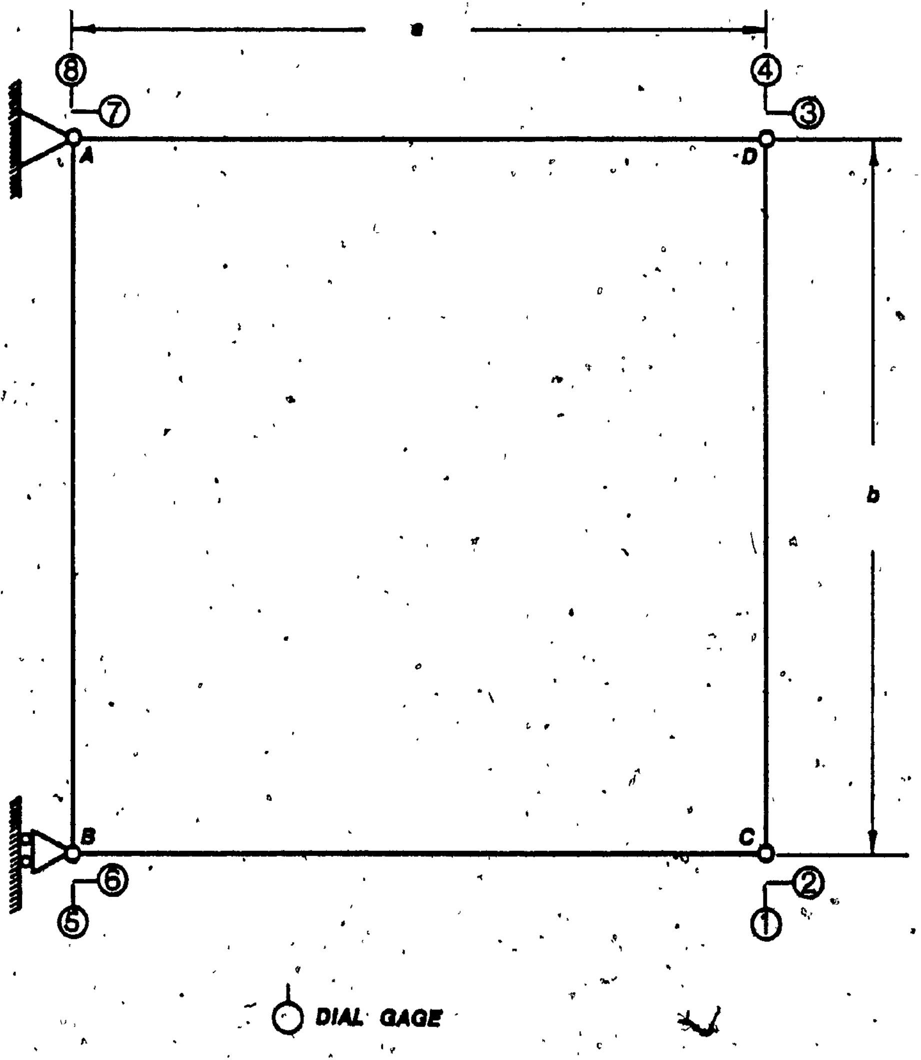

FIG. 3.2 CANTILEVER TEST FRAME METHOD

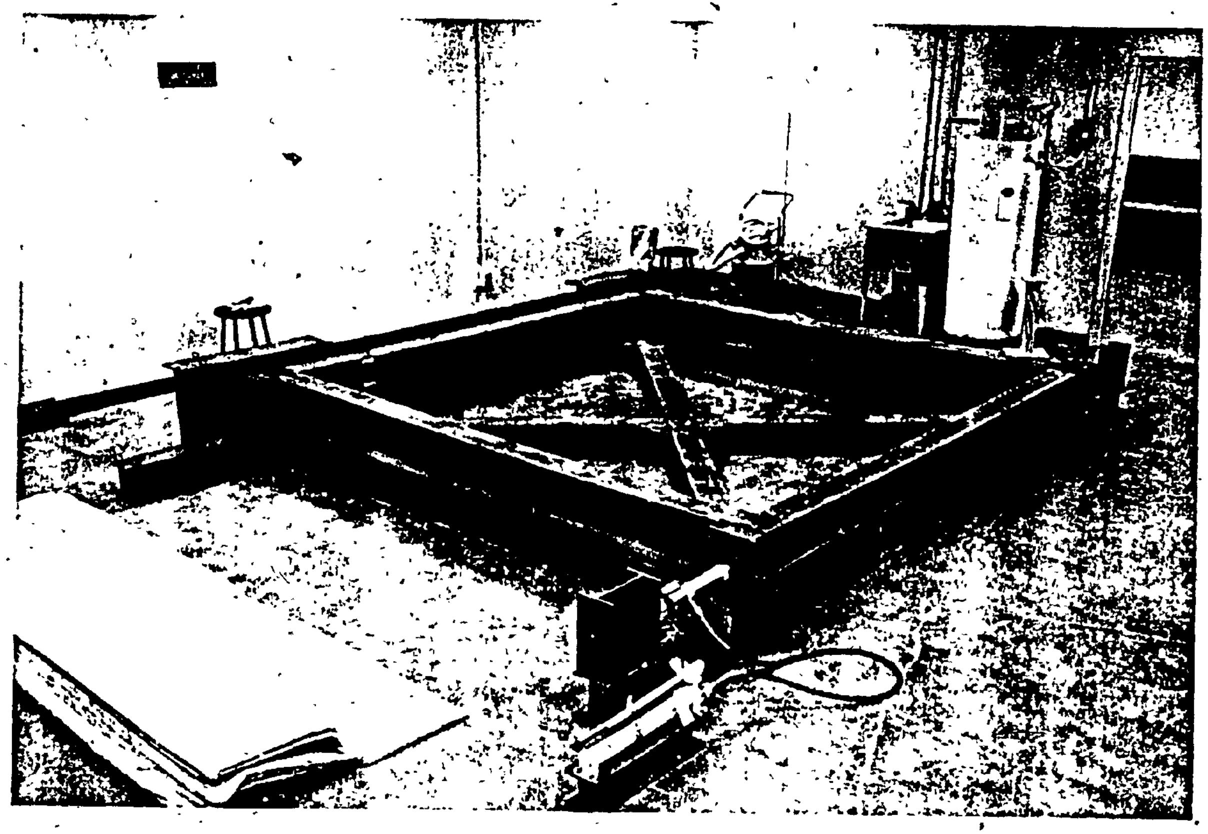

FIG. 3.3 TEST FRAME AND SUPPORTING BASE FRAME

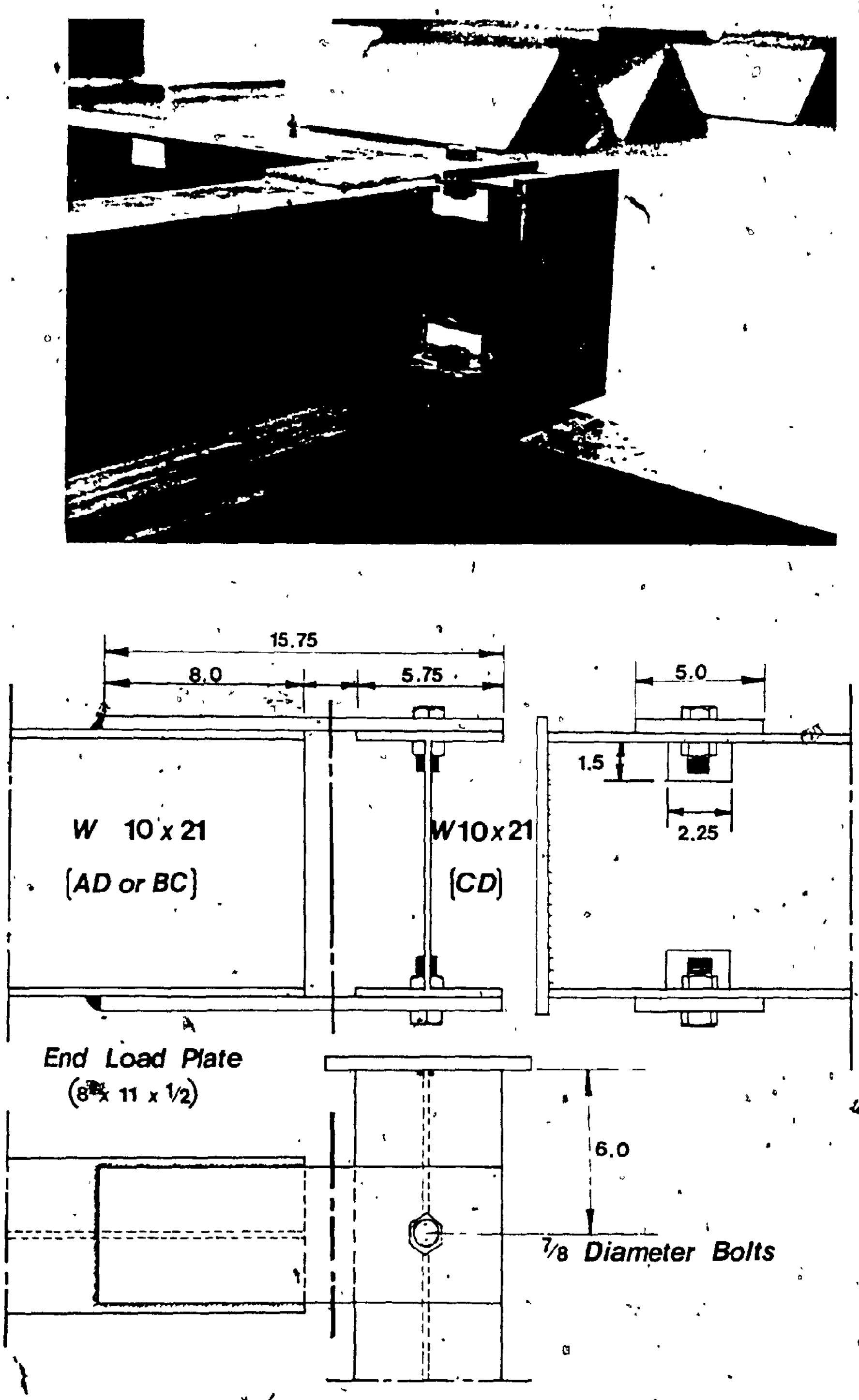

Detail at Corner C or D.

FIG 3.4 TEST FRAME CONSTRUCTION DETAIL AT CORNERS C AND D.

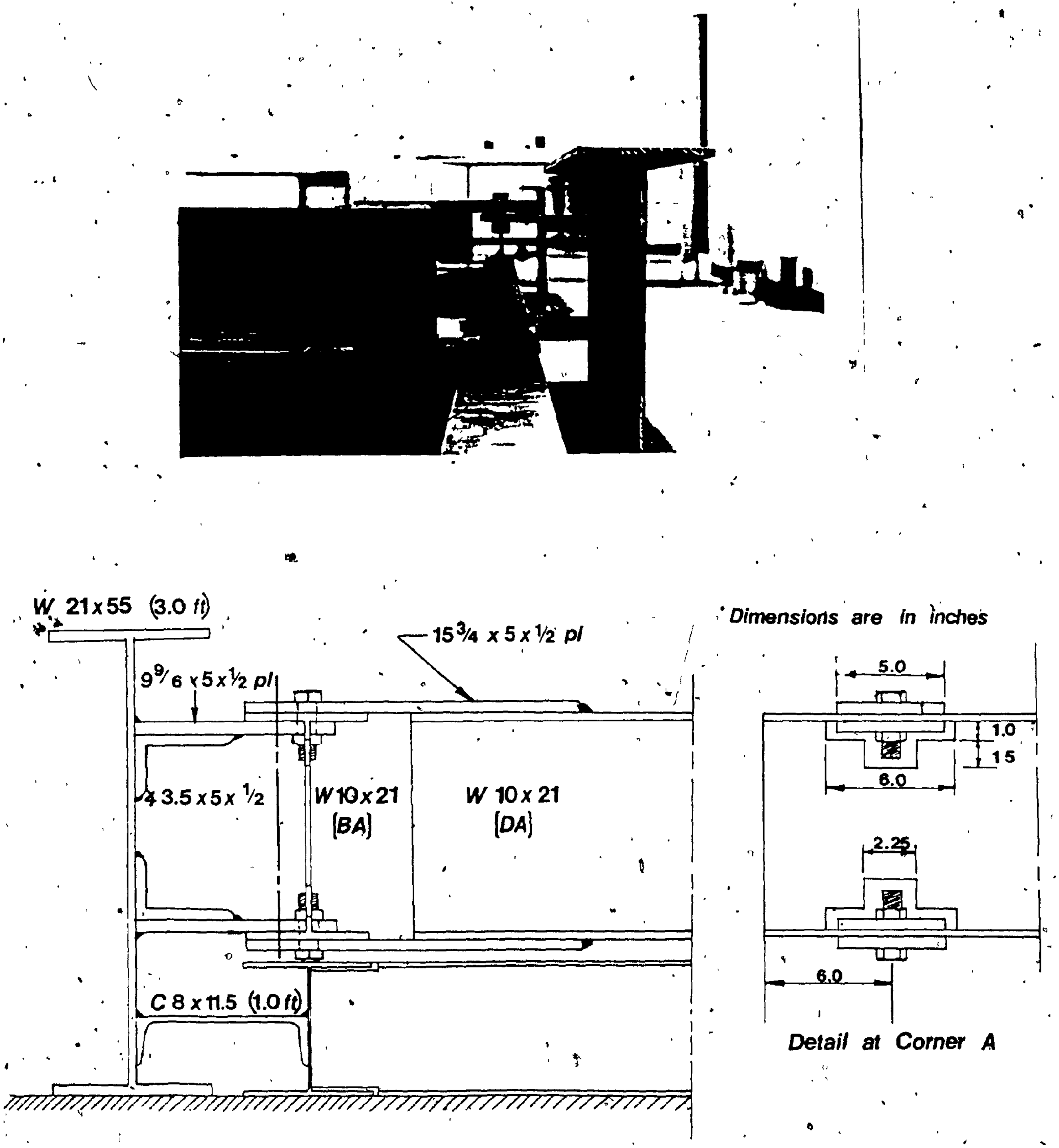

FIG. 3.5 TEST FRAME CONSTRUCTION DETAIL AT CORNER A [HINGED SUPPORT]

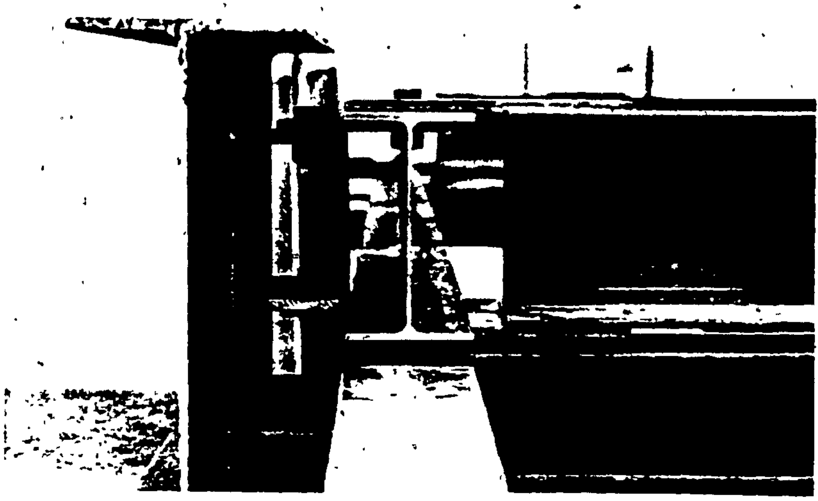

Dimensions are in inches

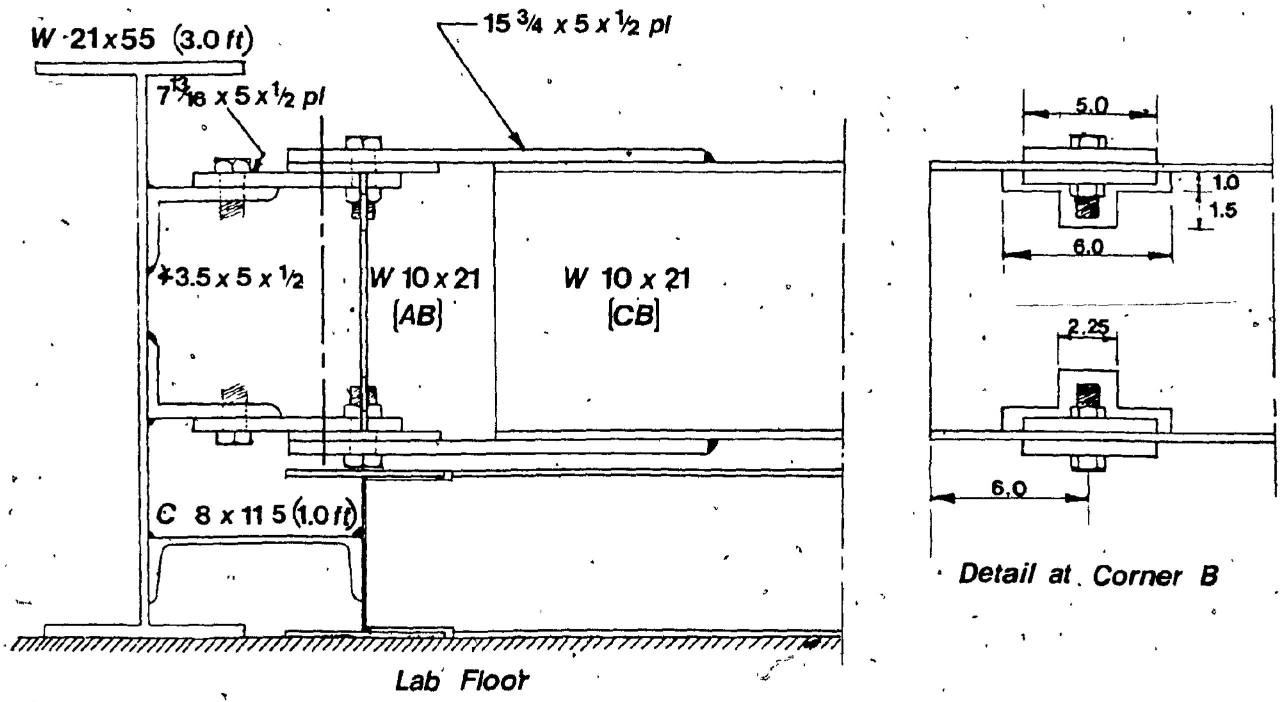

FIG. 3.6 TEST FRAME CONSTRUCTION DETAIL AT CORNER B [MOVABLE SUPPORT]

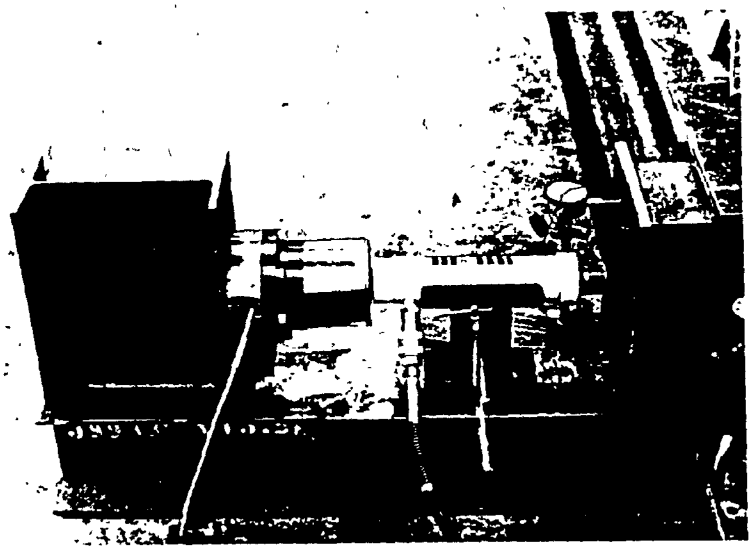

FIG. 3.7 LOAD SOURCE (HYDRAULIC JACK) AND INSTRON LOAD CELL.

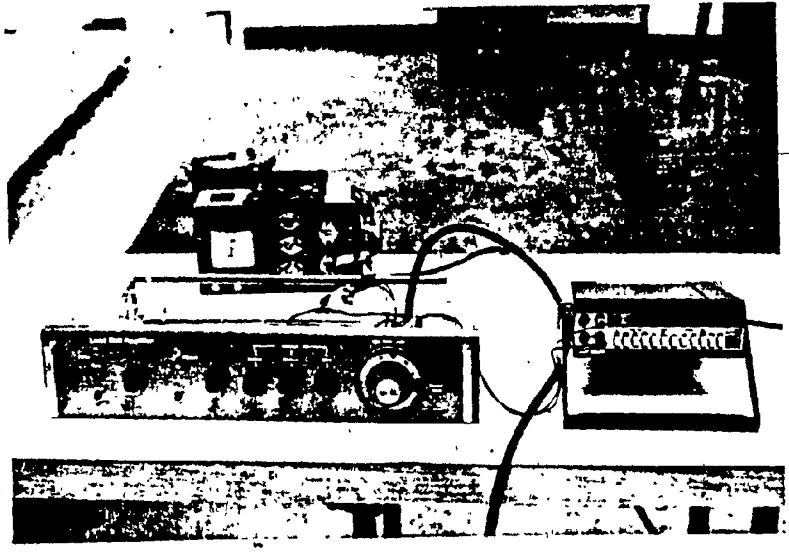

FIG. 3.8 INSTRON LOAD CELL AMPLIFIER UNIT AND DIGITAL VOLTMETER FOR LOAD MEASUREMENT

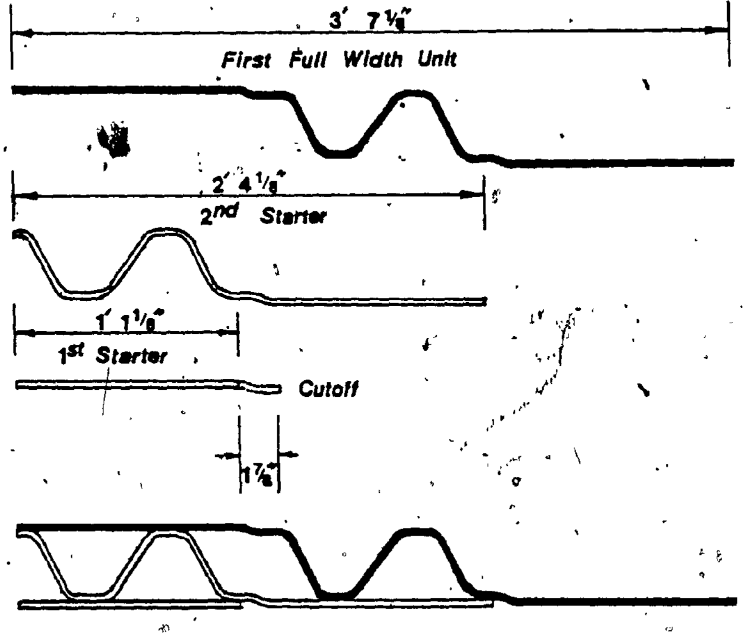

ASSEMBLY OF STARTERS

(a) Starting Units

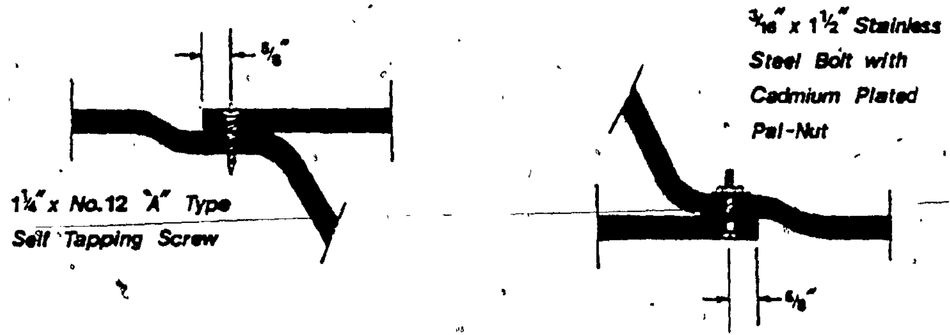

(c) Overlapping Edge Fixing

(b) Underlapping Edge Fixing

FIG. 3.9 CONSTRUCTION DETAILS - CAVITY DECKING

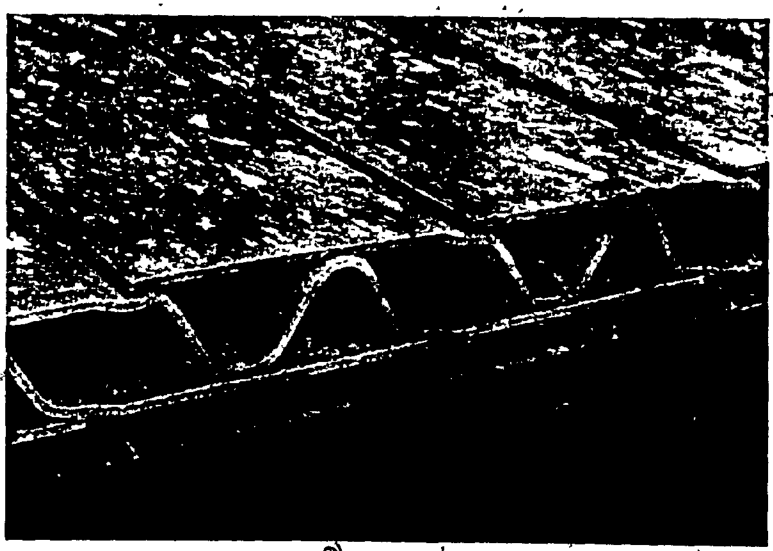

FIG. 3.10 END FASTENERS IN CAVITY DECKING DIAPHRAGM C-7

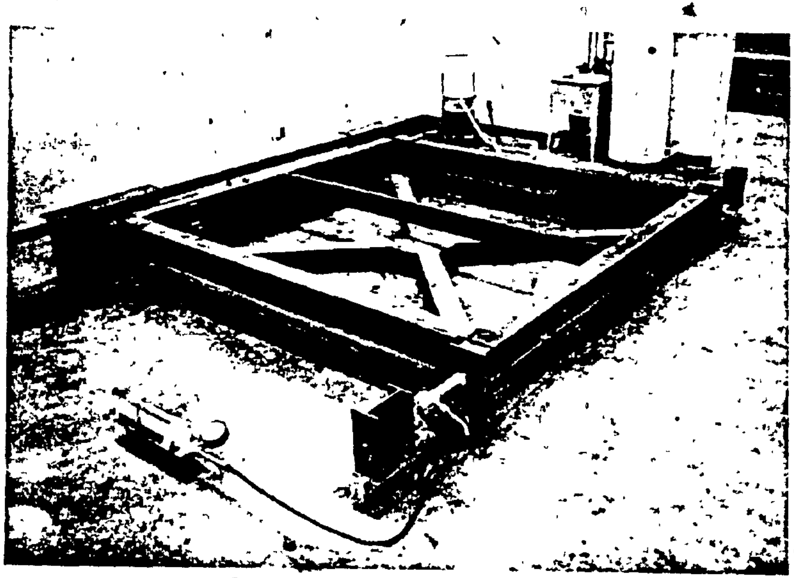

FIG. 3.11 INTERMEDIATE PURLIN IN CAVITY DECKING DIAPHRAGM C-8

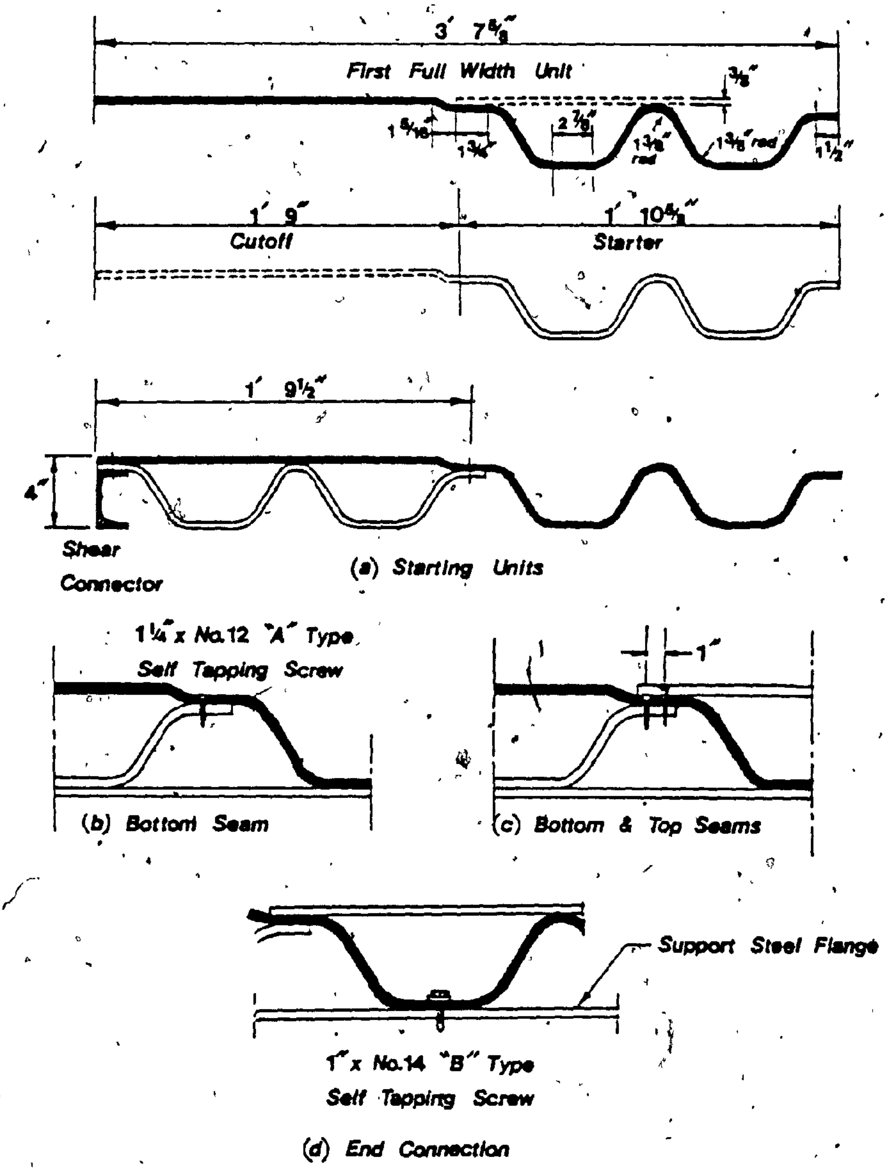

(a) Starting Units

(b) Bottom Seam

(c) Bottom & Top Seams

(d) End Connection

FIG. 3.12 CONSTRUCTION DETAILS - "T" DECK

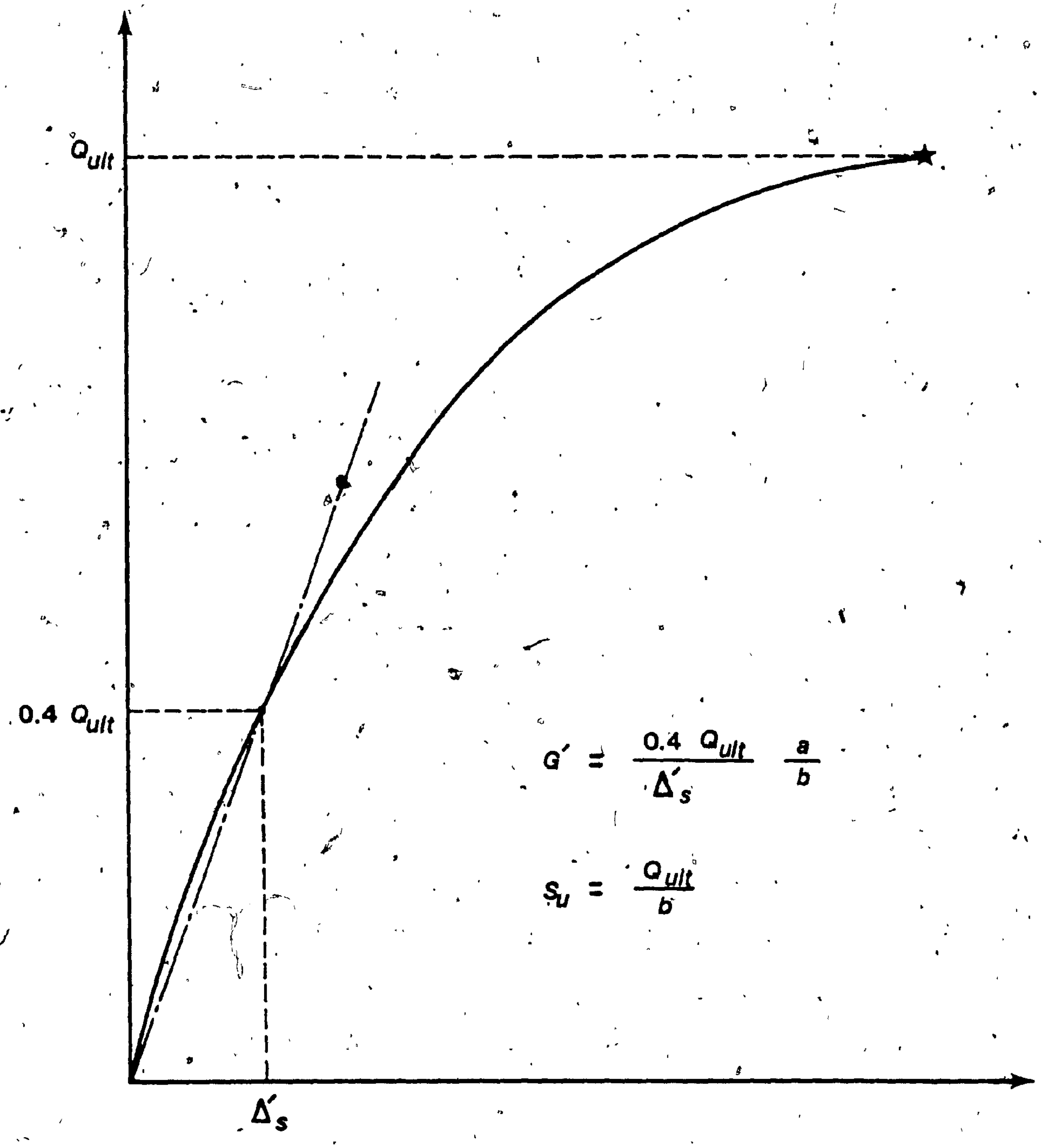

FIG. 3.13 EVALUATION OF SHEAR PARAMETERS

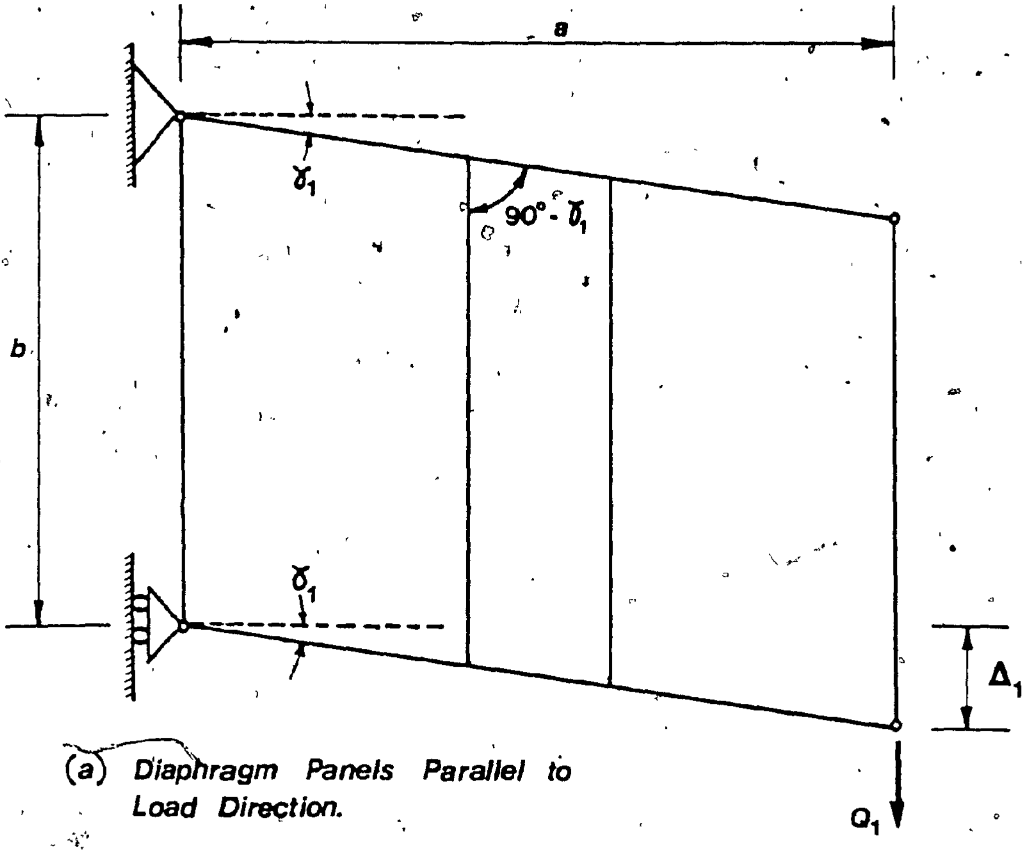

(a) *Diaphragm Panels Parallel to Load Direction.*

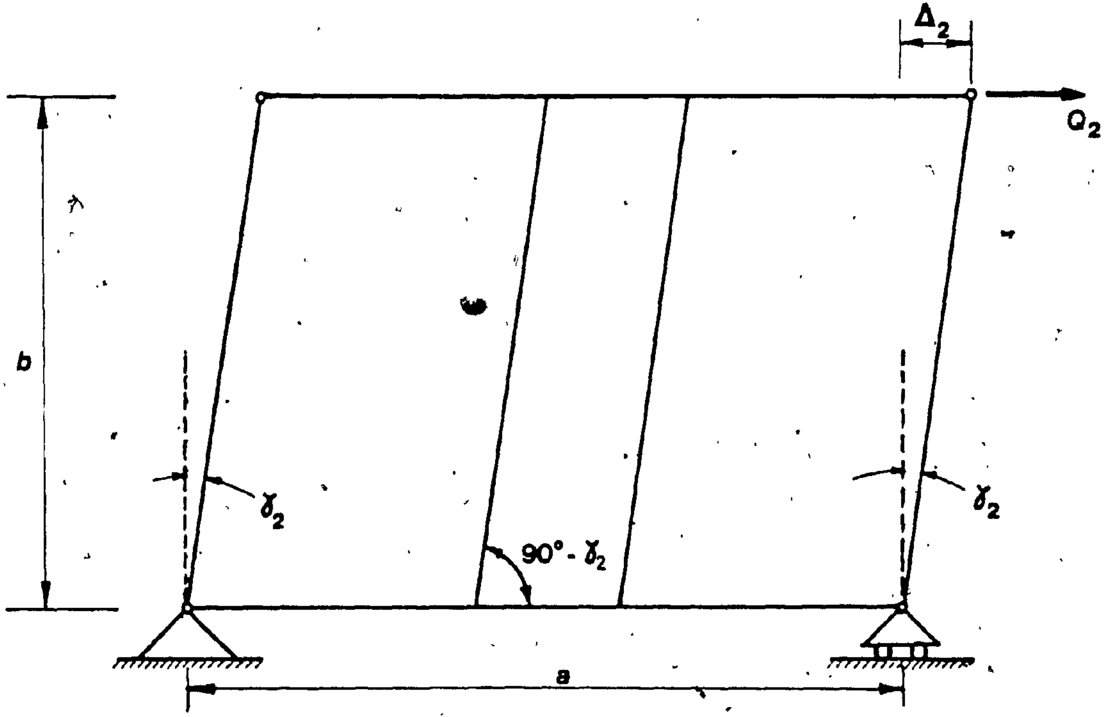

(b) *Diaphragm Panels Perpindicular to Load Direction.*

FIG. 3.14 INDEPENDENCE OF DIAPHRAGM SHEAR MODULUS G' OF LOAD DIRECTION

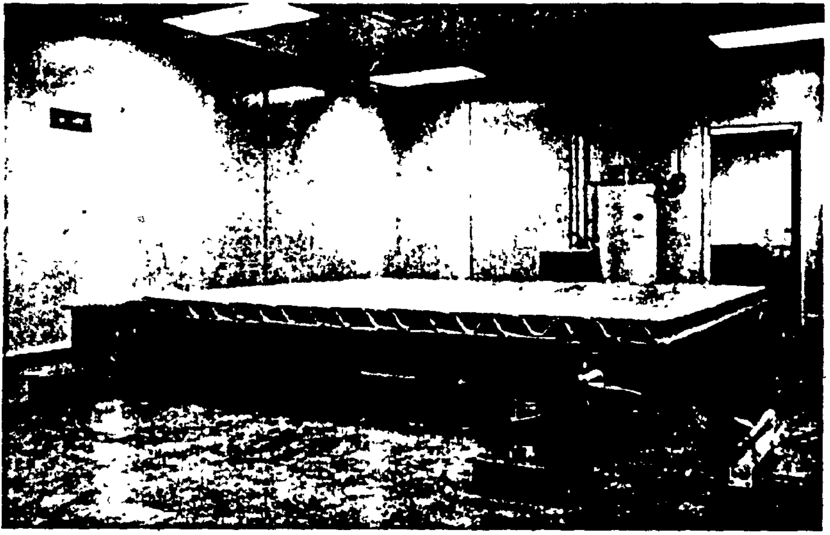

FIG. 3.15 VIEW OF TESTING SET-UP OF CAVITY DECKING DIAPHRAGM C-1

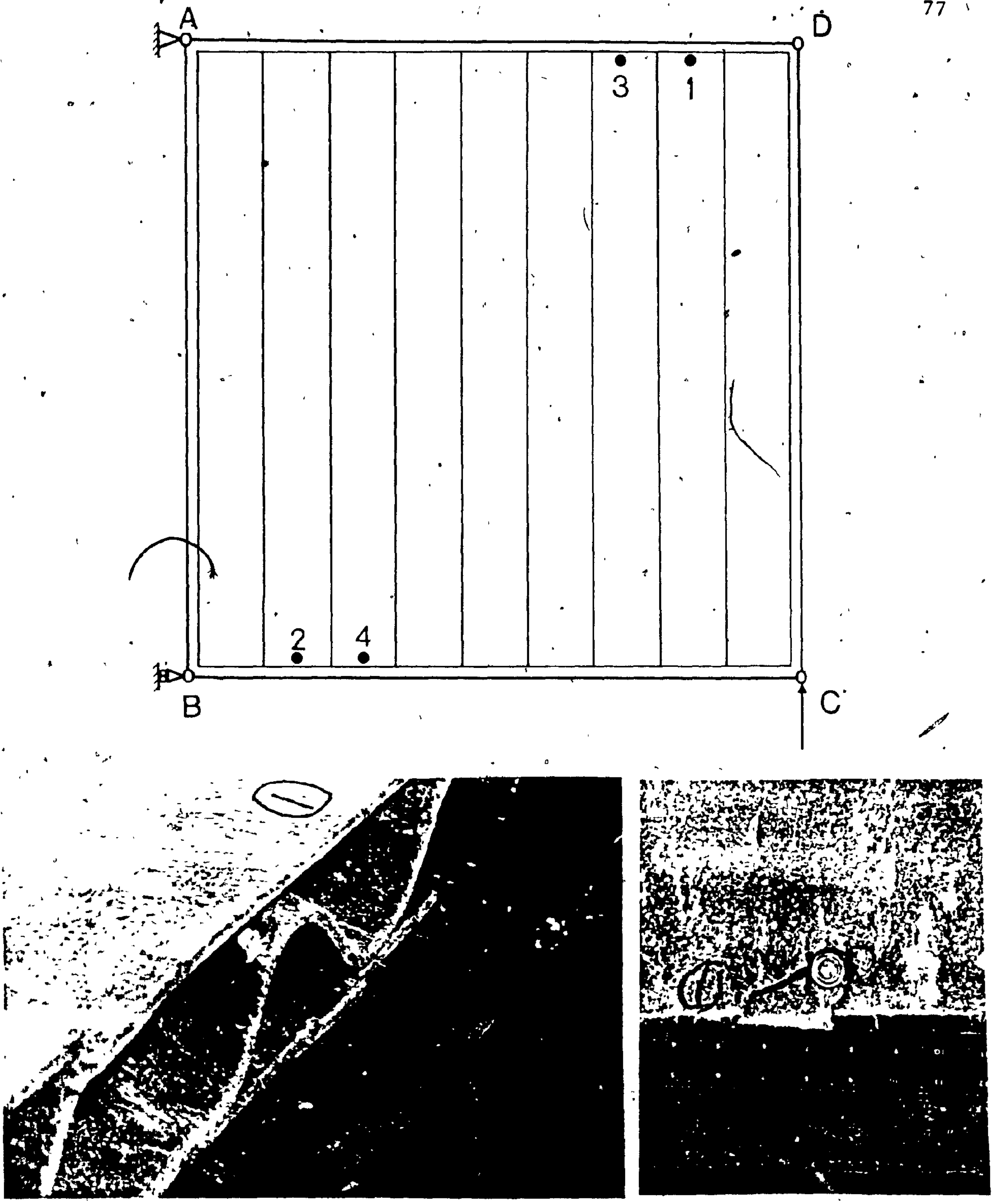

FIG. 3.16 FAILURES AT THE END FASTENERS OF DIAPHRAGM C-1

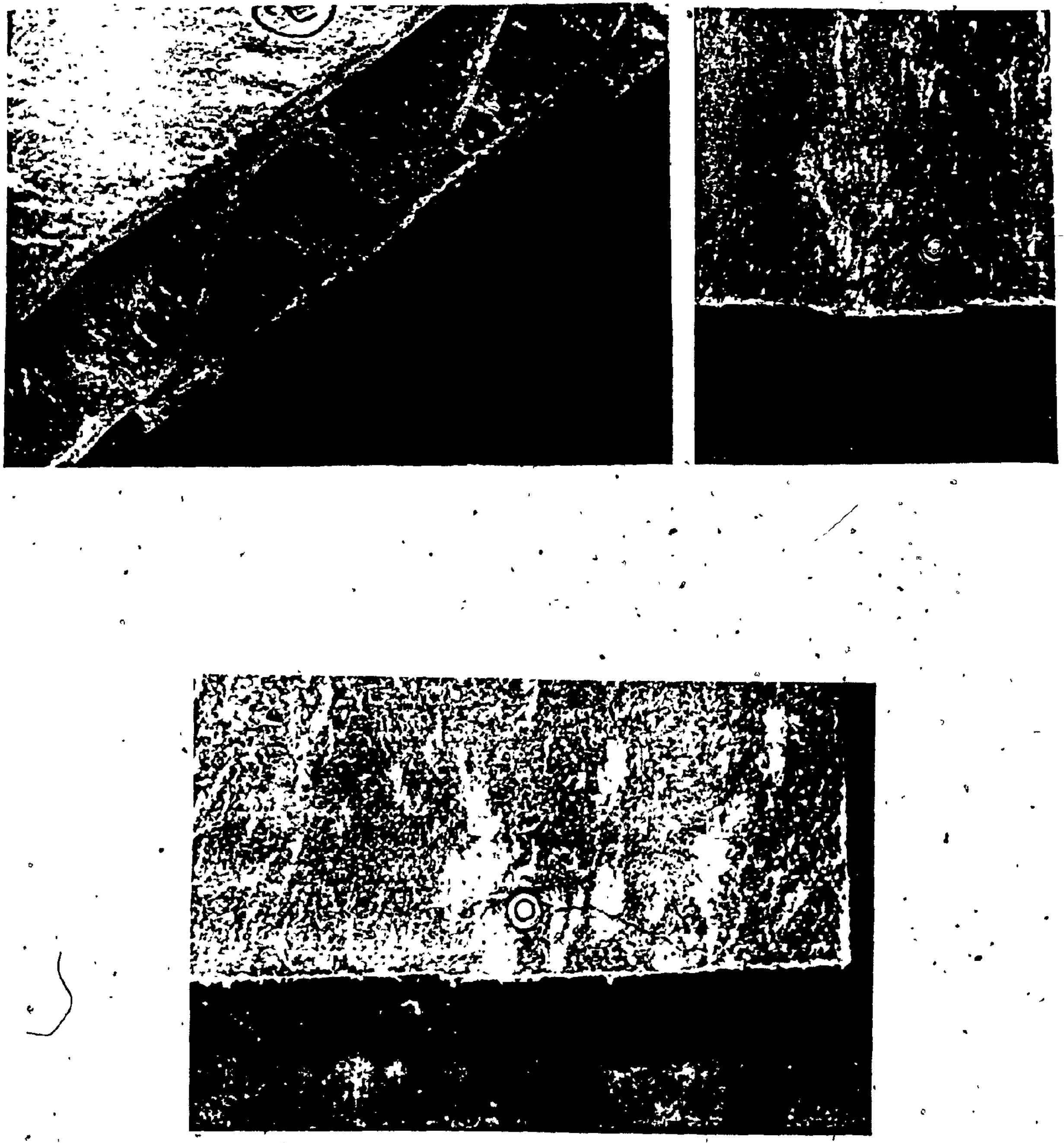

FIG. 3.16 (Cont'd) FAILURES AT THE END FASTENERS OF DIAPHRAGM C-1

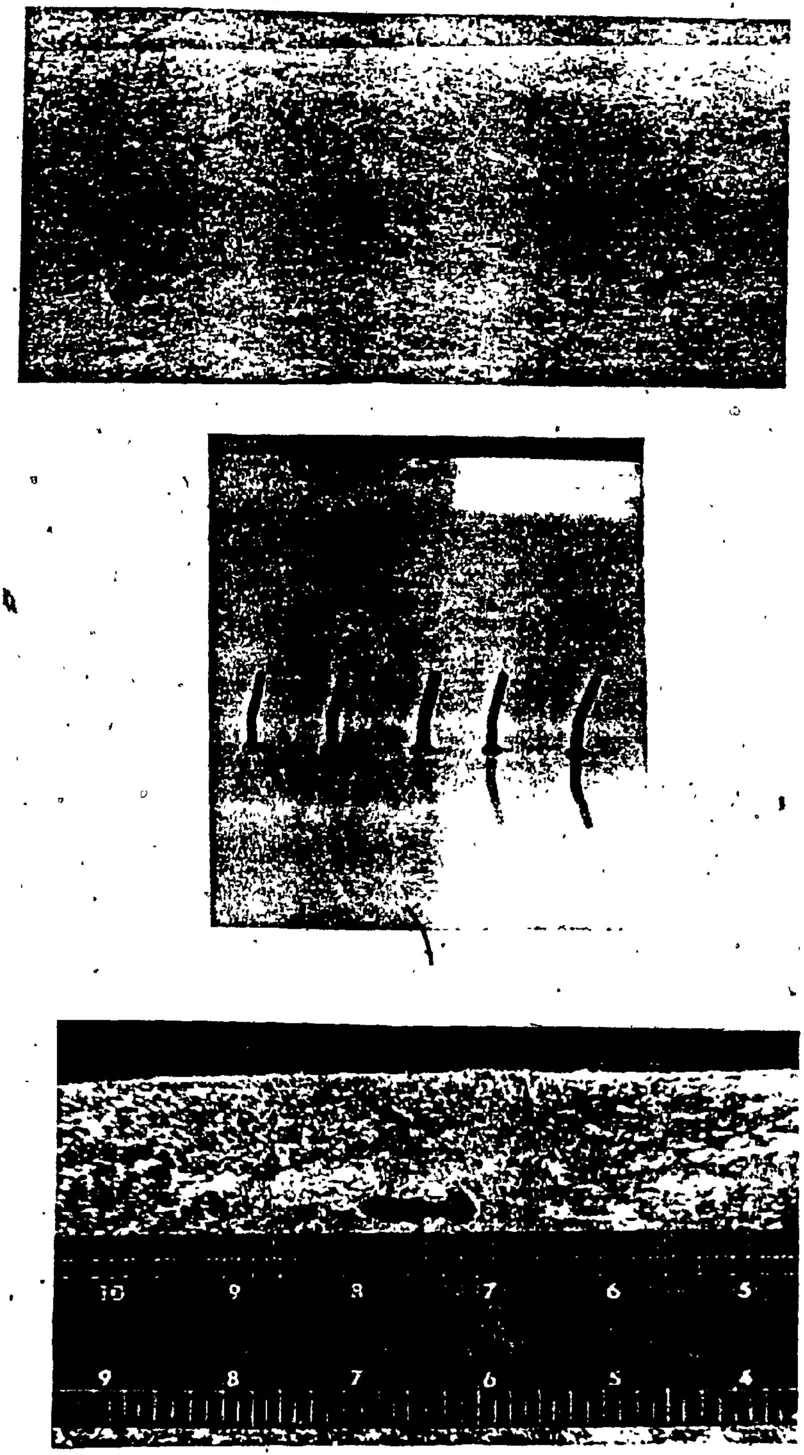

FIG. 3.17 DEFORMATION OF SEAM FASTENERS

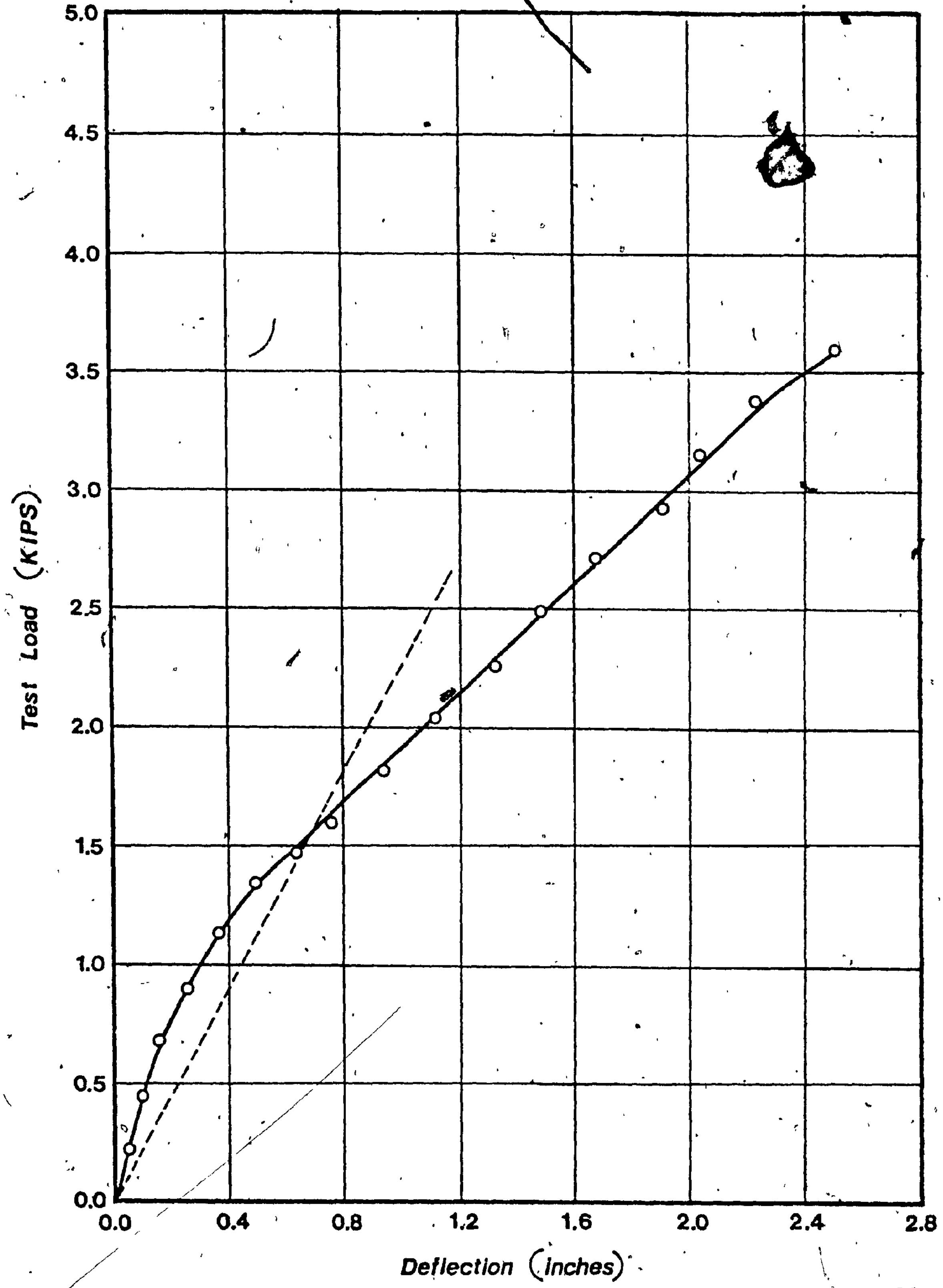

FIG. 3.18 LOAD-DEFLECTION CURVE FOR CAVITY DECKING DIAPHRAGM C-1

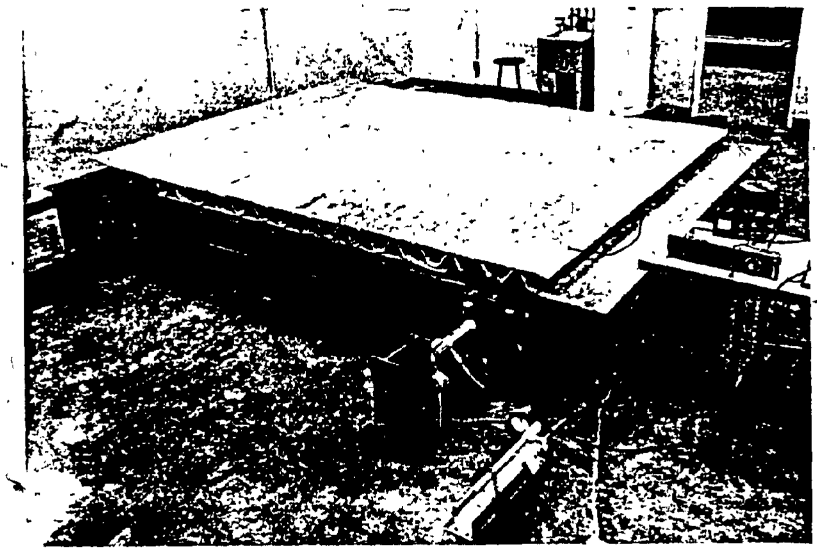

FIG. 3.19 VIEW OF TESTING SET-UP OF CAVITY DECKING DIAPHRAGM C-2

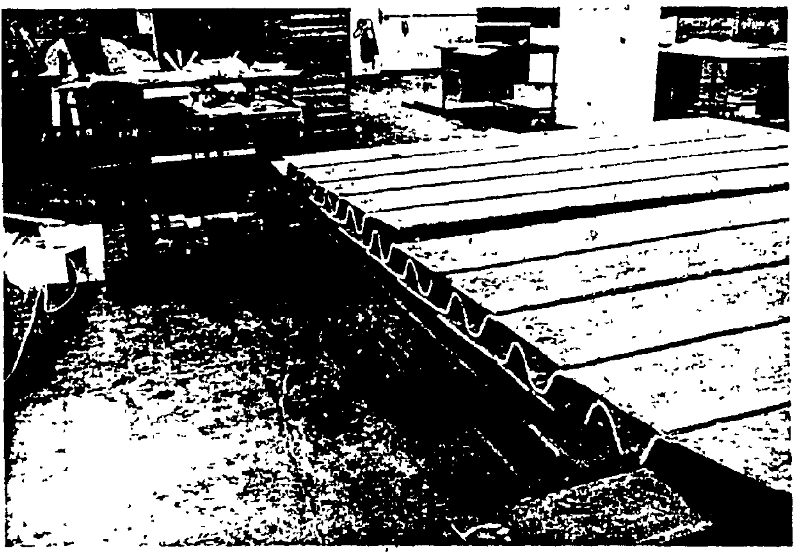

FIG. 3.20 SEPARATION OF UNITS AT TOP SEAM OF DIAPHRAGM C-2

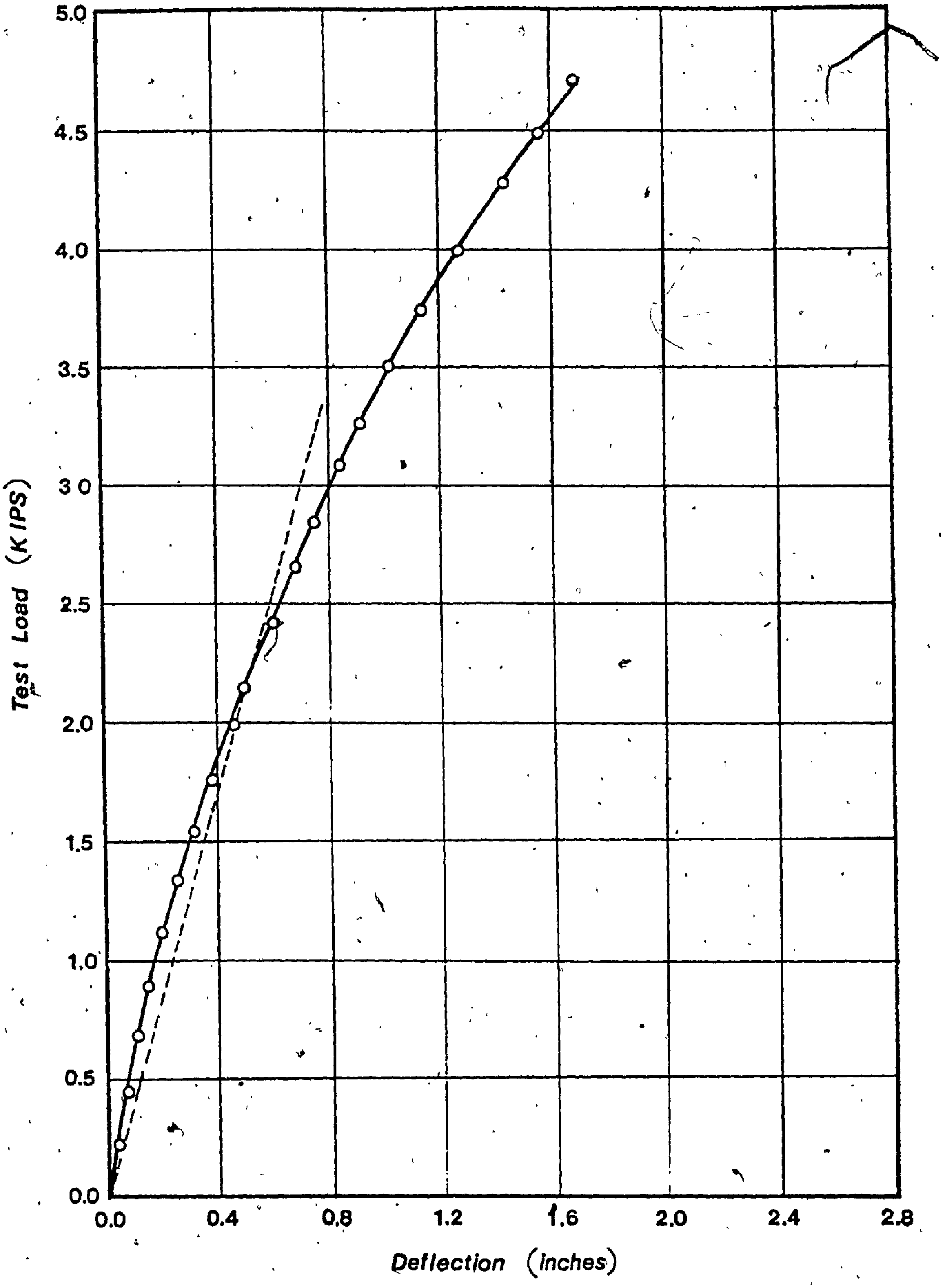

FIG. 3.21 LOAD-DEFLECTION CURVE FOR CAVITY DECKING DIAPHRAGM C-2

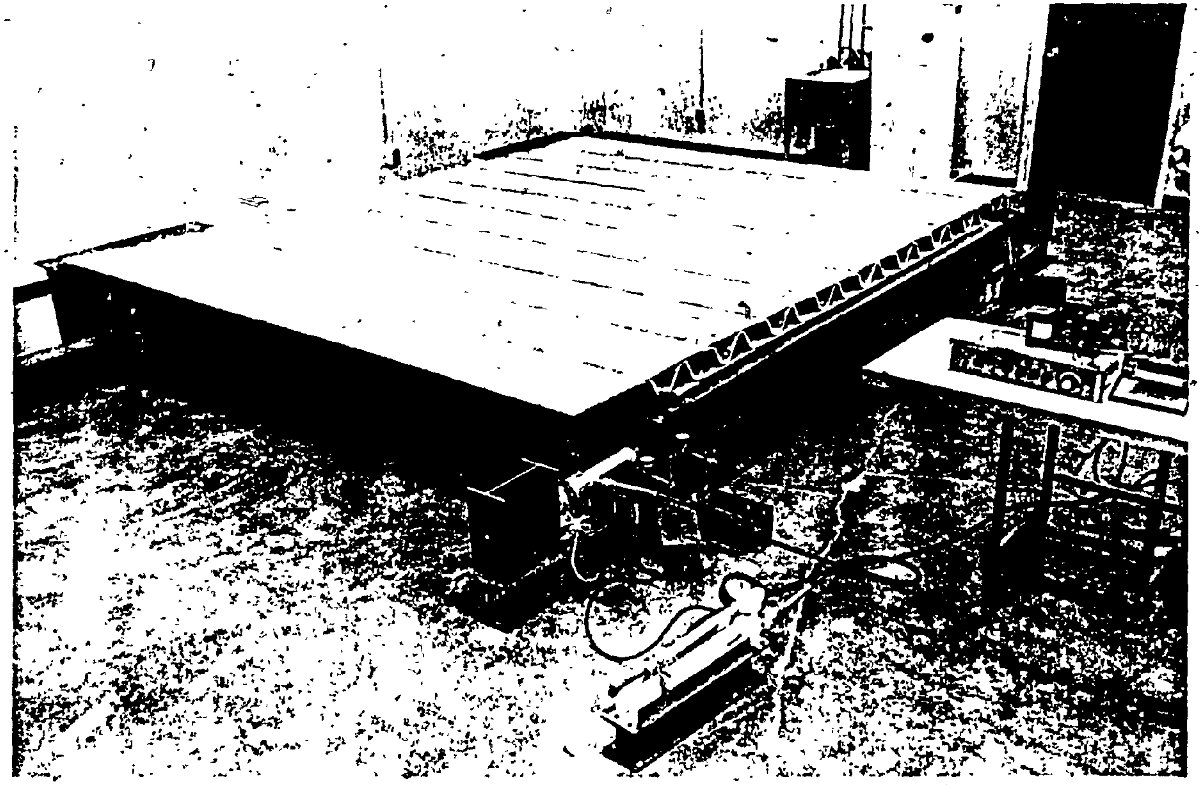

FIG. 3.22 VIEW OF TESTING SET-UP OF CAVITY DECKING DIAPHRAGM C-3.

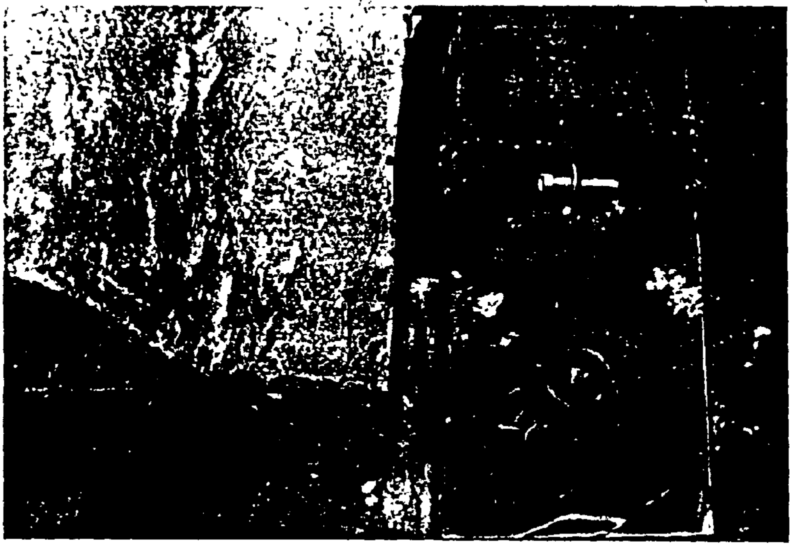

A) FAILURE AT END FASTENER

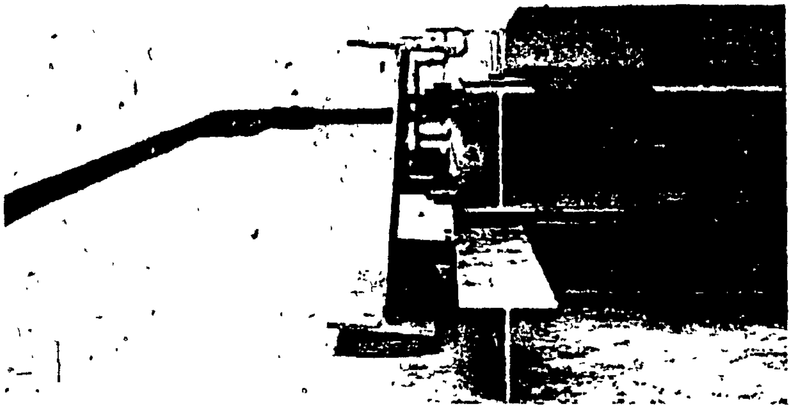

B) TWIST OF REACTION-TRANSMITTING BEAM

FIG. 3.23 AT ULTIMATE LOAD OF DIAPHRAGM C-3

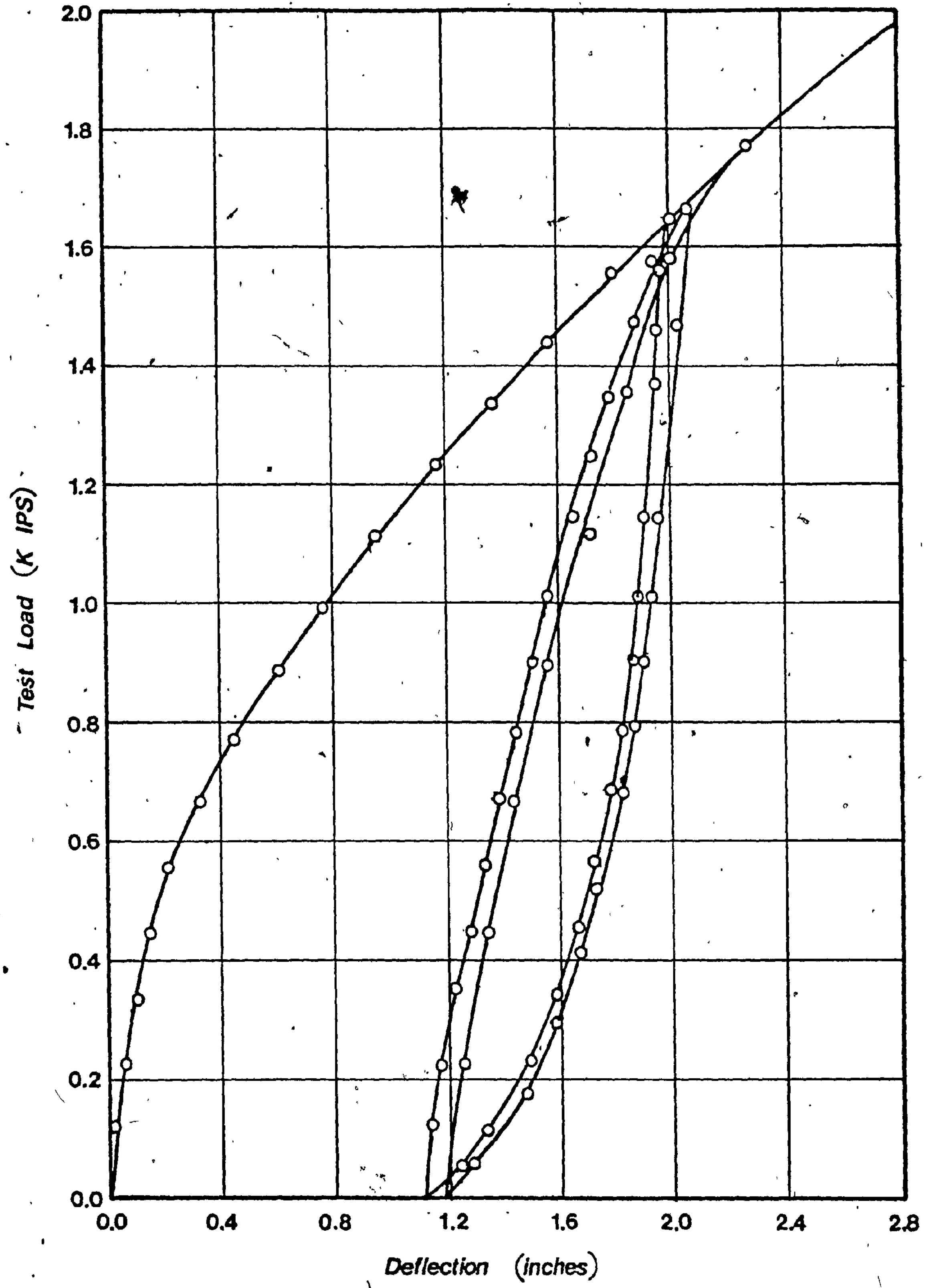

FIG. 3.24 LOAD-DEFLECTION CURVE FOR CAVITY DECKING DIAPHRAGM C-3 - TWO CYCLES OF LOADING-UNLOADING

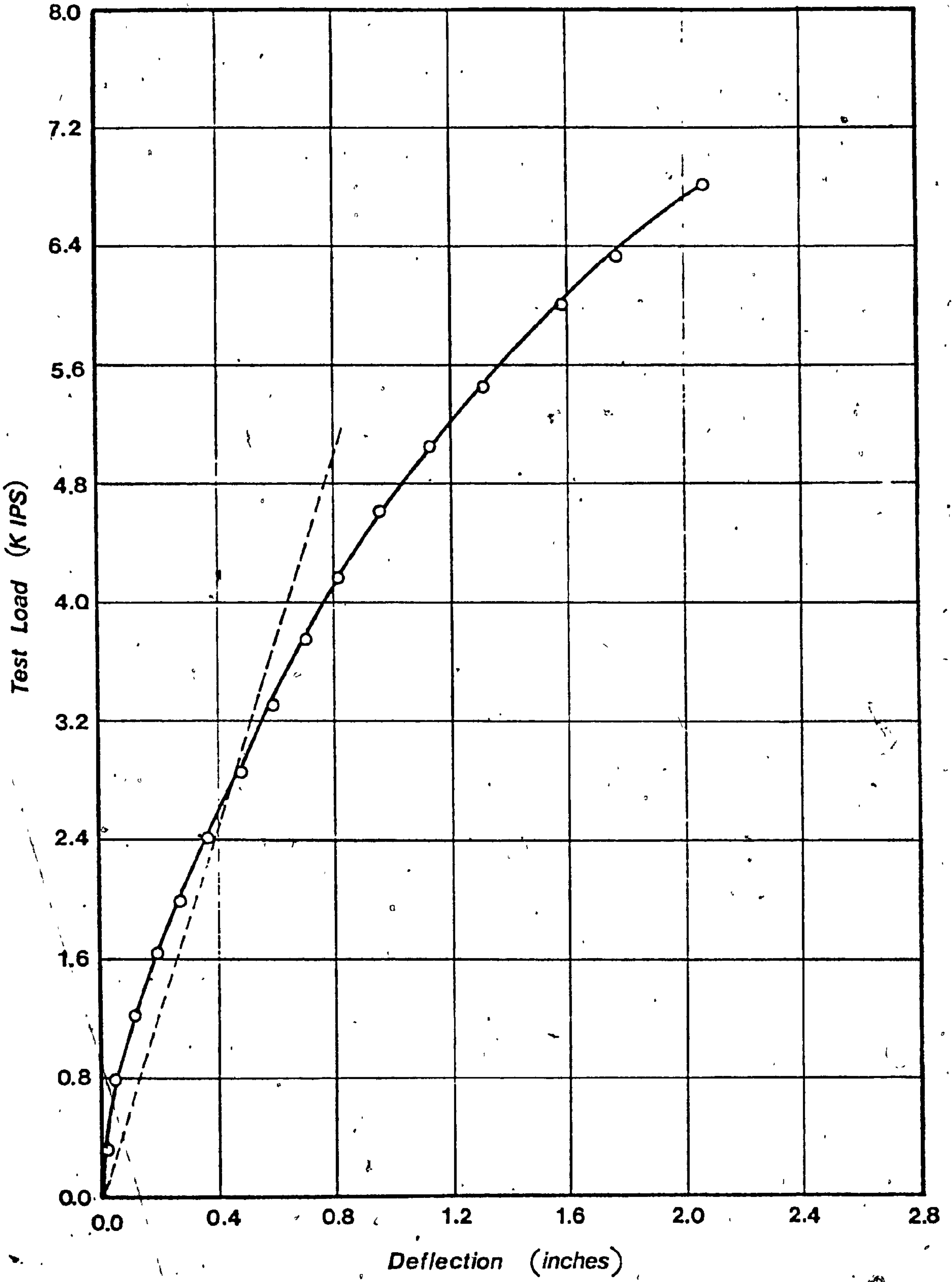

FIG. 3.25 LOAD-DEFLECTION CURVE FOR CAVITY DECKING DIAPHRAGM C-3

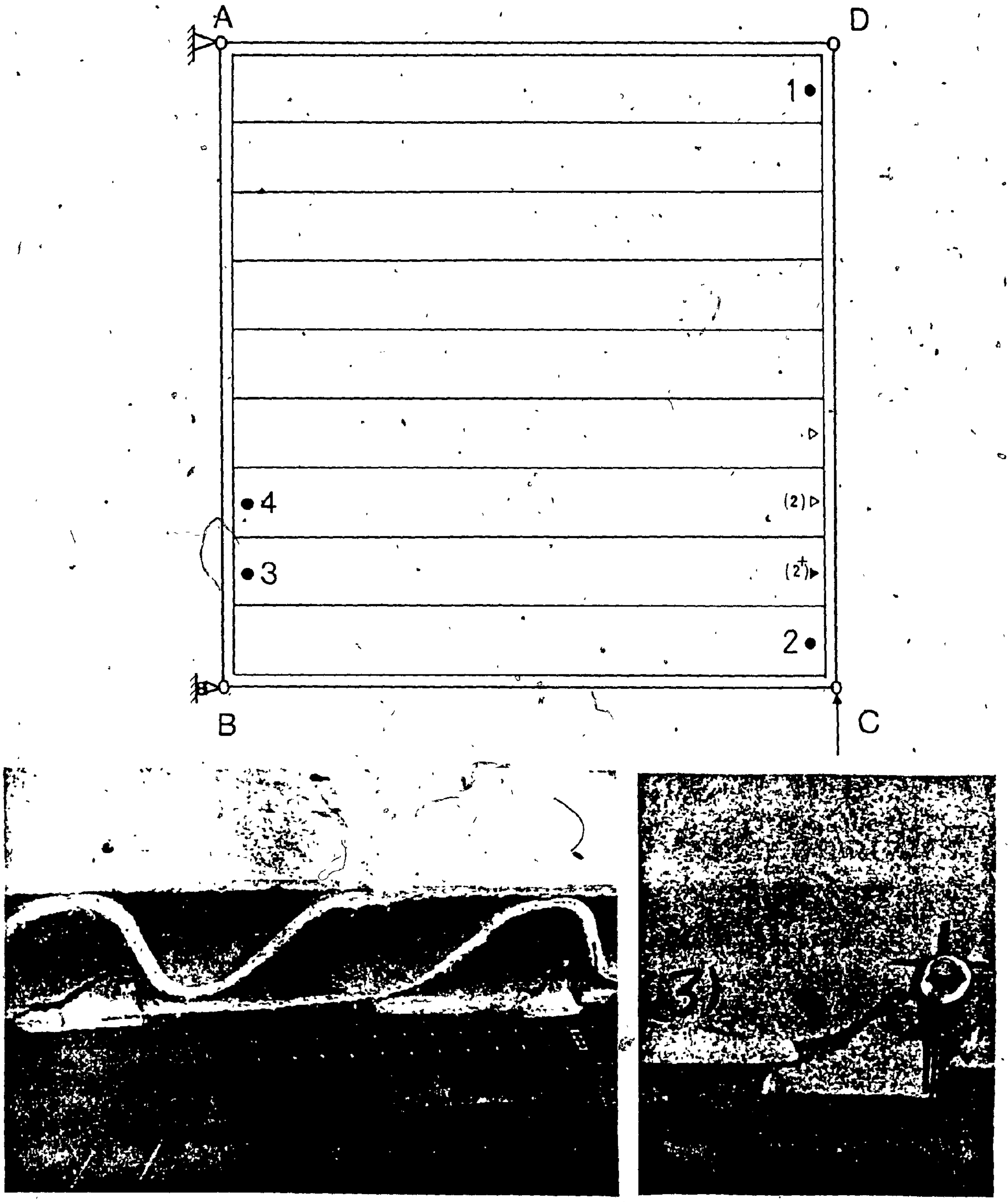

FIG. 3.26 FAILURES AT THE END FASTENERS OF DIAPHRAGM C-4

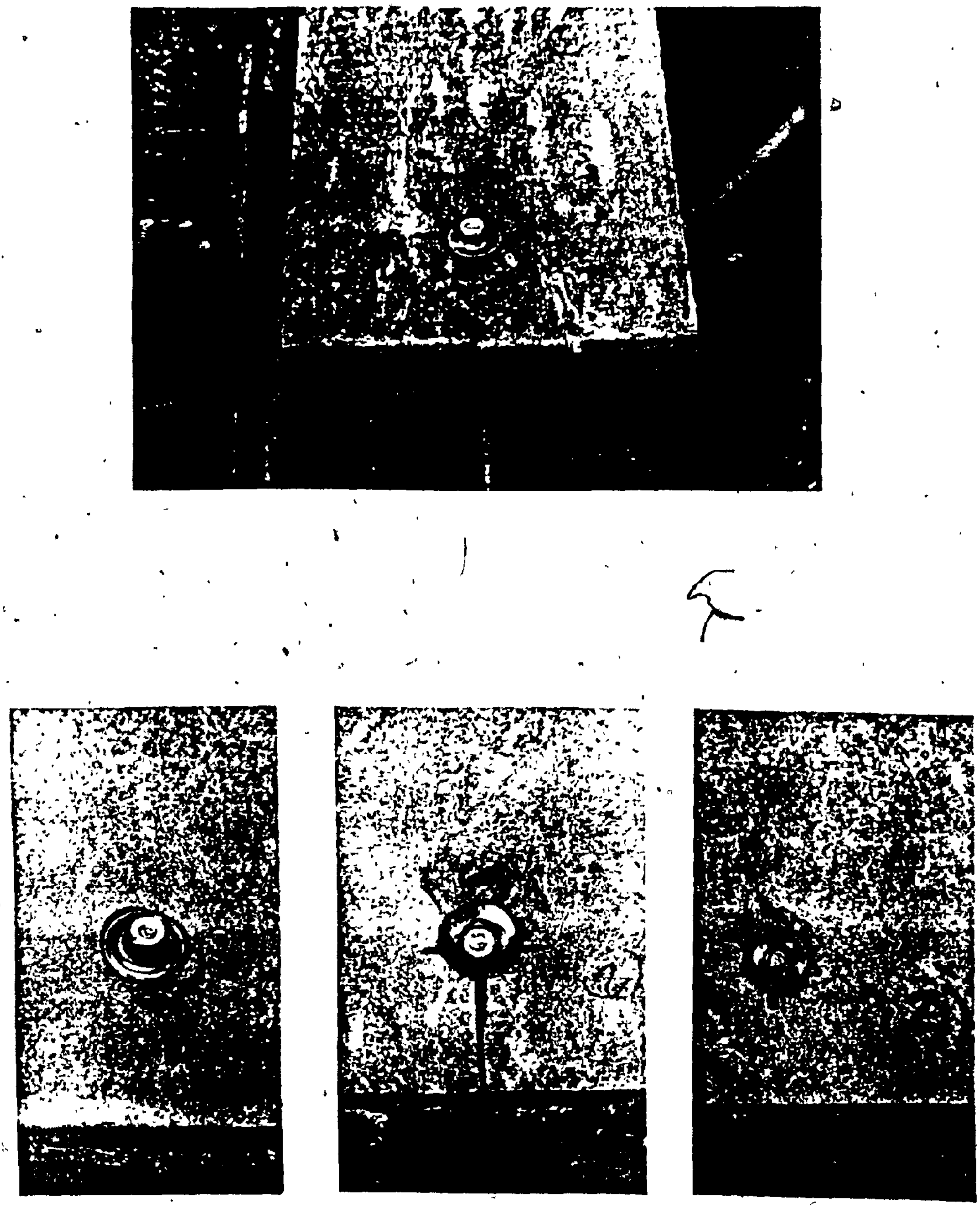

FIG. 3.26 (Cont'd) FAILURES AT THE END FASTENERS OF DIAPHRAGM C-4

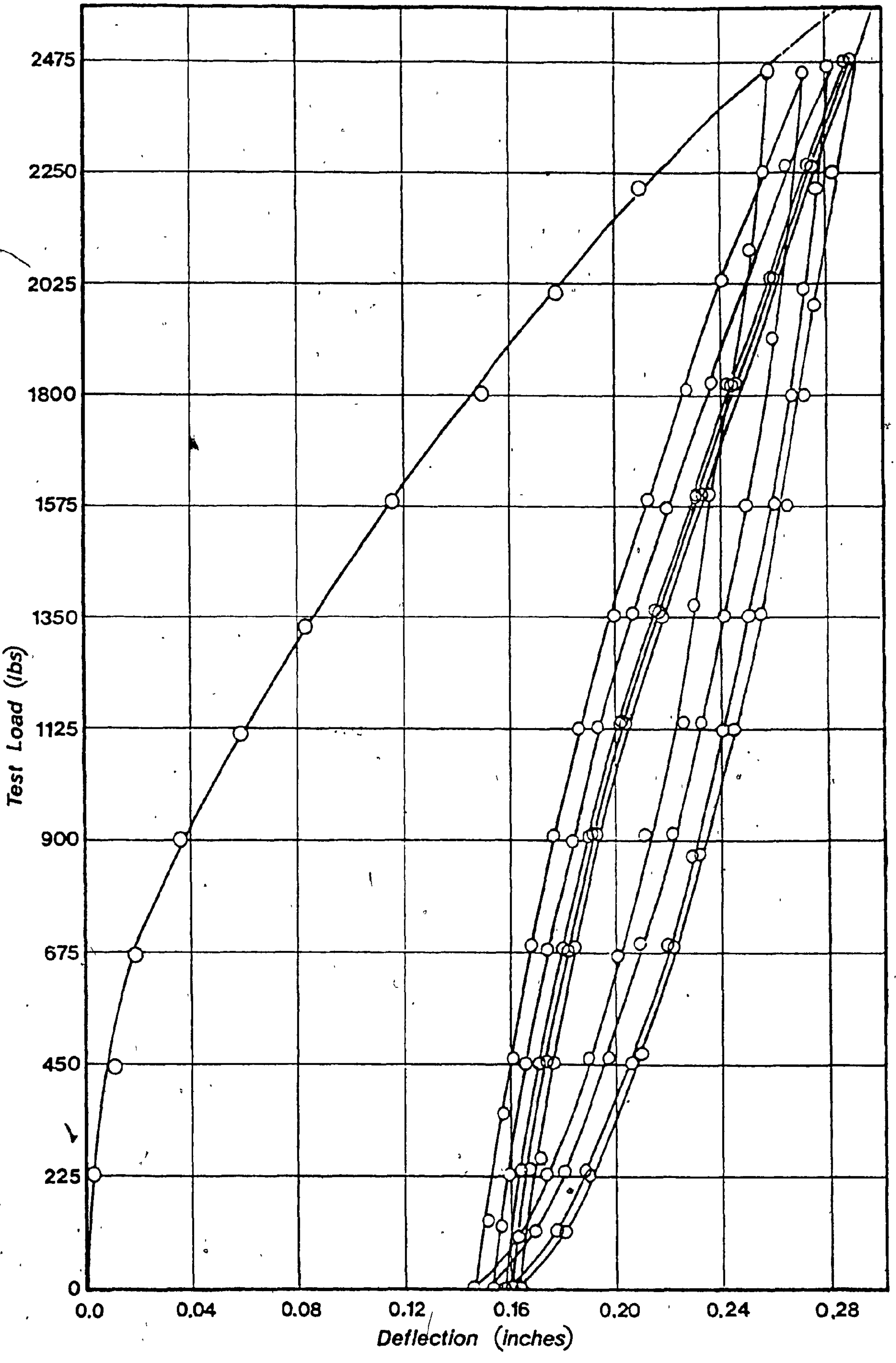

FIG. 3.27 LOAD-DEFLECTION CURVE FOR CAVITY DECKING DIAPHRAGM C-4 - FIVE CYCLES OF LOADING - UNLOADING

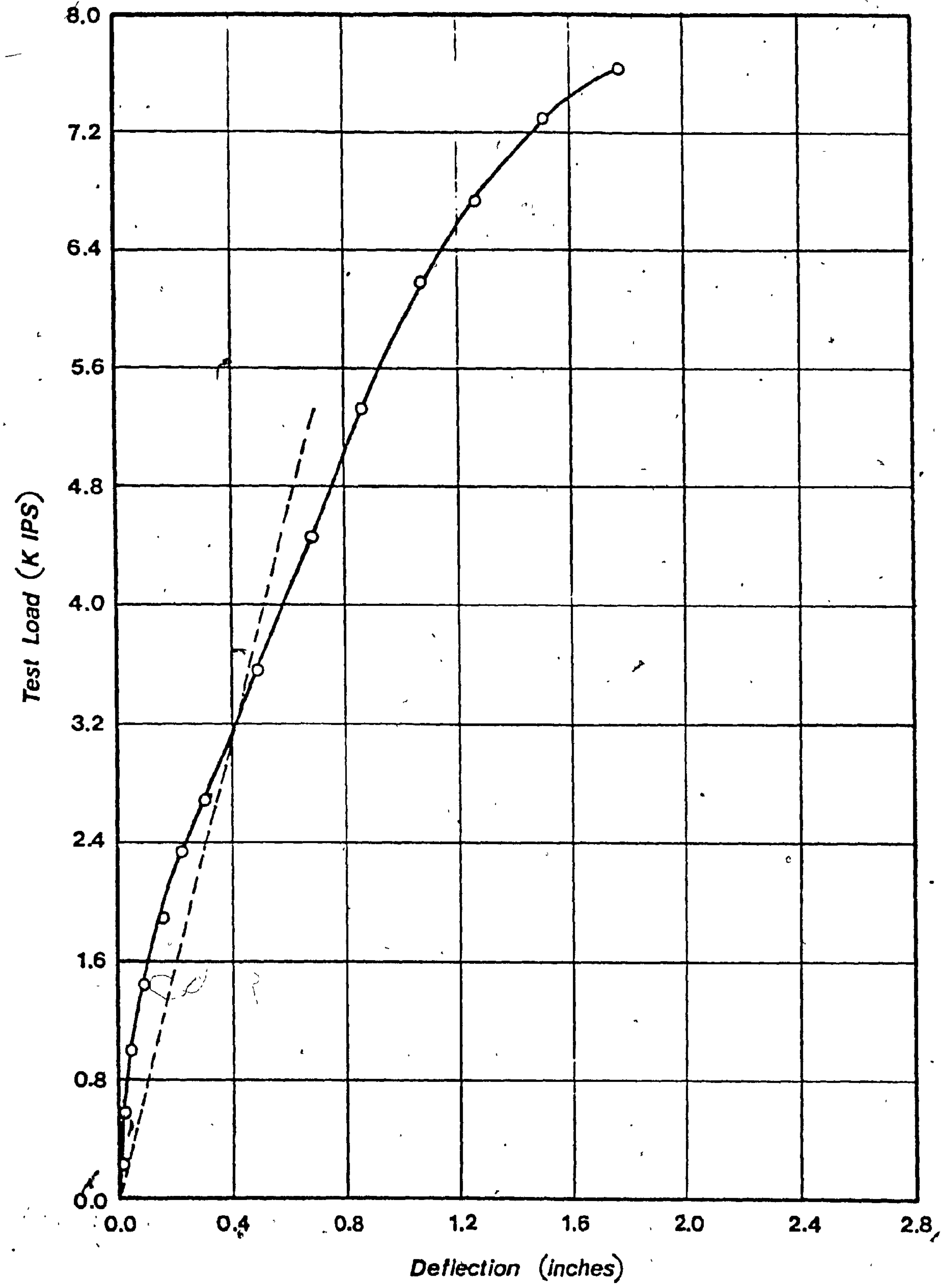

FIG. 3.28 LOAD-DEFLECTION CURVE FOR CAVITY DECKING DIAPHRAGM C-4

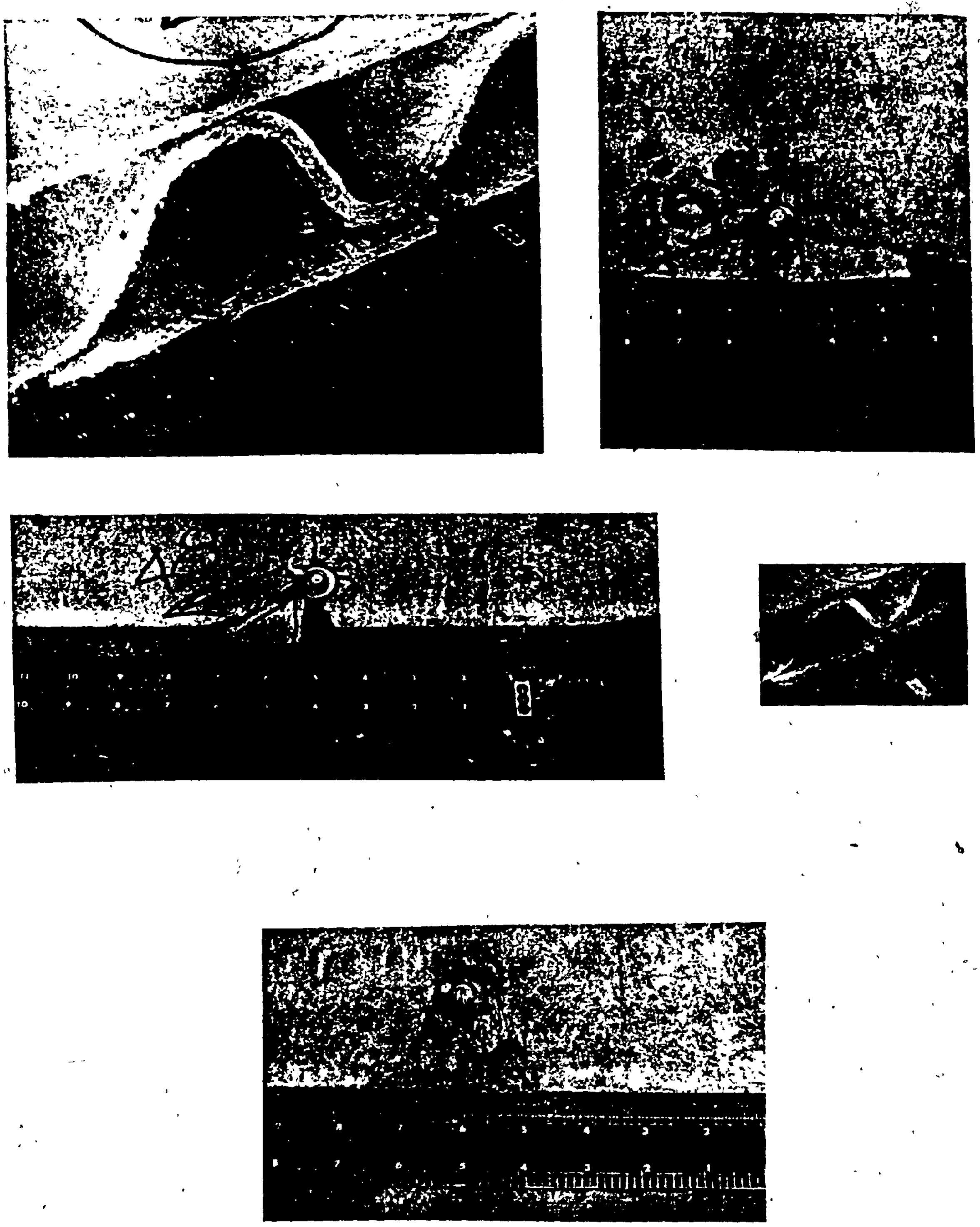

FIG. 3.29 FAILURES AT THE END FASTENERS OF DIAPHRAGM C-5

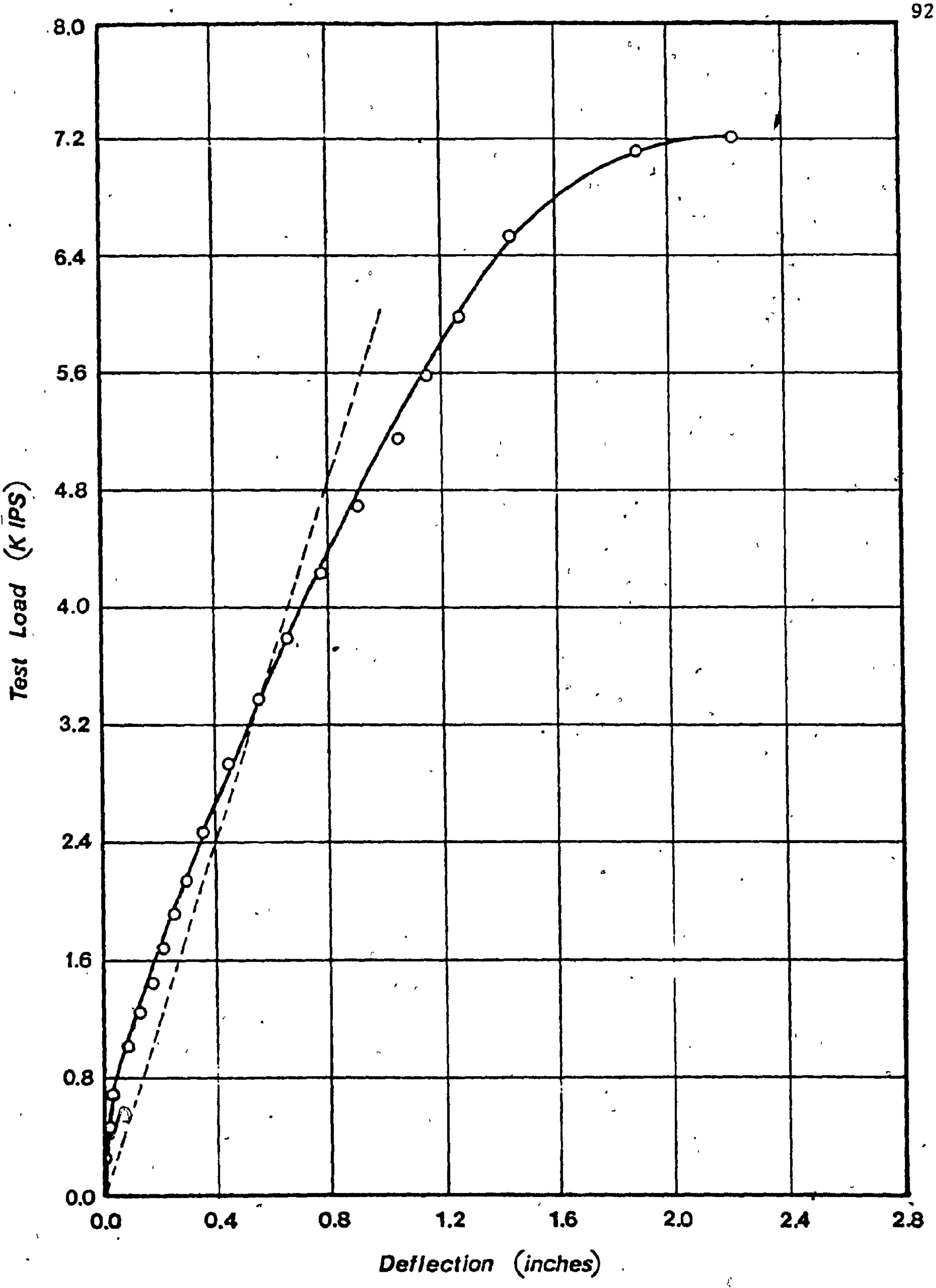

FIG. 3.30 LOAD-DEFLECTION CURVE FOR CAVITY DECKING, DIAPHRAGM C-5

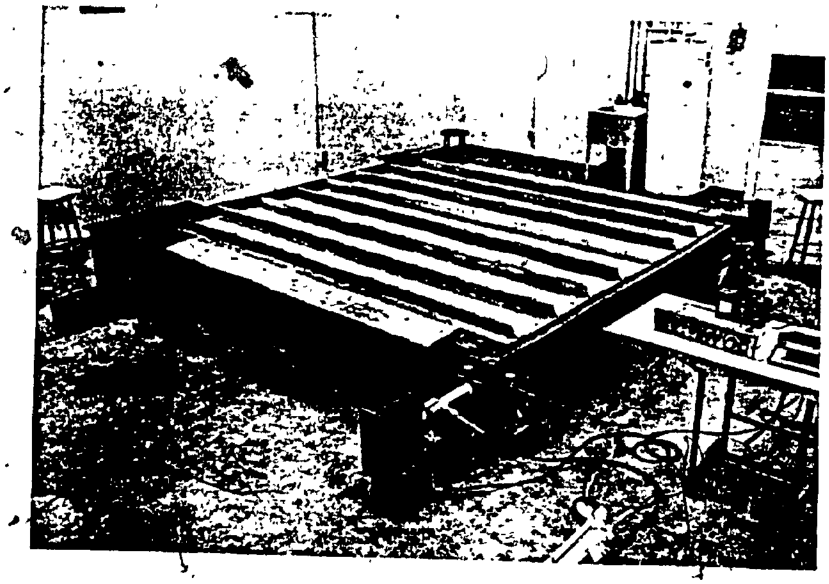

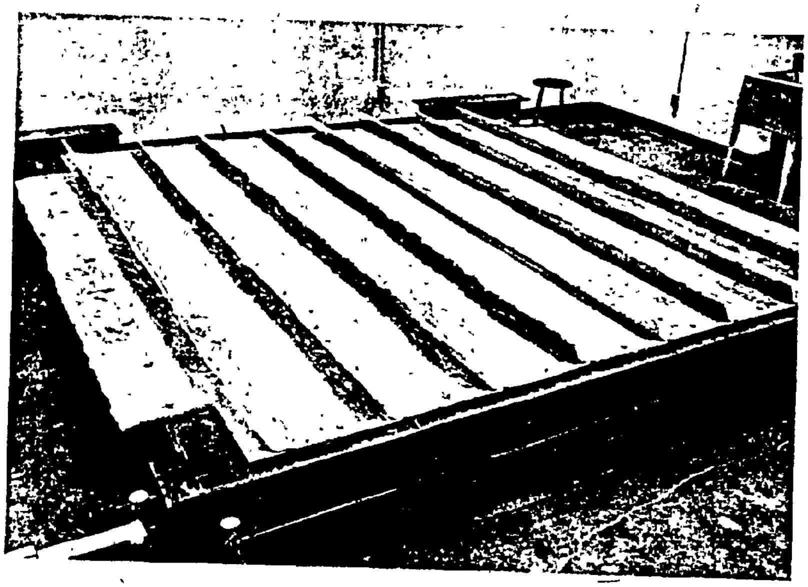

FIG. 3.31 VIEW OF TESTING SET-UP OF CAVITY DECKING DIAPHRAGM C-6

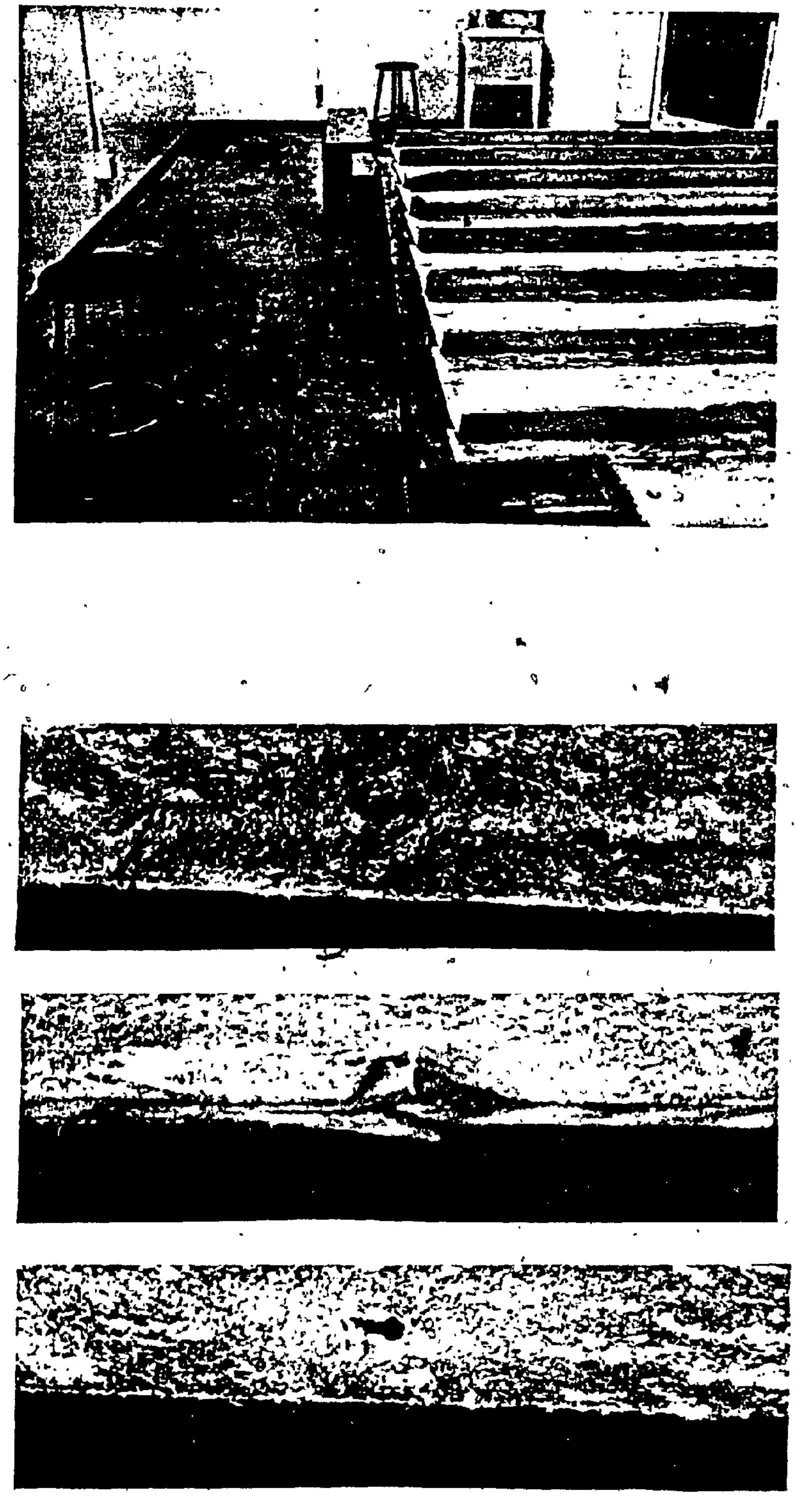

FIG. 3.32 RELATIVE DISPLACEMENT OF ADJACENT UNITS OF DIAPHRAGM C-6

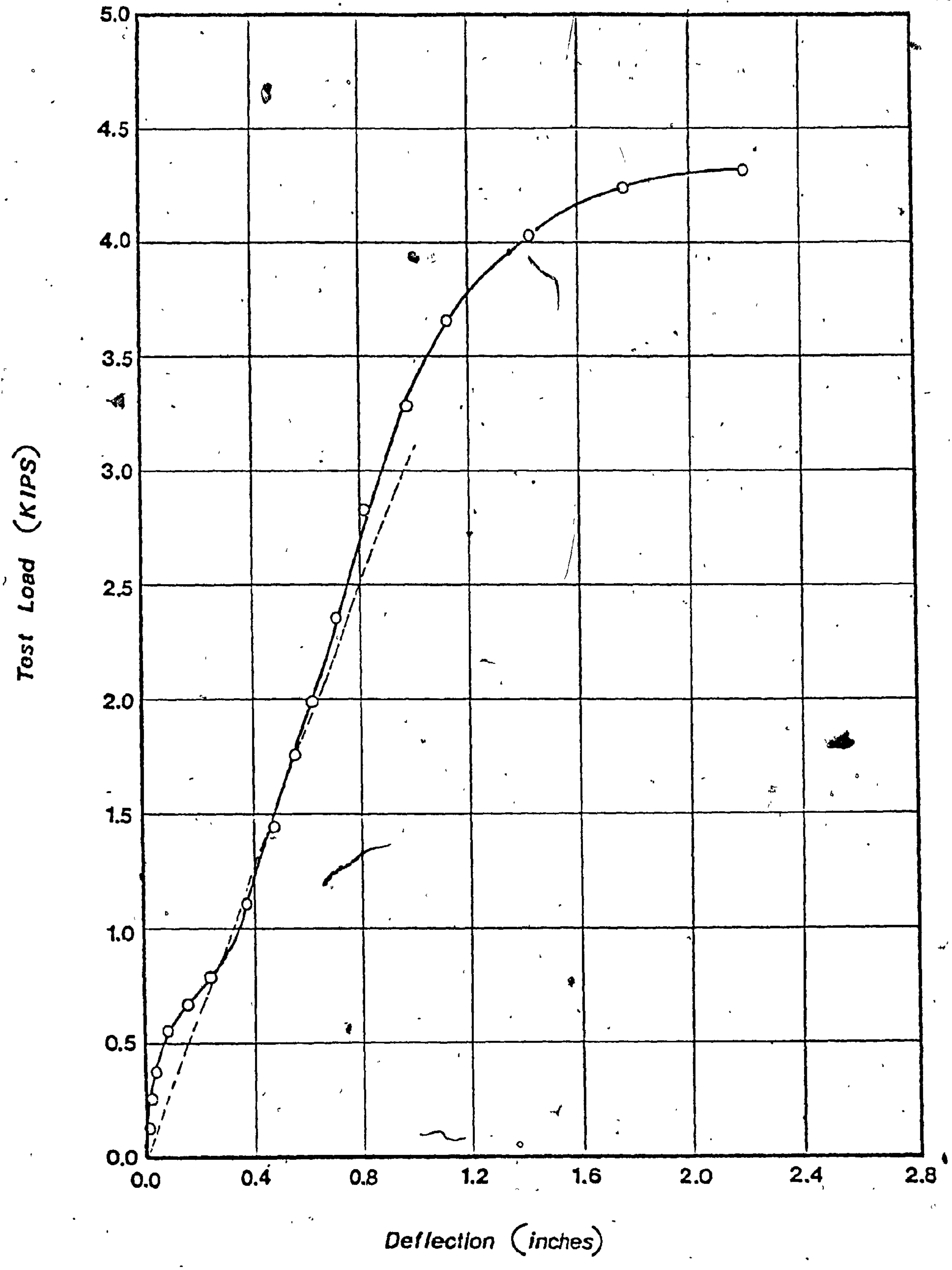

FIG. 3.33 LOAD-DEFLECTION CURVE FOR CAVITY DECKING DIAPHRAGM C-6

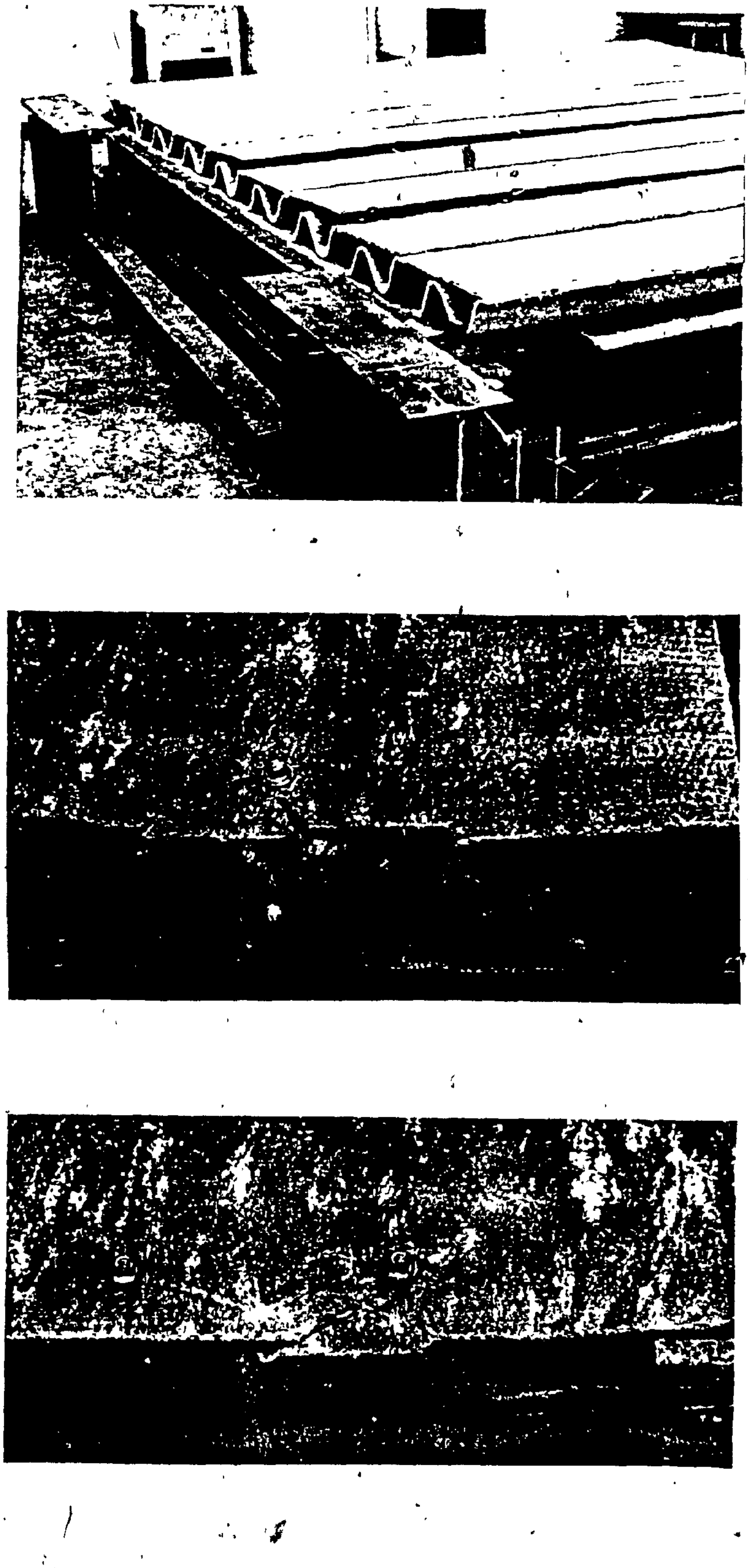

FIG. 3.34 FAILURES AT THE END FASTENERS OF DIAPHRAGM C-7

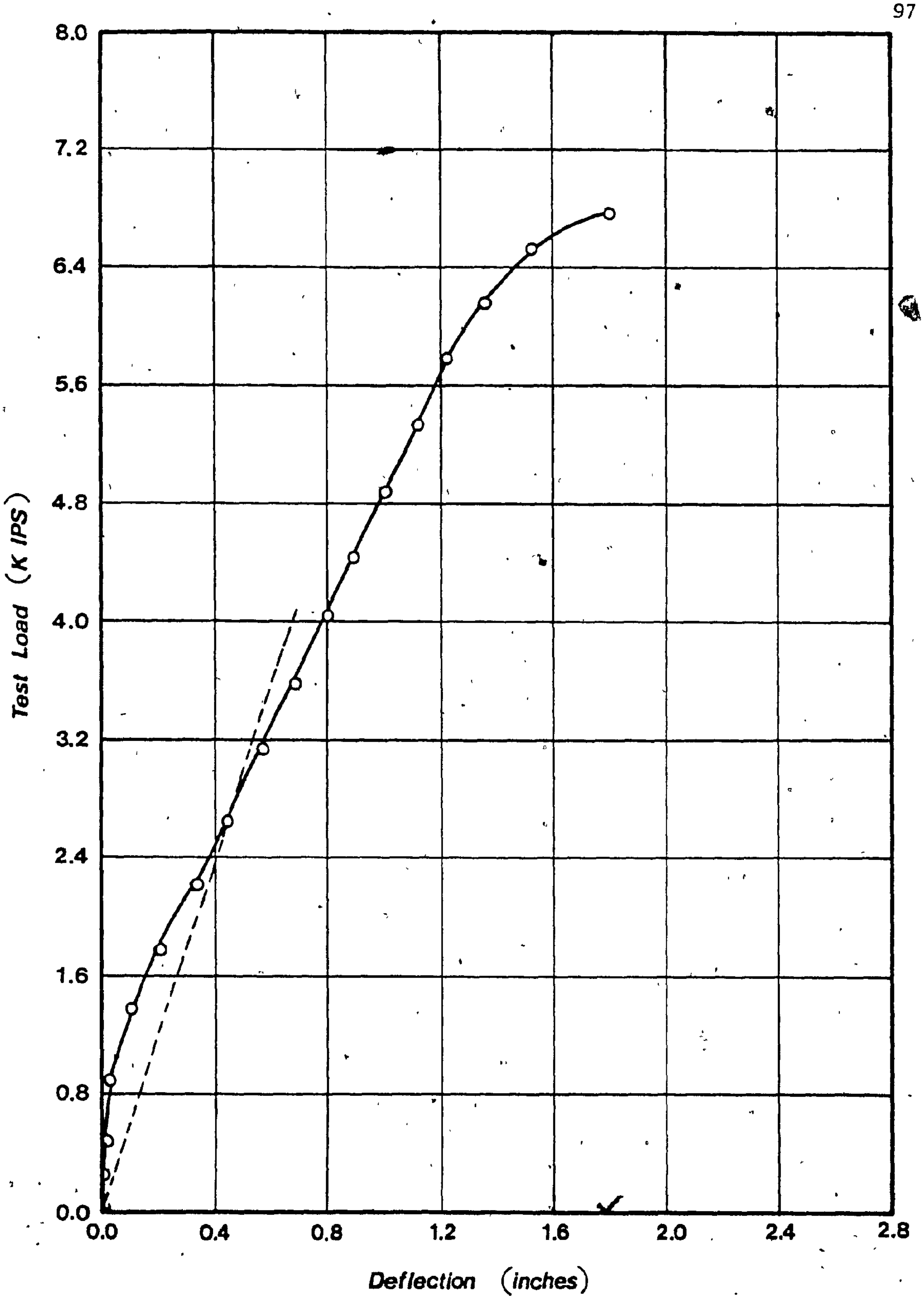

FIG. 3.35 LOAD-DEFLECTION CURVE FOR CAVITY DECKING DIAPHRAGM C-7

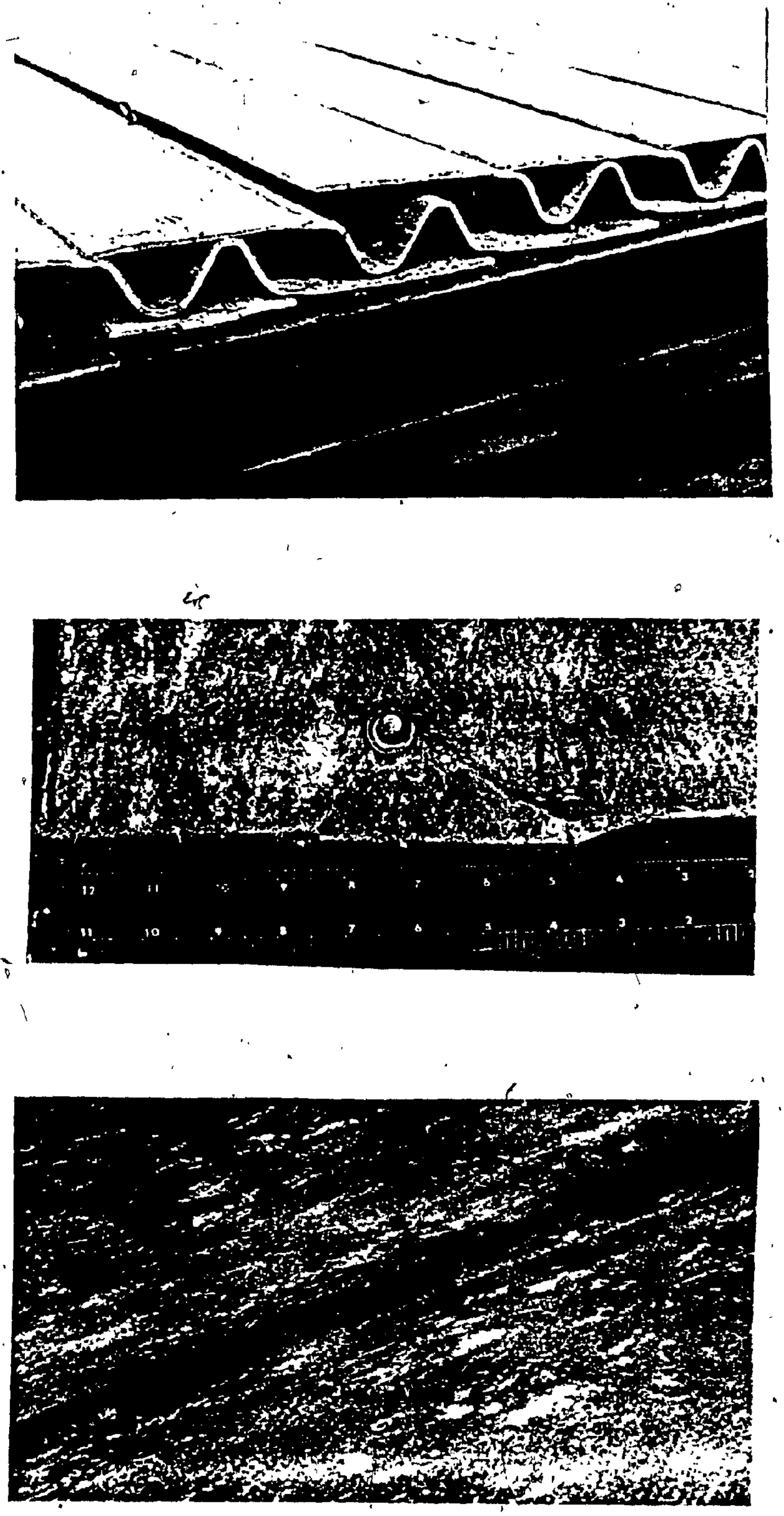

FIG. 3.36 OBSERVATIONS AT FAILURE OF DIAPHRAGM C-8

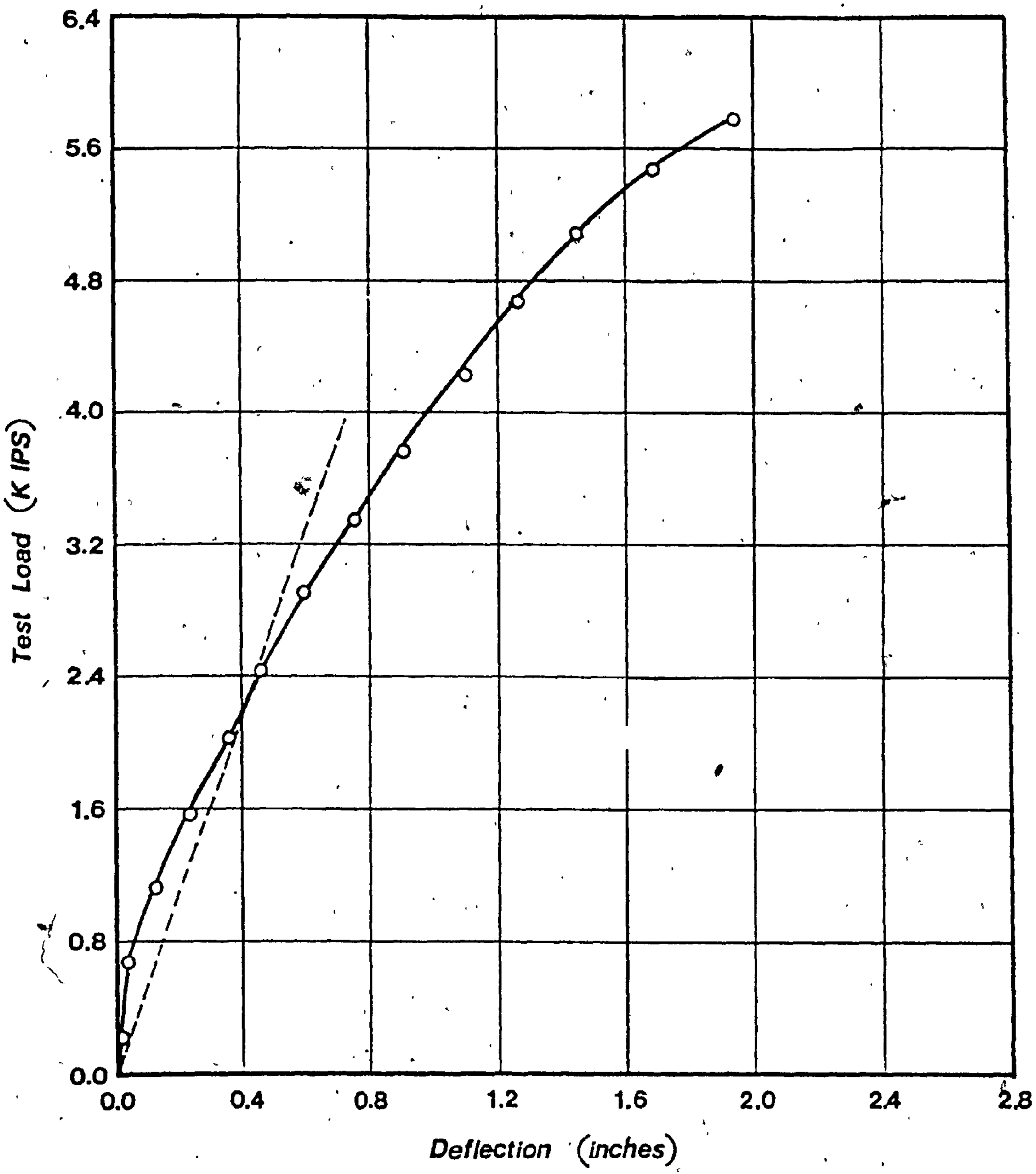

FIG. 3.37 LOAD-DEFLECTION CURVE FOR CAVITY DECKING DIAPHRAGM C-8

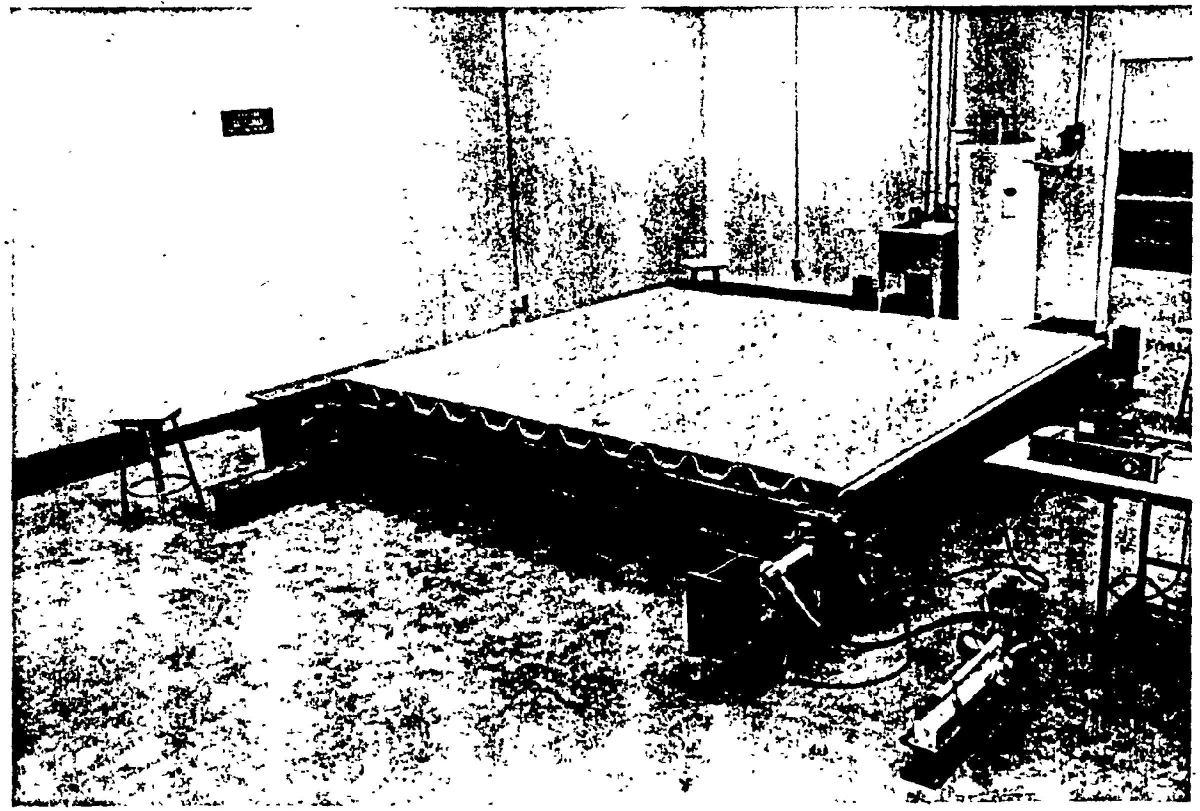

FIG. 3.38 VIEW OF TESTING SET-UP OF "T" DECK DIAPHRAGM T-1

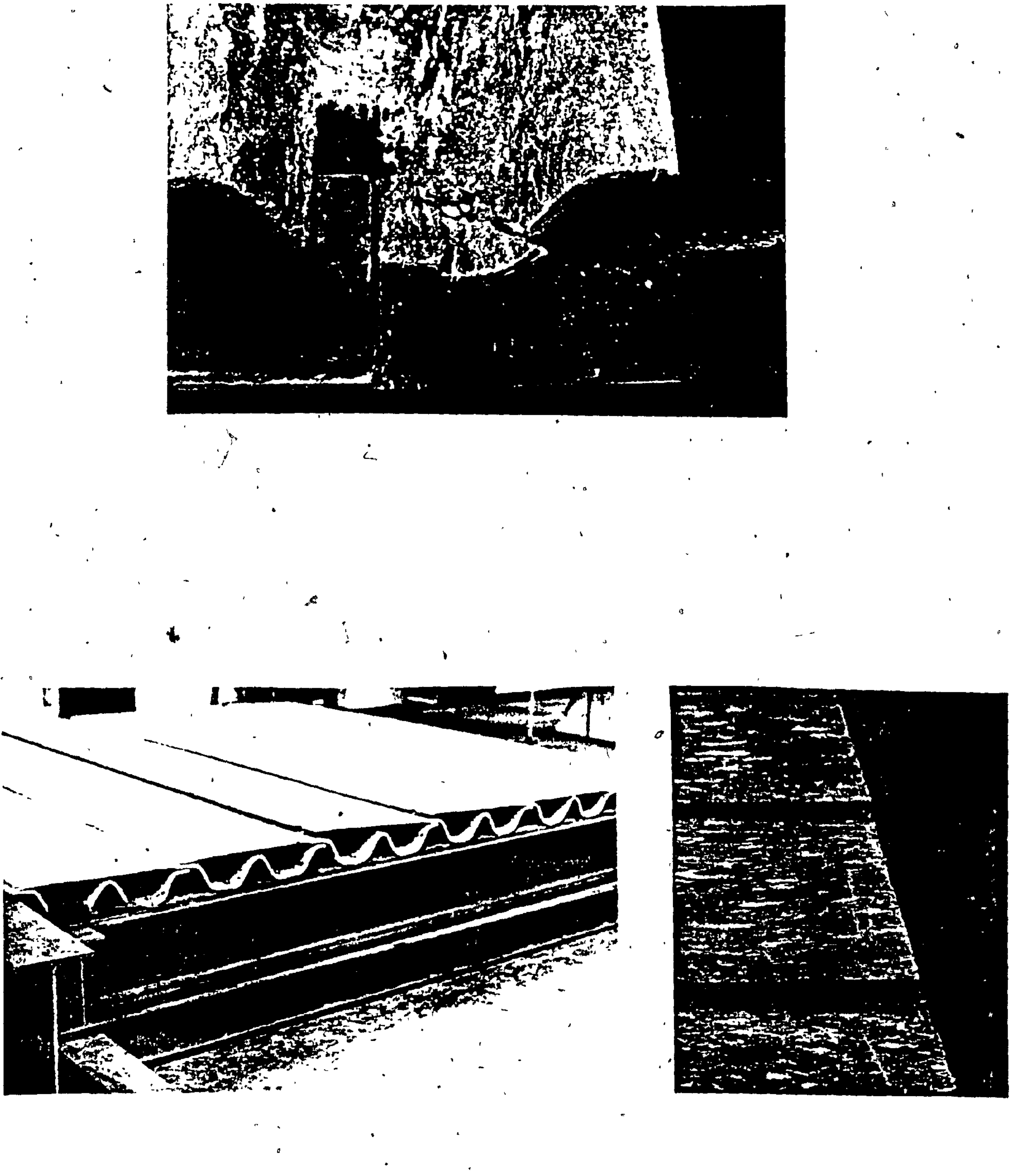

FIG. 3.39 OBSERVATIONS AT FAILURE OF DIAPHRAGM T-1

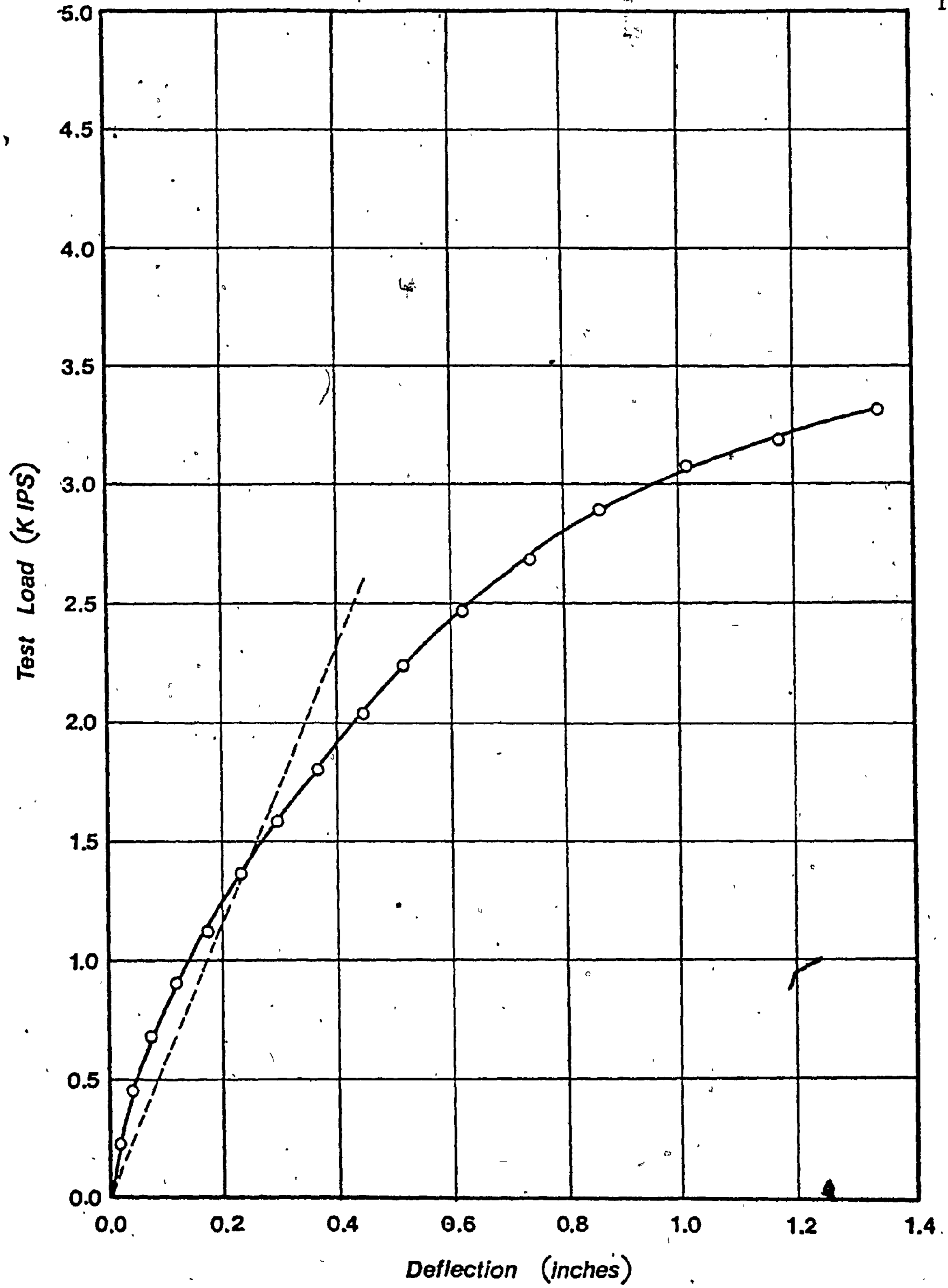

FIG. 3.40 LOAD-DEFLECTION CURVE FOR "T" DECK DIAPHRAGM T-1

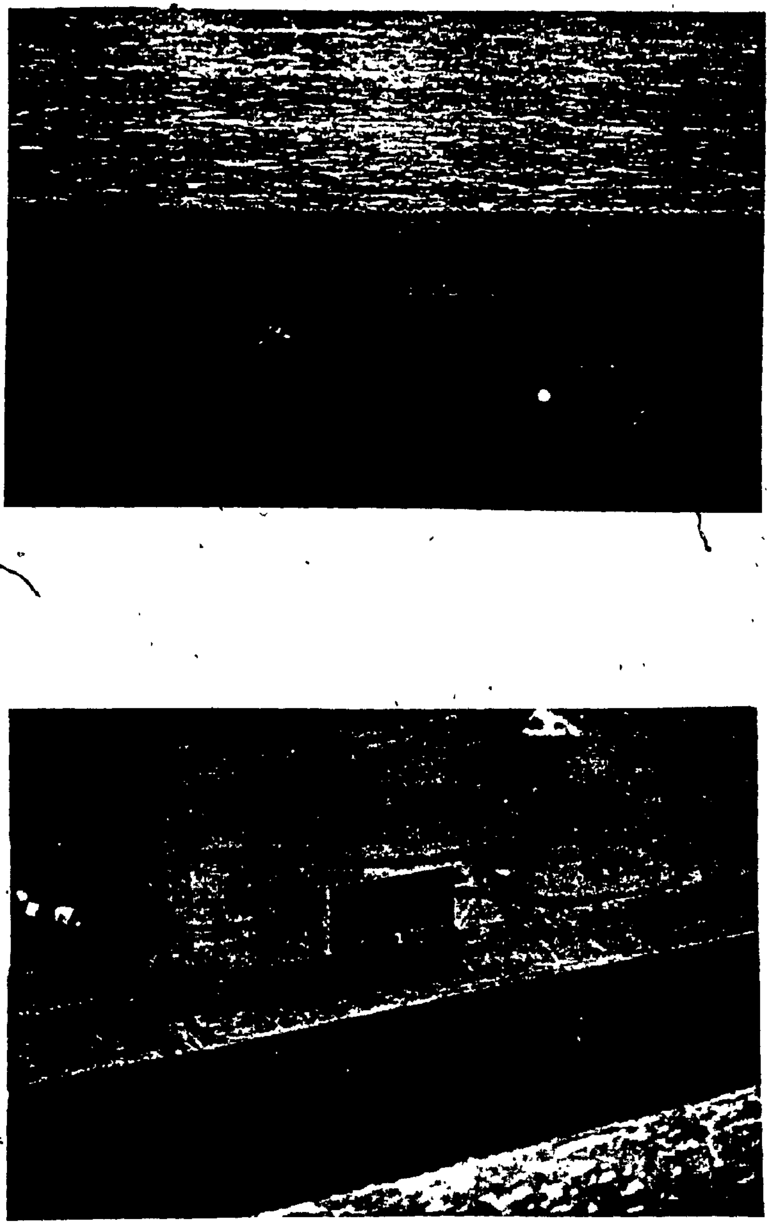

FIG. 3.41 SHEAR CONNECTORS IN DIAPHRAGM T-2

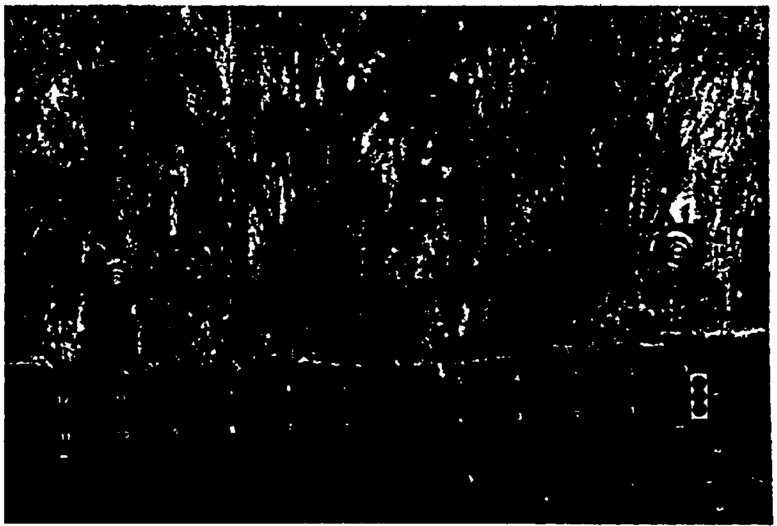

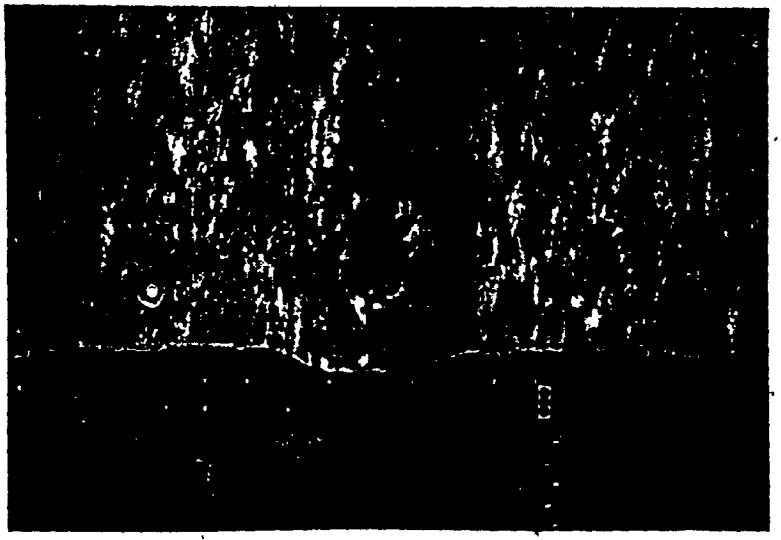

FIG. 3.42 FAILURES AT THE END FASTENERS OF DIAPHRAGM T-2

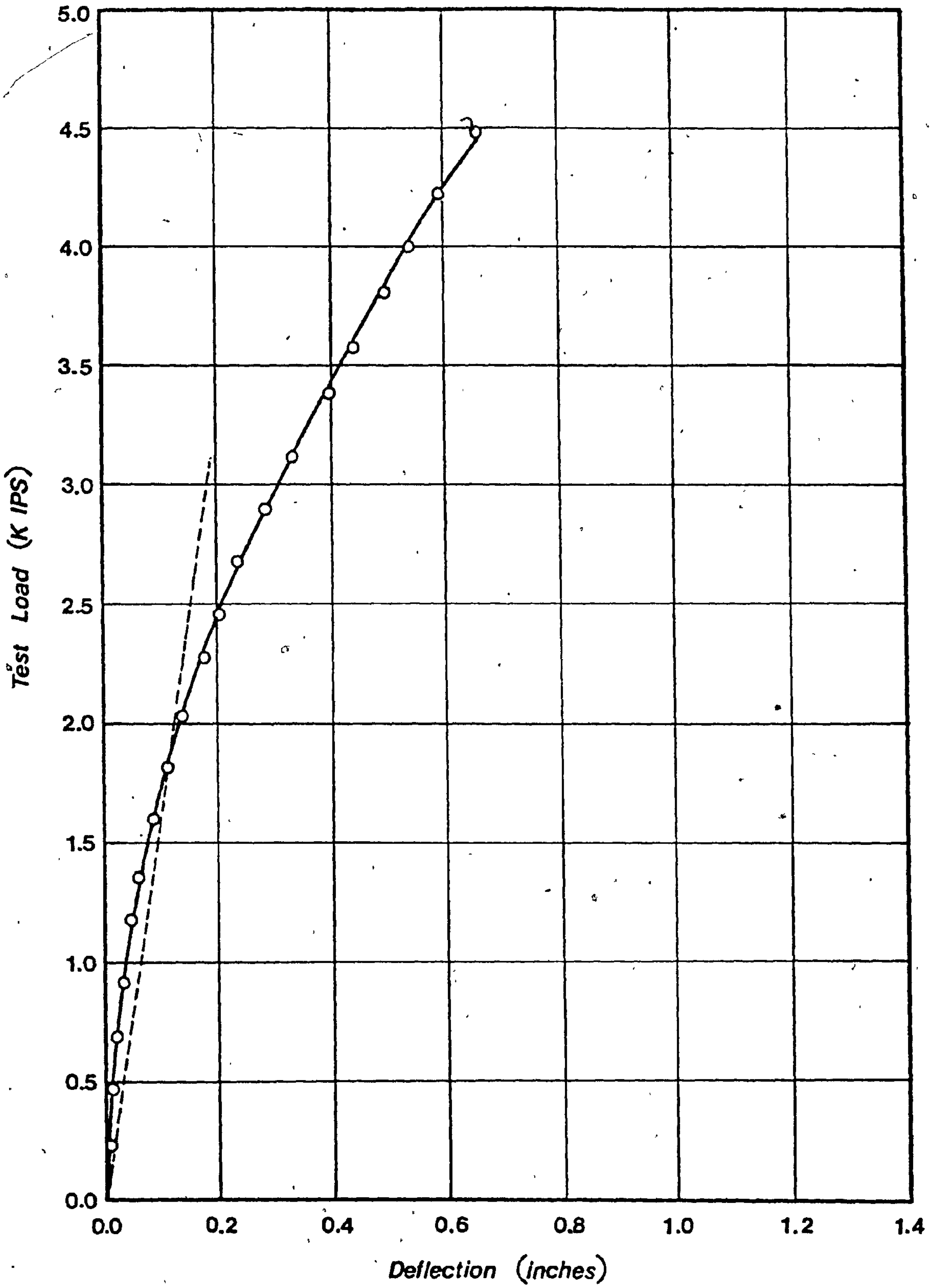

FIG. 3.43 LOAD-DEFLECTION CURVE FOR "T" DECK DIAPHRAGM J-2

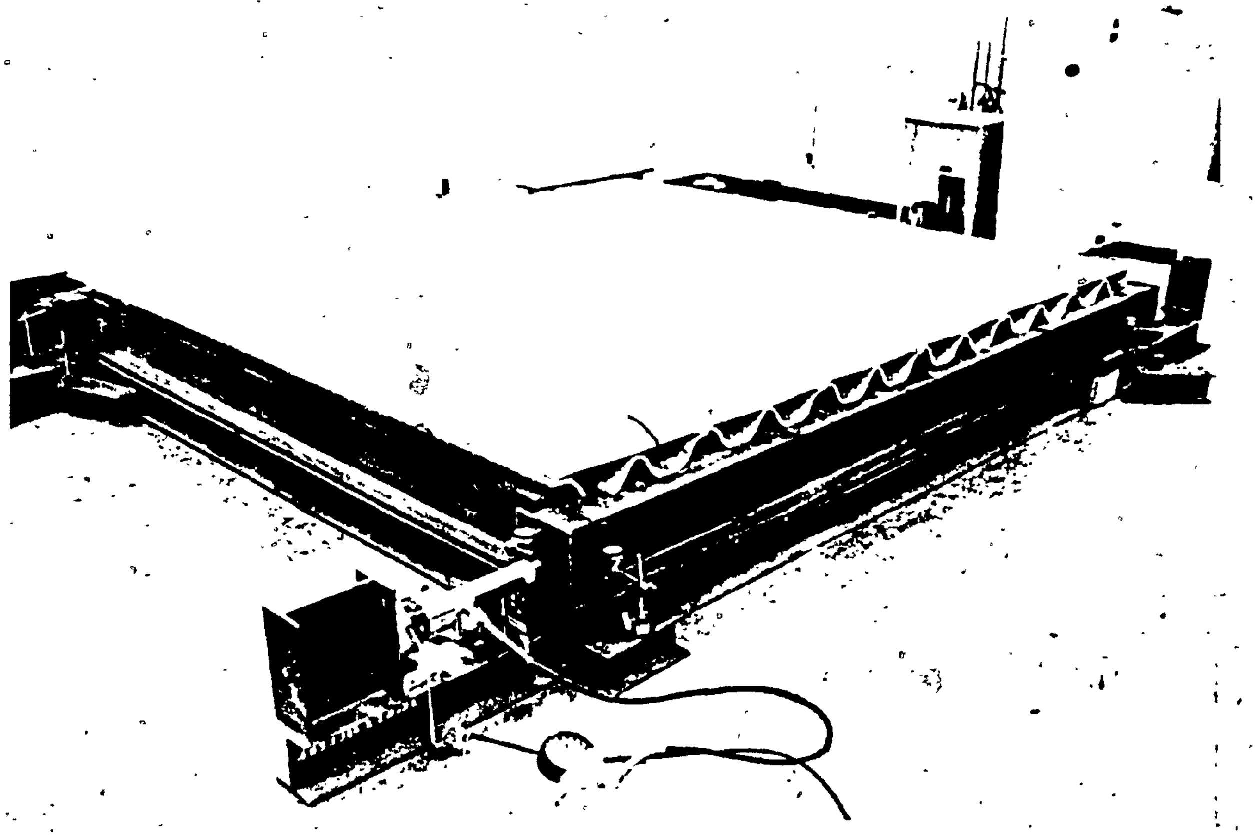

FIG.- 3.44 VIEW OF TESTING SET-UP TO "T" DECK DIAPHRAGM T-3

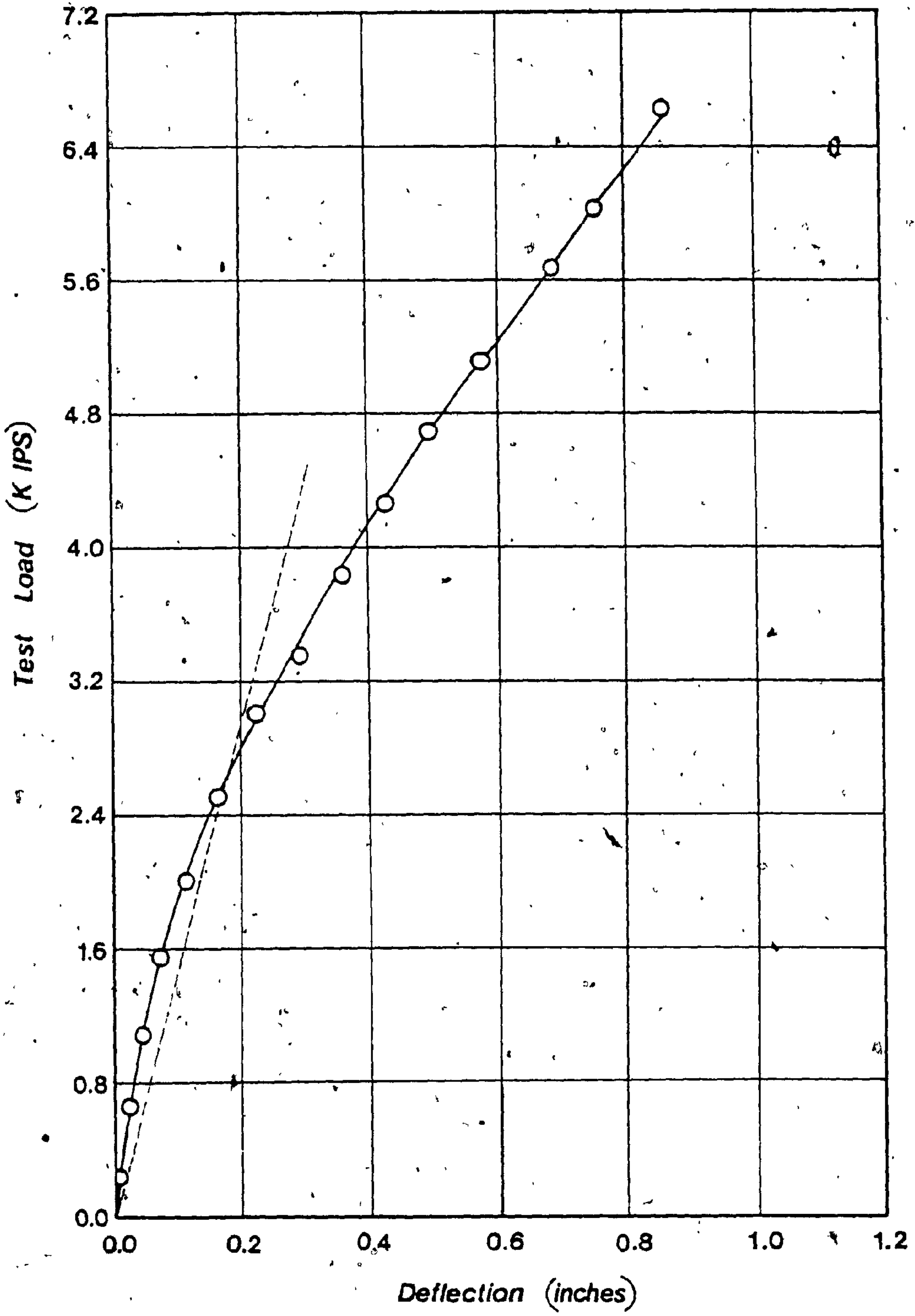

FIG. 3.45 LOAD-DEFLECTION CURVE FOR "T" DECK DIAPHRAGM T-3

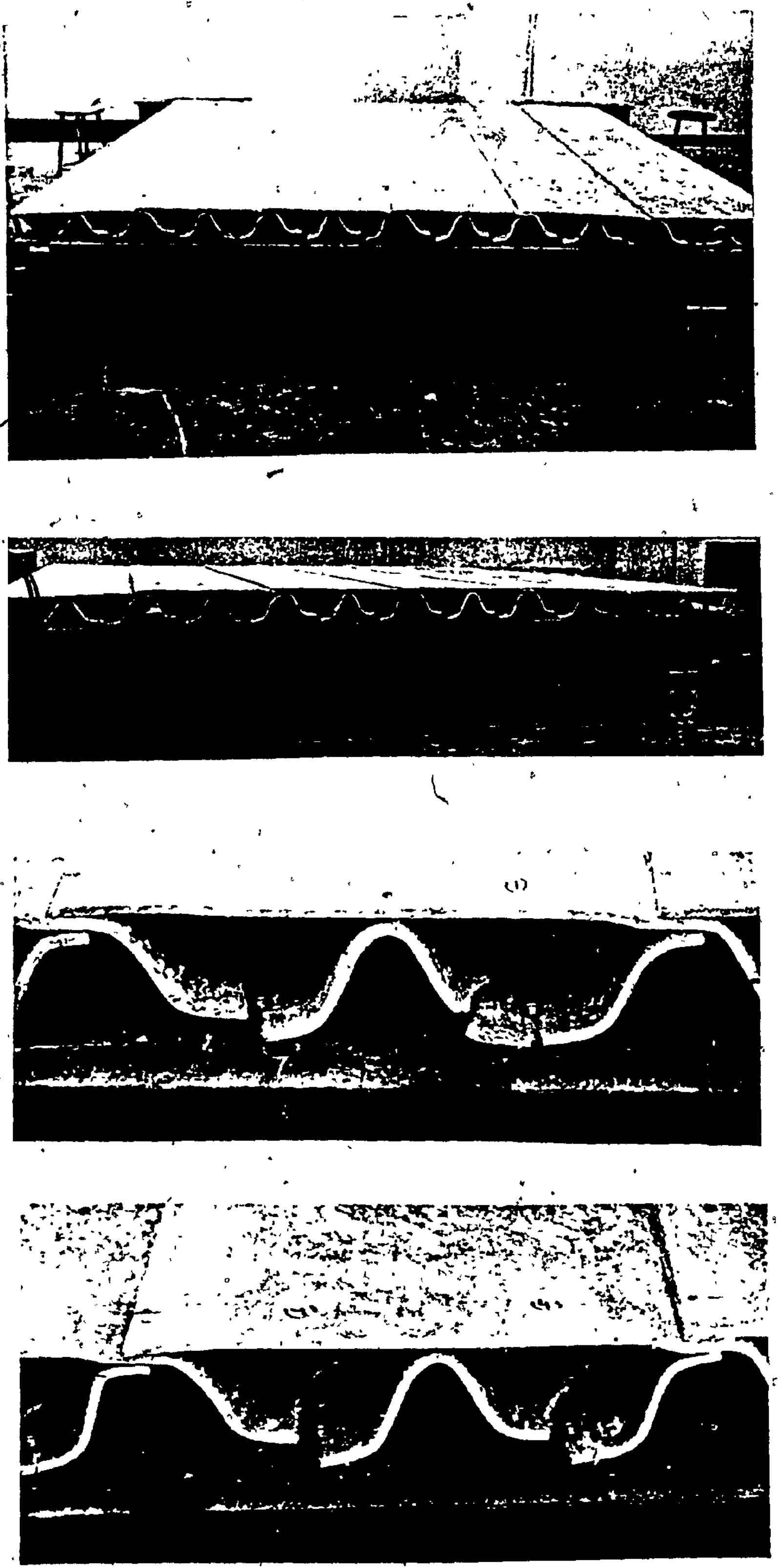

FIG. 3.46 OBSERVATIONS AT FAILURE OF DIAPHRAGM T-4

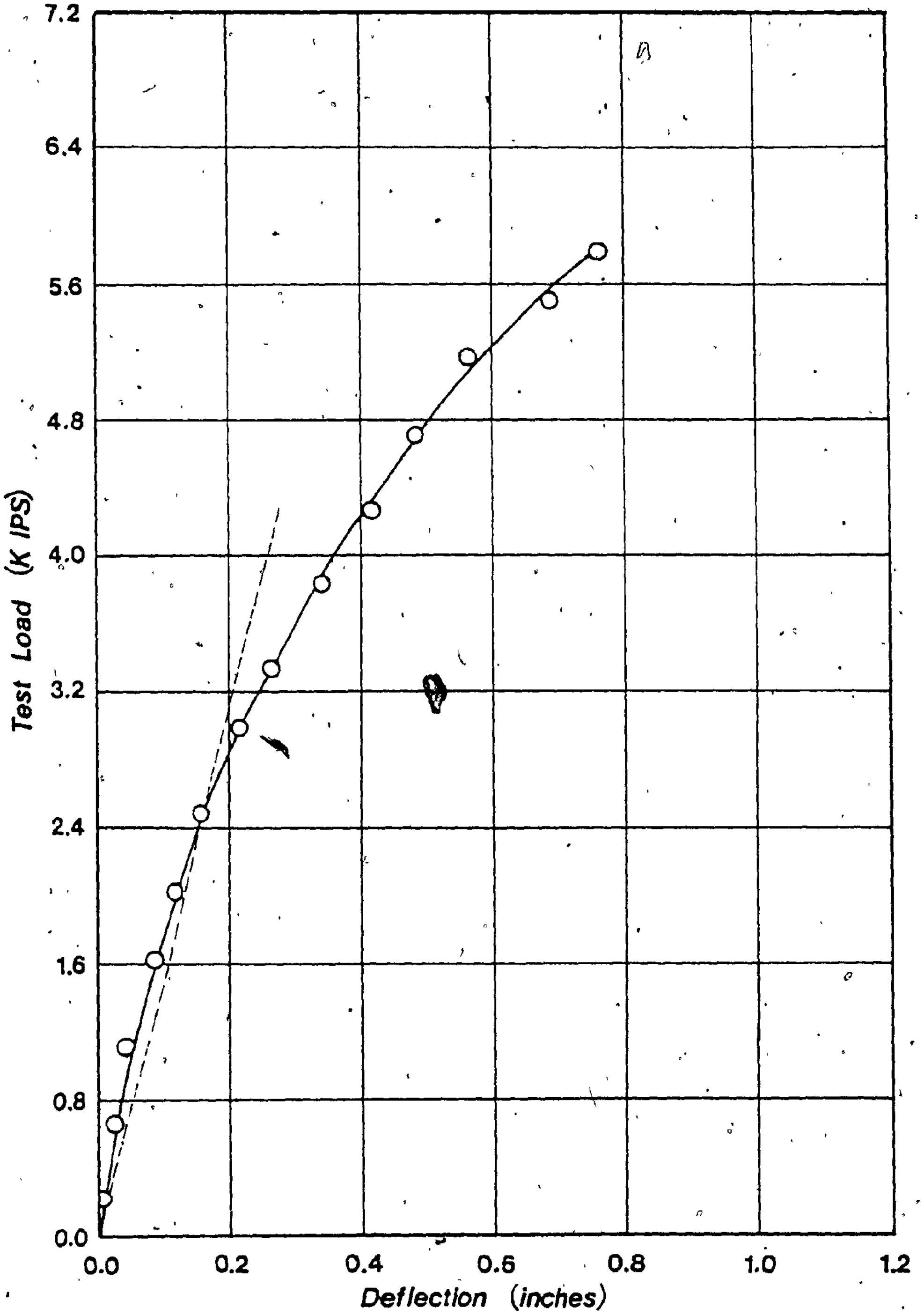

FIG. 3.47 LOAD-DEFLECTION CURVE FOR "T" DECK DIAPHRAGM T-4A

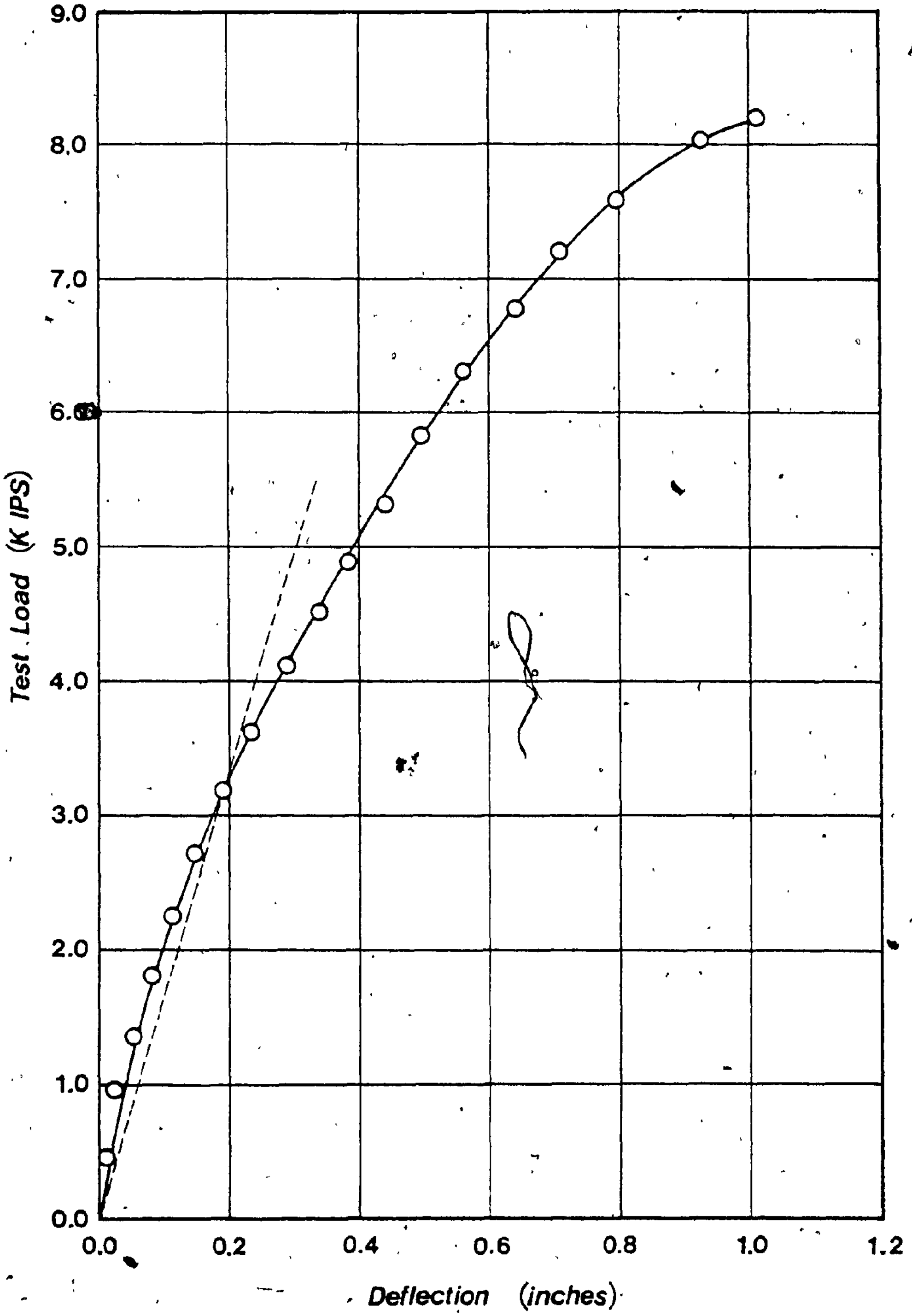

FIG. 3.48 LOAD DEFLECTION CURVE FOR "T" DECK DIAPHRAGM T-4

CHAPTER IV

LOAD-DEFORMATION CHARACTERISTICS OF DIAPHRAGM CONNECTIONS

CHAPTER IV

LOAD-DEFORMATION CHARACTERISTICS OF DIAPHRAGM CONNECTIONS

4.1 INTRODUCTION

In all the tests performed and reported in the previous chapter, it has been observed that the connections, type and pattern, play a major role in the behaviour of diaphragms, influencing both stiffness and ultimate strength. Also, it was clear that failure of all diaphragms was initiated at the weakest connection.

This chapter is concerned with the experimental evaluation of the load-displacment response of the connections used in the two decking systems. The stiffness and strength of the connections as w ll as their failure mode are of main interest. Parameters affecting the mechanical behaviour of the connections are also investigated. The data for the stiffness and strength of the connections are required for the analytical prediction of the performance of the complete diaphragn system as will be shown later in the next two chapters.

4.2 LAPPED-JOINTS AND TEST METHOD

Diaphragm connections fall into two categories, those connecting sheeting units along their seams and those connecting the sheeting to the supporting structural members. In most of the previously reported tests on connections of light-gauge steel sheetings [35,37,46-52], the mechanical characteristics of connections were established by subjecting lapped joints to direct tension till failure. These single shear connections were composed of two parts, either two light-gauge steel sheets, or a thin sheet and a hot-rolled flat section, and joined together by means of an appropriate fastening device.

In the present investigation, tension tests on lapped-joints were conducted in two series. The first are for seam connections which serve to fasten adjacent units, and the second for edge connections which are used to fasten panel edges or panel ends to the flanges of marginal beams. Thus, the first series dealt with the connection of two asbestos-cement sheets of the same thickness (3/8"), Fig. 4.1a, whereas the second was concerned with the attachment of an asbestos-cement sheet to a steel plate 1/2" thick (note that W10X21 steel marginal beams used in full-scale tests have a flange of 7/16" thick), Fig. 4.1b. The specimens tested were fabricated to produce as close as possible the connections used in practice and in the full-scale test diaphragms. Due to the orthotropic nature of the sheeting specimens of the sheeting cut in both the longitudinal (parallel to corrugations) and transverse directions.

For each type of connection, the following variables (Fig. 4.1) were considered: i) diameter of drilled screw holes, ii) edge distance from center of screw in direction of load, and iii) edge distance from center of screw in perpendicular direction to stress (or full width of test specimen).

To minimize the scatter of test results, special emphasis was placed on the:

(1) measurement of the connection dimensions
(2) drilling of the fastener hole
(3) consistency of screw tightening, and
(4) measurement of connection "slip" and applied load.

All tests were performed using the Instron Universal Testing Machine (model 1125) of 100 kN (20,000 lbs) capacity load cell, equipped with six load ranges. The two lowest ranges (2 and 5 kN) were used for most of the tests.

4.2.1 Lapped-Joint Deformation

The total deformation in the connection at a given load consists of a number of components. First, the deformation due to the clearance between the fastener and oversize hole results in a rigid body slip of the sheeting until bearing is established. Second, further slip is due to deformation (mostly plastic) of the joined elements and/or the bolt, in the vicinity of the hole. And finally, a negligible amount of sheet deformation also occurs.

4.2.2 Test Procedure

After appropriate centering and vertical alignment of the connection installed in the test fixtures (grips); first, a relatively small load (0.2 kN) was applied then released to produce initial fit. Load was then applied continuously (till failure) and the total deformation recorded automatically by the strip chart recorder. Different tests were conducted with different cross-head travel speeds of 0.02, 0.05 and 0.1 in/min.

The inherent deflections of the load cell and the machine, and also the slippage of the joint parts from the grips could be sufficient to affect the accuracy of the recorded displacements. To compensate for these errors, a direct calibration of the machine deflections was obtained by running a "no-stretch" curve, as recommended by the Instron machine manual. This test was simply conducted on a rigid specimen (steel or asbestos-cement), with virtually zero gauge length (grips are touching), a load-deformation curve was obtained, which was used to correct for the measured displacements of a lapped-joint at any level of loading. The accuracy of this method was proved satisfactory when checked against measurement of the relative displacements of the two parts of a number of loaded connections by high precision (1/1000 inch) dial gauges. The two procedures yielded very close load-slip curves for the same connections.

4.3 SEAM FASTENERS

Two types of seam fasteners are currently used:

(1) $1\frac{1}{2}$" x $\frac{3}{8}$" diameter flat head stainless steel bolts and cadmium plated pal nuts (Fig. 4.2), and

(2) $1\frac{1}{4}$" x No. 2 flat head "A" type self-tapping screws (Fig. 4.3).

The first type, only used with the cavity decking system, is for connecting the underlapping edges of the sheets (Fig. 3.9b). According to Atlas' application instructions [44], the holes in the asbestos sheets are drilled with a $\frac{1}{4}$" diameter bit. These slightly oversized holes are in fact intended to facilitate the placing of the bolts from the bottom side of the sheeting. The underlap is then tightened up using the nuts. This type of fastener ensures that the sagging bottom flat wing of the sheet (due to its weight), is lifted up and leveled with a horizontal continuous plane provided by the rest of the decking sheets.

The second type, is used to connect the top seams of cavity decking units (Fig. 3.9c), and in connecting the top and bottom seams of the "T" deck sheets (Figs. 3.12b and 3.12c). Self-tapping screws are perhaps the most popular fixing almost universally used today. As the name implies, self-tapping screws tap their own thread in the two sheets to be connected after a slightly undersize pilot hole has been drilled through the sheets (3/16" size bit, as recommended by Atlas [44]). This type of fixing is more practical as it can be used from one side of the sheeting.

4.3.1 Test Results of First Type

In this test series, the following variables were considered: diameter of drilled bolt hole (3/16", 7/32" and 1/4"), full width of test specimen (1", $\underline{1\frac{1}{4}}$" and 2"), and edge distance from center of bolt in the direction of the load (5/8", 1" and 2"). Each two of the underlined values were kept unchanged while considering the variations of the third. For every such combination of the variables, two tests were conducted. In cases of large discrepancies, a third test was performed.

A set of load-displacement curves was obtained. In general, the curves were found to have essentially the same characteristic shape. The average load-displacement behaviour from zero to failure is shown in Figure 4.4 and 4.5 for the longitudinal (L) and transverse (T) directions, respectively. The following values for the stiffness (K) and the ultimate load (F_u) are then obtained from these curves:

$$K_L = 8400 \text{ lb/in.}$$

$$F_{uL} = 450 \text{ lbs.}$$

and

K_T = 6720 lb/in.

F_{uT} = 330 lbs.

It can be seen that the two curves are expressing similar behaviour; with higher values for both the stiffness and failure load in the "longitudinal" direction. The two curves are characterized by an initial slip stage at very low levels of loading (this stage being shorter in the case of smaller predrilled hole), then both followed almost a linear behaviour till about 85% of the failure load. From this level of loading to failure, the connection exhibits a slight nonlinear behaviour.

The effects of the connections three design parameters on its stiffness and ultimate strength are summarized in the following:

(1) A decrease in the hole diameter slightly increases (5-10%) both the ultimate load and stiffness of the connection.

(2) An increase of the edge distance in the direction of loading increases significantly the ultimate load (20-30%) while affects very little the connection stiffness. And,

(3) An increase of the specimens width increases the connection ultimate load (20-30%) and only slightly the stiffness (10%).

As for the failure mode, tilting of the bolt and bending of the pal nut was always present at high loads close to the ultimate, this is being followed by a transverse tension-tearing across the specimen's net section (Fig. 4.6). Failure of all specimens was sudden with chart pen dropping to almost zero load (complete separation). Finally, it is interesting to recall the behaviour of this type of fastener in the full-scale tests on cavity decks (see Section 3.6.2.1 and Fig. 3.17) and observe the great similarity to its behaviour in the current lapped-joint tests.

4.3.2 Test Results of Second Type

The main parameters considered in this test series were: the diameter of the predrilled screw hole (11/64", 3/16", and 7/32"), the width of the test specimen (1", $1\frac{1}{4}$", and 2"), and the edge distance from the center of screw in the direction of loading (5/8", 1" and 2"). As in the previous test series, 9 combinations of these variables were considered for testing, by keeping each two of the underlined values of the parameters unchanged while varying the third parameter.

Similar to the results obtained for the first type, average load-displacement curves in both the longitudinal and transverse directions were obtained (Figures 4.7 and 4.8, respectively). Each curve shows two distinguished stages. The first stage is linear up to approximately 50% of the ultimate load, and in the second stage, the curve deviates progressively in another linear path with a reduced stiffness till failure. The two curves were used to establish the following values for the initial stiffness and ultimate load, in the two directions:

$$K_L = 19600 \text{ lb/in.}$$
$$F_{uL} = 500 \text{ lbs.}$$

and

$$K_T = 11760 \text{ lb/in.}$$
$$F_{uT} = 330 \text{ lbs.}$$

Comparing the above results to those obtained for the first type of seam connections, it is clear that the present connection (self-tapping screws) exhibited substantially higher rigidity, in the two directions, than those for the first type. However, the ultimate loads of the present connection are only slightly higher. This is quite expected, as failure of both types occurs in the asbestos plate across its net section (Fig. 4.9).

The results of the parametric study of these test series were found to be similar to those of the first type, with the scatter of results being within a slightly lower range.

4.4 PANELS TO FRAME CONNECTIONS

In the two decking systems, the connections between the asbestos sheets and the steel framing members (end, side, shear connector or purlin) are effected by the self-tapping screw #14 x 1" type "B" (hexagonal headed) with a 3/4" x 9/32" washer (Fig. 4.10). The washer is known to help in spreading the load over a larger area of the sheeting and to ensure a more uniform tightness which is essential to obtain a consistently rigid and strong connection.

In current practice, the hole drilled in the asbestos sheet is 1/4" diameter while that in the steel flange is 3/16" diameter. In this test series, the specimen size as well as the main parameters are similar to those of the previous test series (second type of seam fasteners).

4.4.1 Test Results

The average load-displacement curves for this type of connection are shown in Figures 4.11 and 4.12, in the longitudinal and transverse directions, respectively. As can be seen, the two curves are almost linear up to approximately 65% of the ultimate load then showing a more pronounced nonlinear behaviour (especially in the longitudinal direction) till failure. The two curves were used to establish the following values for the initial stiffness and ultimate load, in the two directions:

$$K_L = 28000 \text{ lb/in.}$$

$$F_{uL} = 850 \text{ lbs.}$$

and

$$K_T = 28000 \text{ lb/in}$$

$$F_{uT} = 670 \text{ lbs.}$$

It is to be noted that scatter of this test series results was much less than that in the seam connections tests. The reason for this could be attributed to the use of the washer as previously mentioned. It is also believed that the much higher values for the load carrying capacity and stiffness for this connection type when compared to seam connections, is due to the presence of the heavy steel plate, thus restraining the tilting of screw under load.

4.4.2 Failure Modes

The failure mode of these connections was variable depending on the geometric design and edge distances of the connection. As can be seen in Fig. 4.13, failure was either due to transverse tension-tearing across the specimen's net section (for large edge distances), or due to horizontal and vertical cracking (small edge distances). A third mode of failure was also observed (Fig. 4.14a), where failure occurred due to a diagonal and vertical cracking of the asbestos sheet at the screw. The latter mode was associated with specimens of typical representation of the actual connections in the full-scale tests. Fig. 4.14b shows the most common failure mode at the end fasteners observed in the full-scale tests reported in the previous chapter. Comparing the two photographs, it is interesting to note the great similarity between the performance of the prototype and its model.

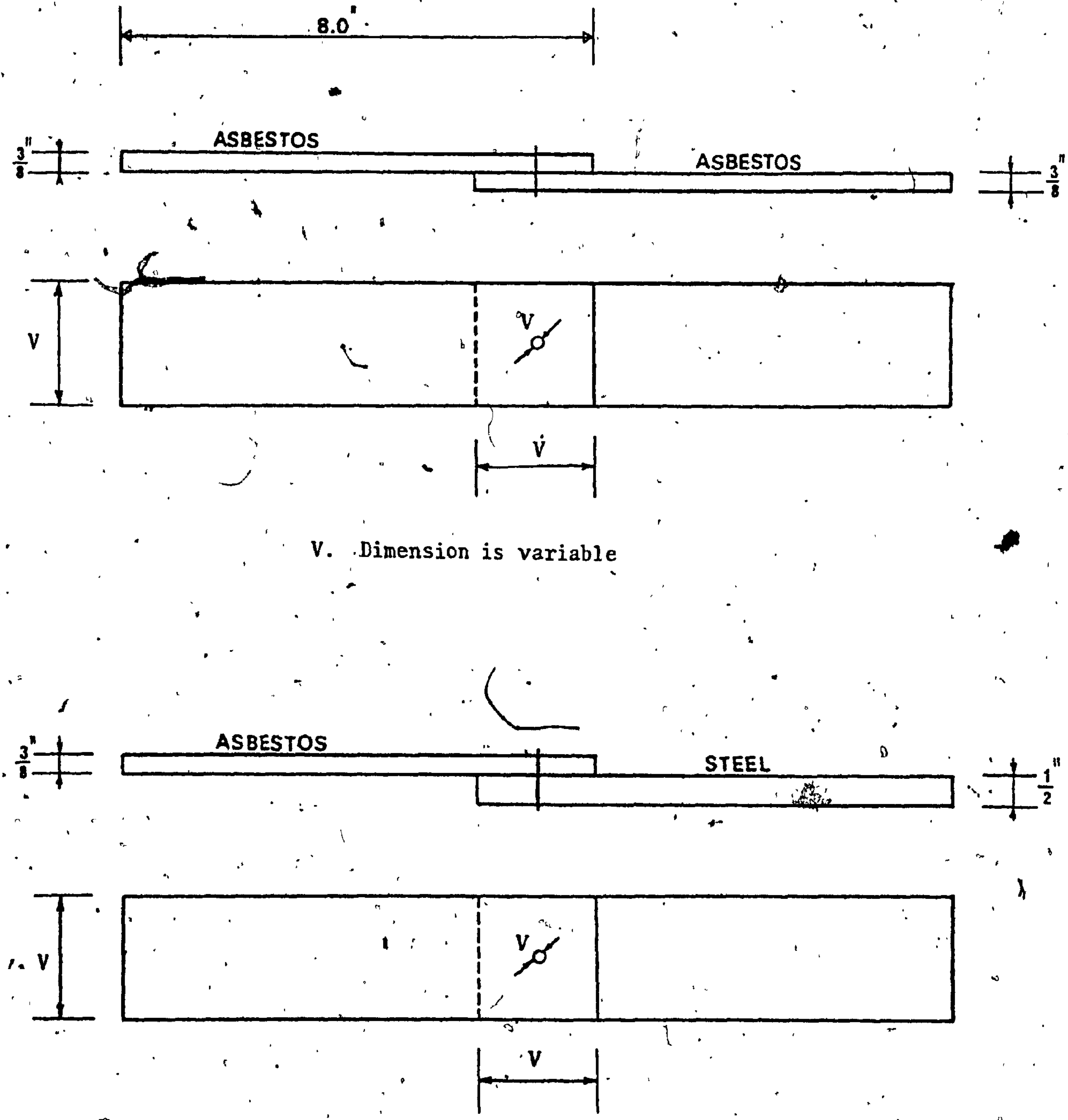

V. Dimension is variable

FIG. 4.1 LAPPED-JOINTS TENSION TEST SPECIMENS

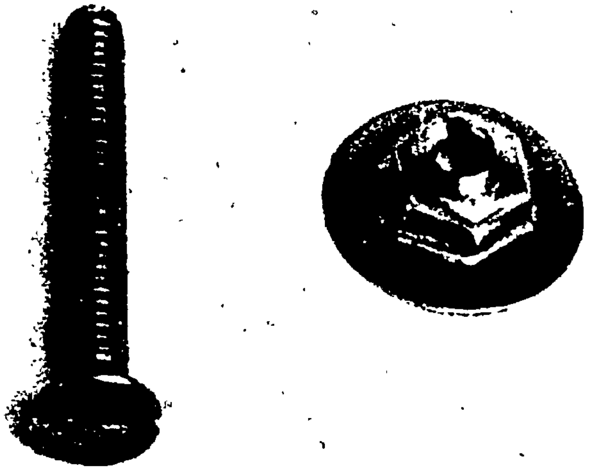

FIG. 4.2 FIRST TYPE OF SEAM FASTENERS: 1½" X 3/8" DIAMETER FLAT HEAD STAINLESS STEEL BOLT AND CADMIUM PLATED PAL NUT

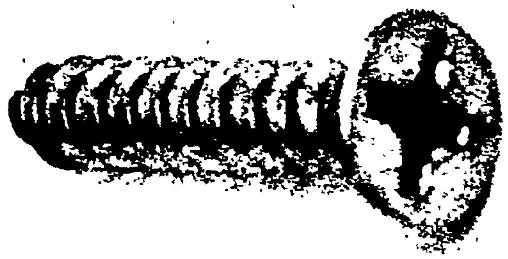

FIG. 4.3 SECOND TYPE OF SEAM FASTENERS: 1¼" X NO. 2 FLAT HEAD "A" TYPE SELF-TAPPING SCREW

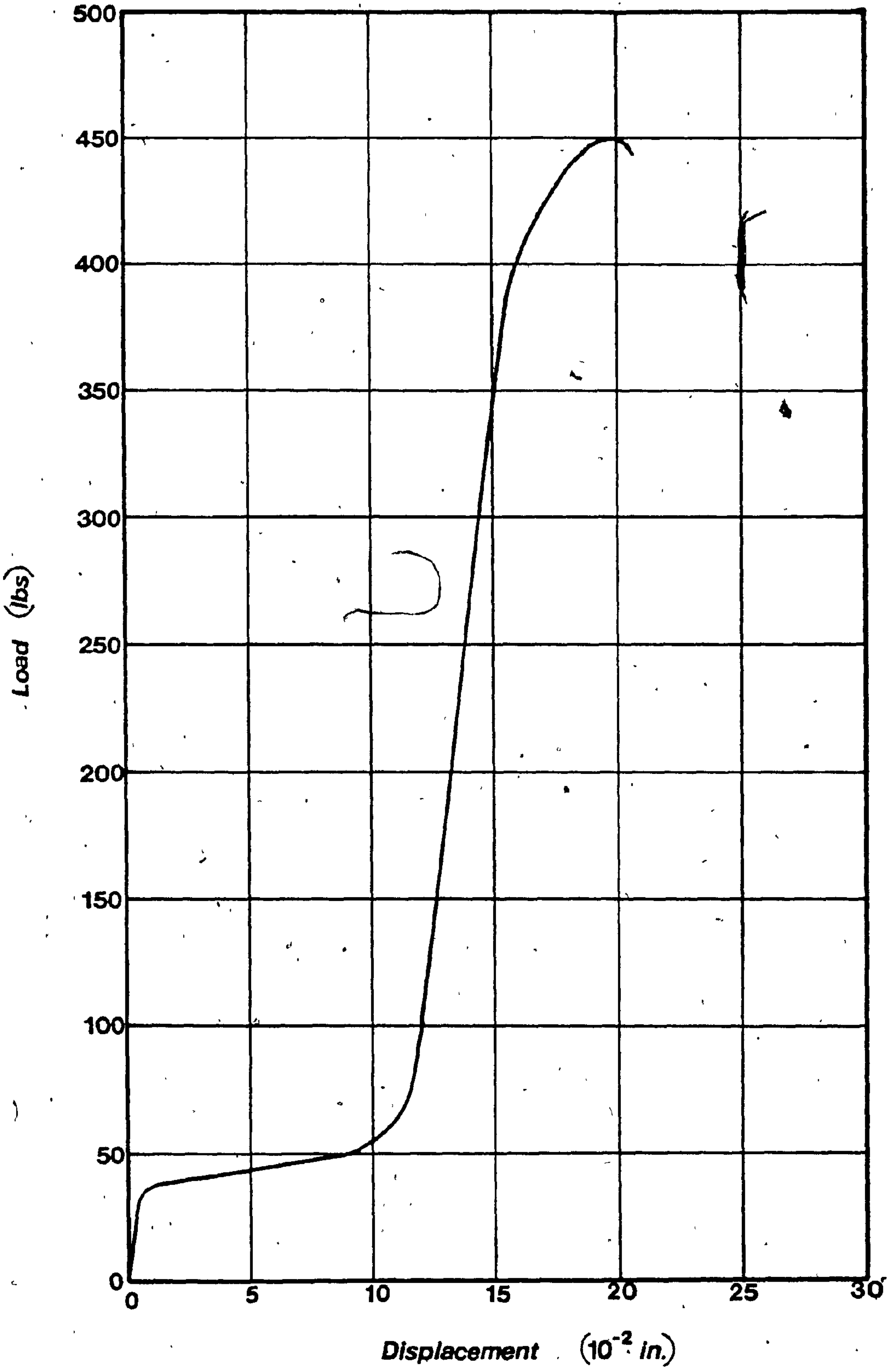

FIG. 4.4 LOAD VS. SLIP FOR FIRST TYPE OF SEAM CONNECTIONS - IN THE LONGITUDINAL DIRECTION

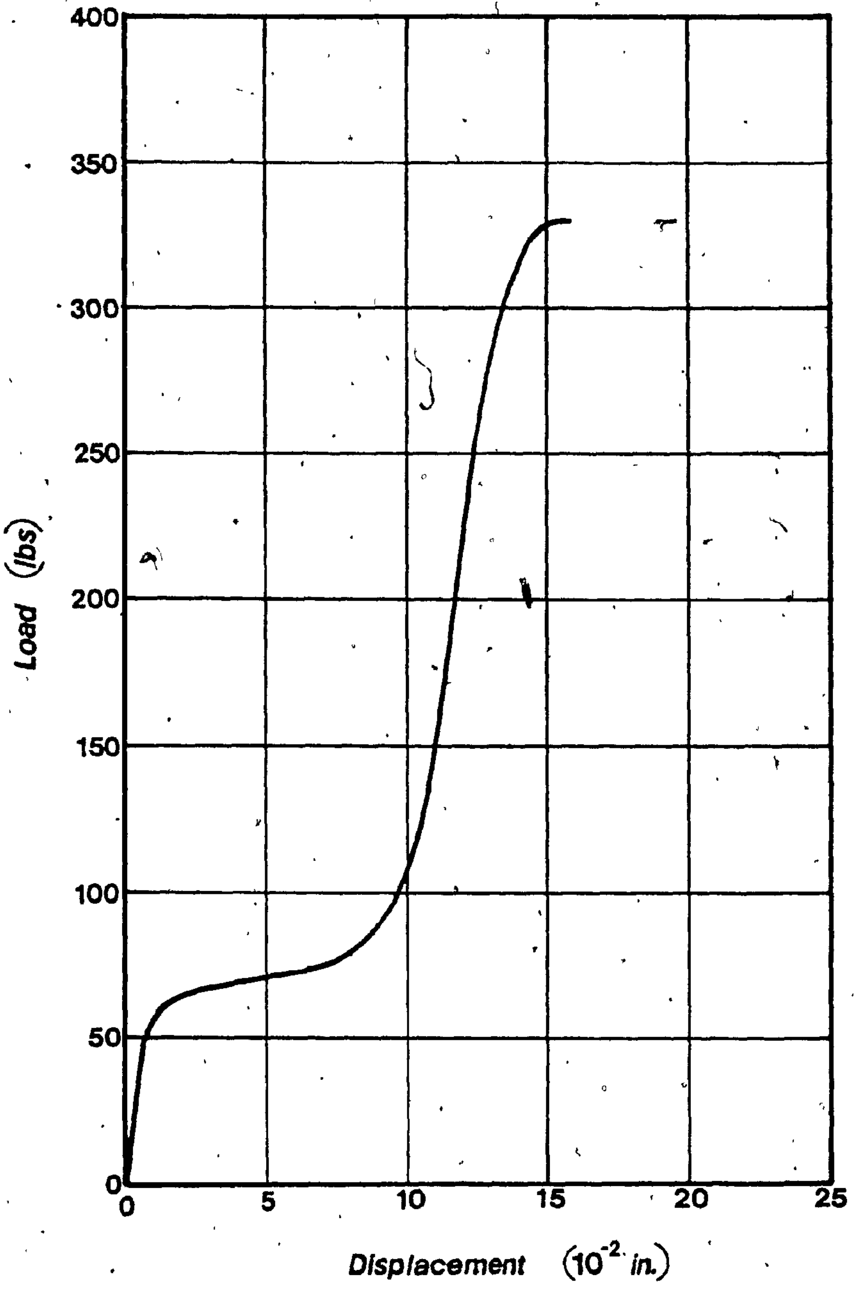

FIG. 4.5 LOAD VS. SLIP FOR FIRST TYPE OF SEAM CONNECTIONS – IN THE TRANSVERSE DIRECTION

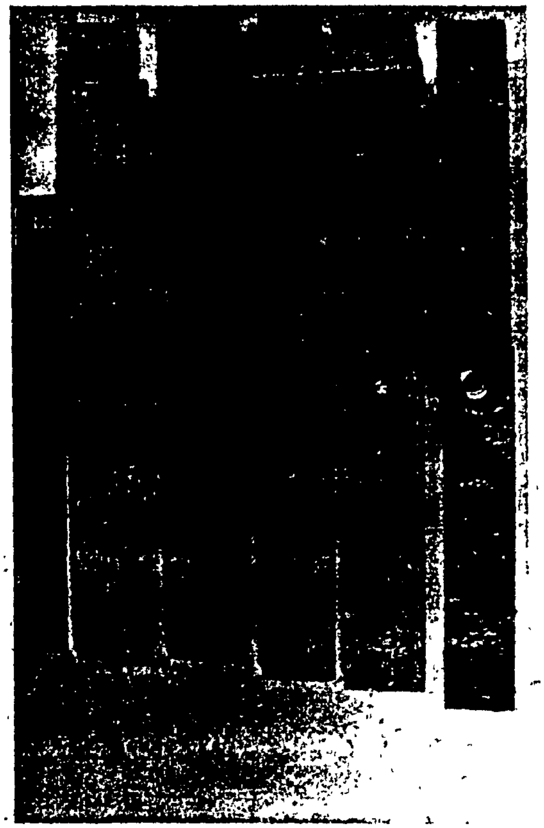

FIG. 4.6 FAILURE MODE - FIRST TYPE OF SEAM FASTENERS

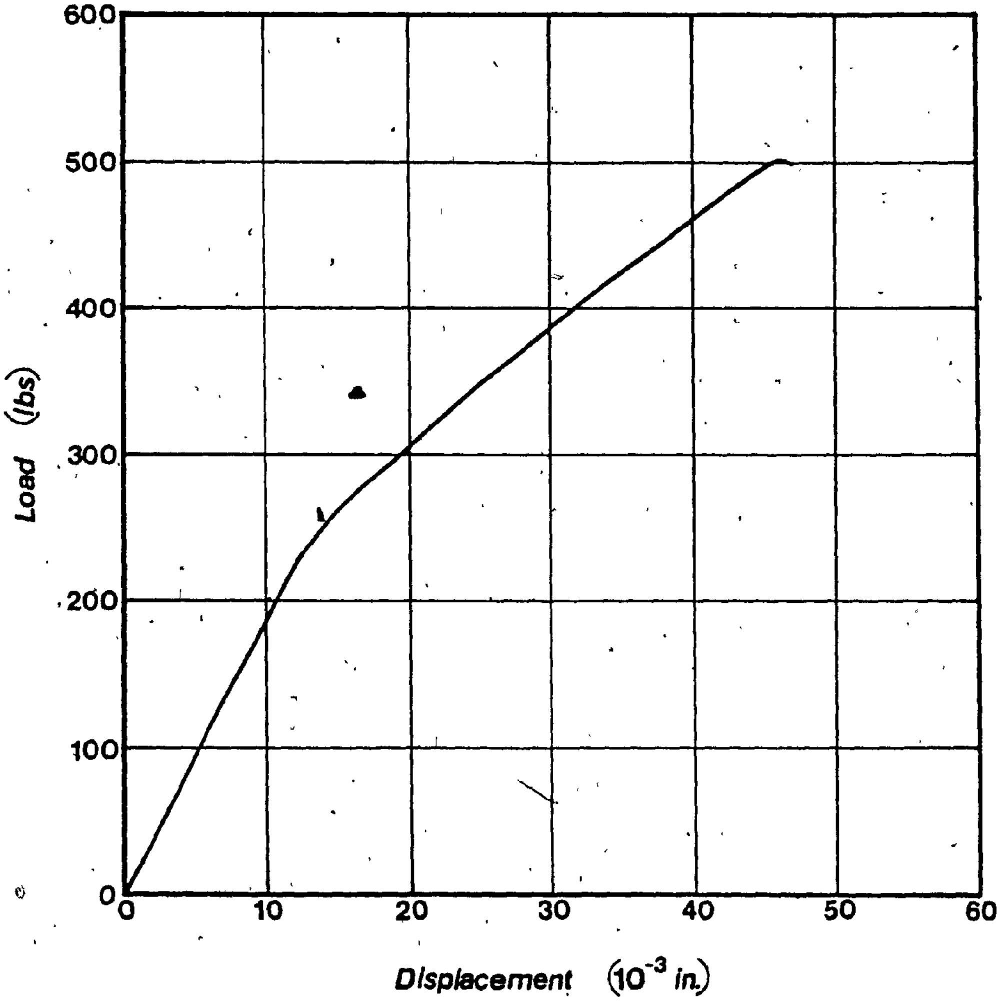

FIG. 4.7 LOAD VS. SLIP FOR SECOND TYPE OF SEAM CONNECTIONS - IN THE LONGITUDINAL DIRECTION

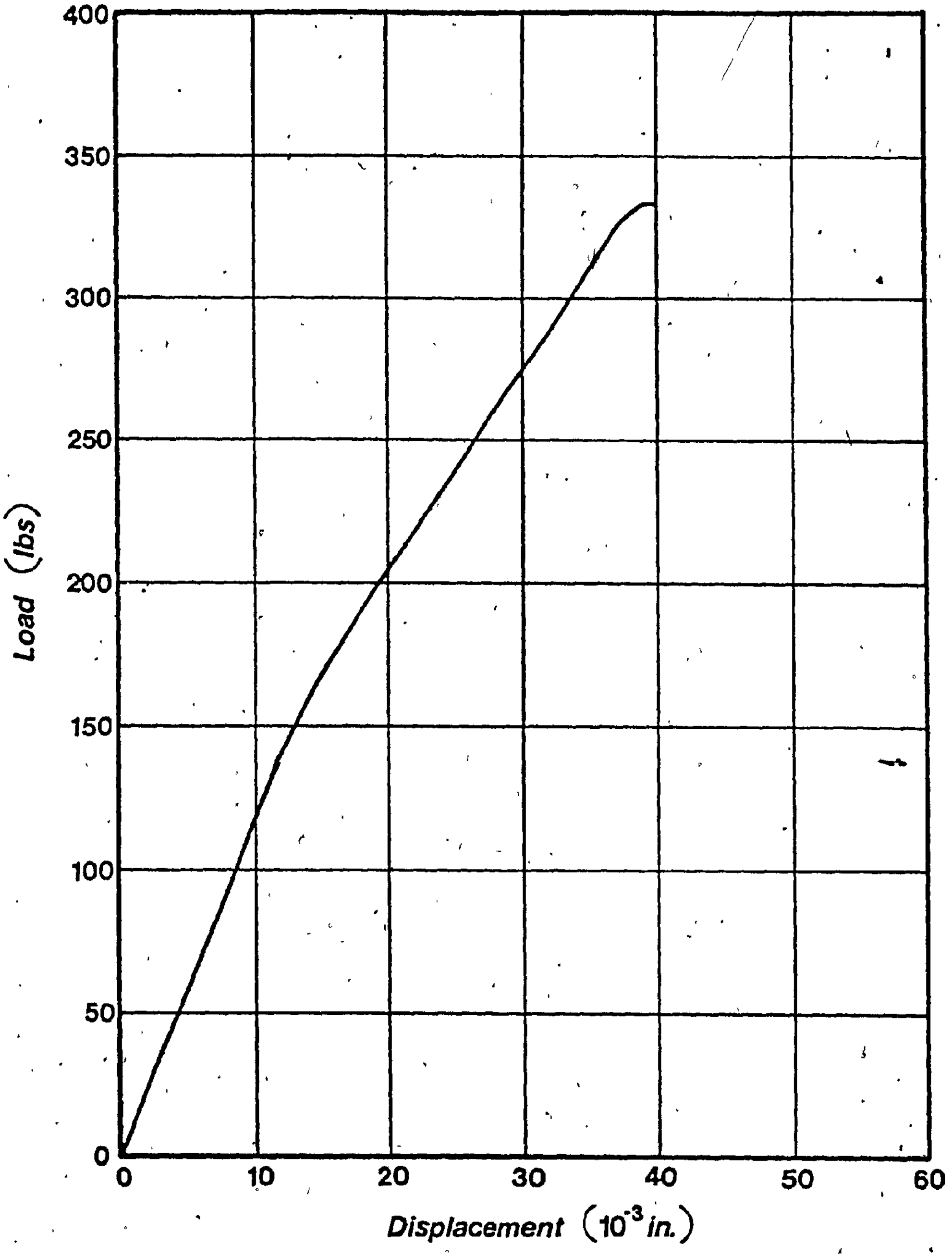

FIG. 4.8 LOAD VS. SLIP FOR SECOND TYPE OF SEAM CONNECTIONS - IN THE TRANSVERSE DIRECTION

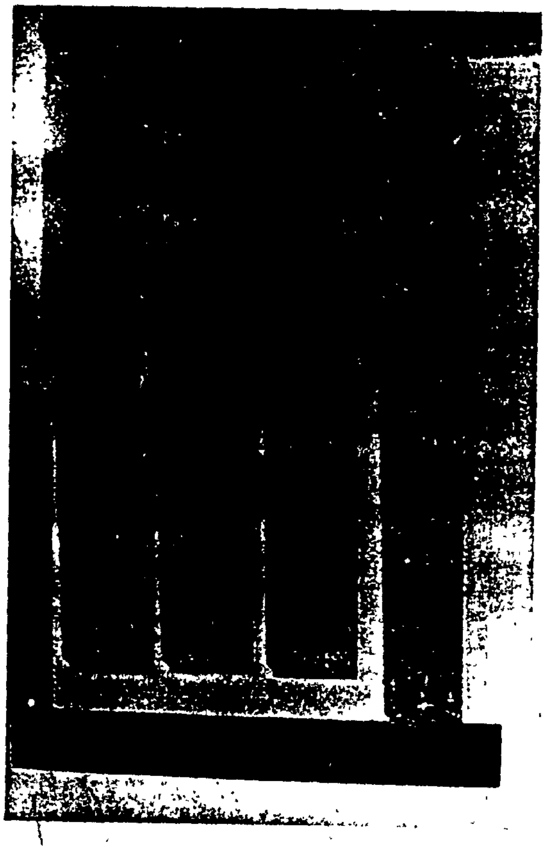

FIG. 4.9 FAILURE MODE - SECOND TYPE OF SEAM FASTENERS

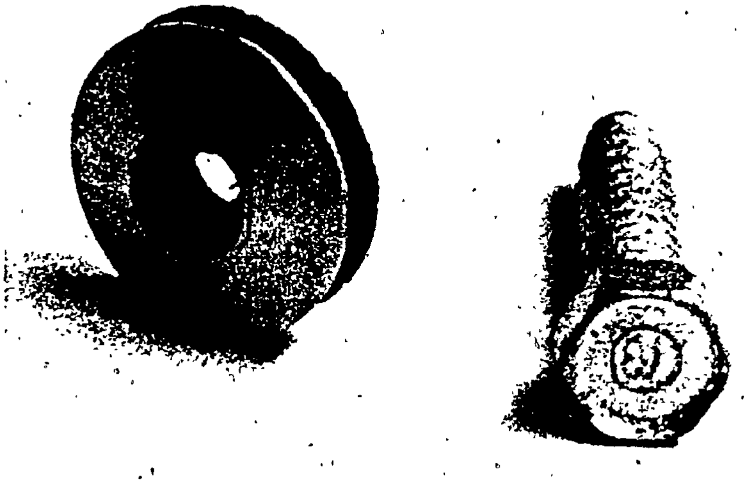

FIG. 4.10 ASBESTOS-TO-STEEL FASTENER: #14X1" TYPE "B" SELF-TAPPING SCREW AND 3/4" X 9/32" WASHER

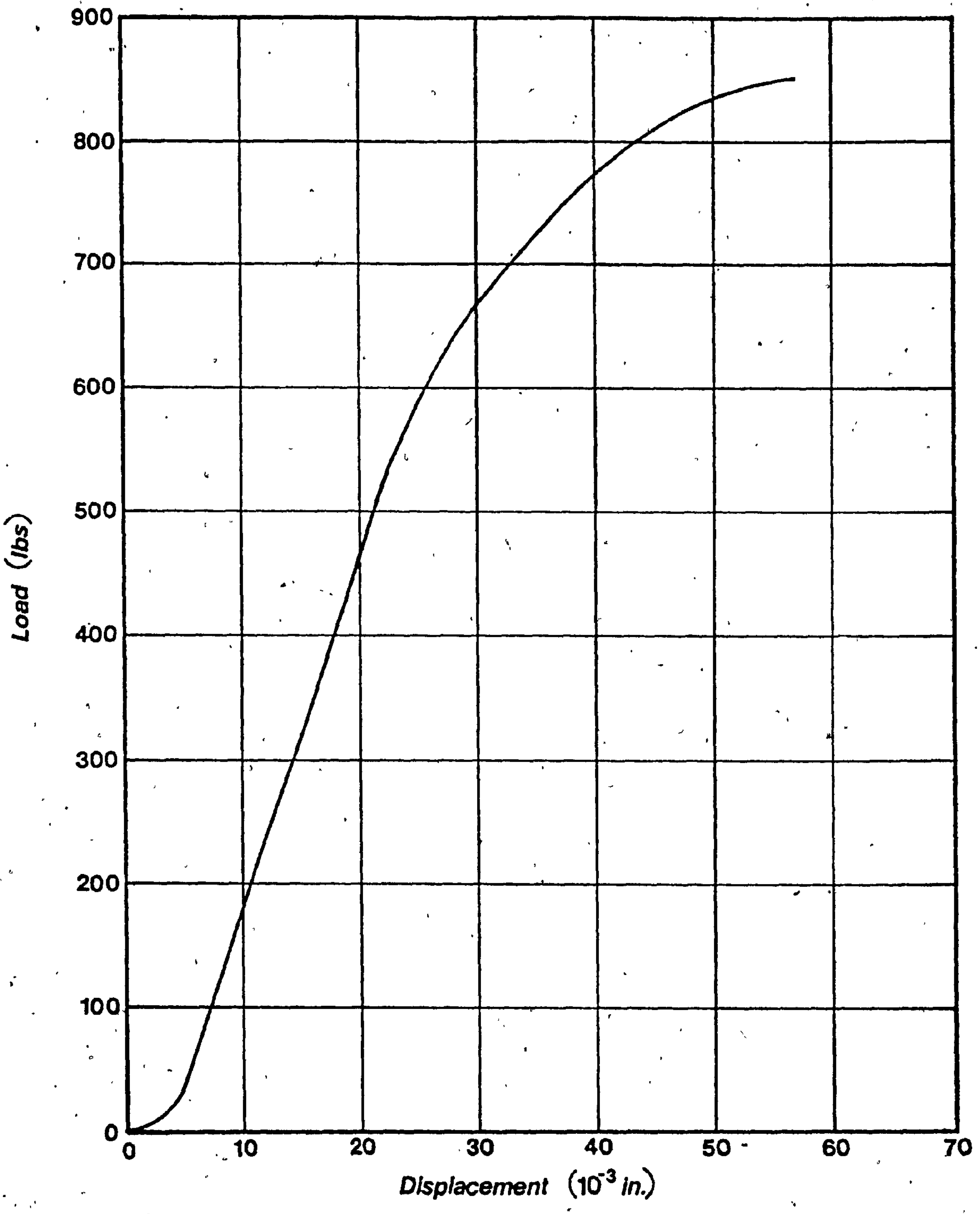

FIG. 4.11 LOAD VS. SLIP FOR @14 SCREW FASTENED PANEL TO FRAME CONNECTIONS - IN THE LONGITUDINAL DIRECTION

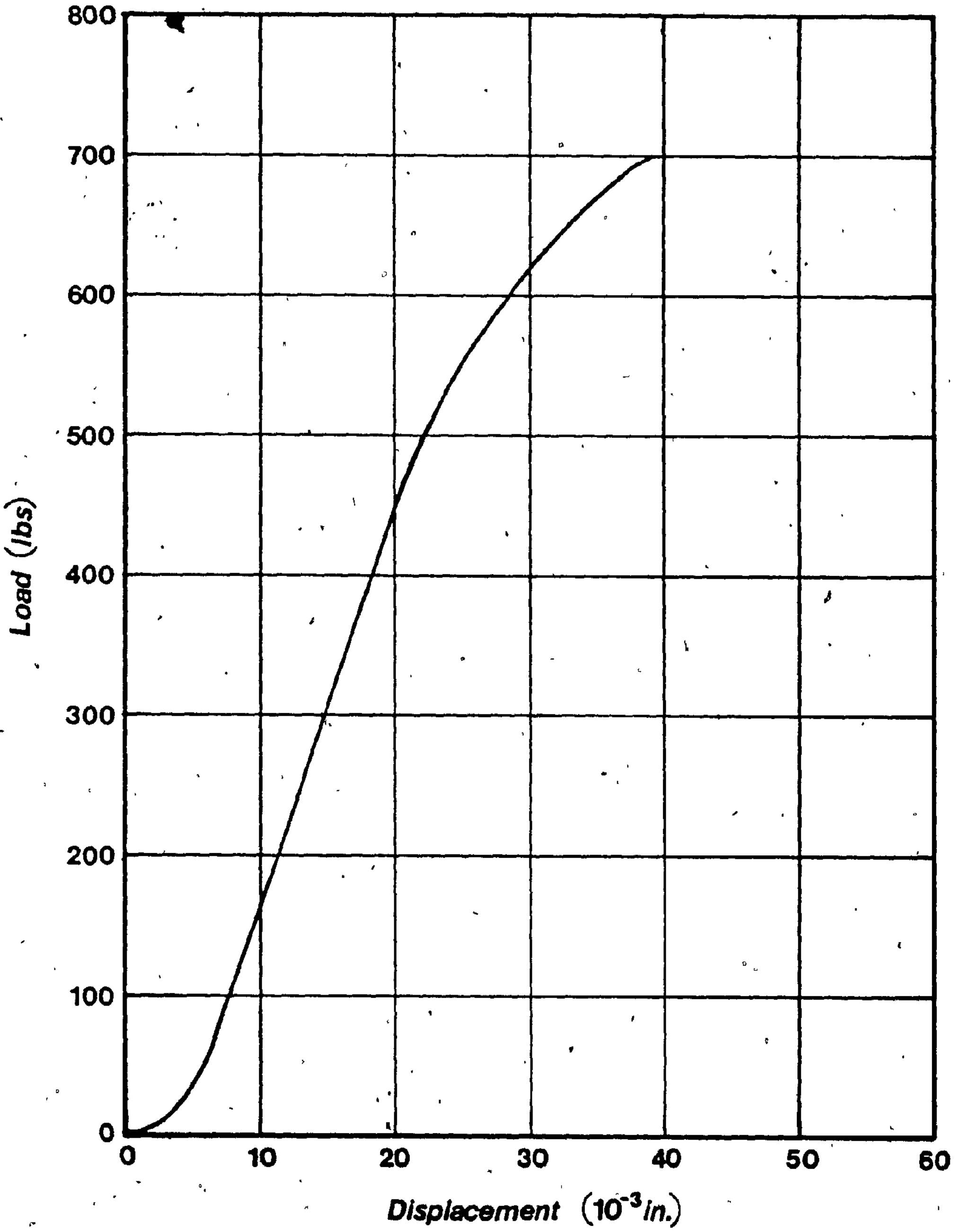

FIG. 4.12 LOAD VS. SLIP FOR @14 SCREW FASTENED PANEL TO FRAME CONNECTIONS - IN THE TRANSVERSE DIRECTION

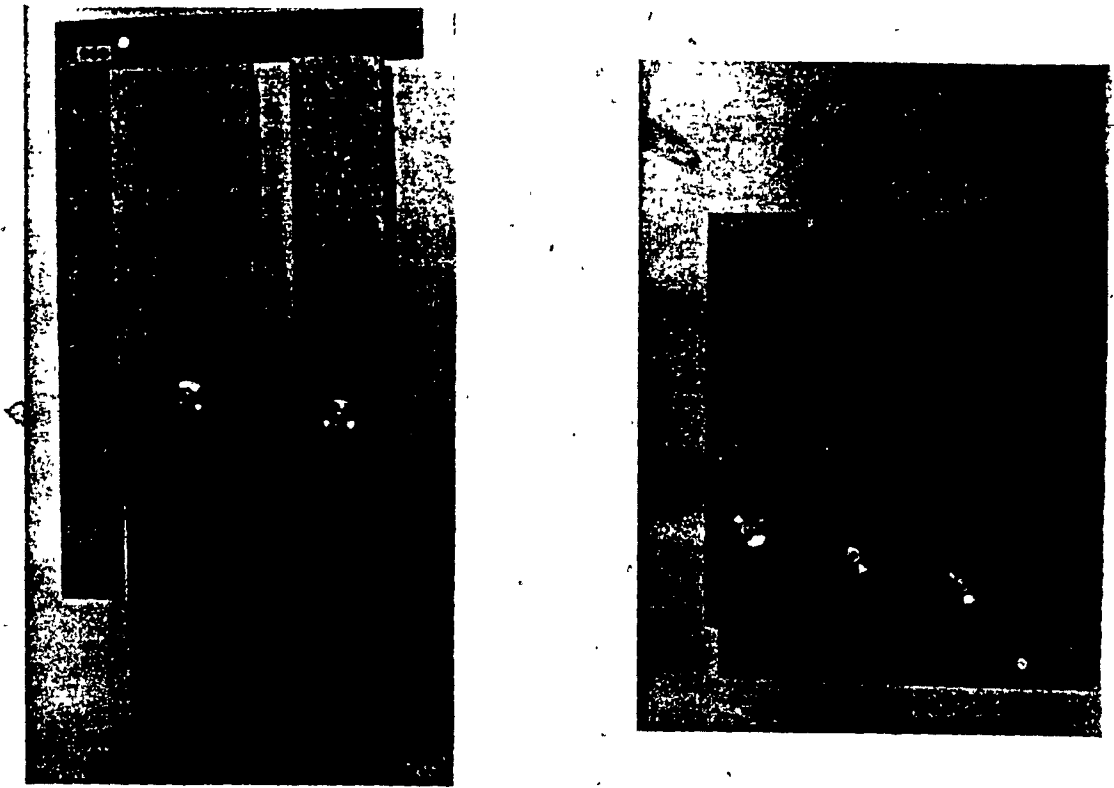

FIG. 4.13 FAILURE MODES - ASBESTOS-TO-FRAME FASTENERS

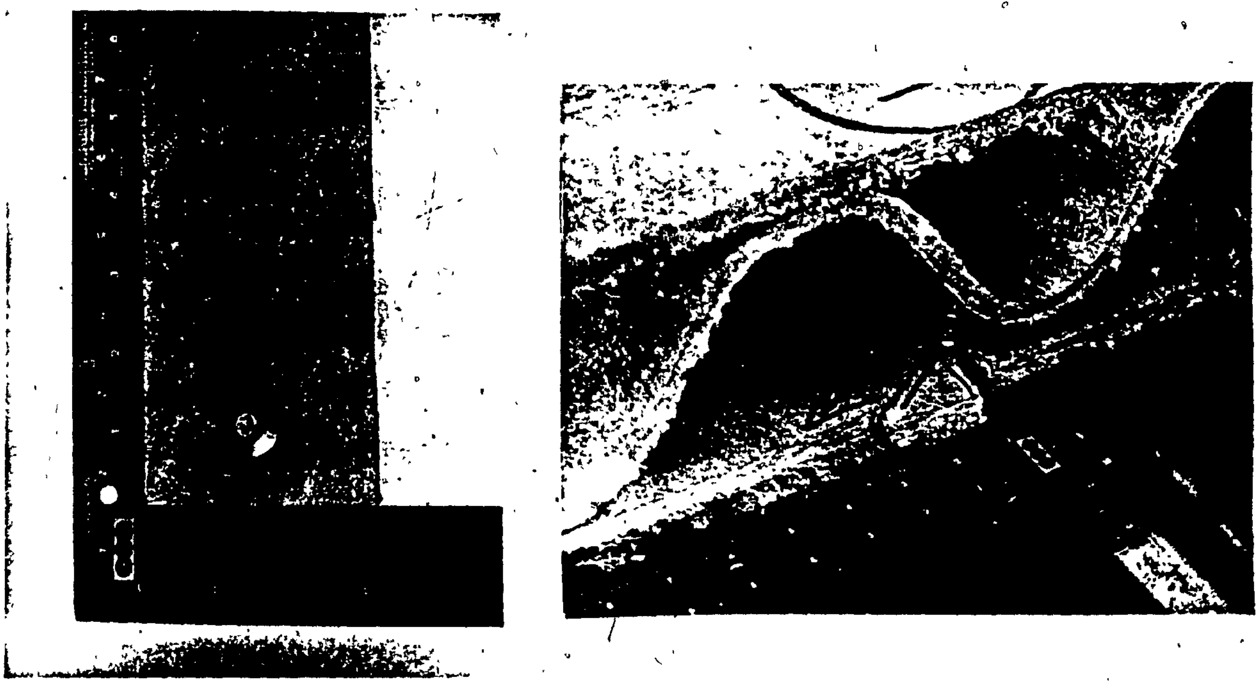

FIG. 4.14 FAILURE MODE OF ASBESTOS-TO-FRAME CONNECTION IN TESTED SPECIMEN AND IN ACTUAL DIAPHRAGM

CHAPTER V

FINITE ELEMENT ANALYSIS AND CORRELATION WITH EXPERIMENTAL RESULTS

CHAPTER V

FINITE ELEMENT ANALYSIS AND CORRELATION WITH EXPERIMENTAL RESULTS

5.1 INTRODUCTION

The finite element method has been extensively developed to a stage where it becomes a powerful numerical technique for solution of a large variety of physical problems. A comprehensive presentation of the method and its many applications has been given by Zienkiewicz [53] and many others [e.g., 54-57]. In the application of the finite element method to structural problems, the structure is idealized to consist of a large number of interconnected elemental regions in which the relationship between force, displacement and strain may be determined by using energy methods. The behaviour within a region (or element) is specified in terms of some parameters at the nodal points which are the points where the elements are joined together. In simple elements, nodal points are often located at the element corners, and in more complex elements additional nodal points may be assigned at the mid-points of the element sides.

The nodal parameters are usually specified in terms of displacements and rotations. Since these nodal parameters are common to the adjacent elements, compatibility of the element deformations is achieved at the nodes. Along the element edges, compatibility may or may not be maintained depending on the theoretical basis upon which the element behaviour is derived.

For solutions, the direct stiffness method is employed to determine the nodal parameters satisfying the overall equilibrium of the structure, the elements and of the nodal points. In general, only approximate solutions can be obtained with this technique since the differential equations of equilibrium and compatability may be violated within the element and along the element edges.

The application of the finite element method to the analysis of shear diaphragms is not new. It was initiated both in the U.S. [45, 58-60] and Australia [61]. Since then, it has been regarded as the most accurate and reliable analytical technique to predict the diaphragm responses, and it has often been used to check the accuracy of other approximate methods [62-68].

The finite element method has several advantages, which include:

(1) A realistic idealization of a complex structure.

(2) A large variety of elements of different types and shapes.

(3) The ability to accommodate arbitrary support conditions and loading, and

(4) The ability to provide detailed information on the distribution of internal forces on the constituent components.

In this chapter, the application of the finite element method is extended to predict the response of absestos-cement diaphragms.

5.1.1 Basic Assumptions

It has been observed in the full-scale tests already performed (Chapter III) that:

(1) The connections play a major role in the behaviour of diaphragms influencing both the stiffness and ultimate strength.

(2) The failure modes are characterized by localized failures at the connections.

(3) At low levels of loading, the shear is mainly transmitted through the continuous flat surface part of the decking.

Based on the above observations and also on previous experience on the finite element analysis of light-gauge steel diaphragms, the following assumptions are made:

(1) All diaphragm components (asbestos sheeting, steel framing members and connections) have linearly elastic behaviour.

(2) The full shear load is transmitted through the flat sheets of the profiles, which span continuously from one side marginal member to the other. The other parts of the profile are considered effective only for stiffening the diaphragm against overall buckling and transverse bending.

The first assumption ignores the nonlinear behaviour of connections and thus neglects the possible redistribution of fastener forces at collapse. However, small-scale tests on connections have shown that they behave linearly to about 50-65% of their ultimate load. Also, in the full-scale tests, it has been observed that only a small number of connections (characteristically near the diaphragm corners) are stressed beyond this linear range. The second assumption related to the neglect of the stiffness of the corrugated part of the profile seems to be reasonable for the case of cavity decking due to the existence of the continuous and interconnected flat sheet. In the case of T-deck diaphragms, because the sheets are actually connected to the end framing members at the corrugations and not directly at the top continuous flat sheets (see Fig. 3.12d), this assumption may be questionable. However, because of the large disparity between the stiffnesses of the sheeting and the connections, the error introduced is negligible. These assumptions are adopted in order to avoid an overly complex modelling of the diaphragms.

In spite of the above simplifying assumptions, the finite element analyses of tested diaphragms will be shown to predict the diaphragm behaviour satisfactorily.

5.1.2 Type of Analysis

Matrix methods of structural analysis based on discrete element idealization may be classified broadly into two groups:

(1) Displacement methods (stiffness methods), in which geometrically compatible states in individual elements are combined to give equilibrium, and

(2) Force methods (flexibility methods), in which equilibrium states in individual elements are combined to give geometric compatibility.

Historically, when computers came into use for structural analysis, it was soon recognized that the displacement methods could be easily formulated for computer programming, and it has become the dominating approach in the finite element methods.

One of the characteristic features of the displacement methods is that the question of statical redundancy does not arise, as the direct solution is for the unknown displacements at the nodal points. These nodal displacements are used to calculate the resulting stress distributions (or internal forces) within the individual elements. Since shear diaphragms are highly redundant structures, the displacement method is therfore adopted in the present work.

5.2 FINITE ELEMENT IDEALIZATION AND ELEMENTS STIFFNESSES

The main components of the structural idealization of a diaphragm system are the marginal framing members, the purlins, the panel sheets and the connections. Similar to previous investigations [58-60], three basic elements are used in the finite element modelling of asbestos diaphragms. For illustration, the analytical finite element model for a simple diaphragm with four panels and its attachment is shown in Fig. 5.1. The steel perimeter members are simulated by beam type elements having axial and bending stiffnesses. The sheeting is simulated by plane stress plate elements. Finally, the different discrete connections are represented individually by two-dimensional linkage elements of zero size. In the following, the three basic elements will be described and their stiffness matrices are given.

5.2.1 Marginal Frame Members and Purlins

The frame members and purlins are idealized by one-dimensional linear elastic prismatic beam elements having three degrees of freedom at each of its two nodes as shown in Fig. 5.2a. The three degrees of freedom at each node represent the axial and the transverse displacements in the plane of the diaphragm, and the rotation about the vertical axis to diaphragm surface. The stiffness matrix of this element is well known and can be found in many texts [e.g. 69,70].

Based on a cubic displacement function, the stiffness matrix is given by

$$[K_{bx}] = \begin{bmatrix} \frac{EA}{L} & 0 & 0 & -\frac{EA}{L} & 0 & 0 \\ & \frac{12EI}{L^3} & \frac{-6EI}{L^2} & 0 & -\frac{12EI}{L^3} & -\frac{6EI}{L^2} \\ & & \frac{4EI}{L} & 0 & \frac{6EI}{L^2} & \frac{2EI}{L} \\ & & & \frac{EA}{L} & 0 & 0 \\ & \text{Symmetric} & & & \frac{12EI}{L^3} & \frac{6EI}{L^2} \\ & & & & & \frac{4EI}{L} \end{bmatrix} \qquad (5.1)$$

where

L is the length of element

A is the cross sectional area of element

and I is the moment of inertia about the axis of bending.

It should be noted that the above stiffness matrix corresponds to elements in the modelling of marginal members or purlins positioned parallel to the x-direction (Fig. 5.1), where the local axes of the element and the global axes of the system are the same. In the case of side members (the marginal members parallel to the y-direction), Fig. 5.2b, the stiffness matrix of the element after transformation from local to global system coordinates is given by

$$[K_{by}] = \begin{bmatrix} \frac{12EI}{L^3} & 0 & -\frac{6EI}{L^2} & -\frac{12EI}{L^3} & 0 & -\frac{6EI}{L^2} \\ & \frac{EA}{L} & 0 & 0 & -\frac{EA}{L} & 0 \\ & & \frac{4EI}{L} & \frac{6EI}{L^2} & 0 & \frac{2EI}{L} \\ & & & \frac{12EI}{L^3} & 0 & \frac{6EI}{L^2} \\ & & & & \frac{EA}{L} & 0 \\ & & & & & \frac{4EI}{L} \end{bmatrix} \qquad (5.2)$$

5.2.2 Deck Panels

The continuous flat sheeting is modelled by two-dimensional plane stress orthotropic plate elements. As shown in Fig. 5.3, this element is a basic four-noded rectangle having two translational degrees of freedom at each node. The derivation of the element stiffness matrix was carried out by Ammar [45] in the standard way. Based on a bilinear displacement function, the element stiffness matrix is given by

$$[K_p] = \begin{bmatrix} B_1 & B_2 & B_3 & B_4 & -\frac{B_1}{2} & -B_2 & B_5 & -B_4 \\ & B_6 & -B_4 & B_7 & -B_2 & -\frac{B_6}{2} & B_4 & B_8 \\ & & B_1 & -B_2 & B_5 & B_4 & -\frac{B_1}{2} & B_2 \\ & & & B_6 & -B_4 & B_8 & B_2 & -\frac{B_6}{2} \\ & & & & B_1 & B_2 & B_3 & B_4 \\ & \text{Symmetric} & & & & B_6 & -B_4 & B_7 \\ & & & & & & B_1 & -B_2 \\ & & & & & & & B_6 \end{bmatrix} \qquad (5.3)$$

where the expressions B_1 to B_8 are given by:

$$\begin{aligned} B_1 &= \frac{t}{3}\left(\frac{E_{xx}}{r\lambda} + r\,G_{xy}\right) \\ B_2 &= \frac{t}{4}\left(\frac{\nu_{yx}E_{xx}}{\lambda} + G_{xy}\right) \\ B_3 &= \frac{t}{6}\left(\frac{-2E_{xx}}{r\lambda} + r\,G_{xy}\right) \\ B_4 &= \frac{t}{4}\left(\frac{\nu_{yx}E_{xx}}{\lambda} - G_{xy}\right) \\ B_5 &= \frac{t}{6}\left(\frac{E_{xx}}{r\lambda} - 2r\,G_{xy}\right) \\ B_6 &= \frac{t}{3}\left(\frac{rE_{yy}}{\lambda} + \frac{G_{xy}}{r}\right) \end{aligned} \qquad (5.4)$$

$$B_7 = \frac{t}{6}\left(\frac{rE_{yy}}{\lambda} - \frac{2G_{xy}}{r}\right)$$

$$B_8 = \frac{t}{6}\left(\frac{-2rE_{yy}}{\lambda} + \frac{G_{xy}}{r}\right)$$

where E_{xx}, E_{yy}, ν_{yx} and G_{xy} are the elastic constants of the orthotropic medium; t is the plate thickness; r = a/b is the aspect ratio of the rectangle used, and $\lambda = (1 - \nu_{xy}\nu_{yx})$. The material elastic constants are those found experimentally (Chapter II). For details on the derivation of the $[K_p]$ matrix, refer to Ref. 45.

5.2.3 Connections

In a diaphragm installation, four types of connections can be present, those between the sheets and themselves (seam connections), or those connecting the sheets to the end marginal members (end connections), or those connecting the sheets to the side marginal members (side connections) and finally the fasteners connecting the sheets to intermediate purlins. In the finite element model, dual points are established at such locations and the connection is modelled by a zero size linkage element connecting the two nodal points. A linkage element have two mutually perpendicular springs (Fig. 5.4) of stiffness K_x and K_y, to account for slip resistance in each direction, parallel and perpendicular to the panel edge, respectively. The linkage element is represented by a 4x4 matrix formed by two uncoupled 2x2 submatrices as:

$$[K_c] = \begin{bmatrix} K_x & -K_x & 0 & 0 \\ -K_x & K_x & 0 & 0 \\ 0 & 0 & K_y & -K_y \\ 0 & 0 & -K_y & K_y \end{bmatrix} \qquad (5.5)$$

The values of K_x and K_y have been determined experimentally for the different types of fasteners used in the two decking systems as reported in the previous chapter.

5.3 METHOD OF ANALYSIS

Once the element stiffness matrices have been established, the next step is the assembly of the overall or global stiffness matrix for the entire structure. The most common assembly technique is known as the "direct stiffness method", in which the coefficients of the global stiffness matrix are computed by simply adding relevant coefficients of the element stiffness matrices for common degrees of freedom (unknown displacements) at any node. This is traditionally achieved through what is termed, the element's "connectivity" matrix, relating two degrees of freedom (DOF) numbering systems, one for the overall structure and another assigned to the individual element. The relation between the two numbering systems determines the location in the global stiffness matrix to which coefficients of elements matrices are assigned.

By the direct stiffness method, a set of simultaneous linear algebraic equations will be obtained, relating loads to unknown displacements through the assembled structure stiffness matrix, as:

$$[K]\ \{U\} = \{P\} \tag{5.6}$$

in which

[K] - Structure's stiffness matrix

{U} - Unknown displacement vector

{P} - Load vector.

These equations cannot be solved until the geometric boundary conditions are taken into account by appropriate modification of the equations. The most straight forward approach, is to consider all nodes as being free when forming the global stiffness matrix and then introduce the boundary conditions afterwards. To preserve the banded nature of the equations, the row and column of [K] corresponding to each geometric boundary condition (support constraints in shear diaphragm analysis) are made null with the exception of the diagonal element, which is made unity [54].

5.4 SOLUTION OF EQUATIONS

The solution of the linear load-displacement equations (Eq. 5.6) is usually the most time-consuming computation step in the displacement method. Therefore, one of the most important features of a finite element program package is its ability of efficiently solving very large sets of linear equations.

The two basic approaches for the solution of large systems of equations are elimination and iteration. The former, also known as the direct approach and typified by Gaussian elimination, is a procedure wherein the matrix [K] is transformed to a triangular form which can be solved directly for the unknowns. The latter is a series of successive corrections to an initial estimate for the unknowns, the process being carried out repeatitively until the size of the necessary corrections becomes negligible.

Survey of the literature reveals that iterative methods for the solution of the load-deflection equations are seldom provided as a standard facility in the larger finite element computer packages. On the other hand, direct methods are used almost exclusively in finite element analysis programs. They have proved to be more versatile and reliable.

Direct (closed) methods as distinct from iterative methods yield the solution by performing a fixed number of arithmetic operations. There is no direct method possible which solves a general system of linear algebraic equations by a smaller total number of arithmetic operations than that which is required by Gaussian elimination [71,72]. Considerable research has been devoted towards finding very efficient equation solving algorithms. Although a great number of these algorithms are based on Gauss elimination, they differ in: the required data organization, the arrangement of the intermediate calculations, and their simplicity to be incorporated into structural analysis programs.

Based on the above discussion, it was decided to incorporate an efficient equation solver that uses Gauss elimination into a computer program specially developed for shear diaphragm analysis. The routine developed by Wilson et al. [73] is believed to provide the best compromise among efficiency, generality and ease of use. This routine (SESOL) has been used in a general structural analysis program [74] and demonstrated the desirable economy and efficiency. Basically the routine uses Gauss elimination on positive-definite symmetrical systems. The specific features are that systems of very large size and bandwidth can be solved and that all operations on zero elements are eliminated. Also, the routine is very simple and can be incorporated into existing or developed programs with minimum effort.

5.5 COMPUTER PROGRAM

Computer program SHEAR was developed to perform a linear-elastic analysis of shear diaphragms, employing the direct stiffness method of analysis. The program incorporates the equation solver (SESOL) [73] to effect an efficient solution of the system equations. The program was written in FORTRAN IV and run on a CDC 6600 computer.

Finite element computer programs are often criticized when involving a large volume of input data. Preparation of the input of a finite element grid (nodal coordinates, node and element numbering, elements' connectivities, element material properties, ...etc) is not only tedious and time-consuming, but it is also liable to error unless great care is taken in checking. This problem has been overcome to a large extent by the present program, which includes a special-purpose automatic data generator, thus reducing the input data to a few number of cards.

The program has the capability to analyse diaphragms with load configuration either parallel or perpendicular to panel's corrugations. In addition to the solution for nodal displacements, it provides detailed information regarding the distribution of internal forces in the constituent components.

A detailed description of the program, user's guide and FORTRAN listing are presented in Appendix C. Also, a sample input and output of the analysis of diaphragm C-2 is included.

5.6 DIAPHRAGM SIMULATION AND CORRELATION WITH EXPERIMENTAL RESULTS

To verify the validity of the basic assumptions made in Section 5.1.1, and to illustrate the efficiency and capabilities of the developed computer program, ten asbestos-cement diaphragms were analysed. The full-scale testing of these diaphragms, 6 of the cavity deck type and 4 of the "T" deck type, have been fully described in Chapter III. The main objective is to predict the diaphragm shear stiffness (or flexibility) and strength for each case, and to compare the results with experimental data.

As it is not practical to present here a detailed description of the finite element simulation of all the diaphragms analysed, only a typical one is described below. The cavity deck diaphragm of Test C-2 was chosen as a demonstrative example, as it involves the least number of elements, which makes it easier to display the idealization and results.

5.6.1 Diaphragm C-2, Finite Element Simulation

A schematic diagram of the structural model of the diaphragm and sequential numbering of the different types of elements is shown in Fig. 5.5. The assignment of coordinate (or degree of freedom DOF) numbers at the nodes is shown in Fig. 5.6. The two numbering schemes were generated automatically by the program. It should be noted that the DOF numbering scheme (Fig. 5.6) was such that it would yield the minimum bandwidth for the overall structure stiffness matrix, an essential feature for storage savings and speed of execution.

Each of the marginal test frame members AB and DC (in the y-direction) is modelled into six linear beam elements each 20" long; while each of members AC and BD (in the x-direction) is modelled into 18 elements each 7.5" long, as described in Section 5.2.1. For each element, longitudinal, transverse and rotational degree of freedom are assigned at each end, thus, axial deformation and bending about the vertical axis - z (normal to the diaphragm plane) are considered. This results in a 6x6 stiffness matrix expressing the contribution of a segment. At each of the four end corners of the test frame, a double node is used to model the hinged connections. These two nodes occupy the same position in space and have the same translational displacents but distinct rotations.

Each of the nine panels comprising the deck (only the bottom flat wings), is modelled into 12 plane stress orthotropic plate elements, giving a total of 108 elements. The size of each plate element is 20" (in the y-direction) by 7.5" (in the x-direction) producing an aspect ratio of $2\frac{2}{3}$. The thickness is taken as that of the flat plate 3/8", the elastic constants in the two principal directions were taken as those of the base material, determined experimentally (Chapter II) as: $E_L = 2.25 \times 10^6$ psi, $E_T = 1.70 \times 10^6$ psi, $\nu_{LT} = 0.2$, $\nu_{TL} = 0.15$ and $G_{LT} = 0.9 \times 10^6$ psi.

As for the three types of connections present in this diaphragm (end, side and seam fasteners), these are each idealized by two orthogonal springs as described in 5.2.3. The end fasteners, 7 in number at each end (the exterior panels were not connected in the test), are each modelled by two orthogonal springs with the stiffnesses: $K_x = K_y = 28000$ lb/in. The same spring constants are given to the connections modelling the side fasteners (5 on each side). The spring constants for the seam fasteners (5 in number for each seam), connecting the 9 cavity decking panels at their underlapping edges (bottom seams), are $K_x = 6720$ lb/in., and $K_y = 8400$ lb/in.

It can be noted from Fig. 5.5 that the lengths of the beam and the dimensions of plate elements are thus chosen to match the spacing pattern of the diaphragm connections. The resulting finite element model was found to be satisfactory, and it was felt that further refinement is

Another important aspect worth mentioning is in relation to the dimensional properties of the plate elements used in the analysis. Ammar [45] investigated the effect of the element's aspect ratio on the accuracy of results. His findings were: for the isotropic case (i.e., $E_L = E_T = E$, $\nu_{LT} = \nu_{TL} = \nu$ and $G = \frac{E}{2(1+\nu)}$), the aspect ratio should be kept below 3. However, in the orthotropic case, larger aspect ratios can be tolerated and may even be beneficial. Study of the terms on the main diagonal of the element stiffness matrix (Eqs. 5.3 and 5.4) discloses that the modulus of elasticity in the strong direction (E_{yy}) is multiplied by the ratio of the width to the length, i.e., the inverse of the aspect ratio. On the other hand, in the "weak direction", the modulus (E_{xx}) is multiplied by the aspect ratio itself. A large aspect ratio will thus have the effect of increasing the smaller terms and reducing the larger ones on the diagonal, resulting in a better conditioning of the matrix. In the present study, aspect ratios in the range of 1.5 to 3.0 have been used.

It is well known that with the use of conforming displacement finite element model, the solutions obtained provide an upper bound to the true stiffness of the structure. On the other hand, in the modelling of the two decking systems, only the flat part of the decking assembly is considered (Section 5.1.1). Thus, these two opposite effects make it impossible to predict whether the finite element solutions are truly the upper bound solutions. In addition, the large variation in the connections' stiffnesses and strengths may further accentuate the discrepancies between the finite element solutions and the experimental data.

5.6.2 Diaphragm Shear Flexibility

The computed shear flexibilities of the 10 diaphragms are compared with full-scale test results in Table 5.1. The computed diaphragm flexibilities can be seen to be in good agreement with those obtained from tests, especially for the cavity decks (discrepancy is less than 10%). The higher discrepancy observed in the results for the "T" deck diaphragms can be attributed to the second basic assumption made earlier in the finite element modelling of the diaphragm assembly (see section 5.1.1). It has been assumed that the presence of the profile corrugations and the warping in the case of "T" decks are ignored. The warping results in some reduction in the diaphragm's shear stiffness and strength.

5.6.3 Diaphragm Shear Strength

While the true strength of a diaphragm cannot be found from the elastic analysis, previous workers [45,62] have noted that a lower bound on the strength can be obtained by extrapolating from the results of the elastic analysis up to that load which produces failure in the most highly stressed part (usually a connector). In tests, because of the local inelastic deformations at the connections and the resulting redistribution of internal forces, diaphragms are expected to carry higher loads than those predicted based on an elastic analysis. Neglect of this redistribution will theoretically give a conservative estimate of the strength.

The results of finite element analysis provide extensive information regarding the distribution of internal forces in the panels, the fasteners and the test frame members. Although this additional data has no experimental counterpart, nevertheless, it provides a new insight into the diaphragm behaviour and thus, would permit more rational design.

The distributions of internal forces obtained for most of the diaphragms analysed followed a similar pattern as that for diaphragm C-2, which is described in detail and its strength estimate calculations in the following.

Figure 5.7 shows the distribution of forces imposed on the marginal beams BC and AD from the diaphragm end fasteners, in the lateral direction (transverse to beam length). A tensile force between beam and panel is considered to be positive.

For diaphragms having a single end fastener per panel end (the case in all tested cavity decking diaphragms, except for C-7), a typical pattern of lateral forces on end marginal beams is shown in Fig. 5.7. It can be observed that compression is present at one corner of the diaphragm and tension at the other corner. The distribution of lateral forces at the end fasteners between the two corners approximately fits a 3rd degree parabola along the beam length. In the other diaphragms (C-7 and "T" decks), the panel ends are connected with two fasteners per end. Distribution of lateral forces on end beams in this case also followed a typical pattern in which tension was present at one end fastener and compression at the other, at the same panel end.

The longitudinal forces transferred at each end fastener between marginal beams BC and AD and diaphragm panels are shown in Fig. 5.8. These forces are approximately proportional to the tributary area of the connections. They are more or less uniform at the interior fasteners and slightly higher at the two exterior fasteners (note that the two end fasteners at the exterior panels are absent). It can also be noted that the highest of longitudinal fastener forces are near the reaction ends of each member (i.e. ends A and B).

Figure 5.9 shows the variation of lateral and longitudinal forces imposed on the members AB and DC from the deck side fasteners. It is clear that the transmittal of shear into the diaphragm along the two beams, is more or less uniform over their lengths, with somewhat higher values being obtained near the jack (end C) and near the hinge (end A), than the other two ends.

The shear transfer (longitudenal or vertical forces) at the seam fasteners is shown in Fig. 5.10. Seam No. 1 is 15" from side marginal member DC, while seam No. 8 is 15" from side marginal member AB. It can be observed that a uniform shear transfer is obtained. The same behaviour was found in all diaphragms analysed. The slightly higher values at the seams 1 and 8 for this particular diaphragm (C-2) are due to the absence of the end fasteners in the two exterior panels. The lateral (horizontal) force distribution at the seam fasteners are not plotted as they were extremely small compared to the longitudenal forces.

Equilibrium checks of the results of the computer analysis were made, both of the entire diaphragm assembly and the individual panels and marginal beams. These checks indicated satisfaction of the requirement of equilibrium for all components.

A strength estimate was made on the basis of the elastic analysis, neglecting redistribution of internal forces due to local plasticity as previously mentioned. Also, based on experimental observations of the full-scale testing, ultimate fialure of the diaphragm was reached when local failure at an end fastener occured. Inspection of the internal force distributions at the end fasteners (Figures 5.7 and 5.8) revealed that the end fastener nearest to corner B was the most highly stressed end connection. With an applied load of 1 kip, the force components on that connector, in the directions parallel and perpendicular to the panel axis, were computed at 19.2 lbs and 139.0 lbs, respectively. Accordingly, the resultant force is

$$F = \sqrt{(19.2)^2 + (139)^2} = 140.3 \text{ lbs}$$

On the basis of tests on the sheet-to-frame fasteners lapped joints (Chapter IV), it is known that the strength of end connections in the longitudenal direction is 850 lbs and in the transverse direction is 670 lbs. Accordingly, the strength prediction, based on the connection strength along the major force component is:

$$Q_{ult} = 1.0 \times (\frac{670}{140.3}) = 4.78 \text{ kips}$$

The above predicted failure load for diaphragm C-2 is only 1% higher than the experimentally determined value of $Q_{ult} = 4.72$ kips.

It is interesting to note that the analysis is also in agreement with the full scale testing regarding the sequence of end fastener failures, where the second end fastener occured at the connection nearest to corner D, the second highly stressed connection as predicted by the analysis (Figures 5.7 and 5.8).

Another interesting observation is that the analysis predicts quite closely the level of loading at which the early failure at the seam lines took place in the full-scale tests (in cavity decking diaphragms, Sec. 3.6.2). The average longitudinal force in the first seam line is predicted as 205.5 lbs (Fig. 5.10). The strength of seam connections (First type, Chapter IV) in the longitudinal direction is 450.0 lbs. Thus, the predicted failure load is given as

$$Q_{ult}(\text{seam}) = 1.0 \times \frac{450.0}{205.5} = 2.19 \text{ kips}$$

The load at which failure of seam line connections of diaphragm C-2 was first observed is 2.36 kips.

In the same manner, the ultimate strength of all diaphragms has been predicted and are compared with full-scale test results in Table 5.2.

Finally, it is of interest to consider the computer time needed for the analysis of diaphragm C-2, which involved a system of equations containing 526 unknowns (Fig. 5.6). The time required for program compilation was 18 seconds, while execution required 7.5 seconds. These numbers are by far less than those quoted by Ammar [45] for problems of the same size or even less, using the program developed at Cornell which was operated on an IBM 360 computer. The advantage of data generation routine developed and incorporated in the present computer program becomes apparent when the two programs are compared. For example, the program developed at Cornell required 172 input data cards for the analysis of a very simple diaphragm assembly as reported by Ammar in Ref. 45. Using the present program, only 12 input data cards are needed to analyse the same diaphragm.

5.7 RESPONSE OF DIAPHRAGMS TO CHANGES IN MAIN PARAMETERS

An important advantage of the developed computer program for the analysis of shear diaphragms is that it permits study of the influence of the different parameters on the general performance of the diaphragm. As has been seen in Chapter III, results obtained from full-scale testing apply only to the specific layout of connectors used for each test. If any significant change in the size of the frame marginal members, or if a different type or layout of connectors is adopted, or either the length of the decking panels or the diaphragm width (i.e. No. of panels) is varied, a new test is required. On the other hand, effects of such changes can easily be evaluated by using the present computer program. The cost of an analysis run on the computer is much less when compared to that of full-scale testing.

In the following paragraphs, comparative studies of diaphragm behaviour are presented to illustrate the influence of certain factors on performance (stiffness and strength). Basically, these studies were conducted using the data of the first four cavity decking finite element structural models C-1 to C-4.

5.7.1 Fastener Stiffness

The basic data set of diaphragm C-1 was altered to study the influence of connection stiffness on the diaphragm's shear flexibility and fastener forces. Increase of the stiffness of all diaphragm connections (seam and end fasteners, no side fasteners) by 20% resulted in a decrease of 15% in the diaphragm flexibility and slightly (1 to 6%) increased fastener forces. On the other hand, decrease of the stiffness of all connections by 20% increased the diaphragm flexibility by 22% and slightly decreased the fastener forces.

Reducing the stiffness of only the end and side fasteners to half their actual values in the analysis of diaphragm C-2 (i.e. from 28000 lb/in to 14000 lb/in, in both directions) increased the diaphragm's flexibility by 11%, and decreased the lateral force of the first end fastener by 78% and its longitudinal force by only 10%. Side fastener forces also decreased by 17%, while seam fastener forces slightly decreased (1%).

5.7.2 Size of Marginal Frame Members

Changing the marginal members dimensions by reducing both the area and moment of inertia by 50% did not affect the behaviour of diaphragm C-2 significantly. More specifically, such change resulted in a 0.5% increase in tip deflection, and less than 3% change in fastener forces. This conclusion confirms what has been observed in previous experimental studies [27,45].

5.7.3 Plate Element Material Properties

The effect of changing the orthotropic properties of the plate element in the analysis of diaphragm C-2 was investigated. Reduction of the material shear modulus G_{LT} to one tenth its test value, resulted in an increase of 15% in the diaphragm's flexibility and almost 50% decrease in the end fastener forces. A very slight decrease (1 to 5%) in the seam and side fastener forces was obtained. Increase of the material elastic modulus in the fibres direction, E_L, ten times its test value, resulted in a decrease of only 1% in the diaphragm's flexibility and a very small change in the fastener forces. Finally, setting equal to zero the values of Poisson's ratios in the two orthotropic directions ν_{LT} and ν_{TL} resulted in almost no change in the diaphragm beahviour. This finding shows that because of the already large stiffness of the sheetings in comparison to that of the other components, change in the former induces little change in the diaphragm response.

5.7.4 Panel Length

This parameter is of major interest since in practice, panel length may vary from 6.0 to 10.0 ft depending on the supporting joists. Two studies were thus considered. In the first, the side and seam fastener spacing was kept constant, while allowing the number of these fasteners to change according to the length of the decking. In the second, the number of side and seam fasteners per line was kept constant regardless of diaphragm length.

In the diaphragm tests C-2, C-3 and C-4, the spacings of both the side and seam fasteners were 20", 15" and 12", respectively, corresponding to 5, 7 and 9 fasteners, respectively, over a span of 10 ft. Based on the data for the finite element models of these three diaphragms, the variation in panel length with a constant spacing of side and seam fasteners was first studied. In the first study, 12 diaphragms were analysed (for an applied load of 1000 lbs) and the results are summarized in Table 5.3. Inspection of the results reveals that the shorter the diaphragm length the smaller its shear modulus (G') capacity. This is expected, since the number of fasteners transmitting the shear forces are smaller in the shorter diaphragm. Fig. 5.11 shows the variation of the diaphragm shear modulus G' versus the diaphragm length for the three spacings of fasteners.

In the second study, the number of fasteners per side or seam line was kept constant. The results obtained for this study are summarized in Table 5.4. It is interesting to note that shorter diaphragms are stiffer (higher G'), while their carrying capacities are slightly lower. Fig. 5.12 shows the variation of the diaphragm shear modulus G' versus the diaphragm length for the three layouts of constant number of side and seam fasteners.

5.7.5 Diaphragm Width

In practice, the number of decking panels between supporting framing members is usually greater than that used in the present full-scale testing, thus, it is necessary to investigate the influence of diaphragm width (or number of decking units) on its performance. Analysis of 6 Cavity decking diaphragms was performed. The diaphragms were common in their fasteners layout (5 fasteners on each side and per seam line, and one fastener per panel end, i.e., as in Test C-2) and were different in their covering width (or No. of decking units). The results obtained from these analyses are summarized in Table 5.5. As can be seen, the diaphragm width has a very moderate influence on the shear modulus (G') and very little effect on the shear strength (or fastener forces).

5.8 CONCLUSIONS

In the previous section, it has been demonstrated that the results obtained by the finite element method yield satisfactory accuracy without the use of excessive computer time. In addition, the following points can be emphasized:

(1) The finite element model data generator routine specially developed for diaphragm analysis has proved to be an excellent feature by which the required input data is kept to the minimum.

(2) The equation solver incorporated in the program has proved to be quite effective and the computer execution time remained in a very acceptable range.

(3) The length of the decking unit has a significant influence on the diaphragm stiffness and capacity. Decrease in the decking length while keeping the fastener spacing constant tends to reduce the two behavioural parameters. On the other hand, decrease in the decking length while keeping the fastener number constant produces the opposite effect.

(4) Changes in the number of decking units has practically no influence on the diaphragm shear modulus or its capacity. This fact has great implications in selecting the diaphragm size for testing.

TABLE 5.1

DIAPHRAGM SHEAR FLEXIBILITY FROM FINITE ELEMENT ANALYSES COMPARED TO FULL-SCALE TEST RESULTS

DIAPHRAGM	DIAPHRAGM SHEAR FLEXIBILITY (in/kip)		F.E. RESULT / TEST RESULT
	F.E. ANALYSIS	FULL-SCALE TEST	
C-1	0.455	0.417	1.03
C-2	0.224	0.240	0.93
C-3	0.159	0.163	0.98
C-4	0.127	0.130	0.98
C-7	0.149	0.160	0.93
C-8	0.218	0.200	1.09
T-1	0.134	0.167	0.80
T-2	0.071	0.060	1.18
T-3	0.051	0.069	0.74
T-4	0.048	0.060	0.80

TABLE 5.2

DIAPHRAGM FAILURE LOAD AS PREDICTED BY FINITE ELEMENT ANALYSES COMPARED TO FULL-SCALE TEST RESULTS

DIAPHRAGM	FAILURE LOAD (KIPS)		
	F.E. ANALYSIS	FULL-SCALE TEST	F.E. RESULT / TEST RESULT
C-1	3.89	3.60	1.08
C-2	4.78	4.72	1.01
C-3	7.23	6.80	1.06
C-4	7.73	7.64	1.01
C-7	7.47	6.75	1.11
C-8	4.82	5.76	0.84
T-1	3.97	3.33	1.19
T-2	5.58	4.50	1.24
T-3	7.36	6.52	1.13
T-4	7.44	8.14	0.91

TABLE 5.3

COMPARATIVE STUDY OF DIAPHRAGM BEHAVIOUR

VARIABLE: DIAPHRAGM LENGTH

CONSTANT: SPACING OF SIDE AND SEAM FASTENERS (p)

	DIAPHRAGM LENGTH (b)	NO. FASTENERS/LINE	TIP DEFLECTION	G'	AVERAGE FASTENER FORCES (lbs)			
	ft		inches	lb/in	SIDE (F_d)	SEAM (F_s)	END (F_{ev})*	END (F_{eh})*
p = 20"	10	5	0.21843	4578	231	203	72.80	99.64
	8-1/3	4	0.027466	4369	295	253	81.02	124.90
	6-2/3	3	0.36920	4063	404	336	99.92	168.88
p = 15"	10	7	0.15966	6263	161	145	56.80	91.37
	8-3/4	6	0.18751	6095	190	169	64.37	106.07
	7-1/2	5	0.22695	5875	232	203	74.10	128.13
	6-1/4	4	0.28694	5576	295	253	86.99	163.77
p = 12"	10	9	0.12694	7878	123	113	46.75	85.38
	9	8	0.14379	7728	139	127	51.75	95.46
	8	7	0.16572	7543	161	145	57.92	108.98
	7	6	0.19540	7311	191	170	65.62	128.30
	6	5	0.23770	7012	233	203	75.44	157.49

* First end fastener from support [F_{ev}: lateral or vertical force; F_{eh}: longitudinal or horizontal force]

TABLE 5.4

COMPARATIVE STUDY OF DIAPHRAGM BEHAVIOUR

VARIABLE: DIAPHRAGM LENGTH

CONSTANT: NO. OF FASTENERS PER SIDE AND SEAM LINES (n)

	DIAPHRAGM LENGTH (b) ft.	FASTENER SPACING inches	TIP DEFLECTION inches	G' lb/in	AVERAGE FASTENER FORCES (lbs)			
					SIDE (F_d)	SEAM (F_s)	END (F_{ev})*	END (F_{eh})*
n = 5	10	20	0.21843	4578	231	203	72.80	99.64
	9	18	0.22103	5027	231	203	73.21	109.05
	8	16	0.22462	5565	231	203	73.72	120.93
	7	14	0.22979	6217	231	203	75.36	157.51
n = 7	10	15	0.15966	6263	161	145	56.80	91.37
	9	13.5	0.16220	6850	161	145	57.20	99.22
	8	12	0.16572	7543	161	145	57.84	109.00
	7	10.5	0.17079	8365	161	145	58.75	121.69
	6	9	0.17852	9336	162	146	60.14	139.00
n = 9	10	12	0.12694	7878	123	113	46.75	85.38
	9	10.8	0.12944	8584	123	113	47.18	92.20
	8	9.6	0.13291	9405	123	113	47.91	100.58
	7	8.4	0.13790	10359	123	113	48.99	111.38
	6	7.2	0.14550	11455	124	114	50.71	126.13

*First end fastener from support [F_{ev}: lateral or vertical force; F_{eh}: longitudinal or horizontal force]

TABLE 5.5.

COMPARATIVE STUDY OF DIAPHRAGM BEHAVIOUR

VARIABLE: DIAPHRAGM WIDTH

DIAPHRAGM WIDTH (a) ft	NO. OF DECKING PANELS	TIP DEFLECTION inches	G' lb/in	AVERAGE FASTENER FORCES (lbs) SIDE (F_d)	SEAM (F_s)	END (F_{ev})*	END (F_{eh})*
10	8	0.19277	5188	230.37	202.35	72.71	99.35
15	12	0.29575	5072	231.85	203.77	72.93	100.00
20	16	0.39976	5003	232.17	204.06	73.01	100.11
25	20	0.50506	4950	232.34	204.19	73.09	100.15
30	24	0.61198	4902	232.49	204.31	73.18	100.18
35	28	0.72083	4856	232.64	204.42	73.26	100.20

* First end fastener from support [F_{ev}: lateral or vertical force; F_{eh}: Longitudinal or horizontal force]

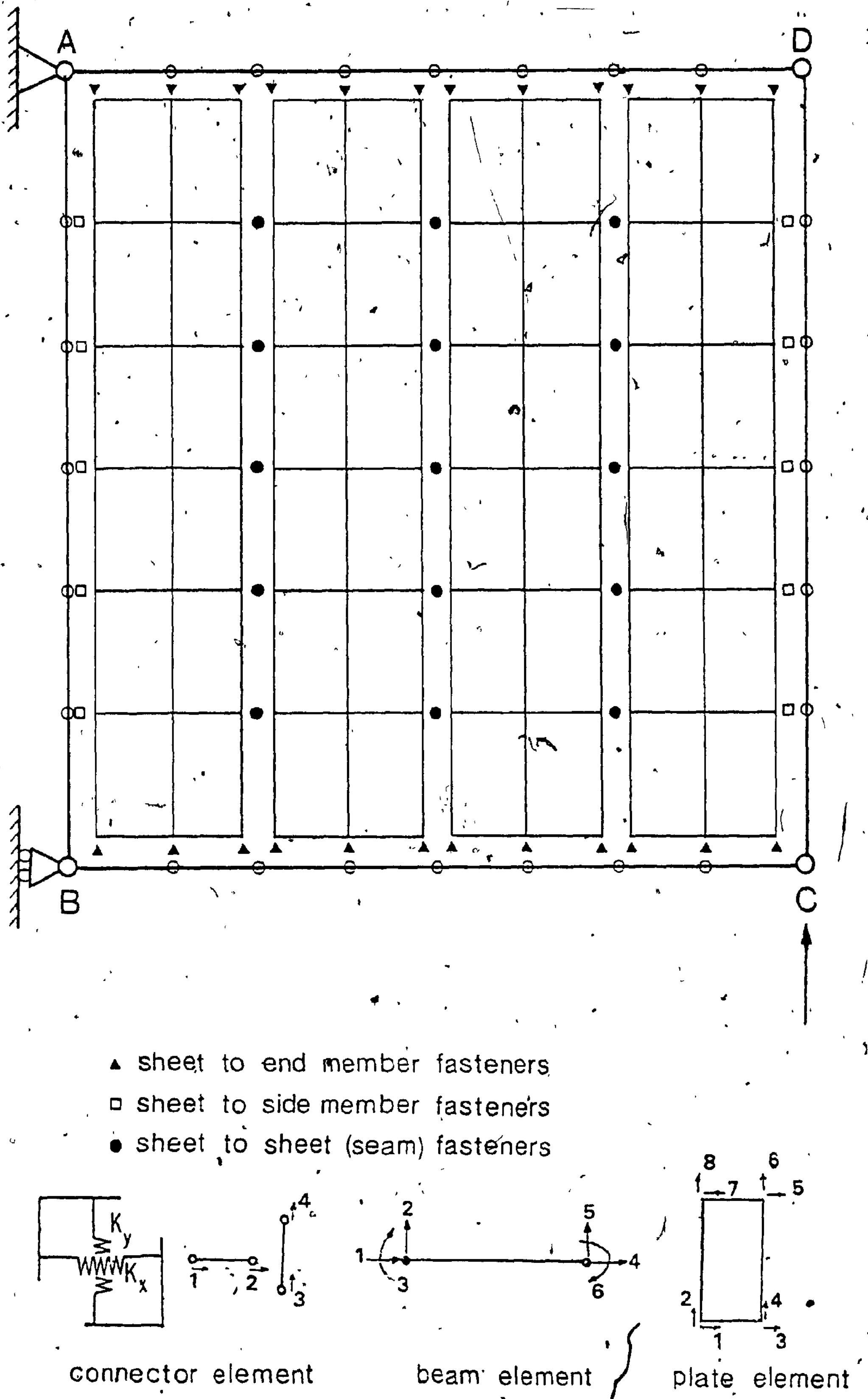
A
D
B
C
▲ sheet to end member fasteners
□ sheet to side member fasteners
● sheet to sheet (seam) fasteners
K
y
K
x
1
2
4
3
connector element
1
2
3
4
5
6
beam element
8
7
6
5
2
4
1
3
plate element

FIG. 5.1 FINITE ELEMENT MODEL OF A SIMPLE DIAPHRAGM

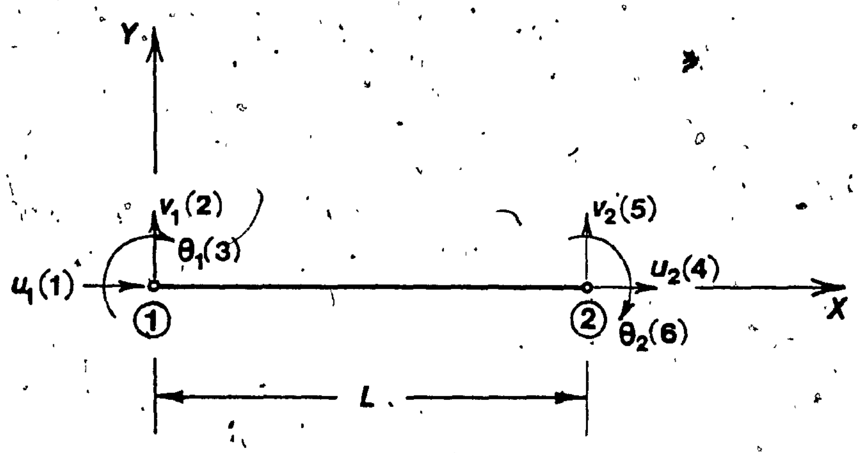

(*a*) *BEAM ELEMENTS IN THE X-DIRECTION*

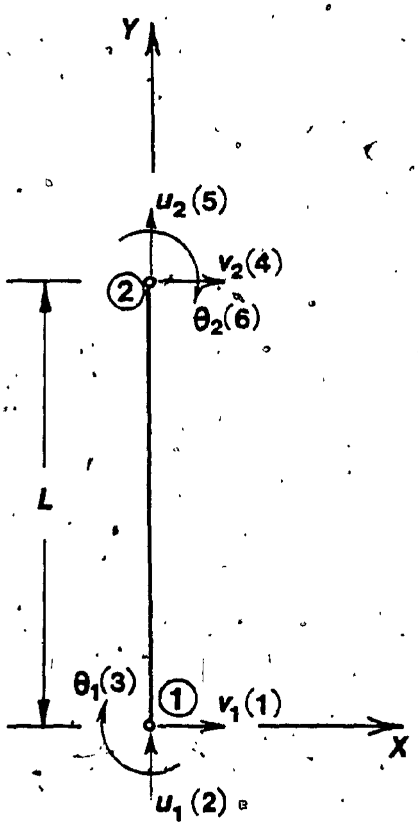

(*b*) *BEAM ELEMENTS IN THE Y-DIRECTION*

FIG. 5.2 DEGREES OF FREEDOM AND SEQUENTIAL NUMBERING FOR BEAM ELEMENTS

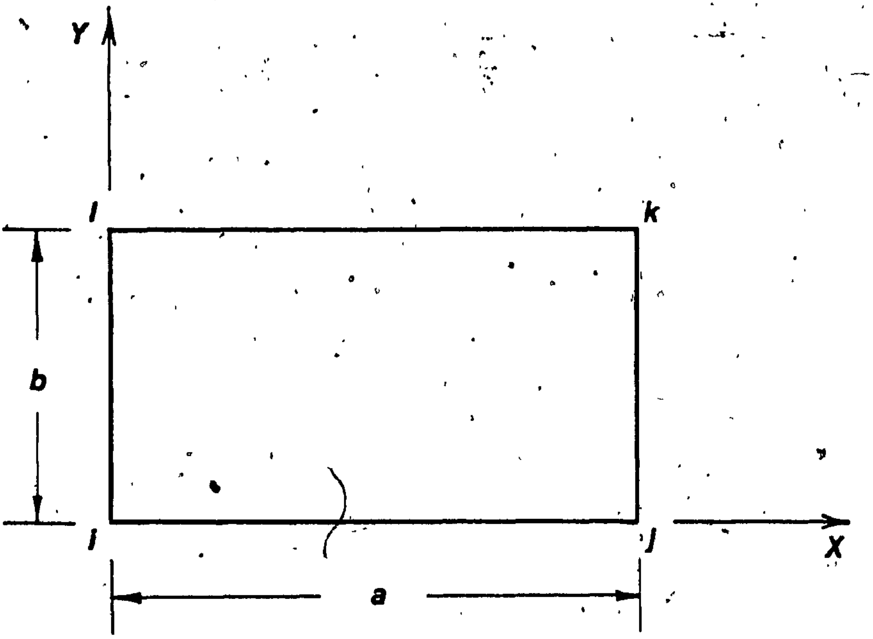

LOCAL COORDINATES

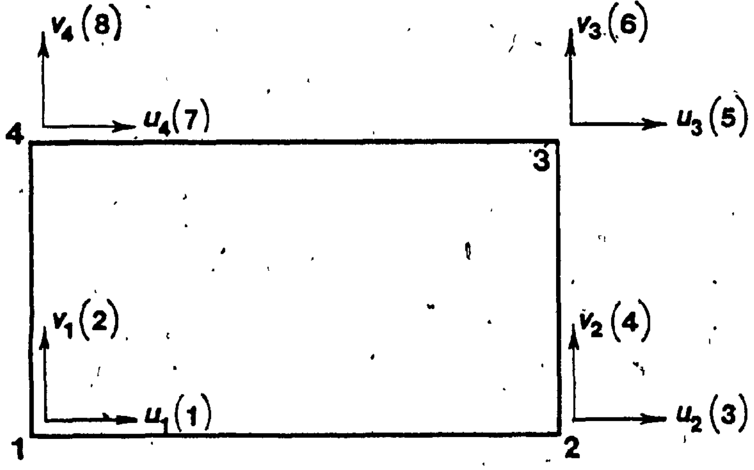

DEGREE OF FREEDOM AND SEQUENTIAL NUMBERING

FIG. 5.3 PLATE ELEMENT

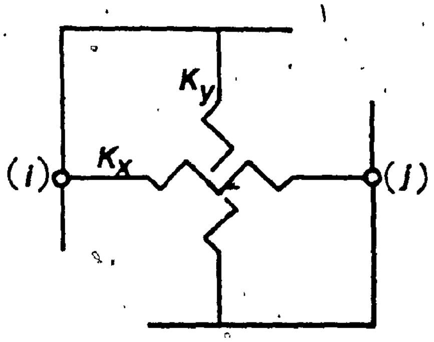

MODELING OF CONNECTION

SEQUENTIAL NUMBERING OF FREEDOMS

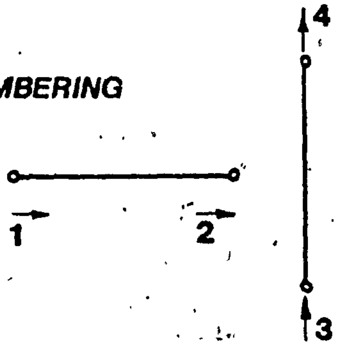

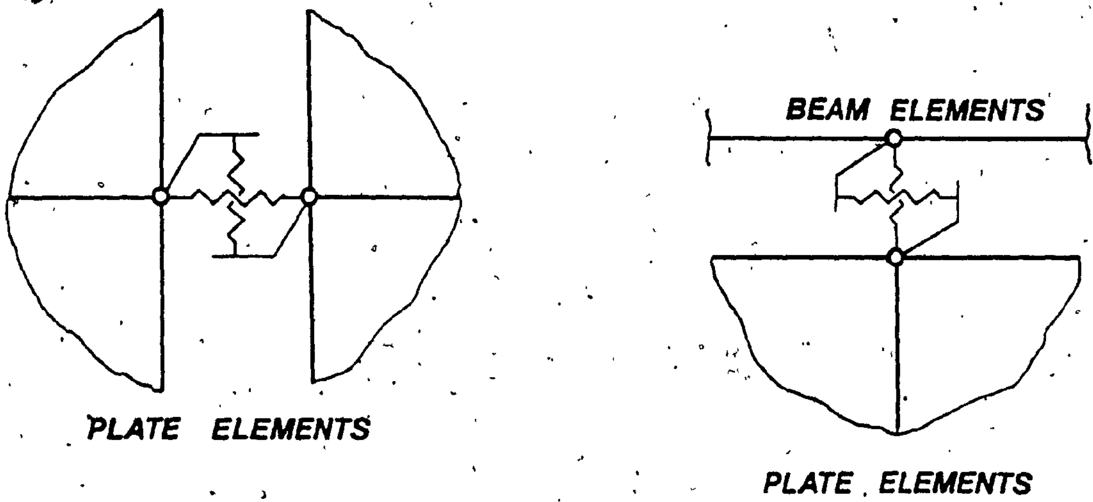

SEAM CONNECTOR

END CONNECTOR

FIG. 5.4 CONNECTOR ELEMENT

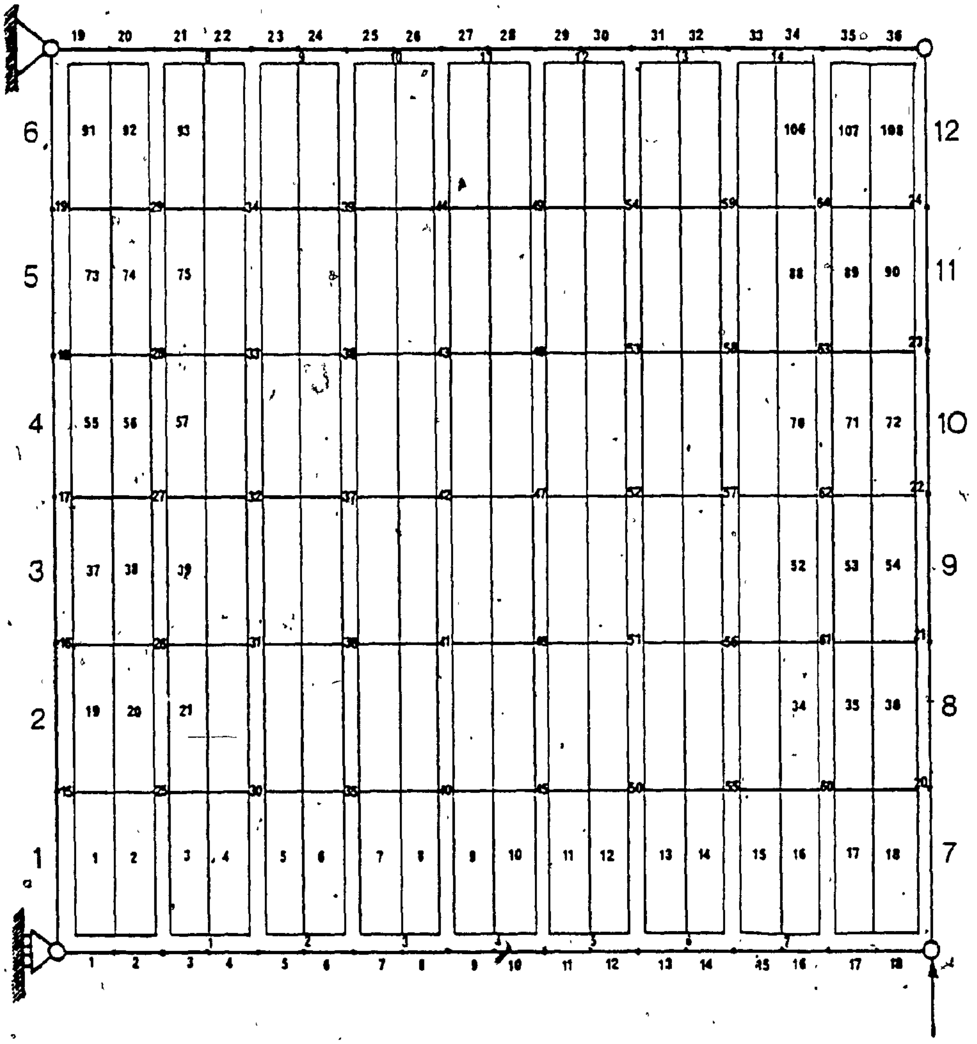

FIG. 5.5 SEQUENTIAL NUMBERING OF ELEMENTS - DIAPHRAGM C-2 FINITE ELEMENT MODEL

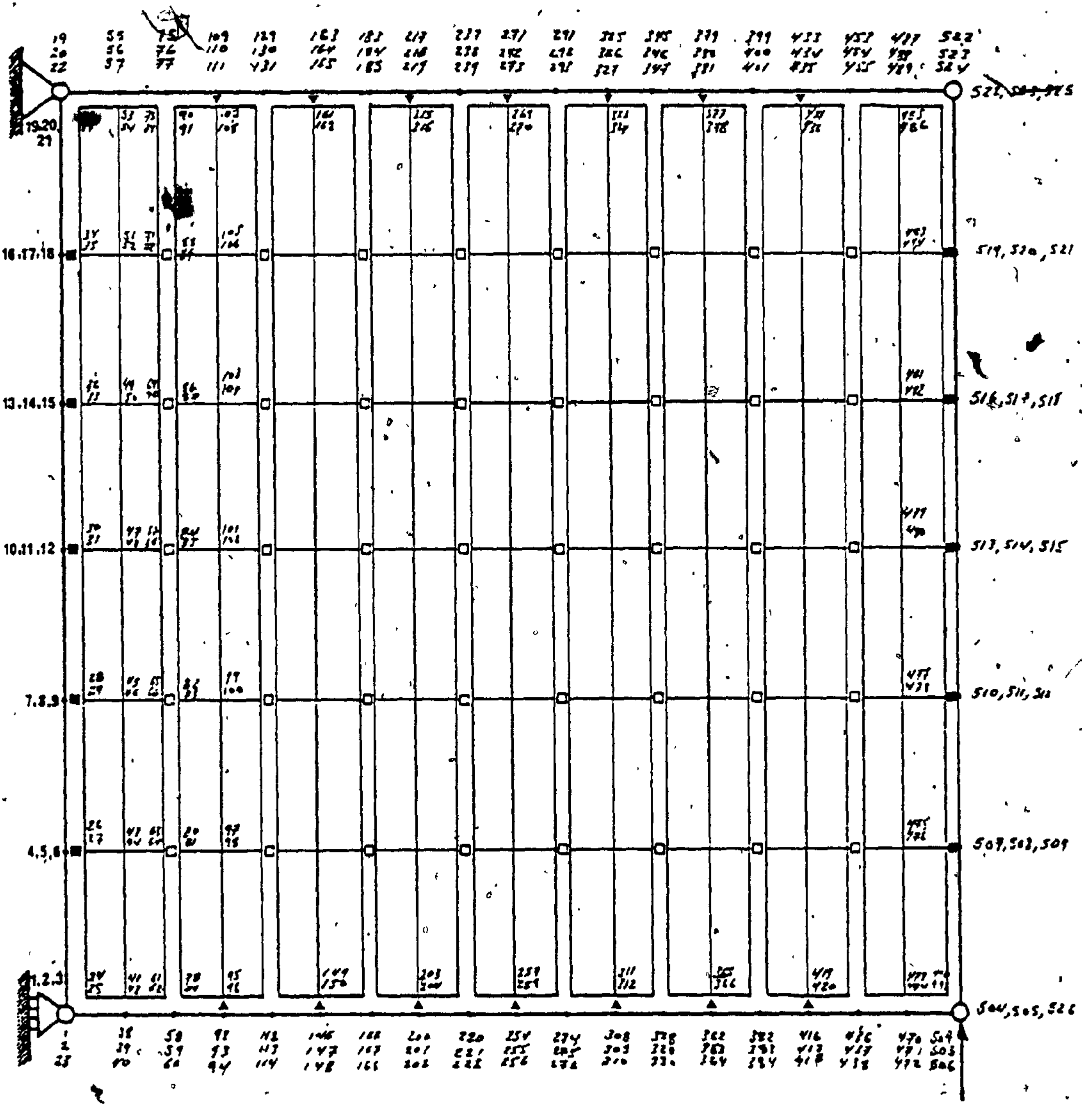

FIG. 5.6 NODAL DEGREE OF FREEDOM NUMBERING - DIAPHRAGM C-2 FINITE ELEMENT MODEL

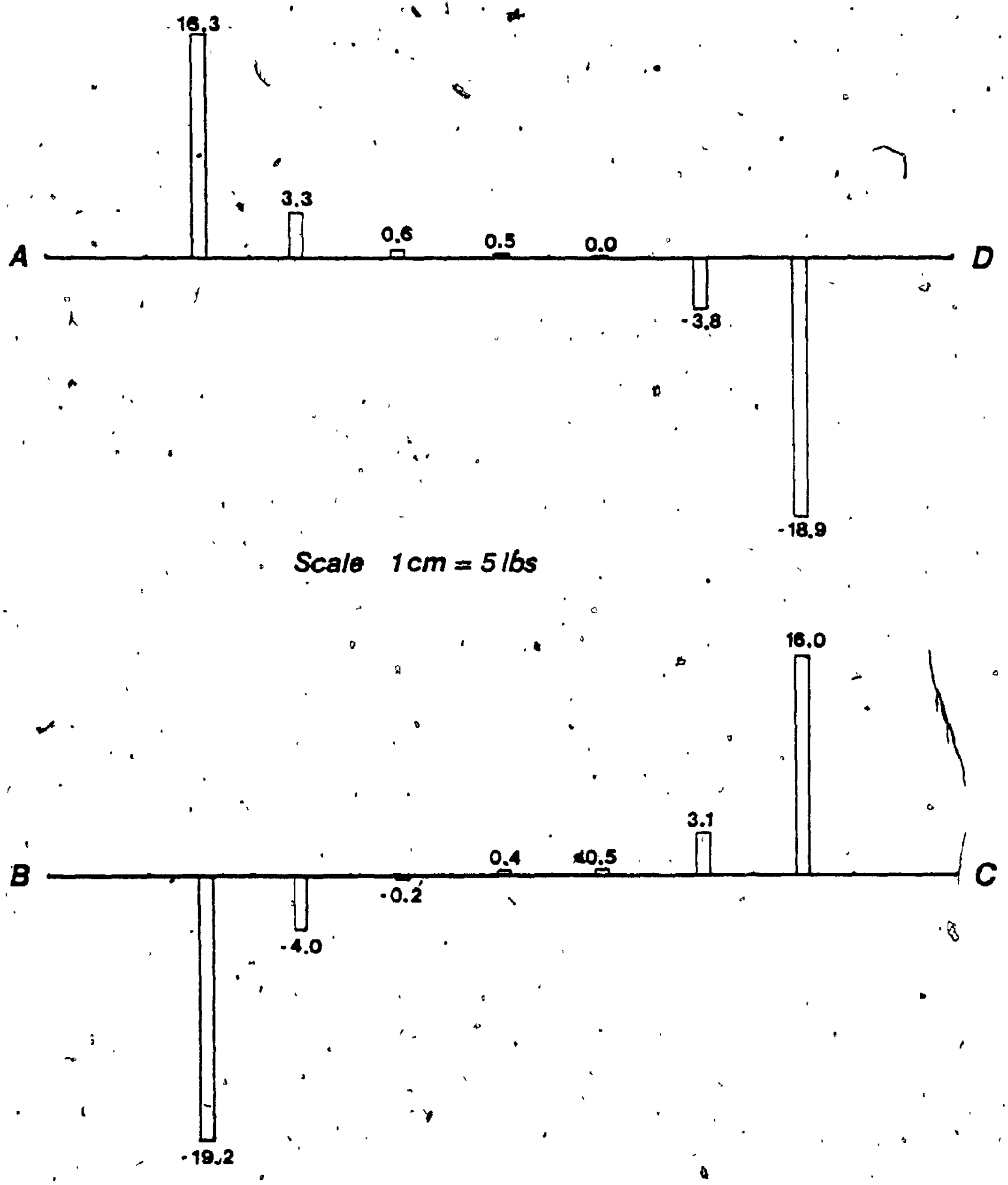

FIG. 5.7 LATERAL FORCES ON MARGINAL BEAMS AD AND BC FROM CAVITY DECKING C-2 DIAPHRAGM ANALYSIS

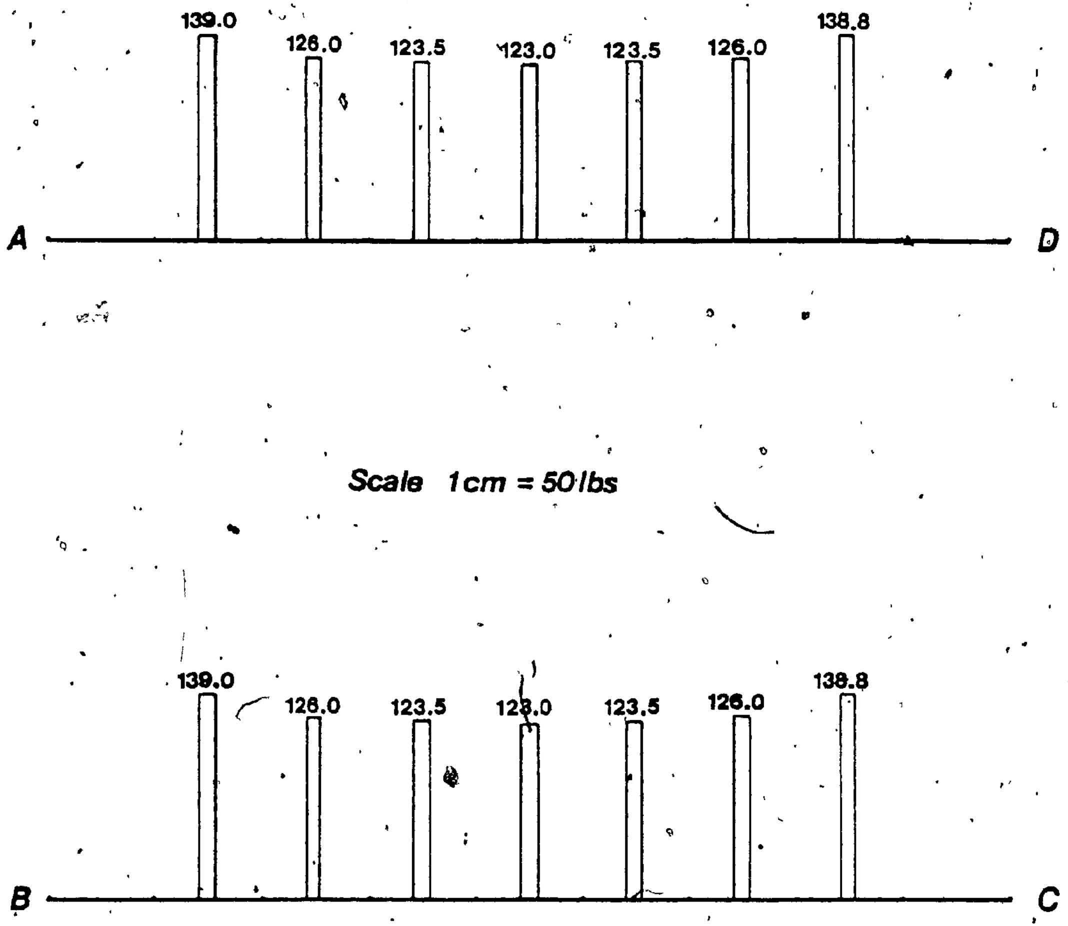

FIG. 5.8 LONGITUDINAL FORCES ON MARGINAL BEAMS AD AND BC FROM CAVITY DECKING C-2 DIAPHRAGM ANALYSIS

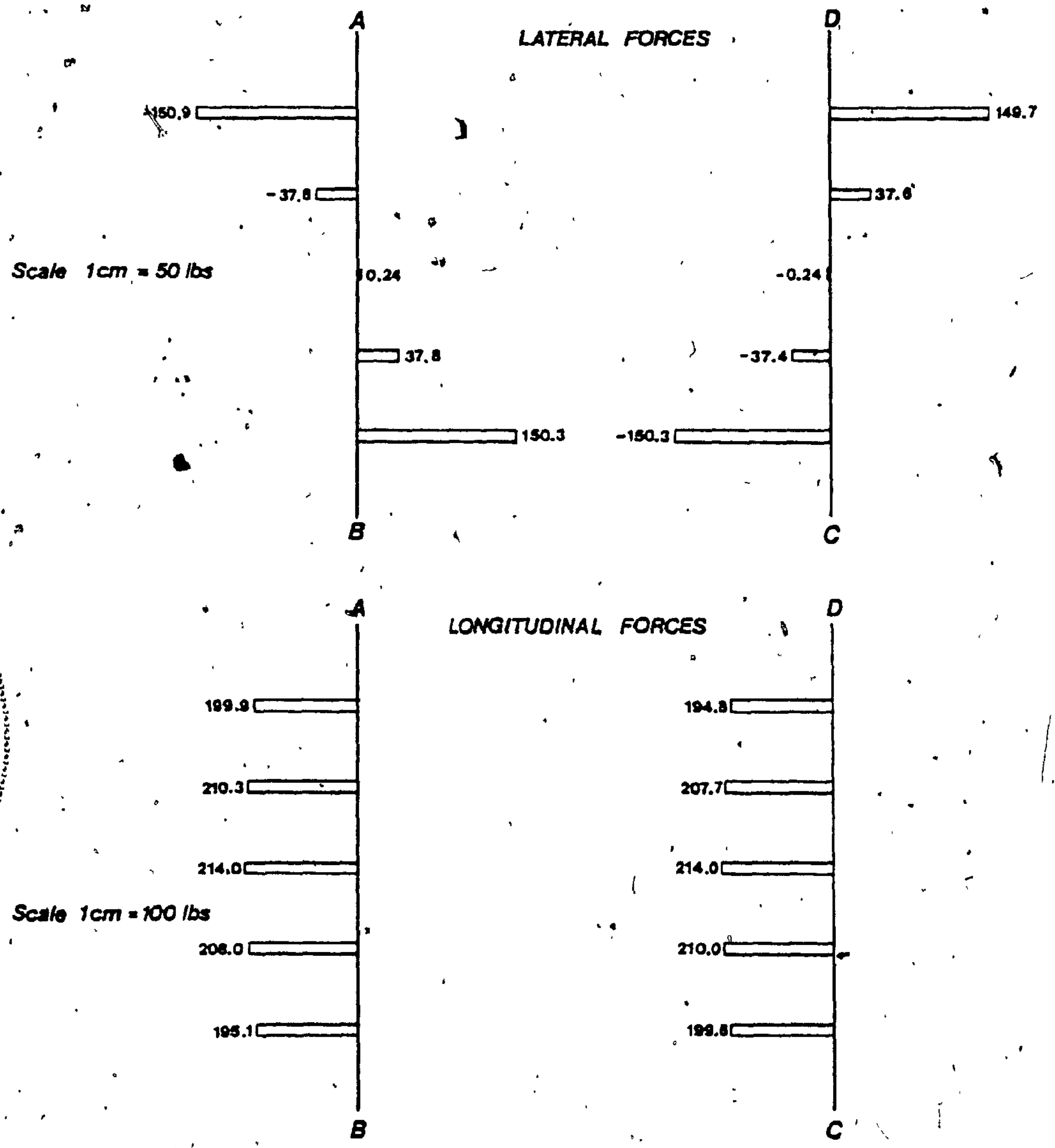

FIG. 5.9 LATERAL AND LONGITUDINAL FORCES ON MARGINAL BEAMS AB AND DC FROM CAVITY DECKING C-2 DIAPHRAGM ANALYSIS

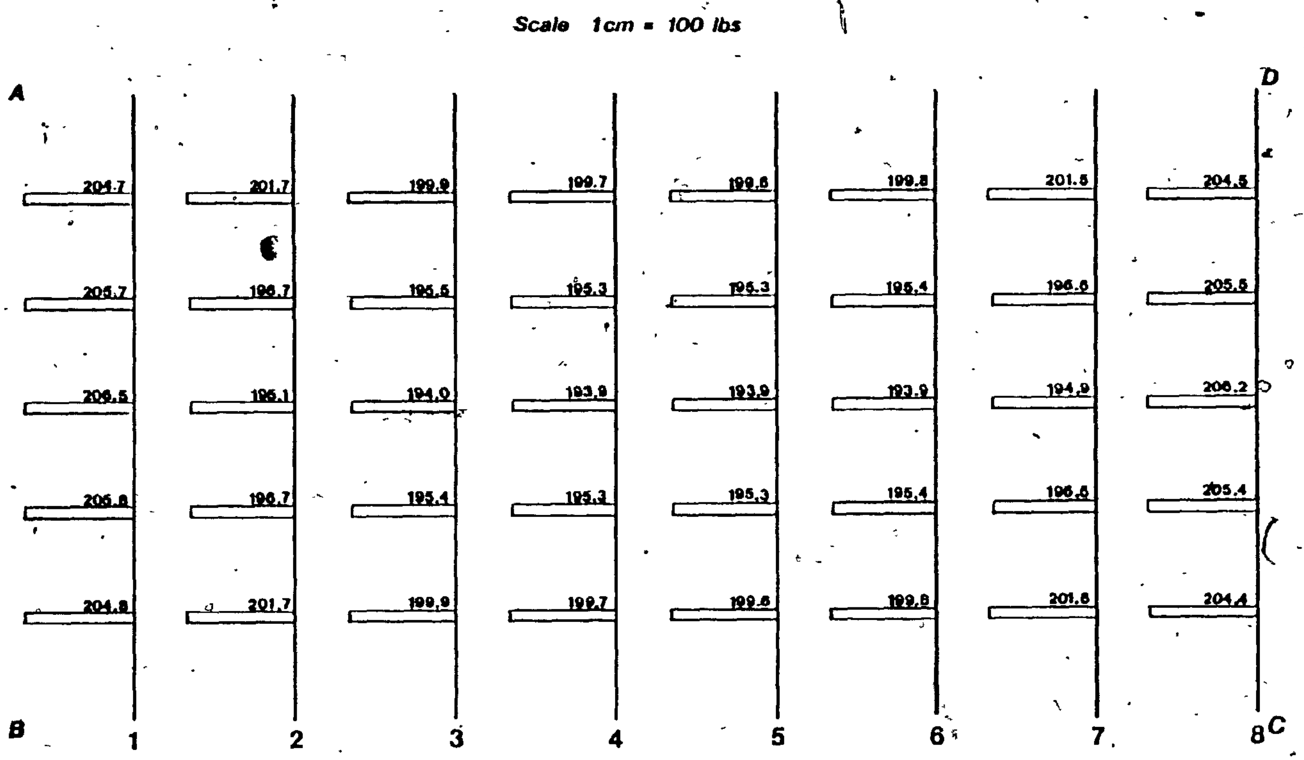

FIG. 5.10 LONGITUDINAL FORCES ON SEAM FASTENERS FROM CAVITY DECKING
C-2 DIAPHRAGM ANALYSIS

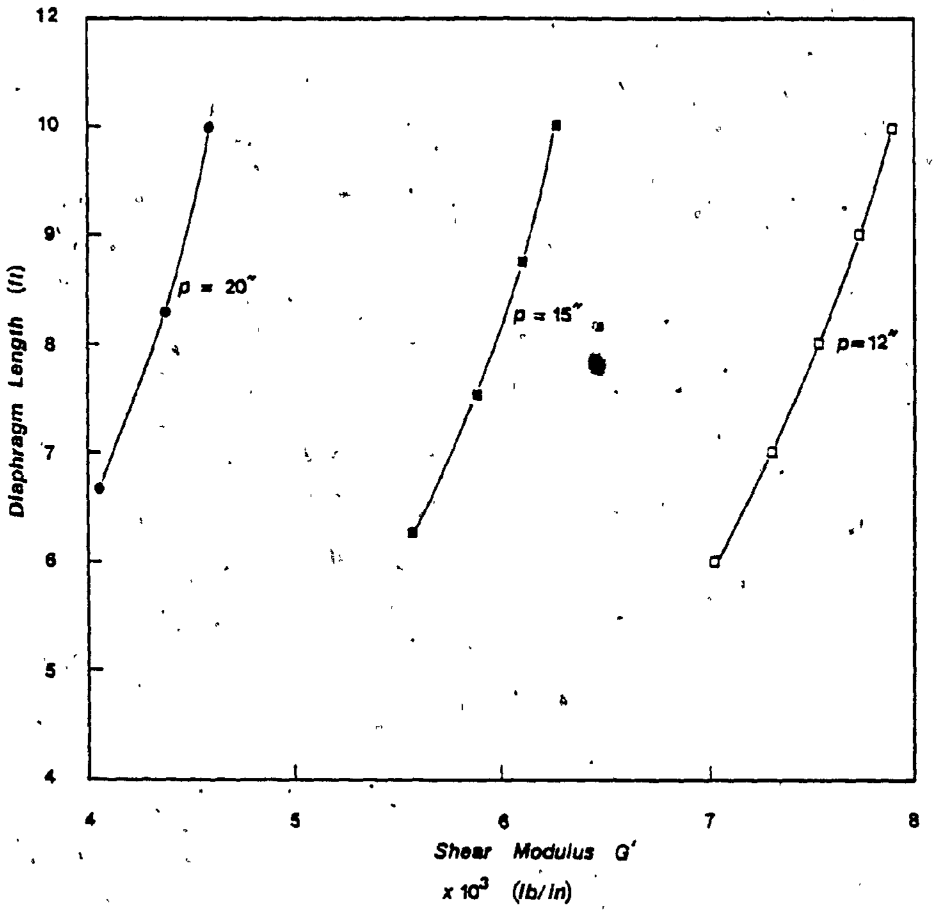

FIG. 5.11 VARIATION OF G' vs. DIAPHRAGM LENGTH CONSTANT: SPACING OF SIDE AND SEAM FASTENERS (P)

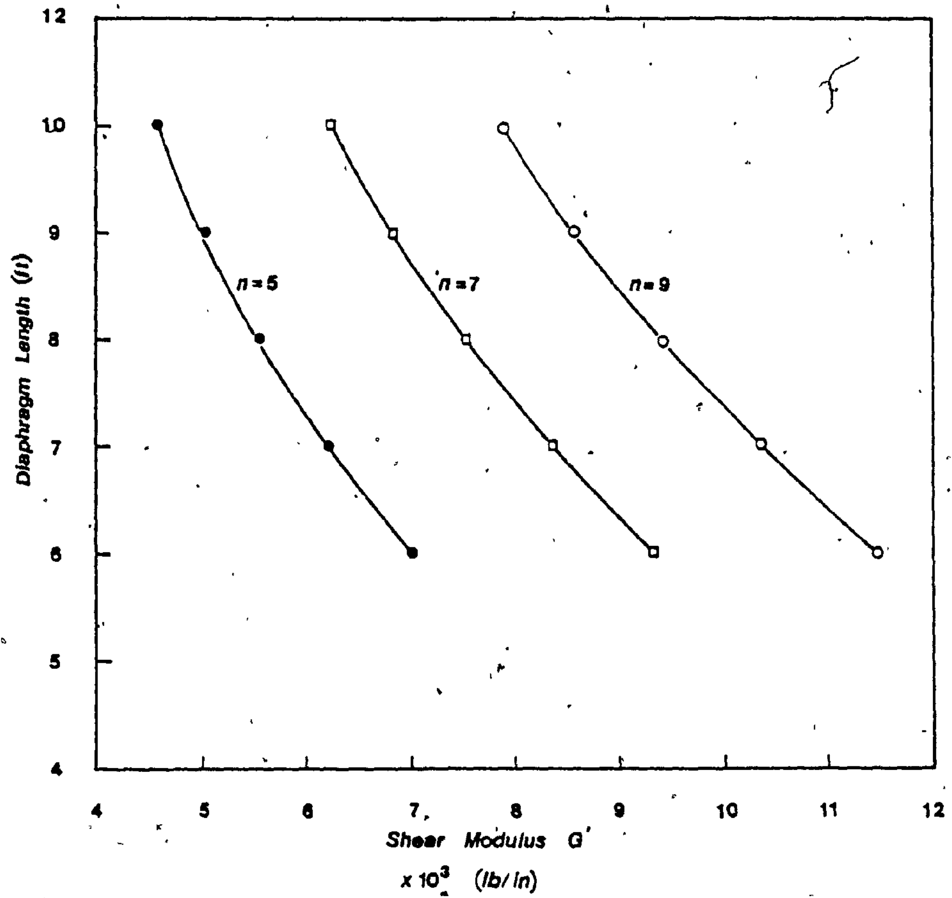

FIG. 5.12 VARIATION OF G' vs. DIAPHRAGM LENGTH CONSTANT: NO. OF FASTENERS PER SIDE AND SEAM LINES (n)

CHAPTER VI

A SIMPLIFIED METHOD FOR DIAPHRAGM ANALYSIS

CHAPTER VI

A SIMPLIFIED METHOD FOR DIAPHRAGM ANALYSIS

6.1 INTRODUCTION

Full-scale testing and finite element analysis (or computer based methods) has been regarded as the most reliable approaches to predict a diaphragm shear flexibility (or stiffness) and strength. However, the two methods are often labelled as too expensive and complex for routine use, and consequently, interest has been growing in deriving simple analytical expressions for predicting the two parameters.

The earliest analytical approach was that advanced by Bryan et al. [34,35,75] a decade ago, and was based on a series of simplifying assumptions regarding the distribution of internal forces within the diaphragm. The flexibility of a diaphragm, expressed as the amount of tip deflection per unit load, was evaluated by simple summation of individual flexibilities of the different components. Mathematical expressions were derived for these components flexibilities using energy methods, and some of these expressions contained data to be obtained by tests on components (e.g., the slip value per unit load and ultimate tearing value of different sheet fasteners). Expressions to predict the shear strength and based on tearing strengths of the different fasteners were also derived. An evaluation of tip deflections and strengths of some diaphragms, using the above approach, compared fairly well with experimental results obtained for full-scale installations.

A discussion by Falkenberg [76] implied some deficiencies regarding the establishment of corrugations flexibility, and proposed a variation of the method, claiming better results. More recently, Davies [62,63] put forward an improved version of Bryan's expressions based on improvements in the assumed internal force distribution. Modified expressions were derived using static equilibrium.

Also worth mentioning, the work by Libove and Lin [77,79], regarding the analytical investigation of corrugated panels subjected to the action of shear load, also used the same energy principles as Bryan, with even more rigorous concepts, but failed to obtain more accurate results when compared with experiments. The study was very thorough and the reason for the relatively poor correlation may reside in the difficulty to define the boundary conditions correctly.

A new different approach was followed by Easley [80], and based on an experimentally observed mode of diaphragm deformations [81,82]. Easley developed formulas for the fastener forces and the diaphragm flexibility, taking into account only the fastener deformations and shear strains in the sheetings. By adjusting the fastener stiffnesses and strength, Easley has obtained consistent and good comparisons with his experimental data. However, when applied to other investigator's experimental works, Easley's formulas produced erroneous results. This is due to three main factors:

(i) the theory assumes that all panels deform identically;

(ii) the seam slip was erroneously taken to be the same as the deformation of the corner end fastener; and

(iii) neglect of possible profile distortion

The theory is further limited to diaphragms where all fasteners possess the same stiffnesses and strength.

It should be emphasized that, all the above mentioned analytical works were basically developed to predict the behaviour of light-gauge metal shear diaphragms. Again, it was also the only attempt of investigation into the structural behaviour of asbestos-cement shear diaphragms [1], that Bryan applied his early analytical expressions. The correlation obtained between calculated and test results varied greatly.

In this chapter, a simple analytical method is presented for the analysis of shear diaphragms. The method is inspired by the simplicity of Easley's theory, however, the present work not only corrects the deficiencies of Easley's theory, but also extends its applicability to a more general class of practical diaphragms.

6.2 ASSUMPTIONS

The expressions for the shear deflections and fastener forces are developed based on an assumed mode of deformation in conjunction with an assumed internal force distribution, from which failure loads can also be estimated.

A diagramatic arrangement of a typical isolated diaphragm is shown in Fig. 6.1. It comprises several panels connected together and to the perimeter members and purlins with a variety of fasteners. The deformed shape of this diaphragm due to vertical deformations of the connections is assumed as shown in Fig. 6.2. This simple mode of deformation is based on many experimental observations and extensive finite element analyses. Implicit in this assumed mode are the following assumptions:

(1) Interior panels deform in approximately the same manner, thus; the seam slips are the same, that is the vertical components of seam fasteners forces are constant. The reasonableness of this assumption is borne out by the F.E. study of the previous chapter showing the tip deflection is linearily proportional to the number of panels, i.e. G' is independent of the number of panels.

(2) The horizontal components of the seam and side fastener forces are negligible, and the vertical components of the side fastener forces are also constant.

(3) The vertical components of the end fastener forces vary linearly within the sheet width.

Although the last assumption may not be realistic under some circumstances, it gives rise to simple expressions for the flexibility and fastener forces with reasonable accuracy when compared to experimental data and finite element results [67]. A more refined distribution of the fastener forces has been incorporated by modifying assumption (3), to allow the vertical components of the end fastener forces to vary linearly within an interior panel, and parabolically in the exterior panels (Fig. 6.3). This has shown to yield a better prediction of diaphragm behaviour [68].

Experimental data and finite element analyses have also shown that failure of the diaphragm is invariably initiated in the exterior panels; thus greater emphasis should be placed on these panels by ensuring their complete equilibrium. In contrast, Bryan and Davies' approach ensures equilibrium of the interior panels, but violates moment equilibrium equation of the exterior panels.

6.3 DERIVATION OF FORMULAS

In the following, the expressions derived are relevant to the assumed mode of deformation of Fig. 6.2, those for the mode of Fig. 6.3 are presented in Appendix A.

Similar to Bryan's method, the tip deflection of a complete diaphragm is obtained as the sum of the following component deflection:

D_1 = deflection due to deformation of all connections except that due to the horizontal force components in the end fasteners which is denoted D_2; D_3 = deflection due to shear strains in the sheeting and warping of the corrugation profiles; and D_a = deflection due to axial deformations of the perimeter members. The present work differs from that of Bryan and Davies in the derivation of the expressions for D_1 and the fastener forces.

6.3.1 Expressions for D_1 (Deflection Due to Vertical Deformations of all Connections) and Fastern Forces

With reference to Fig. 6.2, the deflection component D_1 can be written as:

$$D_1 = 2D_e + 2(N-1)\ D_s \qquad (6.1)$$

in which D_e, D_s = the vertical separations between the end member and the panels at the diaphragm corners and at the seam lines, respectively, and N = number of panels in the diaphragm.

To determine D_e and D_s, equilibrium of the exterior panel is considered. Fig. 6.4 shows the forces acting on the left exterior panel. The vertical component of the forces in the end fasteners are given by the equation (positive for upward force):

$$F_{vi} = K_e\ (1 - \frac{x_i}{x_o})\ D_e \qquad (6.2)$$

in which K_e = stiffness of the end connections; x_i = horizontal distance from the left edge of the panel to the fastener i, and x_o is as defined in Fig. 6.4. The vertical forces in the sheet-to-purlin fasteners can also be evaluated by Eq. 6.2 with K_e being replaced by K_p which is the stiffness for these connections. By making use of Eq. 6.2, the vertical equilibrium of the panel may be written as

$$n_dF_d - n_sF_s + 2D_ek_e \sum_{i=1}^{n_e} (1 - \frac{x_i}{x_o}) + M\ D_ek_p \sum_{i=1}^{n_p} (1 - \frac{x_i}{x_o}) = 0 \qquad (6.3)$$

in which n_d, n_e, n_s = the numbers of fasteners in the side, and end, and the seam connections, respectively; F_d, F_s = vertical forces in the side and the seam fasterners, respectively; n_p = number of sheet to purlin fasteners; and M = number of purlins.

From the assumed mode of deformation in Fig. 6.2, the deformations in the side and seam connections are seen to be D_e and $2D_s$, respectively. Thus;

$$F_d = k_d\ D_e \qquad (6.4)$$

and

$$F_s = k_s(2D_s) = 2k_s(\frac{w}{x_o} - 1)\ D_e \qquad (6.5)$$

in which w = width of the panel. Substituting Eqs. (6.4) and (6.5) into Eq. (6.3) and solving for x_o yields

$$x_o = \frac{2n_sk_s + 2k_eg_{1e} + Mk_pg_{1p}}{n_dk_d + 2n_sk_s + 2n_ek_e + Mn_pk_p}\ w \qquad (6.6)$$

in which $g_{1e} = \frac{1}{w} \sum_{i=1}^{n_e} x_i$ and $g_{1p} = \frac{1}{w} \sum_{i=1}^{n_e} x_i$ (6.7)

Moment equilibrium of the panel about the lower left corner can be expressed as:

$$n_sF_sw - 2k_eD_r \sum_{i=1}^{n_e} (1 - \frac{x_i}{x_o})x_i - MD_ek_p \sum_{i=1}^{n_p} (1 - \frac{x_i}{x_o})x_i = Qw \qquad (6.8)$$

This equation together with Eqs. 6.4 and 6.5 yields the following expression for D_e

$$D_e = Q/k \qquad (6.9)$$

in which

$$k = 2n_s k_s \left(\frac{w}{x_o} - 1\right) + 2k_e(g_{2e} - g_{1e}) + Mk_p(g_{2p} - g_{1p}) \tag{6.10}$$

$$g_{2e} = \frac{1}{wx_o} \sum_{i=1}^{n_e} x_i^2;$$

and (6.11)

$$g_{2p} = \frac{1}{wx_o} \sum_{i=1}^{n_p} x_i^2$$

The deflection component D_1 of Eq. (6.1) becomes

$$D_1 = \frac{2Q}{k} \left[1 + (N-1)\left(\frac{w}{x_o} - 1\right)\right] \tag{6.12}$$

and for the fastener forces

$$F_d = k_d \, Q/k \tag{6.13}$$

$$F_s = 2k_s\left(\frac{w}{x_o} - 1\right) Q/k \tag{6.14}$$

$$F_{vi} = k_e\left(1 - \frac{x_i}{x_o}\right) Q/k \tag{6.15}$$

and

$$F_{pi} = k_p\left(1 - \frac{x_i}{x_o}\right) Q/k \tag{6.16}$$

in which F_p = vertical force in the sheet-purlin fasteners.

As has been mentioned earlier, the diaphragm deflection D is obtained as the sum of several components. Apart from D_1, the other component deflections D_2, D_3 and D_a are closely the same as those derived by Bryan and Davies [37,62]. However, for the sake of completeness, the derivation for these component deformations is also presented in Appendix B.

6.3.2 Failure Load Expressions

In most practical diaphragms, the number of fasteners is inadequate to develop the full strength of the diaphragm by overall shear buckling. Thus, the connections are often the weakest component of the system. Failure of these diaphragms is caused either by shear failure of the fasteners or by tearing of the sheeting at the fasteners.

A conservative estimate of diaphragm strength can be made on the basis of elastic behaviour, neglecting redistribution of internal forces due to fasteners yielding. Failure of a diaphragm can occur along a vertical line of fasteners (side or seam connections) or at the end fasteners of the exterior panels.

6.3.2.1 Failure at the seam:

Let F_{su}, F_{pu} and F_{eu} be the strengths of the individual fasteners at the seam, purlin and end connections. The capacity of the seam connection is $n_s F_{su} + MF_{pu} + 2F_{eu}$, in which the last two terms account for any sheet-to-framing member connections in line with the seam. From Eqs. (6.14) to (6.16), the failure load is obtained as

$$Q_f = \frac{K(n_s F_{su} + MF_{pu} + 2F_{eu})}{(\frac{w}{x_o} - 1)(2n_s k_s + Mk_p + 2k_e)} \tag{6.17}$$

6.3.2.2 Failure at the side:

The total vertical force along the side is

$$n_d F_d + MF_{pl} + 2F_{el} = \frac{Q}{k}(n_d k_d + Mk_p + 2k_e) \tag{6.18}$$

Equating the above force to the capacity of the side and the in-line sheet to purlin fasteners gives

$$Q_f = \frac{k(n_d F_{du} + MF_{pu} + 2F_{eu})}{n_d k_d + Mk_p + 2k_e} \tag{6.19}$$

in which F_{du} = strength of an individual side fastener.

6.3.2.3 Failure at the end:

The end fasteners are subject to both horizontal and vertical forces. In general, the horizontal components are small compared to the vertical forces, and thus diaphragm failure associated with the horizontal shear forces is rare. However, if the number of end fasteners in a diaphragm is small, their horizontal force components should not be ignored. The maximum vertical force occurs in the fasteners closest to the panel corners and can be evaluated from Eq. (6.15). By equating the magnitude of the resultant force to the fastener capacity (F_{eu}), the failure load Q_f can be evaluated.

6.3.3 Diaphragm Orientation - Relative to Load

The above derivation of D_1 and fastener forces is based on the configuration where the applied load is in the direction of corrugations (Fig. 6.5a). Fig. (6.5b) shows the alternate configuration where the load is applied in a direction normal to the corrugations, and whose flexibility would be different from that of the other case if the diaphragm is not square in shape. A more intrinsic property of shear diaphragms which is invariant with respect to loading configuration is the "diaphragm shear modulus" defined as

$$G = \frac{q}{\gamma} \tag{6.20}$$

in which q = shear flow, equal to Q/b for configuration of Fig. 6.4a and to Q'/a for configuration of Fig. 6.5b; and γ = shear angle, equal to D/a and D'/b for configurations (a) and (b), respectively. Note that the diaphragm length a is in the direction perpendicular to the corrugations, whereas b is the panel span.

Let S be the diaphragm stiffness derived from configuration (a), i.e.

$$Q = SD \tag{6.21}$$

The diaphragm stiffness S' for configuration (b); i.e. Q' = S'D', may be derived from S as follows. Expressing Q and D of Eq. (6.21) in terms of q and γ, the diaphragm shear modulus is obtained as

$$G = S\frac{a}{b} \tag{6.22}$$

Similarly, for configuration (b)

$$G = \frac{q'}{\gamma'} = \frac{Q'/a}{D'/b} \tag{6.23}$$

Equating G in Eqs. (6.22) and (6.23) leads to

$$Q' = S\frac{a^2}{b^2}D' \tag{6.24}$$

The diaphragm stiffness S' is then seen to be

$$S' = S\frac{a^2}{b^2} \tag{6.25}$$

The fastener forces for configuration (b) can also be obtained from those of configuration (a) by recognizing that the two configurations are statically equivalent if $Q = Q'\frac{b}{a}$. Substitution of this equation to Eqs. (6.13) - (6.16) gives the appropriate expressions for the fastener forces.

6.3.4 "Direct" and "Indirect" Shear Transfer Cases

Past research has shown that a panel of profiled sheeting is most efficient as a diaphragm when it is connected on all four edges [36]. This may be achieved either by ensuring that the framing members and purlins form a flat surface, or as has been shown in Chapter III, by using "shear connectors" as side fasteners. This form of construction results in what is termed "direct shear transfer" case. Absence of the side fasteners will force the shear loads to be transferred through the end and purlin connections, and will result in the "indirect shear transfer" case.

While Bryan and Davies derived separate expressions for the fastener forces and the deflection component D_1 for the two cases, the present expressions are applicable to both. To obtain solutions for indirect shear transfer diaphragms, one needs only to set the number of side fasteners (n_d) and their stiffness (k_d) to zero in all expressions.

6.4 CORRELATION WITH TEST RESULTS AND FINITE ELEMENT ANALYSES

The validity of the present simple method of previous sections and its refinement (Appendix A) have been verified in references 67 and 68. The expressions were applied to the analysis of 8 light-gauge steel diaphragms, which have been tested and reported in the literature, and having a wide range of constructional details, such as fastener type (welded and screw fastened), panel type (flat stiffened with hat sections and corrugated sheets), diaphragm size and direction of load application. The expressions have shown to be general, easy to apply and also have been shown to yield reasonably good results (for diaphragm flexibility and strength) when compared to test results and to finite element analyses.

In this section, the expressions are applied to the analysis of 10 tested asbestos-cement diaphragms (6 of the cavity deck type, and 4 of the "T" deck type), to evaluate further its applicability to asbestos diaphragms. These diaphragms are fully described in Chapter III and also their finite element analyses in Chapter V, thus, only those data relevant to the present formulation are tabulated in Table 6.1.

The calculated diaphragm flexibilities and strengths are compared to finite element results and experimental data on Tables 6.2 and 6.3, respectively. Inspection of Table 6.2 shows excellent agreement between the present method (and its refined version) and finite element analyses regarding the diaphragm shear flexibility. The calculated flexibilities for all "direct shear transfer" diaphragms are shown to be lower than finite element results by less than 9%, with the results from the refined theory being more accurate. On the other hand, higher discrepancy is obtained in the case of "indirect shear transfer" diaphragms (C-1 and T-1). The diaphragm strengths are calculated based on the strength of the end fasteners, as discussed in the previous chapter (see Section 5.6.3). As shown in Table 6.3, the predicted failure loads are, in general, on the conservative side, again with higher discrepancy in the case of diaphragms C-1 and T-1.

It should be mentioned that in the analysis of the indirect shear transfer diaphragms, i.e. C-1 and T-1, the diaphragm constant K (Eq. 6.10) was multiplied by the ratio $2(N-1)/N$, where N is the number of panels in the diaphragm. This modification is explained by the fact that the end fasteners at the exterior panels are loaded with a horizontal shear force half that of the end fasteners at the internal panels, as revealed by the corresponding finite element analyses. Thus, the shear force at the exterior panel end is equal to $\frac{Qa}{2(N-1)b}$ instead of $\frac{Qa}{Nb}$ (Figures 6.3 and A.1).

A summary of the fastener forces is presented in Tables 6.4 and 6.5. The results are compared to those obtained by finite element analyses. The tabulated fastener forces are for an applied load of 1 kip. It should be noted that the finite element results for the forces in the seam and side fasteners vary very little from one fastener to another (as evident in Figures 5.9 and 5.10), thus the average values of these forces are used for comparison in Table 6.4. It can be seen that the present method, with its linear variation of the vertical end fastener forces, predicts the fastener forces more accurately than its refined version. This clearly indicates that the refined theory is suitable only when there are three or more fasteners per panel end (see Appendix A), and only then a quadratic variation in the end fastener forces is justified.

6.5 CONCLUSIONS

A simple method for the design of diaphragms has been presented. The present method has the advantage that only one single mode of deformation has been assumed in the derivation of the expressions for both the fastener forces and the diaphragm flexibility and strength. The formulas are applicable to both direct and indirect shear transfer cases. The application of the method to asbestos-cement diaphragms shows that the calculated strengths and flexibilities generally agree with finite element analyses and experimental data. Although the refined expressions accurately predicted diaphragm flexibilities, poor correlation with finite element results was obtained regarding the fastener forces.

TABLE 6.1

DIAPHRAGM DATA

Diaphragm	No. of Different Types of Connections			Fastener Stiffness (kip/in)				Fastener Ultimate Strength (lb)					
	n_e	n_s	n_d	K_e	K_s		K_d	F_{eu}		F_{su}		F_{du}	
				L&T	L	T	L&T	L	T	L	T	L	T
C-1	1	5	-	28	8.4	6.72	-	850	670	450	330	-	-
C-2	1	5	5	28	8.4	6.72	28	850	670	450	330	850	670
C-3	1	7	7	28	8.4	6.72	28	850	670	450	330	850	670
C-4	1	9	9	28	8.4	6.72	28	850	670	450	330	850	670
C-7	2	7	7	28	8.4	6.72	28	850	670	450	330	850	670
C-8	1	5	5	28	8.4	6.72	28	850	670	450	330	850	670
T-1	2	8	-	28	19.6	11.76	-	850	670	500	330	-	-
T-2	2	8	3	28	19.6	11.76	28	850	670	500	330	850	670
T-3	2	12	4	28	19.6	11.76	28	850	670	500	330	850	670
T-4	2	12	5	28	19.6	11.76	28	850	670	500	330	850	670

Data Common to Diaphragms:

$a = b = 120''$, $w = 15''$, (Cavity Decking) = 21'' (T-decks)

$N = 9$ (Cavity Decking) = 6 (T-decks)

TABLE 6.2

SUMMARY OF CALCULATED DIAPHRAGM SHEAR FLEXIBILITIES (inch/kip)

Diaphragm	Simplified Method	Refined Simplified Method*	Finite Element Analysis	Full-Scale Test
C-1	0.3372	0.5468	0.455	0.417
C-2	0.2094	0.2187	0.224	0.240
C-3	0.1551	0.1598	0.159	0.163
C-4	0.1245	0.1274	0.127	0.130
C-7	0.1409	0.1494	0.149	0.160
C-8	0.2060	0.2176	0.218	0.200
T-1	0.0870	0.131	0.134	0.167
T-2	0.0644	0.0646	0.071	0.060
T-3	0.0480	0.0482	0.051	0.069
T-4	0.0450	0.0451	0.048	0.060

* See Appendix A

TABLE 6.3

SUMMARY OF CALCULATED ULTIMATE LOADS (kips)

Diaphragm	Simplified Method	Refined Simplified Method*	Finite Element Analysis	Full-Scale Test
C-1	1.50	1.50	3.89	3.60
C-2	5.44	6.03	4.78	4.72
C-3	5.70	6.03	7.23	6.80
C-4	5.80	6.04	7.73	7.64
C-7	6.25	10.15	7.47	6.75
C-8	5.54	6.02	4.82	5.76
T-1	2.17	1.92	3.97	3.33
T-2	5.14	6.15	5.58	4.50
T-3	5.95	6.64	7.36	6.52
T-4	6.77	7.15	7.44	8.12

* See Appendix A

TABLE 6.4

SUMMARY OF CALCULATED SIDE (F_d) AND SEAM (F_s) FASTENER FORCES, in lbs

Diaphragm	Simplified Method		Refined Simplified Method*		Finite Element Analysis+	
	F_d	F_s	F_d	F_s	F_d	F_s
C-1	-	225	-	225	-	185
C-2	211	189	201	199	231	203
C-3	149	137	143	142	161	145
C-4	115	108	112	111	123	113
C-7	147	128	145	137	159	136
C-8	214	186	201	199	236	201
T-1	-	130	-	117	-	149
T-2	265	141	302	131	232	142
T-3	207	93	231	86	184	83
T-4	173	90	189	86	158	83

* See Appendix A

+ Average Values

TABLE 6.5

SUMMARY OF CALCULATED END FASTENER FORCES, IN LBS, OF EXTERIOR PANEL

Diaphragm	Simplified Method		Refined Simplified Method*		Finite Element Analysis+	
C-1	562.5		562.5		462.5	
C-2	53		4.1		70	
C-3	40		3.0		54	
C-4	32		2.3		44	
C-7	27	-92	9	-37	29	-109
C-8	48		4.0		65	
T-1	+378	+143	432	34	+351	+170
T-2	+143	+21	70	-0.4	+128	+ 23
T-3	+116	+ 25	57	-0.03	+104	+ 29
T-4	+ 94	+ 15	43	-0.41	+ 87	+ 17

* See Appendix A

+ Average Values

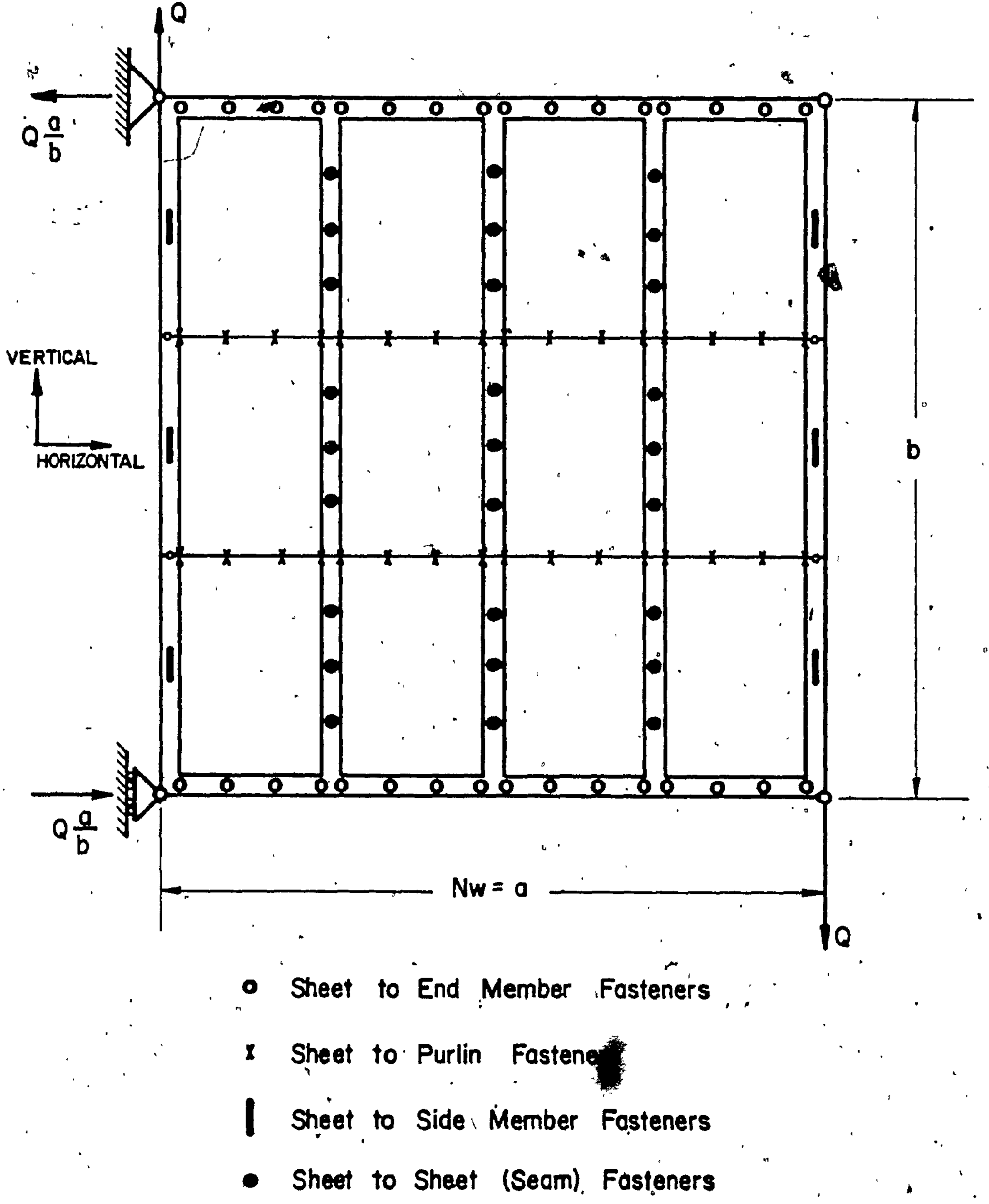
Q
Q a/b
VERTICAL
HORIZONTAL
b
Q a/b
Nw = a
Q
o Sheet to End Member Fasteners
x Sheet to Purlin Fasteners
| Sheet to Side Member Fasteners
● Sheet to Sheet (Seam) Fasteners

FIG. 6.1 COMPONENTS OF A TYPICAL DIAPHRAGM

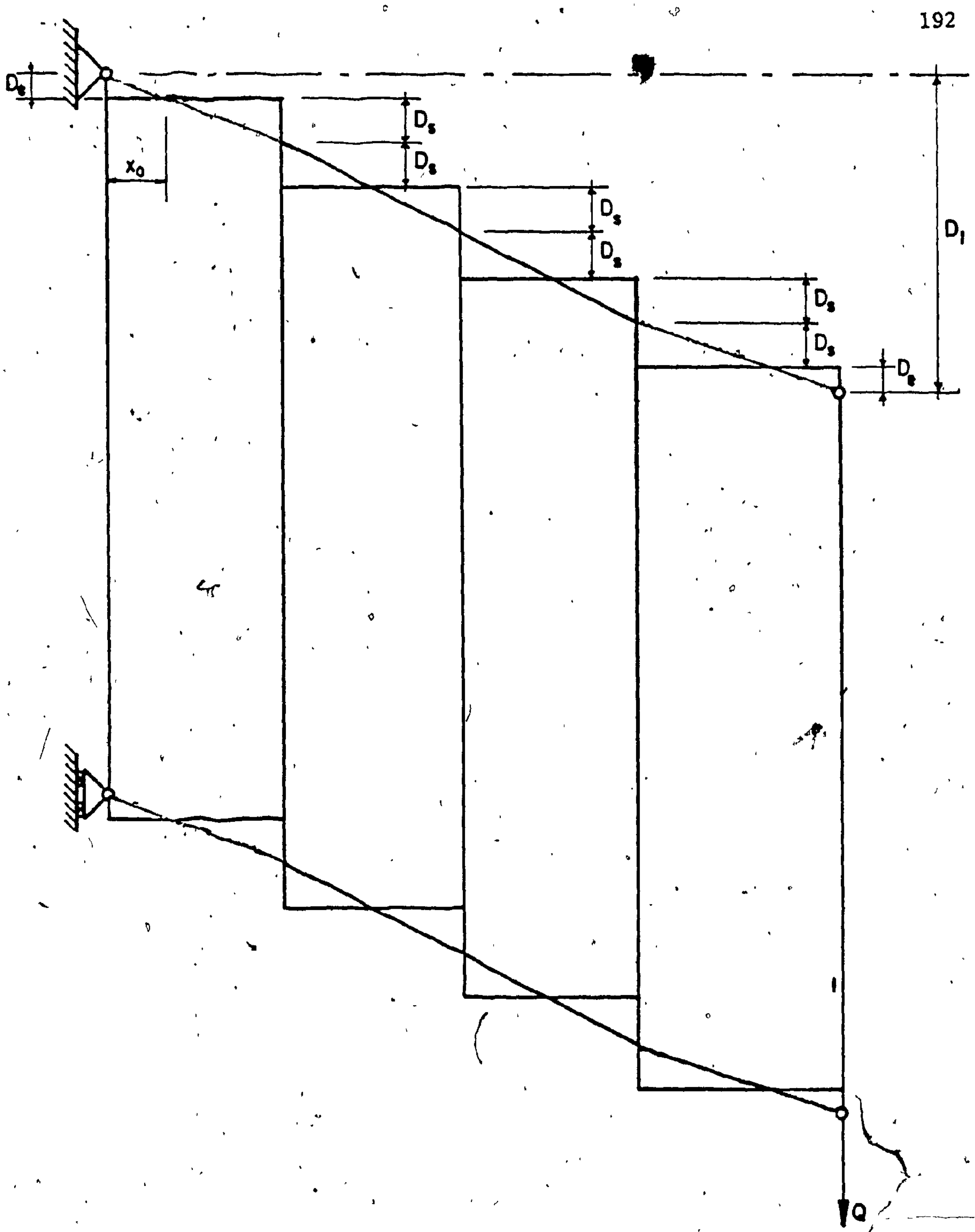

FIG. 6.2 DIAPHRAGM DEFORMATION MODE DUE TO FASTENER FLEXIBILITY

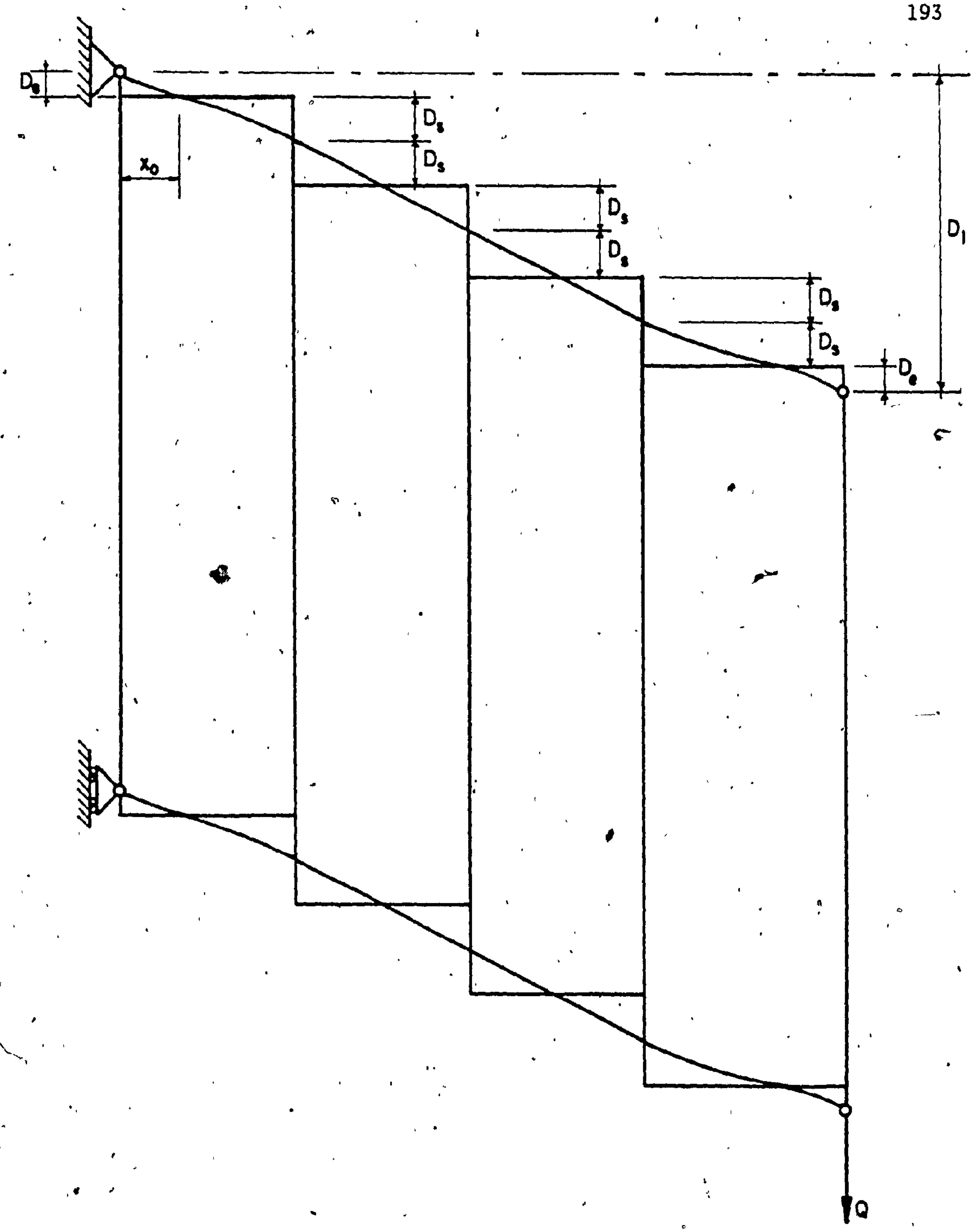

FIG. 6.3 DIAPHRAGM DEFORMATION MODE DUE TO FASTENER FLEXIBILITY (REFINED DISTRIBUTION)

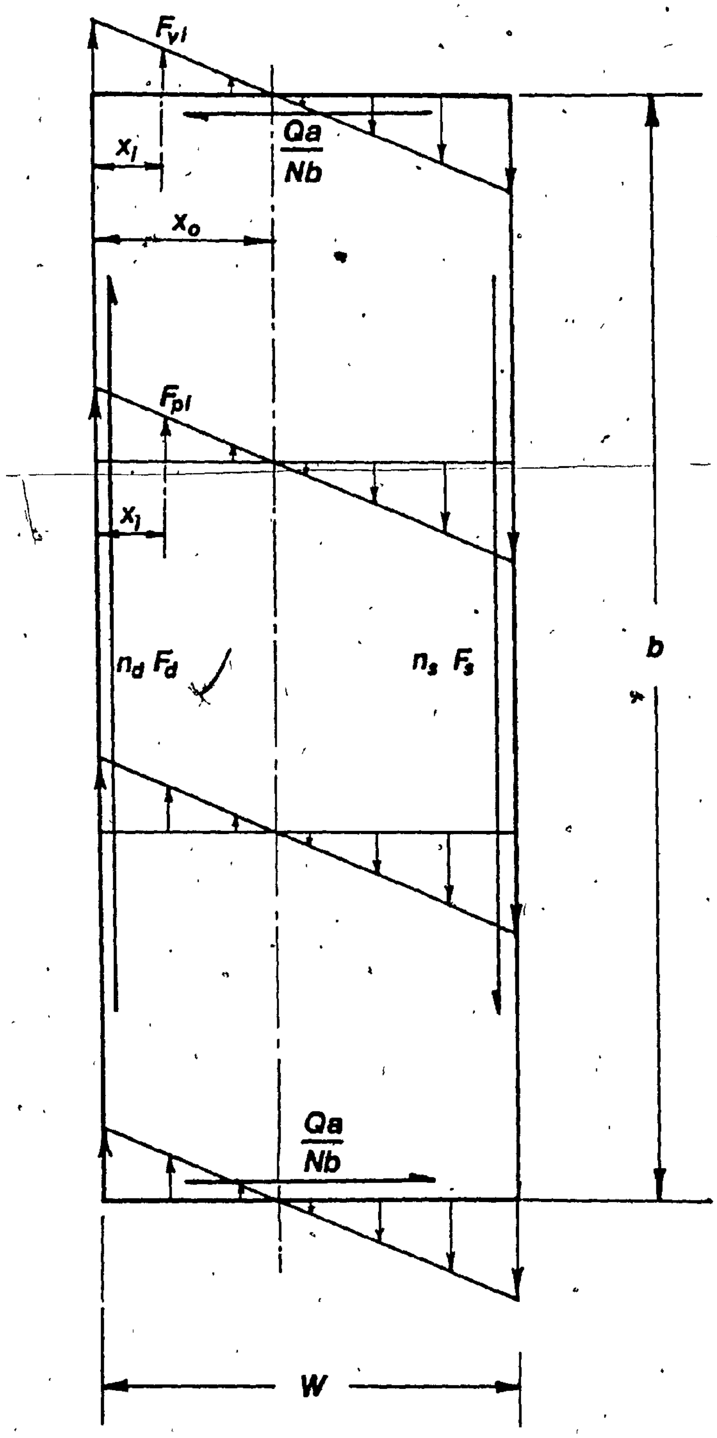

FIG. 6.4 FORCES ACTING ON THE LEFT EXTERIOR PANEL

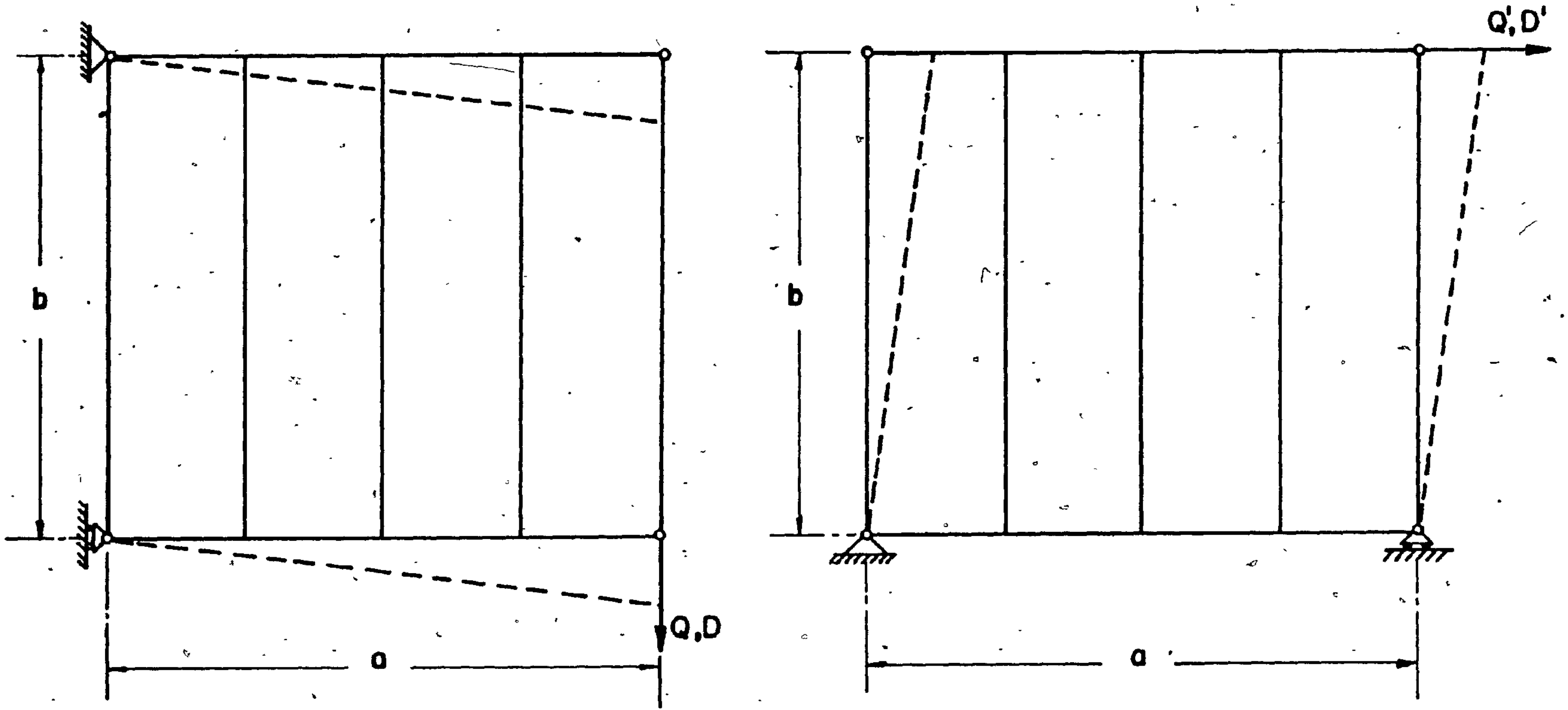

(a) (b)

FIG. 6.5 LOADING CONFIGURATIONS: (a) LOAD PARALLEL TO CORRUGATIONS; (b) LOAD PERPENDICULAR TO CORRUGATIONS

CHAPTER VII

DESIGN OF ASBESTOS-CEMENT DIAPHRAGMS

CHAPTER VII

DESIGN OF ASBESTOS-CEMENT DIAPHRAGMS

7.1 INTRODUCTION

Full-scale test results (Chapter III) have shown that both the cavity and "T" deck roofing panels possess definite and useful diaphragm capabilities. Thus, if properly designed and constructed, the two decking system would be capable of resisting shear forces in their own planes in addition to those forces acting normal to their surface. The effective use of their shear resistance can therefore supplement or eliminate conventional separate bracing systems and reduce building costs. Towards that goal, design and construction guidelines and recommendations are presented in this chapter. An application of the design criteria is demonstrated by a practical design example.

7.2 CONDITIONS FOR DIAPHRAGM DESIGN

To insure proper diaphragm action, methods of erection and maintenance used for the construction of shear diaphragms should be carefully evaluated [21]. In general, in order that a roof decking system may act as a shear diaphragm, certain conditions must be fulfilled [20,21,37,38,40, 41]:

(1) There must be vertical walls or bracings at the ends of the deck so that the diaphragm forces may be taken down to the foundations.
(2) The connections between the roof steelwork and the main frames must be adequate to carry the diaphragm forces from the deck into the main frames.

(3) The decking and fasteners must be regarded as structural components. It is imperative that proper inspection and quality control procedures be established to insure the soundness and spacing of the connections.

(4) Temporary bracing should be introduced wherever necessary during initial construction or when replacing panel sections.

(5) The deck must be provided with longitudinal edge members which are adequate to carry the axial flange forces arising from the deck acting as a plate girder. The connections between adjacent lengths of these members must also be adequate to carry the flange forces.

7.3 DESIGN CRITERIA

Similar to the case of light-gage steel diaphragms, asbestos cement diaphragms may be designed on the basis of a limiting horizontal deflection, or of the ultimate strength. In the first case, the shear flexibility of the decking and the slip at the fasteners have to be taken into account; and in the second the usual criterion is tearing of the sheet at the fasteners. In most designs, both stiffness and strength have to be considered.

7.3.1 Deflection

The permissible deflection of a given diaphragm depends on the type of building construction and the type of occupancy. When diaphragms are supporting masonry or concrete walls, it is recommended that the maximum deflection of the diaphragm computed be limited to the amount by the formula given in Bulletin No. 1 of the Structural Engineers Association of Southern California. This formula is as follows:

$$\Delta_{max} = \frac{100\ h_w^2\ f_c}{E_w t_w} \qquad (7.1)$$

where

Δ_{max} = maximum permissible deflection of the wall (in.)

h_w = height of wall between horizontal supports (ft.)

f_c = allowable flexural compressive strength of wall material (psi)

E_w = modulus of elasticity of wall material (psi)

t_w = thickness of wall (in.)

In addition to the consideration of deflection from the viewpoint of structural safety, under certain circumstances an analysis of shear reactions, shear, and bending moments may depend on a deflection study. For example, intermediate shear walls may be present in addition to the usual shear walls at the ends of a building (end-gables), in which case a deflection analysis is mandatory in order to determine the distribution of reactions to the various resisting elements [30,31,37].

The method adopted in North America in calculating the total deflection of shear diaphragms is based on arithematically summing up two components of deflection [e.g. 20,21,27,30,31,33,43].

(1) Flexural Deflection (Δ_b)

The flexural deflection of a diaphragm is determined by conventional beam deflection formulas as given in Table 7.1 for the two diaphragm span conditions: the simple beam type (Fig. 7.1(a)), and the cantilever type (Fig. 7.1(b)). The moment of inertia of the diaphragm is computed considering only the moment of inertia of the marginal beams about the mid-depth of the diaphragm, neglecting the small contribution of the diaphragm web (see Appendix B, B.3).

(2) Web Shear Deflection (Δ_s)

The shear deflection of the diaphragm is the sum of the deflections due to: (i) the shear stress in an assumed solid web (flat plate), (ii) the seam slip between adjacent panels; and (iii) the relative movement between marginal beams and shear web at end connections. The diaphragm shear deflection (Δ_s) can be seen to be inversly proportional to the diaphragm shear modulus (G') as given by the formulas in Table 7.1.

It is also customary to express the web shear deflection using a proportional constant (F) termed the "Flexibility factor" [30, 31] measured in micro-inches per pound. It represents the average micro-inches a diaphragm web will deflect in a span of one foot under a shear of one pound per foot of diaphragm width. Formulas for "Δ_s" in terms of "F" are also given in Table 7.1. As can be seen, the diaphragm constants "F" and "G" are related by the equation:

$$G' = \frac{10^6}{F} \qquad (7.2)$$

7.3.2 Strength

Due to the fact that the roof decking panels are often relatively stiff compared with the steel framework, they may attract a considerable shear load. This load may be in excess of what can be borne by the sheet-to-purlin and seam fasteners at the usual spacings. It is therefore always important to check the diaphragm strength of a deck, even if deflection alone is the expected criterion [37,40].

The general procedure is to apply a safety factor to the measured or calculated diaphragm ultimate strength. Thus, the allowable design shear for all diaphragms shall be given as:

$$S_{desg} = \frac{S_u}{S.F.} \qquad (7.3)$$

where

S_{desg} = allowable design shear lb/ft.

S_u = tested or calculated ultimate shear strength lb/ft

S.F = safety factor

The choice of a suitable safety factor must be left to the designer, bearing in mind the nature and use of the building. In the design of screw connected light gage steel diaphragms a safety factor of 2.1-2.5 has been suggested in the United States [21], while in Britain, a factor of 1.7 - 1.8 has been used [40]. For the case of asbestos-cement diaphragms, to account for its unpredictable long-term behaviour (due to carbonation, hydration of free lime and creep [1]) a safety factor of 3.5 to 4.0 is more appropriate.

7.4 DIAPHRAGM DESIGN EXAMPLES

In the following two design examples similar to those in Ref. 31 are presented to illustrate the simplicity of the design procedure.

7.4.1 Example One

Given: A one-storey steel frame building covered with 10 ft. long cavity decking panels. Wall height is 16 ft. and design wind pressure is 20 psf. Lateral deflection of the diaphragm will not adversely affect the cladding. Therefore diaphragm deflection is assumed to be not critical and limiting stress is the design criterion. The building plan is given in Fig. 7.2.

Required: To determine the layout (distribution) of fasteners (seam and side) and the size of the diaphragm perimeter members parallel to the length of the building.

Solution:

(1) Determine the lateral load due to wind acting on the roof diaphragm. Assume this to be a uniform load, W, equal to the wind pressure times half the wall height

$$W = 20 \times 1/2 \times 16 = 160 \text{ lb/ft}$$

(2) Determine the maximum diaphragm shear, q, with diaphragm spanning between end-walls (see Fig. 7.1(a))

$$q = \frac{WL}{2D} = \frac{160 \times 270}{2 \times 120} = 180 \text{ lb/ft}$$

(3) Determine the required number (or spacing) of side and seam fasteners to resist the maximum diaphragm shear. If a safety factor of 3.5 is considered, the layout of fasteners for tested diaphragm C-3 (Chapter III) would be enough, where the allowable diaphragm shear is given as:

$$\frac{680}{3.5} = 194 \text{ lb/ft} > 180 \text{ lb/ft} \quad \underline{\text{OK}}$$

Thus, 7 fasteners per seam line or side (spacing of 15") are to be used.

(4) Select a trial perimeter member. Try L 3-1/2 x 3-1/2 x 3/8 continuous [$A = 2.48 \text{ in}^2$; $r = 1.07$ in; $S = 1.2 \text{ in}^3$]

Determine:

a) axial stress due to diaphragm flexure (f_a)

$$M = \frac{WL^2}{8} = \frac{160 \times 270^2}{8} = 1{,}458{,}000 \text{ ft-lb}$$

$$P_a = \frac{M}{D} = \frac{1{,}458{,}000}{120} = 12{,}150 \text{ lb}$$

$$f_a = \frac{P_a}{A} = \frac{12{,}150}{2.48} = 4899 \text{ psi}$$

b) local bending stress due to wind load acting on perimeter member over its unsupported length equal to the joist spacing of 10 ft. Assume the two perimeter members transverse to the wind direction each take one half the total lateral load on the diaphragm

$$W_1 = \frac{1}{2} W = \frac{1}{2} \times 160 = 80 \text{ lb/ft}$$

For a continuous member

$$M_1 = \frac{W_1 L_1^2}{10} = \frac{80 \times 10^2}{10} = 800 \text{ ft.lb}$$

and $$f_b = \frac{M_1}{S} = \frac{800 \times 12}{1.2} = 8000 \text{ psi}$$

c) check adequacy of beam-column member (combined stresses). For a non-compact section [83]

i. width-to-thickness ratio

$$\frac{b}{t} \leq \frac{75}{\sqrt{F_y}} \qquad \text{(CSA S16 Clause 14.1.1)}$$

assuming F_y = 44,000 psi.

$$\frac{3.5}{3/8} = 10.13 \quad \frac{75}{\sqrt{44}} = 11.31 \quad 10.13 < 11.31 \qquad \underline{\text{OK}}$$

ii. strength

$$\frac{f_a}{0.6 F_y} + \frac{f_b}{F_b} \leq 1.0 \qquad \text{(CSA S16 Clause 17.1.1)}$$

$$F_b = 0.6 F_y \qquad \text{(CSA S16 Clause 16.2.4)}$$

$$\frac{4,899}{26,400} + \frac{8,000}{26,400} = 0.186 + 0.303 = 0.89 < 1.0 \qquad \underline{\text{OK}}$$

iii. stability

$$\frac{f_a}{F_a} + \frac{C_m f_b \alpha}{F_b} \leq 1.0 \qquad \text{(CSA S16 Clause 17.1.1)}$$

in which:

$$F_a = \frac{149,000}{(KL/r)^2} \qquad \text{(CSA S16 Clause 16.2.2)}$$

$$F_b = 0.6 F_y \qquad \text{(CSA S16 Clause 16.2.4)}$$

C_m = 1.0 (equal end moments)

$$\alpha = \text{amplification factor} = \frac{1}{1 - \frac{f_a}{F'_e}}, \quad F'_e = \frac{149,000}{(KL/r)^2}$$

calculate $\frac{KL_1}{r} = \frac{1 \times 10 \times 12}{1.07} = 112$

whence $F_a = 11,878$ psi, and $\alpha = 1.7$

$$\frac{4,899}{11,878} + \frac{1.0 \times 8,000 \times 1.7}{26,400} = 0.412 + 0.515 = 0.927 < 1.0 \quad \underline{\text{OK}}$$

Use L $3\frac{1}{2} \times 3\frac{1}{2} \times \frac{3}{8}$ continuous

7.4.2 Example Two

Given: A one-storey masonry wall building covered with 10 ft. long cavity decking panels. The loading, spans and general design are the same as for Example One, with the exception of the 10 inch thick masonry perimeter walls. In this example the roof diaphragm is tied to, and provides lateral support for the masonry walls. Therefore diaphragm deflection must be limited so as to prevent excessive stresses in the walls due to lateral displacement.

Required: To determine the layout (distribution) of fasteners (seam and side) and the size of the diaphragm perimeter members parallel to the length of the building.

Solution:

(1) Follow steps 1 to 4 inclusive of Example One. This results in a diaphragm design which is sufficiently strong but not necessarily with sufficient stiffness.

(2) Determine limiting deflection of the 16 ft. high masonry wall. Assume 1500 psi concrete block units with types M or S mortar. (See CSA S304-1976 [84]).

$$\Delta_{max} = \frac{100\, h^2\, f_c}{E_w\, t_w} \text{ in.}$$

where: $t_w = 10$ in., $E_w = 1.15 \times 10^6$ psi, $f_c = 0.32 \times 1,150 = 368$ psi

$h = 16$ ft.

$$I = \frac{A\ D^2 (12)^2}{2} \text{ in}^4$$

$$= \frac{2.48 \times 120^2\ (12)^2}{2} = 2.57 \times 10^6 \text{ in}^4$$

$$\Delta_F = \frac{5\ WL^4\ (12)^3}{384\ EI} \text{ in.}$$

$$= \frac{5 \times 160 \times 270^4 \times 12^3}{384 \times 29.5 \times 10^6 \times 2.57 \times 10^6} = 0.252 \text{ in.}$$

b) Web deflection (Δ_W)

$$q = \frac{WL}{4D} = \frac{160 \times 270}{4 \times 120} = 90 \text{ lb/ft}$$

F = flexibity factor = $\frac{10^6}{G'}$

For tested diaphragm C-3 (Chapter III). $G' = 6135$ lb/in

$F = 163$

$$\Delta_W = \frac{qLF}{2 \times 10^6}$$

$$\Delta_W = \frac{90 \times 270 \times 163}{2 \times 10^6} = 1.98 \text{ in.}$$

c) Total deflection

$$\Delta_T = \Delta_F + \Delta_W$$

$$= 0.252 + 1.98 = 2.232 > \Delta_{max}\ (0.820 \text{ in})\ \underline{\text{NG}}$$

Diaphragm stiffness must be increased. Redesign diaphragm so that $\Delta_T \leq \Delta_{max}$.

TABLE 7.1

FORMULAS FOR MAXIMUM DIAPHRAGM DEFLECTION

TYPE OF DIAPHRAGM	DIAPHRAGM LOADING CONDITION	FLEXURAL DEFLECTION Δ_b (inches)	WEB OR SHEAR DEFLECTION Δ_w (or Δ_s) (inches)	
Simple beam	Uniform load	$\frac{5\ wL^4(12)^3}{384\ EI}$	$\frac{wL^2}{8G'b}$	$\frac{q\ LF}{2x10^6}$
	Load P applied at center	$\frac{PL^3(12)^3}{48\ EI}$	$\frac{PL}{4G'b}$	
	Load P applied at each 1/3 point of span	$\frac{23PL^3(12)^3}{648\ EI}$	$\frac{PL}{3G'b}$	
Cantilever beam (at Free End)	Uniform load	$\frac{w\ a^4(12)^3}{8\ EI}$	$\frac{wa^2}{2G'b}$	$\frac{q\ aF}{10^6}$
	Load P applied at free end	$\frac{P\ a^3(12)^3}{3\ EI}$	$\frac{Pa}{G'b}$	

E = modulus of elasticity of steel (29.5 x 10^6 psi)

I = moment of inertia of diaphragm flange (perimeter) members about centroidal axis of diaphragm (in^4)

L = span of simple beam (ft)

a = span of cantilever beam (ft)

P = concentrated lateral load (lbs)

w = uniform lateral load (lb/ft)

F = flexibility factor = $10^6/G'$ (in/lb)

G' = diaphragm shear modulues (lb/in)

q = average shear (per unit of diaphragm width) along L/2 or a (lb/ft)

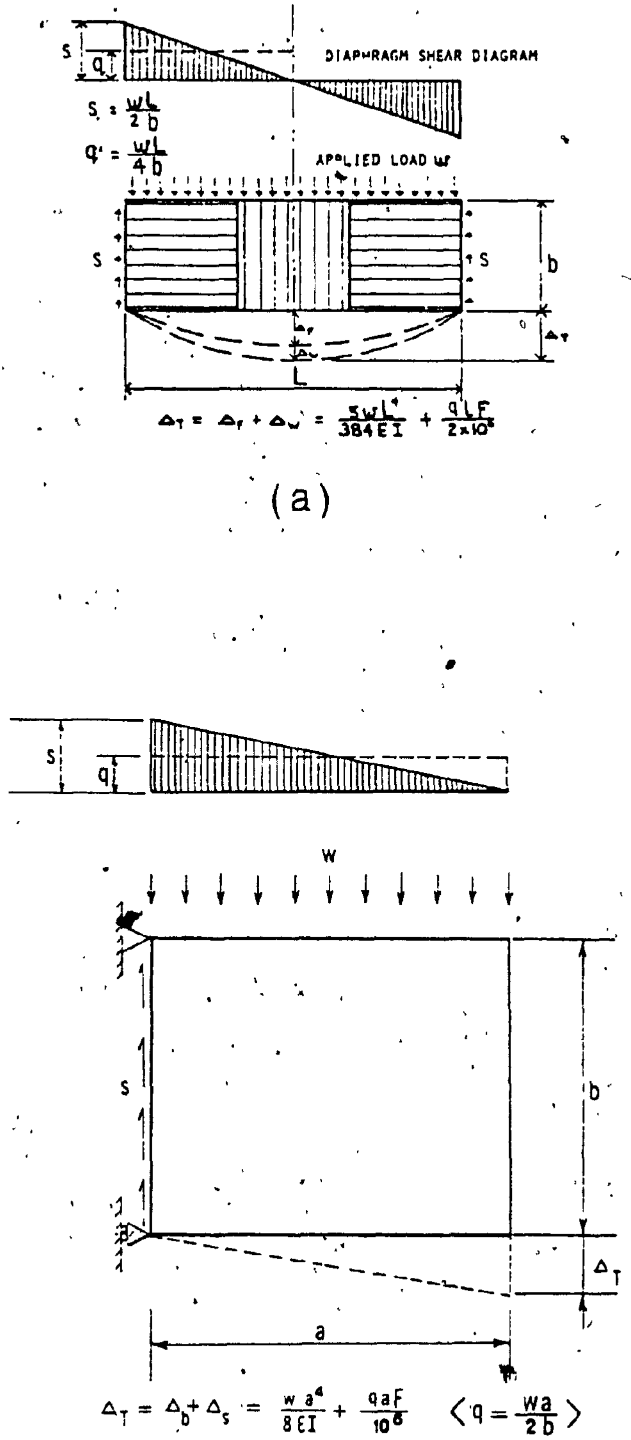

$$S = \frac{wL}{2b}$$

$$q' = \frac{wL}{4b}$$

$$\Delta_T = \Delta_f + \Delta_w = \frac{5wL^4}{384EI} + \frac{q'LF}{2\times10^6}$$

(a)

$$\Delta_T = \Delta_b + \Delta_s = \frac{wa^4}{8EI} + \frac{qaF}{10^6} \quad \langle q = \frac{wa}{2b} \rangle$$

(b)

FIG. 7.1 DIAPHRAGM DEFLECTIONS

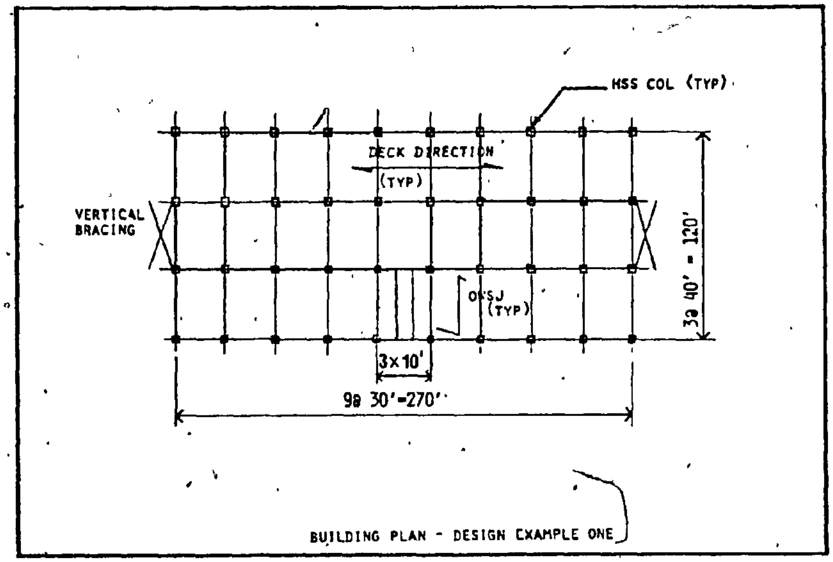

BUILDING PLAN - DESIGN EXAMPLE ONE

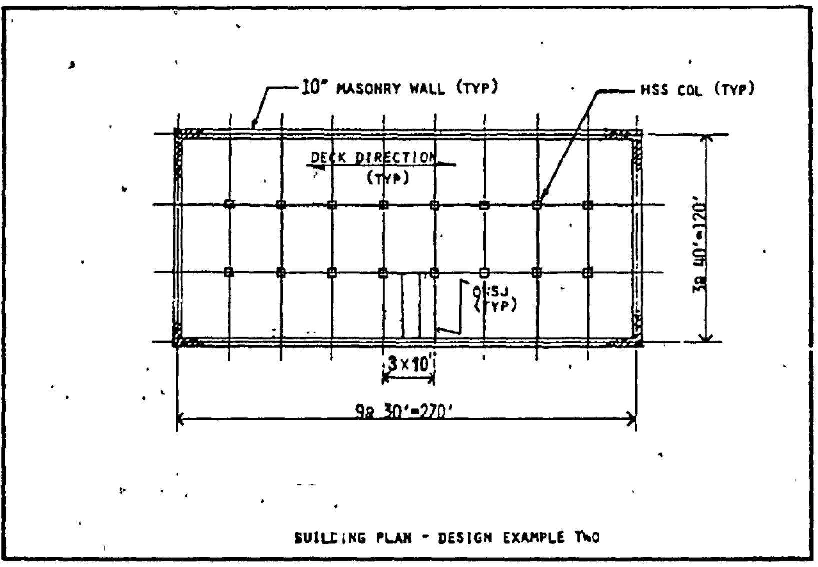

BUILDING PLAN - DESIGN EXAMPLE TWO

FIG. 7.2 BUILDING PLAN - DESIGN EXAMPLES

CHAPTER VIII

SUMMARY, CONCLUSIONS AND RECOMMENDATIONS FOR FURTHER RESEARCH

CHAPTER VIII

SUMMARY, CONCLUSIONS AND RECOMMENDATIONS FOR FURTHER RESEARCH

8.1 SUMMARY OF THE WORK

The present work is the first attempt in North America to study and evaluate the in-plane shear strength and stiffness of asbestos-cement decking assemblies. The study covered both the theoretical and experimental investigation of the diaphragm capabilities of the two decking systems (Cavity and "T" decks) which are manufactured by Atlas Asbestos Company; Quebec, Canada.

The experimental work was directed toward establishing preliminary design information on the diaphragms action of the two decking systems as currently used. For this purpose, a cantilever full-scale test frame was designed and fabricated, and a total number of thirteen diaphragm tests were conducted. Small sample tests were also conducted to determine the mechanical properties of asbestos-cement material, and the strength and stiffness of the fasteners.

The analytical investigation included:

(a) Detailed finite element analyses of the two decking systems. A special-purpose finite element computer program was developed for this purpose.

(b) The development of simple closed-form expressions for the diaphragm shear flexibility and fastener forces. The formulas are applicable to both direct and indirect shear transfer cases. The development was based on a simple deformation mode observed in tests and on an assumed distribution of the internal fastener forces as revealed by finite element analysis.

Guidelines for the design and construction of asbestos-cement shear diaphragms have been outlined and illustrated by a practical design example.

8.2 CONCLUSIONS

On the basis of the work described the following conclusions are drawn:

(1) The results of the full-scale test program indicated that the two asbestos-cement decking systems (cavity and "T" decks) as currently constructed possess a moderate amount of shear strength (360 and 333 lb/ft, respectively) and a low shear stiffness (2400 and 5990 lb/in, respectively). However, when the decks were connected at all four edges, the diaphragm stiffness increased considerably (74% and 178%, respectively) and its strength only moderately (31% and 35%, respectively). Also, it has been shown that by increasing the number of seam and side fasteners, both the stiffness and strength increase substantially.

(2) In general, the two decking systems are very flexible (especially the cavity decking) in comparison with welded light-gage steel diaphragms of the same size. Thus, if diaphragm design is based on deflection limitations, it would become difficult to eliminate the conventional bracing systems normally used. However, in such a situation, use of the deck's shear resistance may still effect some reduction in building costs. On the other hand, the two decking systems possess sufficiently high shear strength to meet the normal requirements of diaphragm design based on

strength alone. A safety factor of 3.5 to 4.0 have been recommended on the basis of the unpredictable long-term behaviour of the asbestos-cement composite.

(3) For similar fastener patterns, "T" deck diaphragms are between 2 to 3 times stiffer than cavity decking diaphragms. This is mainly attributed to the low stiffness (8.4 kip/in) of the seam fasteners used in the cavity decking as compared to that used in the "T" decks (19.6 kip/in), and secondly because of the fewer seam lines (for the same covering width) in the "T" decks, through which the shear force must be transfered. On the other hand, the strength of the "T" deck diaphragms are slightly lower because of its open profile in contrast with the rather closed one in the cavity decking.

(4) The finite element technique in conjunction with the proposed idealized structural systems has yielded results in good agreement with the experimental data. The developed special-purpose computer program requires minimal input and runing time, and has proved very useful and economical in the study of the influence of the different parameters on the general performance of the diaphragm.

(5) As revealed by the finite element analyses, the length of the decking units has a significant influence on the diaphragm stiffness and capacity. Decrease in the decking length while keeping the fastener spacing constant tends to reduce the two behavioural parameters. On the other hand, decrease in the decking length while keeping the fastener number constant produces the opposite seffect. Also, the analyses showed that changes in the number of decking units has practically no influence on the diaphragm shear modulus or its capacity.

(6) The simplified method for shear diaphragm analysis has been shown to be general, easy to apply and yielded reasonably good results when compared to accurate finite element analyses. The method has the advantage that only one single mode of deformation has been assumed in the derivation of the expressions for both the fastener forces and the diaphragm's two basic parameters (flexibility and strength). Thus, the designer can easily acquire a sense of the behaviour of the diaphragm and modify the expressions to suit special diaphragm construction details.

8.3 RECOMMENDATIONS FOR FURTHER RESEARCH

Some recommendations for further study are as follows:

(1) Development of more effective, practical means for the connections. These may be in the form of mechanical fasteners or glue or combination of both. Special water-resistant adhesive applied between the overlapping edges of the decking units may prove to be effective in increasing not only the shear stiffness and strength, but also the bending strength of the decks.

(2) The present investigation with its developed full-scale testing facility, can be extended to the study of the diaphragmic action of other asbestos-cement profiles manufactured by Atlas, e.g. Atlas Trafford Tile and Corrugated Board. These roofing and siding products are used for cladding of all buildings with large wall and/or sloping roof areas, particularly those requiring fireproof construction. They are also used as facing panels or cladding of residential or commerical buildings and for plain roofs of low cost housing.

(3) The present finite element analysis may be extended to cover the nonlinear range of diaphragm performance. The main source of nonlinear response is in the fasteners, while all panels, marginal members, and purlins would be considered elastic up to failure.

REFERENCES

REFERENCES

[1] Bryan, E.R., Kallaur, M., and Akhtar, S., "Asbestos-Cement Roofs and Z Purlins", Civil Engineering and Public Works Review, Vol. 65, March, 1970, pp 249-255.

[2] Bryan, E.R., "Asbestos-Cement Sheeting and Zed Purlins, Under Downward Load and Wind Suction", Civil Engineering and Public Works Review, Vol. 65, April, 1970, pp 375-376.

[3] Bryan, E.R., Balmain, W.A., and Oliver, J., "Testing an Asbestos Cement Building System", BUILD International, January/February, 1971, pp 36-41.

[4] Carnston, W.B., Starrock, R.D., and Clements, S.W., "Structural Effects of Asbestos-Cement Sheeting", Technical Report, Cement and Concrete Association, England, May, 1973.

[5] Godard, P., Delvaux, P., della Faille, M., and Mercier, J.P., "Mechanical Properties of Impregnated Asbestos-Cement", Proc. of the International Symposium RILEM/IUPAC, 'Pore Structure and Properties of Materials', Prauge, Sept. 18-21, 1973, pp D243-D253.

[6] De Bussy, Materials and Technology, Vol. 2, Longman, 1971, pp 33-35.

[7] Ryder, J.F., "Applications of Fibre Cement", RILEM Symposium: Fibre Reinforced Cement and Concrete, Constr. Press, Ltd., Lancaster, England, 1975, pp 23-35.

[8] Sinclair, W.E., Asbestos, 1959, pp 304-308.

[9] Carroll-Porczynski, C.F., Asbestos, 1956, pp 216-229.

[10] Kallaur, M., "The Shear Behaviour of Asbestos Cement Sheeting", MSc Thesis, University of Manchester, Manchester, England, October 1968.

[11] Allen, H.G., "Tensile Properties of Seven Asbestos Cements", Composites, June, 1971, pp 98-103.

[12] Jones, R.M., Mechanics of Composite Materials, McGraw-Hill Book Co., 1975, Chapter 2, pp 31-84.

[13] Ashton, J.E., Primer on Composite Materials: Analysis, Technomic Publ. Co., Stamford, Conn., 1969, Chapter 6, pp 95-114.

[14] Ammar, A.R., and Nilson, A.H., "Analysis of Light Gage Steel Shear Diaphragms - Part I", Research Report No. 350, Department of Civil Engineering, Cornell University, Ithaca, N.Y., August, 1972.

[15] Adsit, N.R., Carnahan, K.R., and Green, J.E., "Mechanical Behaviour of Three-Dimensional Composite Ablative Materials" Composite Materials: Testing and Design (Second Conference), ASTM, STP-497, Anaheim, California, April 20-22, 1971, pp 107-120.

[16] Krenchel, H., and Hejgaard, O., "Can asbestos be completely replaced one day?", RILEM Symposium: Fibre Reinforced Cement and Concrete, Constr. Press Ltd., Lancaster, England, 1975, pp 335-346.

[17] de Mahieu, L. "La Theorie de L'Asbeste-Ciment", S.A. Eternit N.V., Kapell-Op-Den-Bos, Belgium, 1973.

[18] Nilson, A.H., "Deflection of Light Gage Steel Floor Systems Under Action of Horizontal Loads", M.S. Thesis, Cornell University, Ithaca, New York, 1956.

[19] Nilson, A.H., "Report on Tests of Light Gage Steel Floor Diaphragms - 1957 Series", Research Report, Dept of Structural Engineering, Cornell University, Ithaca, N.Y., 1957.

[20] Nilson, A.H., "Shear Diaphragms of Light Gage Steel", J. Struc. Div., ASCE, Vol. 86, No. ST11, Proc. Papaer 2650, Nov. 1960, pp 111-140

[21] "Design of Light Gage Steel Diaphragms", American Iron and Steel Institute, 1967.

[22] Bryan, E.R., and EL-Dakhakhni, W.M., "Shear of Thin Plates with Flexible Edge Members", J. Struc. Div., ASCE, Vol. 90, No. ST4, Proc. Paper 3991, Aug. 1964, pp 1-14.

[23] Bryan, E.R., and EL-Dakhakhni, W.M., "Behaviour of Sheeted Portal Frame Sheds: Theory and Experiments", Proc. Inst. of Civl Engrs. Vol. 29, Dec. 1964, pp 743-778.

[24] Bates, W., Bryan, E.R., and EL-Dakhakhni, W.M., "Full Scale Tests on a Portal Frame Shed", The Structural Engineer, Vol. 43, June 1965,

[25] Luttrell, L.D., "Structural Performance of Light Gage Steel Diaphragms", Research Report No. 319, Dept. of Struc. Engrg., Cornell University, Ithaca, N.Y., Aug. 1965.

[26] Luttrell, L.D., "Light Gage Steel Shear Diaphragms", Civil Engr. Dept. Publication, West Virgina University, 1965.

[27] Luttrell, L.D., "Strength and Behaviour of Light Gage Steel Shear Diaphragms", Cornell University, Engrg. Research Bulletin 67-1, Ithaca, N.Y. July, 1967.

[28] Luttrell, L.D., "Screw Connected Shear Diaphragms", Proc. 2nd Speciality Conference on Cold-Formed Steel Structures, Univ. of Missouri-Rolla, Rolla, Mo., Oct. 1973.

[29] Apparao, T.V.S.R., "Tests on Light Gage Steel Diaphragms", Research Report No. 328, Dept. of Struc. Engrg., Cornell University, Ithaca, N.Y., Dec. 1966.

[30] Levelt, H.L., and Fung, C., "Report on Steel Deck Diaphragms", Research and Development Dept., Westeel-Rosco Ltd., Toronto, Ontario, May 1969.

[31] "Diaphragm Action of Cellular Steel Floor and Roof Deck Construction", Canadian Sheet Steel Building Institute, CSSBI, Mississauga, Ontario, December 1972.

[32] Ellifritt, D.S., and Luttrell, L.D., "Strength and Stiffness of Steel Deck subjected to In-Plane Loading", C.E. Report 2011, Steel Deck Institute, Chicago, 1970.

[33] "Tentative Recommendations for the Design of Steel Deck Diaphragms", Steel Deck Institute, Chicago, 1972.

[34] Bryan, E.R., and EL-Dakhakhni, W.M., "Shear of Corrugated Decks: Calculated and Observed Behaviour", Proc. Inst. of Civ. Engrs., Vol. 41, Nov., 1968, pp 523-540.

[35] Bryan, E.R., and El-Dakhakhni, W.M., "Shear Flexibility and Strength of Corrugated Decks", J. Struc. Div., ASCE, Vol. 94, No. ST11, Proc. Paper 6218, Nov., 1968, pp 2549-2580.

[36] Bryan, E.R., and EL-Dakhakhni, W.M., Shear Tests on Light Gage Steel Decks", Acier-Stahl-Steel, No. 10, Oct., 1969, pp 435-442.

[37] Bryan, E.R., "The Stressed Skin Design of Steel Buildings", CONSTRADO Monograph. Crosby Lockwood Stapes, London, England, 1973.

[38] "European Recommendations for The Stressed Skin Design of Steel Structures", European Convention for Constructional Steelwork (ECCS), ECCS-SV11-77-iE No. 19, CONSTRADO, London, England, March 1977.

[39] "Design Code and Tables for Diaphragm Action in Light Gage Steel Roof Decks", Final Draft, Metal Roof Deck Association (MRDA), London, England, January 1978.

[40] Bryan, E.R., "Stressed Skin Roof Decks for the SEAC and CLASP Building Systems", CONSTRADO, London, England, March, 1973.

[41] Bryan, E.R., "Stressed Skin Design and Construction: A State of Art Report", The Structural Engineer, Vol. 54, No. 9, Sept. 1976, pp 347-351

[42] Bryan, E.R., and Davies, J.M., "Stressed Skin Construction in the U.K.", Proc. 3rd Speciality Conference on Cold-Formed Steel Structures, Univ. of Missouri-Rolla, Rolla, Mo. Nov., 1975

[43] "Standard Method of Static Load Testing of Framed Floor or Roof Diaphragm Construction for Buildings", American Society for Testing and Materials, ASTM Standard E 455-76., 1976.

[44] "Atlas Materials Selection Guide- Asbestos-cement Roof Decking", Atlas Asbestos Company's Selection Guides (general product information), Montreal, Quebec.

[45] Ammar, A.R., and Nilson, A.H., "Analysis of Light Gage Steel Shear Diaphragms - Part II", Research Report No. 351, Department of Civil Engineering, Cornell University, Ithaca, N.Y. April, 1973.

[46] Winter, G., "Tests on Bolted Connections in Light Gage Steel", J. Struc. Div., ASCE, Vol. 82, No. ST2, Proc. Paper 920, Mar. 1956, pp 920-1-920-25.

[47] Innes, P.G., Smith, R., and White, P.E., "Fasteners for Light Gage Steel Structures", International Symposium on Thin Walled Steel Structures, University College of Swansea School of Engineering, Sept. 11-14, 1967, pp 404-419.

[48] Hill, H.V., "Connections and Fasteners for Light Gage Steel Structures", Acier-Stahl-Steel, No. 10, Oct., 1974, pp 412-422.

[49] Bakker, C., and Stark, J., "Requirements Specified for Joints", Acier-Stahl-Steel, No. 10, Oct. 1974, pp 423-426.

[50] Errera, S.J., Popowich, D.W., and Winter, G., "Bolted and Welded Stainless Steel Connections", J. Struc. Div., ASCE, Vol. 100, No. ST7, Proc. Paper 10618, June 1974, pp 1279-1296.

[51] Baehre, R., and Berggren, L., "Joints in Sheet Metal Panels", The National Swedish Institute for Building Research, Document D8: 1973, Stockholm, Sweden.

[52] Nissfolk, B., "Fatigue Strength of Joints in Steel Metal Panels 1 - Riveted Connections", The Swedish Council for Building Research Docment DS: 1977, Stockholm, Sweden.

[53] Zienkiewicz, O.C., The Finite Element Method, 3rd Edition, McGraw-Hill Book Co., London, 1977.

[54] Desai, C.S., and Abel, J.F., Introduction to the Finite Element Method, Van Nostrand-Reinhold Co., New York, 1972.

[55] Cook, R.D., Concepts and Applications of Finite Element Analysis, John Wiley & Sons Inc., New York, 1974.

[56] Huebner, K.H., Finite Element Method for Engineers, John Wiley & Sons Inc., N.Y., 1975.

[57] Gallagher, R.H., Finite Element Analysis Fundamentals, Prentice-Hall, Englewood Cliffs, N.J. 1976.

[58] Nilson, A.H., "Analysis of Light Gage Steel Sheer Diaphragms" Proceedings, 2nd Speciality Conference on Cold-Formed Steel Structures, Univ. of Missouri-Rolla, Rolla, Mo., Oct. 1973 pp 325-363

[59] Nilson, A.H. and Ammar, A.R., "Finite Element Analysis of Metal Deck Shear Diaphragms", J. Struc. Div., ASCE, Vol. 100, No. ST4, Proc. Paper 10467, Apr., 1974, pp 711-726.

[60] Miller, C.J. and Sexsmith, R.G., "Analysis of Multistorey Frames with Light Gage Steel Panel Infills", Research Report No. 349, Dept. of Structural Engineering, Cornell University, Ithaca, N.Y., Aug. 1972, 199p.

[61] Lawrence, S.J. and Sved, G., "A Finite Element Analysis of Clad Structures", Conference on Metal Structures Research and its Applications, Sydney, Australia, Nov., 1972.

[62] Davies, J.M., "The Design of Shear Diaphragms of Corrugated Steel Sheeting", Report Ref. No. 74/50, Department of Civil Engineering, University of Salford, Salford, England, Sept. 1974

[63] Davies, J.M., "Calculation of Steel Diaphragm Behaviour", J. Struc. Div., ASCE, Vol. 102, No. ST7, Proc. Paper 12244, July, 1976, pp 1411-1430.

[64] Davies, J.M., "Simplified Diaphragm Analysis", J. Struct. Div. ASCE, Vol. 103, No. ST11, Proc. Paper 13320, Nov., 1977, pp 2093-2109

[65] Ha, H.K., "Corrugated Shear Diaphragms", J. Struc. Div., ASCE, Vol. 105, No. ST3, Proc. Paper 14449, Mar., 1979, pp 577-587

[66] Ha, H.K., "Lateral Load Behaviour of Multistorey Frames Stiffened with Corrugated Panels", Proc. of the Symposium on Behaviour of Building Systems and Building Components, Vanderbilt Univ., Nashville, Tennesse, March 8-9, 1979, pp. 121-135.

[67] Ha, H.K., EL-Hakim, N., and Fazio, P.P., "Simplified Design of Corrugated Shear Diaphragms", J. Struc. Div., ASCE, Vol. 105 No. ST7, Proc. Paper 14681, July, 1979, pp 1365-1377

[68] Ha, H.K., EL-Hakim, N., and Fazio, P.P., "Refined Calculations for the Strength and Stiffness of Cold-Formed Steel Diaphragms", Canadian Journal of Civil Engineering, Vol. 6, No. 2, 1979, pp 268-275

[69] Ghali, A., and Neville, A.M., Structural Analysis - A Unified Classical and Matrix Approach, 2nd Edition, Chapman and Hall Ltd., London, 1978.

[70] Przemieniecki, J.S., Theory of Matrix Structural Analysis, McGraw-Hill Book Co., N.Y., 1968

[71] Klyuyen, V.V., and Kokovkin-Scherbak, N.I., "On the Minimization of the Number of Arithmetic Operations for the Solution of Linear Algebraic Systems of Equations", Technical Report CS 24, Computer Science Department, Stanford University, Stanford, California, 1965.

[72] Meyer, C., "Solution of Linear Equations - State-of-the-Art", J. Struc. Div., ASCE, Vol. 99, No. ST , Proc Paper 9861, 1973, pp 1507-1526.

[73] Wilson, E.L., Bathe, K.J., and Doherty, W.P., "Direct Solution of Large Systems of Linear Equations", Computers and Structures, Vol. 4, 1974, pp 363-372

[74] Wilson, E.L. et al. "Computer Program for Static and Dynamic Analysis of Linear Structural Systems", EERG Report, No. 72-10, University of California, Berkeley, Nov. 1972.

[75] Bryan, E.R., and Jackson, P., "The Shear Behaviour of Corrugated Steel Sheeting", Symposium on Thin Walled Steel Structures, University of Swansea, Sept. 1967, Proc. publ. by Crosby Lockwood, 1968.

[76] Falkenberg, J.C., discussion of "Shear Flexibility and Strength of Corrugated Decks", by Eric R. Bryan and Wagih M. EL-Dakhakhni, Ref. [35], J. Struc. Div., ASCE, Vol. 95, No. ST6, Proc. Paper 6583, June 1969, pp 1382-1386.

[77] Libove, C., "Survey of Recent Work on the Analysis of Discretely Attached Corrugated Shear Webs", American Institute of Aeronautics and Astronautics, AIAA, Paper No. 72-351, Apr. 1972.

[78] Lin, C., and Libove, C., "Theoretical Study of Corrugated Plates; Shearing of a Trapezoidally Corrugated Plate with Trough Lines Held Straight", Report No. MAE 1833-T1, Syracuse University Research Institute, Syracuse, N.Y. May, 1970.

[79] Lin, C., and Libove, C., "Theoretical Study of Corrugated Plates: Shearing of a Trapezoidally Corrugated Plate with Trough Lines Permitted to Curve", Report No. MAE 1833-T2, Syracuse University Research Institute, Syracuse, N.Y. June 1970.

[80] Easley, J.T., "Strength and Stiffness of Corrugated Metal Shear Diaphragms", J. Struc. Div., ASCE, Vol. 103, No. ST1, Proc. Paper 12675, Jan. 1977, pp 169-180.

[81] Easley, J.T., "Test on Light Gage Steel Shear Diaphragms" Report on CRES Project 85, The University of Kansas, Lawrence, Kans., Feb. 1967.

[82] Easley, J.T., "Tests on Light Gage Steel Shear Diaphragms", Report on CRES Project 85, Part 2, The University of Kansas, Lawrence, Kans., Dec. 1967.

[83] CSA S16.1969, "Steel Structures for Buildings", Canadian Standard Association, Rexdale, Ontario.

[84] CSA S304-1976, "Masonry Design and Construction for Buildings", Canadian Standard Association, Rexdale, Ontario.

APPENDIX A

REFINED CALCULATIONS FOR THE SHEAR FLEXIBILITY AND STRENGTH OF DIAPHRAGMS

APPENDIX A

REFINED CALCULATIONS FOR THE SHEAR FLEXIBILITY AND STRENGTH OF DIAPHRAGMS

The simplified method of diaphragm analysis presented in Chapter 6 is extended here by incorporating a more refined distribution of the diaphragm's end (or sheet-purlin) fastener forces. Expressions for deflection component D_1 and fastener forces are derived based on the deformation mode of Fig. 6.3. In this mode, it is assumed that the vertical components of the end fastener forces vary linearly within an interior panel, and parabolically in the exterior panels.

A.1 EXPRESSIONS FOR D_1 AND FASTENER FORCES

With reference to Fig. 6.3, the deflection component D_1 can be written as

$$D_1 = 2D_e + 2(N-1)D_s \tag{A.1}$$

in which D_e, D_s = the vertical separations between the end member and the panels at the diaphragm corners and at the seam lines, respectively, and N = number of panels in the diaphragm.

To determine D_e and D_s, equilibrium of the exterior panel is considered. Figure A.1a shows the forces acting on the left exterior panel. The vertical components of the forces in the two end fasteners (or sheet-to-purlin fasteners), each located at distance x_i from the panel center line (Fig. A.1b), are given by the equations

$$F_{ei} = (K_e D_e / x_0^2)(w/2 - x_0 + x_i)^2 \tag{A.2}$$

$$F'_{ei} = (K_e D_e / x_0^2)(x_i - w/2 + x_0)^2 \tag{A.3}$$

in which K_e = stiffness of an end fastener, w = width of the panel, and x_0 is as defined in Fig. A.1.

To determine the unknown distance x_0, the equation for vertical equilibrium of the panel may be written as

$$n_d F_d - n_s F_s + n_p \sum_{i=1}^{n_e/2} \frac{K_e D_e}{x_0^2} \left(x_i - \frac{w}{2} + x_0\right)^2 - n_p \sum_{i=1}^{n_e/2} \frac{K_e D_e}{x_0^2} \left(\frac{w}{2} - x_0 + x_i\right)^2 = 0 \qquad \text{(A.4)}$$

in which n_d, n_e, n_s = the number of fasteners in the side, the end, and the seam connections, respectively; F_d, F_s = vertical forces in the side and the seam fasteners, respectively; and n_p = number of end and intermediate purlins. Equation A.4 applies specifically to the case where the purlin fasteners are symmetrically distributed. For simplicity, the small force component of the fastener at the panel center line is neglected.

From the assumed mode of deformation in Fig. 6.3 the deformations in the side and seam connections are seen to be D_e and $2D_s$, respectively. Thus

$$F_d = K_d D_e \qquad \text{(A.5)}$$

$$F_s = K_s(2D_s) = 2K_s \frac{(w - x_0)^2}{x_0^2} D_e \qquad \text{(A.6)}$$

Substitution of A.5 and A.6 into A.4 results in a quadratic equation in the unknown x_0. A meaningful solution for x_0 is given as

$$x_o = w[(1-r^{1/2})/(1-r)] \qquad \text{(A.7)}$$

in which

$$r = \frac{n_d K_d w + 2n_p K_e f}{2(n_s K_s w + n_p K_e f)} \qquad \text{(A.8)}$$

and

$$f = \sum_{i=1}^{n_e/2} x_i \tag{A.9}$$

Moment equilibrium of the panel about its center can be expressed as

$$n_d F_d \frac{w}{2} + n_s F_s \frac{w}{2} + n_p \frac{K_e D_e}{x_o^2}$$

$$\times \left[\sum_{i=1}^{n_e/2} \left(\frac{w}{2} - x_0 + x_i\right)^2 x_i \right.$$

$$\left. + \sum_{i=1}^{n_e/2} \left(x_i - \frac{w}{2} + x_0\right)^2 x_i \right] = Qw \tag{A.10}$$

This equation together with A.5 and A.6 yields the following expression for D_e,

$$D_e = Q/K \tag{A.11}$$

in which

$$K = \frac{1}{2} n_d K_d + n_s K_s \left(\frac{w}{x_0} - 1\right)^2$$

$$+ \frac{2 n_p K_e}{w x_0^2} \left[\left(\frac{w}{2} - x_0\right)^2 f + g\right] \tag{A.12}$$

and

$$g = \sum_{i=1}^{n_e/2} x_i^3 \tag{A.13}$$

The deflection component D_1 of A.1 becomes

$$D_1 = \frac{2Q}{K} \left[1 + (N-1) \left(\frac{w}{x_0} - 1\right)^2\right] \tag{A.14}$$

and for the fastener forces:

$$F_d = K_d Q/K \tag{A.15}$$

$$F_s = 2K_s(w/x_0-1)^2 \; Q/K \tag{A.16}$$

$$F_{ei} = (K_e/x_0^{\,2})(w/2 - x_0 + x_i)^2 \; Q/K \tag{A.17}$$

$$F'_{ei} = (K_e/x_0^{\,2})(x_i - w/2 + x_o)^2 \; Q/K \tag{A.18}$$

A.2 STRENGTH OF DIAPHRAGM

A conservative estimate of diaphragm strength can be made on the basis of elastic behaviour, neglecting redistribution of internal forces due to fasteners yielding. Failure of a diaphragm can occur along a vertical line of fasteners (side or seam connections) or at the end fasteners of the exterior panels.

A.2.1 Failure of the Seam

Let F_{su} and F_{eu} be the strengths of the individual fasteners at the seam and end (or sheet-to-purlin) connections. The capacity of the seam connection is $n_sF_{su} + n_pF_{eu}$ where the second term accounts for those purlin connections in line with the seam. From A.16 and A.17 the failure load is obtained as

$$Q_f = \frac{K(n_sF_{su} + n_pF_{eu})}{(\frac{w}{x_0} - 1)^2 \; (2n_sK_s + n_pK_e)} \tag{A.19}$$

A.2.2 Failure at the Side

The total vertical force along the side is, from A.15 and A.18

$$n_dF_d + n_pF_{ei'}\big|_{x_i=w/2} = (Q/K)(n_dK_d + n_pK_e) \tag{A.20}$$

Equating the above force to the capacity of the side and in-line purlin fasteners, and solving for Q gives

$$Q_f = \frac{K(n_d F_{du} + n_p F_{eu})}{(n_d K_d + n_p K_e)} \tag{A.21}$$

in which F_{du} = strength of an individual side fastener.

A.2.3 Failure at the End

The end fasteners are subject to both horizontal and vertical forces. In general, the horizontal components are small compared to the vertical forces, and thus diaphragm failure associated with the horizontal shear forces is rare. However, if the number of end fasteners in a diaphragm is small, their horizontal force components should not be ignored. The maximum vertical force occurs in the fasteners closest to the panel corners and can be evaluated from A.17 and A.18. By equating the magnitude of the resultant force to the fastener capacity F_{eu}, the failure load Q_f can be evaluated.

A.3 SPECIAL APPLICATION TO CAVITY DECKING DIAPHRAGMS

In the derivation of the above expressions for the deflection component D_1 and fastener forces, the vertical force components of the sheet-to-purlins fasteners at the panel center line was neglected for simplicity. These forces are quite small in the case where there is three or more sheet-to-purlin fasteners per panel width, as verified by many finite element analyses. However, all cavity decking diaphragms, except C-7, are characterized with a single fastener per panel width at its center line. For this special case, the expression are modified to account for these forces.

The vertical component of the force in this single end fastener (or sheet-to-purlin fastener) is given by the equation:

$$F_e = (K_e D_2/x_o^o)(w/2 - x_o)^2 \qquad [A.22]$$

The equation for vertical equilibrium of the panel, Eq. 4, becomes

$$n_d F_d - n_s F_s - n_p \frac{K_e D_e}{x_o^2} (\frac{w}{2} - x_o)^2 = 0 \qquad [A.23]$$

Substitution of A.5 and A.6 into A.23 results in a quadratic equation in the unknown x_o:

$$a\, x_o^2 + b\, x_o + c = 0 \qquad [A.24]$$

in which

$$a = 1$$

$$b = (\frac{4n_s K_s + 2K_e}{n_d K_d - 2n_s K_s - 2K_e})\, W \qquad [A.25]$$

$$c = -(\frac{2n_s K_s + \frac{1}{2} K_e}{n_d K_d - 2n_s K_s - 2K_e})\, W^2$$

For Eq. A.24 there is only one meaningful solution for x_o:

$$x_o = \frac{-b \pm \sqrt{b^2 - 4ac}}{2a} < W \qquad [A.26]$$

Moment equilibrium of the exterior panel about its center can thus be expressed as

$$n_d F_d \frac{W}{2} + n_s F_s \frac{W}{2} = QW \qquad [A.27]$$

This equation together with A.5 and A.6 yields the following expression for D_e

$$D_e = Q/K' \qquad [A.28]$$

in which

$$K' = \frac{1}{2} n_d K_d + n_s K_s (\frac{w}{x_o} - 1)^2 \qquad [A.29]$$

Similarly, the equations for deflection component D_1, fastener forces, failure loads are the same as those of A.14 to A.21 after replacing K with K'.

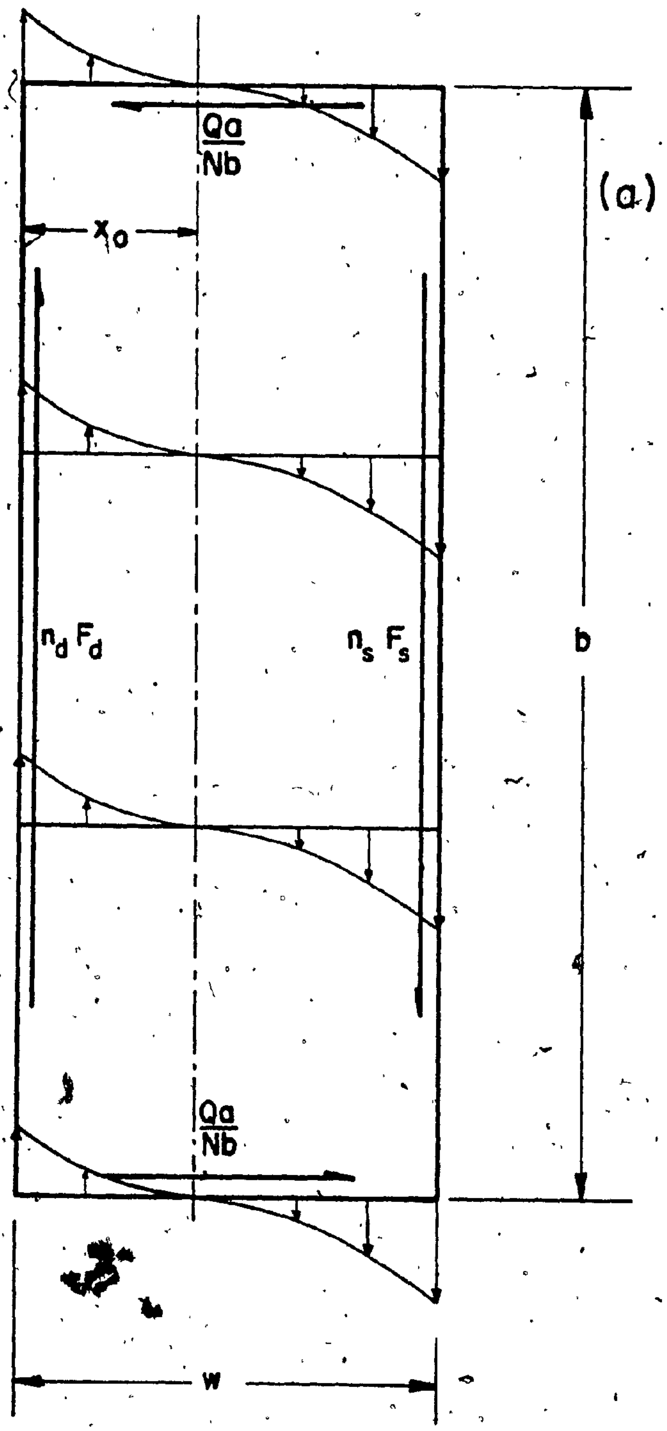

FIG. A.1 FORCES ACTING ON THE LEFT EXTERIOR PANEL (FIG. 6.3)

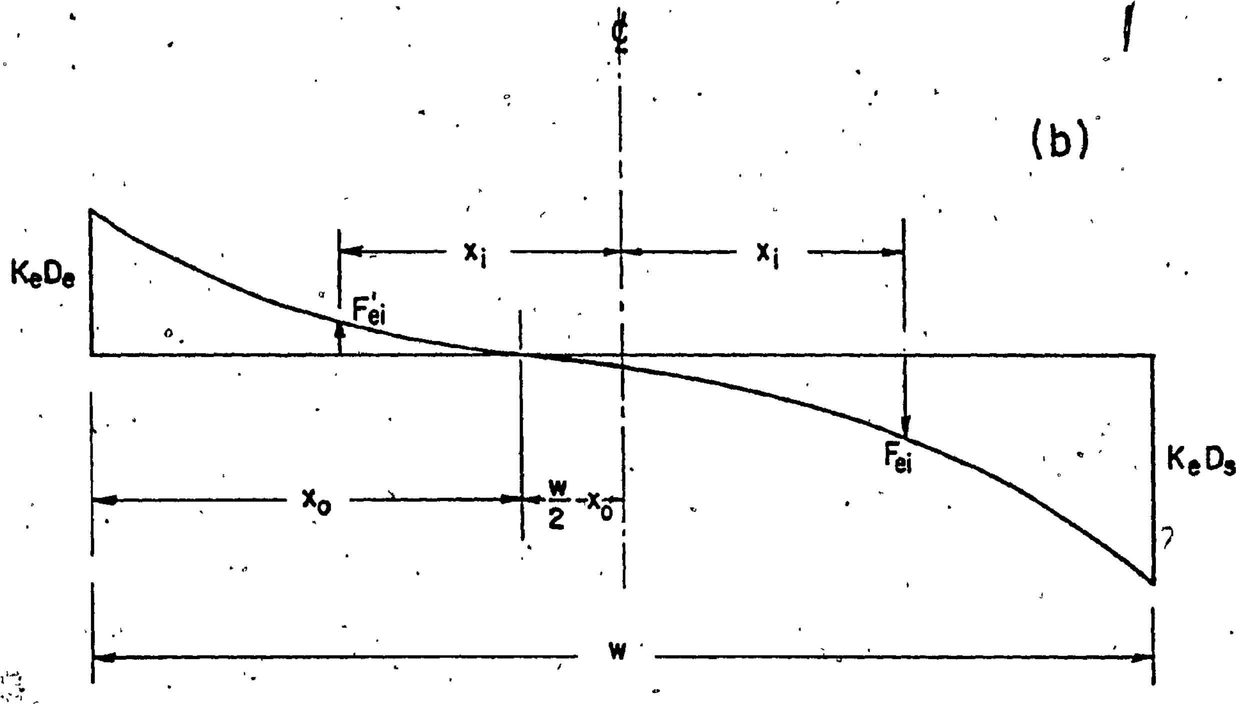

FIG. A.1 FORCES ACTING ON THE LEFT EXTERIOR PANEL

APPENDIX B

EXPRESSIONS FOR DEFLECTION COMPONENTS D_2, D_3 and D_a IN SIMPLIFIED METHOD FOR DIAPHRAGM ANALYSIS

APPENDIX B

EXPRESSIONS FOR DEFLECTION COMPONENTS D_2, D_3 AND D_a IN SIMPLIFIED METHOD FOR DIAPHRAGM ANALYSIS

Calculation of the tip deflection of a complete diaphragm as that of Fig. 6.1 is based on arithematically summing up 4 components of deflection: D_1, contributed by the vertical deformations occurring at the end, sheet-to-purlin, side and seam fasteners; D_2, due to the horizontal slip of the end fasteners; D_3, due to shear strains in the sheeting material and warping of the corrugation profiles; and D_a, due to axial deformations of the marginal frame members. Expression for deflection component D_1 has been derived in Chapter 6. A refined expression for D_1 has also been derived in Appendix A. The derivation of expressions for D_2, D_3 and D_a has been reported in the literature and is presented here for completeness.

B.1 EXPRESSION FOR D_2

This deflection component is calculated based on the following two assumptions:

(1) The total horizontal force Qa/b in each of the two horizontal marginal members of the isolated diaphragm shown in Fig. 6.1 is equally shared between the number of sheets (N) comprising the diaphragm.

(2) The horizontal force component in each of the outer two end fasteners (at panel's edge) is one half the force in each of the internal end fasteners, or in other words, the horizontal forces in the end fasteners are proportional to the tributary area served.

Based on the above assumptions, the edge shear force per sheet is equal to $\frac{Qa}{Nb} = \frac{Qw}{b}$ (where $w = \frac{a}{N}$), and the horizontal force per end fastener is thus given by

$$F_{ex_i} = \frac{Qw}{b(n_e-1)} \qquad (B.1)$$

The horizontal deformation (slip) due to F_{ex_i} can be expressed by

$$\Delta_{ex_i} = \frac{Qw}{b(n_e-1)K_e} \qquad (B.2)$$

Referring to Fig. B.1, the horizontal slip of the end fasteners would cause the sheet to rotate as a rigid body, resulting in a vertical component of deflection (Δ_N) in direction of the applied shear load Q and is obtained by considering the geometry of Fig. B.1:

$$\text{rotation angle} = \phi = \frac{Qw}{b(n_e-1)K_e} \Big/ \frac{b}{2} = \frac{\Delta_N}{w}$$

thus

$$\Delta_N = \frac{2\ Qw^2}{b^2(n_e-1)K_e} \qquad (B.3)$$

Summing over the N sheets comprising the diaphragm results in an expression for D_2 as the overall vertical deformation due to the horizontal slip of the end fasteners

$$D_2 = N\cdot\Delta_N = \frac{a}{w}\ \Delta_N$$

$$D_2 = \frac{2Qaw}{b^2(n_e-1)K_e} \qquad (B.4)$$

B.2 EXPRESSION FOR D_3

When subjected to shear, the shear strain (γ_3) of an open profile corrugated section of the diaphragm panels is dependent on two main factors: (a) the direct shear strain induced in the individual plates forming the corrugation, and (b) the displacements produced by distortion of the open profile due to bending effects. Torsion and membrane stretching effects are also present, but their influence is not significant [45].

An actually corrugated diaphragm panel as that shown in Fig. B.2a can theoretically be replaced by an equivalent continuous homogeneous orthotropic thin plate (Fig. B.2b) which can reproduce the panel's response to load. Two principle directions are established by the paired geometry; the longitudinal direction (identified by the subscript L) denoting the direction parallel to corrugations, and the transverse direction (identified by subscript T) perpendicular to it. Accordingly four equivalent elastic constants designated: E_L, E_T, U_{LT} and G_{LT} can be established in terms of the elastic moduli of the base material and the geometric configuration of the panel cross section. These can be evaluated for the condition that, for given forces at the horizontal projected boundaries of a panel, the displacements of the actual corrugated sheet will be equal to those of the equivalent orthotropic flat plate of same thickness t and equal projected dimensions a and b. The shear strain component γ_3 can thus be expressed as (Fig. B.2c)

$$\gamma_3 = \frac{q}{G_{LT}} = \frac{Q/bt}{G_{LT}} \tag{B.5}$$

Noting that $\gamma_3 = \frac{D_3}{a}$, the deflection component D_3, is then

$$D_3 = \frac{Q\,a}{b\,G_{LT}\,t} \tag{B.6}$$

The value of the equivalent shear modulus, G_{LT}, or often termed the effective shear modulus, G_{eff}, depends on the two main factors mentioned earlier. For corrugated sheets, G_{LT} can be evaluated experimentally or analytically. This has been the subject of several studies. A review of these studies can be found in Ref. 45.

It should be noted that for flat sheets of isotropic (like steel) or orthotropic (asbestos cement) material, G_{LT} is equal to the shear modulus of the material.

B.3 EXPRESSION FOR D_a

In order to compare the calculated value of the total deflection of a shear diaphragm by the current analytical method to that obtained from a finite element analysis or that obtained directly from full-scale testing (Eq. 3.2), the bending deformation of the supporting frame due to the axial strains in the marginal members must be added to D_1, D_2 and D_3.

The test frame with an installed diaphragm behaves under load like a short cantilever. Analogous to a plate girder, the contribution of the diaphragm (the web) to the bending stiffness is negligible. Thus, a conservative estimate of the cantilever bending deflection as a function of the properties of the test frame marginal members (the flanges), Fig. B.3, is the conventional beam deflection formula:

$$D_3 = \frac{Q\,a^3}{3EI}$$

in which

Q = Applied load at cantilever end, perpendicular to the span a.

I = moment of inertia of flange perimeter members about the centroidal axis of the diaphragm = $Ab^2/2$

A = cross-sectional area of perimeter frame members perpendicular to load direction.

and E = modulus of elasticity of steel.

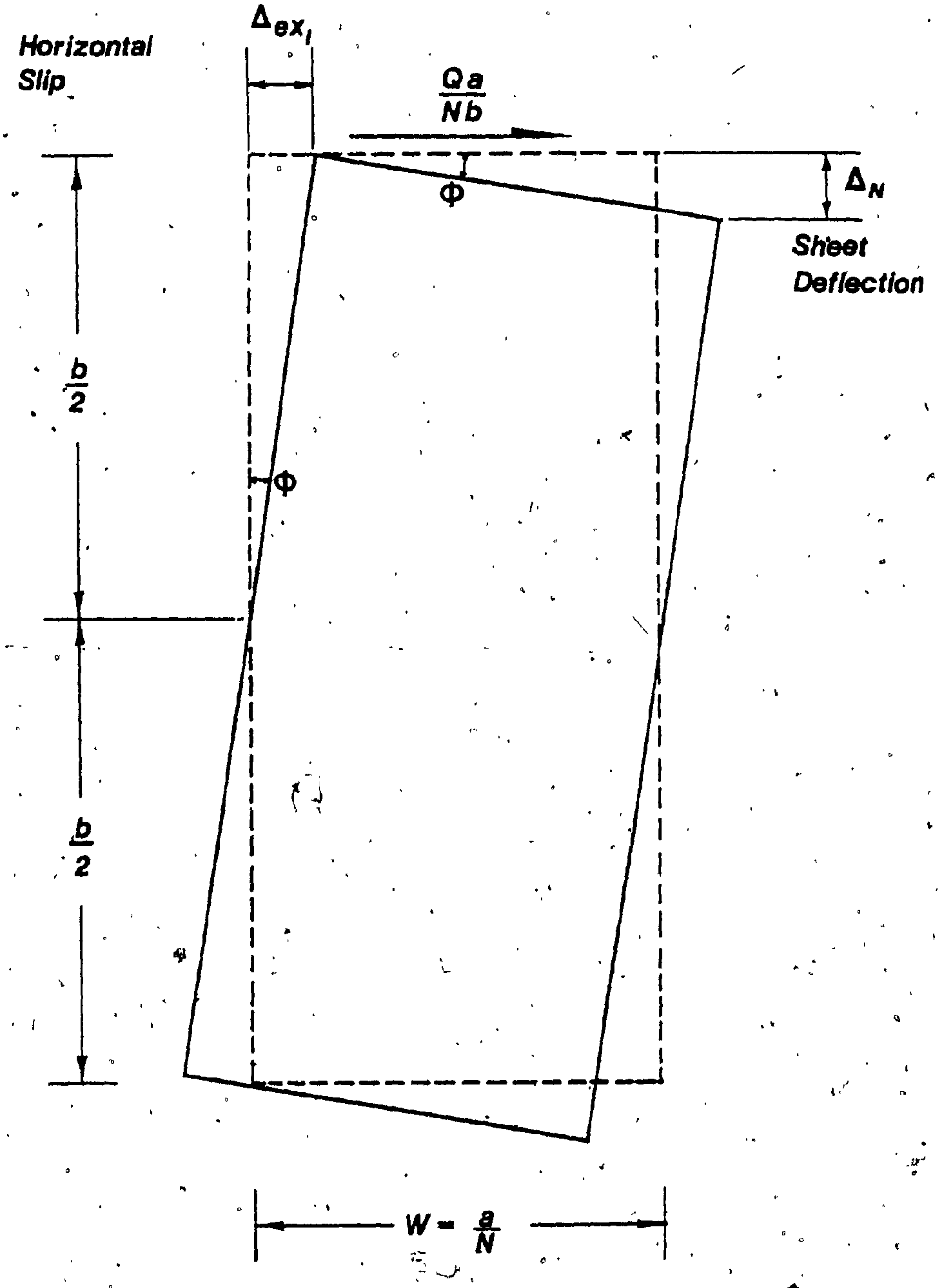

FIG. B.1 SHEET DEFLECTION DUE TO HORIZONTAL SLIP AT THE END FASTENERS

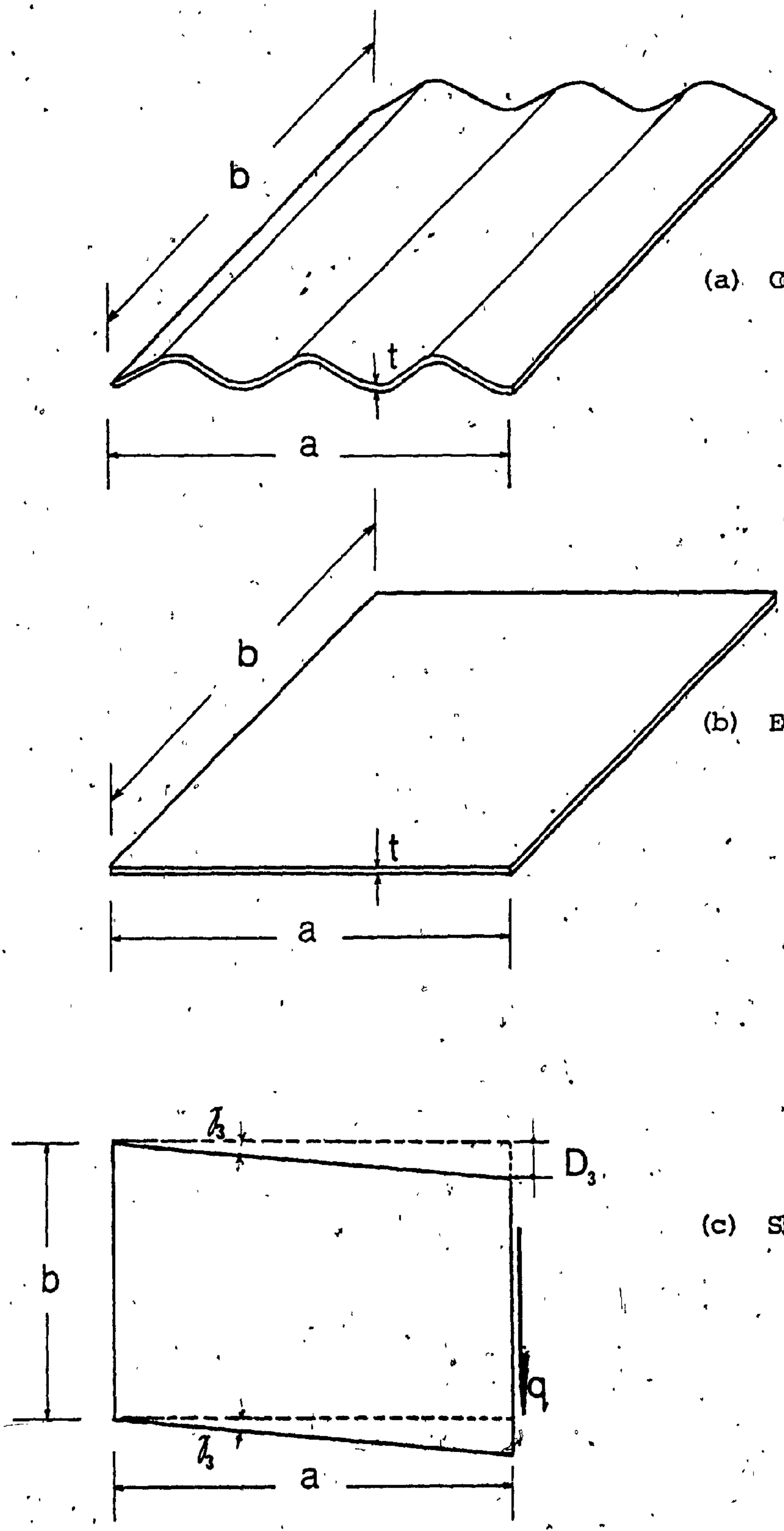

(a) Corrugated Sheet

(b) Equivalent orthotropic plate

(c) Sheet's shear strain γ_3

FIG. B.2 SHEAR STRAIN OF AN EQUIVALENT ORTHOTROPIC PLATE

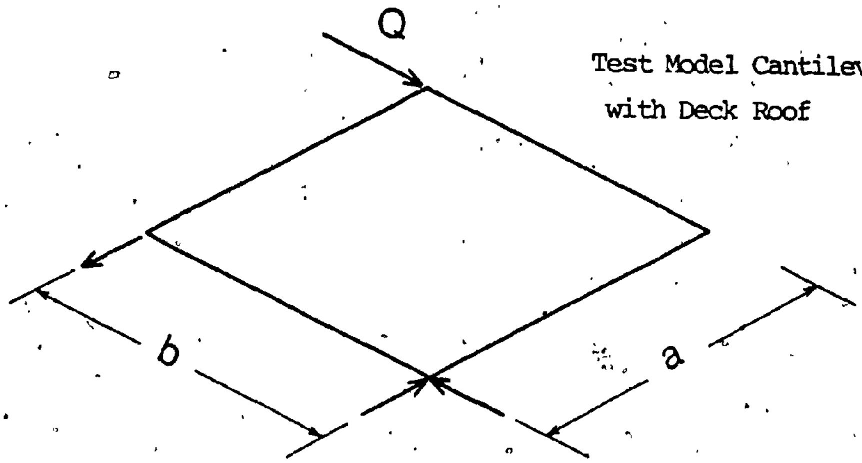

Test Model Cantilever frame with Deck Roof

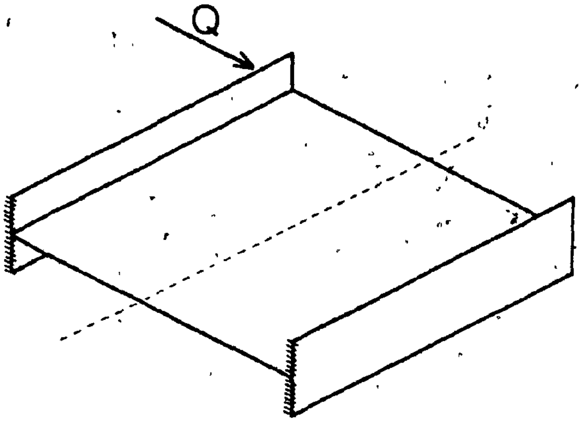

Equivalent Plate Girder

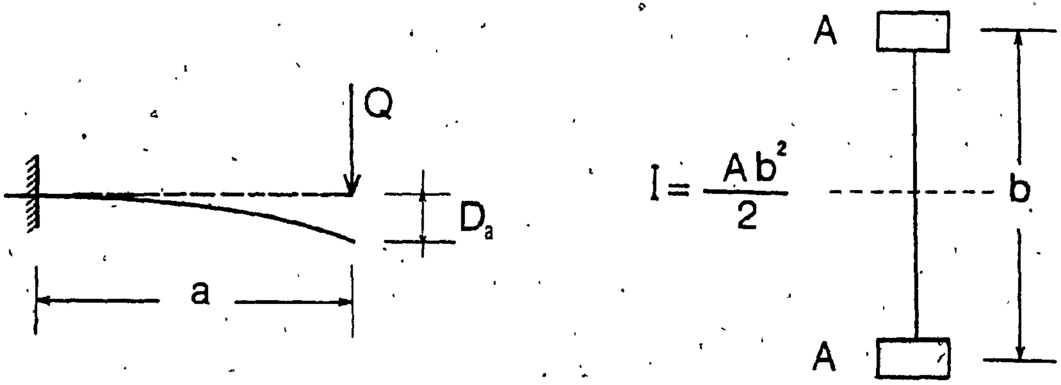

Deflection of a Cantilever Beam

FIG. B.3 BENDING DEFORMATION DUE TO AXIAL STRAINS IN MARGINAL FRAME MEMBERS

APPENDIX C

COMPUTER PROGRAM

APPENDIX C

COMPUTER PROGRAM

C.1 INTRODUCTION

This special-purpose finite element computer program (SHEAR) has been developed to perform a linear elastic analysis of plane rectangular shear diaphragms composed of sheeting panels, marginal beams, purlins, and fastening devices. Load and support conditions are such that the diaphragm analysed is of the simple cantilever type adopted in the full-scale tests (Fig. 3.2, Chapter III). The program calculates displacements at all nodal points and internal forces throughout the diaphragm. It is written in the FORTRAN IV language and is operated on a CDC 66000 Computer. Efficient use of the memory storage has been achieved by employing a dynamic memory allocation scheme and a corresponding addressing procedure. In addition, the program makes use of six auxiliary storage magnetic tapes. Figure C.1 shows a flow chart of the program.

The amount of input data required by the program is kept to a minimum by implementing automatic data generation wherever possible, thus reducing both the effort in data preparation and the chances of data errors.

The objective of this Appendix is to describe the logic of the program and the essential features. This will serve two purposes:

(1) To assist the user in using the program correctly and efficiently.

(2) To facilitate further development or modification of the current version of the program.

C.2 DESCRIPTION OF THE PROGRAM

The program is composed of a main program and 8 subroutines arranged as indicated by the flow diagram of Fig. C.1. The functions of the main routine and subroutines are described in the following.

C.2.1 Program Shear

(1) Reads and prints out problem identification and descriptive title.

(2) Reads and prints out the basic data defining the diaphragm analysed. These are:

- definition of load orientation relative to diaphragm panels (parallel or perpendicular)
- description of the finite element idealization of the diaphragm (number of elements for each type, i.e., plate elements, beam elements in the x-direction, beam elements in the y-direction, and counter elements, respectively); and
- the value of the applied load.

(3) Calls the finite element data generator routine (GENRD)

(4) Sets memory storage scheme and checks storage requirements.

(5) Calls the overall stiffness matrix assembly routine (FORMAK)

(6) Calls the solution routine (SESOL)

(7) Prints out displacements at corresponding degrees of freedom

(8) Retrieves element data from routine GENRD, to be used in elements' nodal forces calculations.

(9) Calls force calculation routine (FORCE).

C.2.2 Subroutine GENRD

(1) Reads and prints out the variables needed for the automatic generation of the diaphragm finite element grid.

(2) Calculates the total number of degrees of freedom (unknown displacements) involved in the analysis.

(5) Generates the element numbering of four groups of elements (plate elements, beam elements in the x-direction, beam elements in the y-direction, and connector elements, respectively). Also, generates the connectivity matrices (degrees of freedom numbering) for each element. These data are stored on TAPE 7 for later retrieval when calculating elements' forces.

(4) Defines the degrees of freedom at which the support boundary conditions are imposed. Also, defines the degrees of freedom corresponding to load application and diaphragm tip displacement in direction of load.

(5) Calculates the maximum half-bandwidth of the overall diaphragm stiffness matrix, including diagonal.

C.2.3 Subroutine PLATE

Generates the element stiffness matrix for an orthotropic plane stress rectangular element with two degrees of freedom at each corner, as given by equations 5.3 and 5.4. When this subroutine is called, it reads and prints out the geometric and elastic properties of the plate element.

C.2.3 Subroutine BEAMX

Generates the stiffness matrix for a marginal end member or purlins positioned parallel to the x-direction and perpendicular to the panels' corrugations. It accounts for axial deformation and bending about a single axis, as given by Eq. 5.1. Also, it reads and prints out the geometric and elastic properties of the element.

C.2.5 Subroutine BEAMY

Generates the stiffness matrix for a marginal side member positioned parallel to the y-direction, i.e., parallel to the panels' corrugations. It also accounts for axial deformation plus bending about a single axis. It gives directly the transformed stiffness matrix in system coordinates, as given by Eq. 5.2.

C.2.6 Subroutine CONNEC

Generates the stiffness matrix of a connector element used to simulate any of the four types of connections in a diaphragm installation (end, side, seam and sheet-to-purlin fasteners), as given by Eq. 5.5.

C.2.7 Subroutine FORMAK

(1) Assembles the diaphragm stiffness matrix (AK) by simply adding the stiffness contributions of each element. At the same time, the kinematic constraints (geometric boundary conditions at the roller and hinge supports) are introduced.

(2) A block storage row-wise scheme of the assembled stiffness matrix and load vector on TAPE 1 (NSTIF) is performed as required by the solution routine (SESOL).

C.2.8 Subroutine SESOL

Solves the equilibrium set of simultaneous linear equations (Eq. 5.6). This routine was developed by E.A. Wilson et. al., and it is fully described and documented in Ref. 73.

C.2.9 Subroutine FORCE

Calculates elements' nodal forces. First, the element nodal displacement vector is extracted from the global displacement vector (solution of equilibrium equations), then multiplied by the elements' stiffness matrix giving nodal forces.

C.3 USER'S GUIDE

C.3.1 Diaphragm Idealization

As already described in Chapter V, the structural idealization involves discretizing the actual system into three basic elements (Fig. 5.1). A proper record of the finite element model should consist of three diagramatic representations of the data:

(1) The finite element model itself.

(2) The F.E. model, with sequential numbering of the different types of elements, and

(3) The F.E. model, with assignment of coordinate (DOF) numbers at the nodal points.

These discriptive sketches are an indispensible aid in preparing and checking input data before the solution, and as a tool to interpret computer output afterwards. It should be noted here that the user needs only to input the data describing the finite element model as given by the first diagramatic representation. The information provided by the other two sketches (i.e., element and DOF numbering) will be automatically generated by the program in a predetermined manner as will be described.

C.3.2 Input Data

As written, the program does no conversion of units. Thus, it is the responsibility of the user to ensure that the units used are consistent. The input data sequence are as follows:

A. Problem identification or descriptive title card. This first card may contain a title of the problem or any other labelling, making use of FORTRAN IV accepted characters. All 80 columns of the card may be used. FORMAT (10A8).

B. Basic data of F.E. grid and loading. One Card. FORMAT (6I5, F15.5) pertaining to the following variables:

ICASE
Col. (1-5)
= 1 Load is applied at corner C in direction CD (i.e., parallel to the panel's corrugations, Fig. C.2a)
= 2 Load is applied at corner B in direction BC (i.e., perpendicular to the panel's corrugations, Fig. C.2b)

NMP
Col. (6-10)
= Total number of plate elements

NMBX
Col. (11-15)
= Total number of beam elements parallel to the X-direction, i.e., of the two end marginal members AD and BC and intermediate purlins

NMBY = Total number of beam elements parallel to the Y-direction, i.e., of the two side marginal members AB and CD.
Col. (16-20)

NMC = Total number of connector elements simulating the end, side, seam, and sheet-to-purlins fasteners.
Col. (21-25)

NLC = No. of load cases, put as 1.
Col. (26-30)

P = Value of the applied Jack Load at diaphragm end.
Col. (31-45)

C. Variables for the automatic generation of element and DOF numbering.

C.1 Data relevant to plate and beam elements generation. One Card. FORMAT (16I15) pertaining to the following variables:

NPANEL = Number of diaphragm panels
Col. (1-5)

NMPPX = Number of plate elements per panel in the X-direction
Col. (6-10)

NMPPY = Number of plate elements per panel in the Y-direction
Col. (11-15)

NY = Number of plate elements in the Y-direction between two purlins. (NOTE: NY=NMPPY if there is no intermediate purlins)
Col. (16-20)

NGIRT = Number of intermediate purlins (girts) positioned parallel to the X-direction (NOTE: the two end marginal members AD and BC are excluded).
Col. (21-25)

C.2 Data relevant to connector elements generation. One Card. FORMAT (16I5) pertaining to the following variables:

NCTS Col. (1-5) = Number of connection types existing in the diaphragm assembly.
= 1 only end fasteners
= 2 end and side fasteners
= 3 end, side and seam fasteners
= 4 end, side, seam and sheet-to-purlins fasteners.

NEND Col. (6-10) = Total number of end connections

NSIDE Col. (11-15) = Total number of side connections

NSEAM Col. (16-20) = Total number of seam connections

NCPS Col. (21-25) = Number of seam connections per seam

NCGIRT Col. (26-30) = Number of sheet-to-purlin connections per purlin.

C.3 Locations of different types of fasteners between the diaphragm panels and the steel frame members. These are determined by a series of integers. Each integer number is equal to the number of plate element widths (in the X-direction) or lengths (in the Y-direction) measured from origin point at corner B to the location of the particular connection. The cards (FORMAT (16I5)) containing the series of integers pertain to the following variables:

(1) X(IN), IN = 1, NEND2.

Locations of end fasteners. NEND2 = Half the number of end fasteners.

(2) Y(IU), IU = 1, NSIDE2

Locations of side fasteners. NSIDE2 = Half the number of side fasteners. NOTE: This card(s) is needed only if NSIDE $\neq$ 0.

(3) YS(IU), IU = 1, NCPS

Locations of seam fasteners. NCPS = Number of seam fasteners per seam line. NOTE: Needed only if NSEAM $\neq$ 0.

(4) XCG(IN), IN = 1, NCGIRT

Location of sheet-to-girts fasteners. NOTE: Needed only if NCGIRT $\neq$ 0.

D. Plate element data. One Card: FORMAT (2F6.4, 2F9.5, 2F15.5, F5.3, F15.5) pertaining to the following variables:

NUXY = Poisson's ratio relating strains in the
Col. (1-6) Y-direction to stresses in the X-direction

NUYX = Poisson's ratio relating strains in the
Col. (7-12) X-direction to stresses in the Y-direction

LX = Length of the element side in the X-direction
Col. (13-21)

LY = Length of the element side in the Y-direction
Col. (22-30)

EX = Modulus of elasticity in the X-direction
Col. (31-45) E_{xx}.

EY = Modulus of elasticity in the Y-direction
Col. (46-60) E_{yy}

T = Thickness of plate element

Col. (61-65)

G = Effective shear modulus

Col. (66-80)

NOTE: If isotropic plate element, $E_{xx} = E_{yy} = E$;

$$\nu_{xy} = \nu_{yx} = \nu; \quad G_{xy} = G. \quad \text{Where } G = \frac{E}{2(1+\nu)}.$$

E. Beam elements in X-direction data. NB Cards, where: NB = 2 + NGIRT. i.e., one card for each steel member parallel to the X-direction (the purlins usually have smaller sections than marginal end members). FORMAT (4F15.5) pertaining to the following variables:

LBX = Length of the beam element

Col. (1-15)

ZIBX = Moment of inertia about axis of bending

Col. (16-30) (perpendicular to diaphragm plane).

ABX = Cross-sectional area

Col. (31-45)

EBX = Steel Young's modulus

Col. (46-60)

F. Beam element in Y-direction data. One Card. FORMAT (4F15.5) pertaining to the variables LBY, ZIBY, ABY, EBY; similar to those described in E.

G. Connector elements data. NCTS Cards. According to the number of connection types, one card a type. FORMAT (2F15.5) pertaining to the variables.

KX = Spring coefficient (stiffness) in the
Col. (1-15) X-direction
KY = Spring coefficient in the Y-direction
Col. (16-30)

The sequence of these cards corresponds to end fasteners, side fasteners (delete if NSIDE = 0), seam fasteners (delete if NSEAM = 0) and sheet-to-purlins fasteners (delete if NGIRT = 0), respectively.

C.4 PROGRAM OUTPUT

In addition to a print-out of most of the input information, the following output is given by the program:

(1) Automatically generated elements' connectivity matrices (see Section 5.3) for the four types of elements (plate elements, beam elements in the X-direction, beam elements in the Y-direction, and connector elements, respectively). The four groups of elements are separately numbered, from 1 to NMP, from 1 to NMBX, from 1 to NMBY, and from 1 to NMC, respectively.

(2) Constrained displacement degrees of freedom corresponding to the supports (one DOF for the roller support and two for the hinge support). Also printed out are: DOF at which the Jack load is applied, DOF at diaphragm tip in load direction, the total number of degrees of freedom in the finite element model, and the maximum half-bandwidth (including the diagonal) of the overall diaphragm stiffness matrix.

(3) A list of displacements at each degree of freedom

(4) Element forces for the four groups of elements (plate elements, beam elements in the X-direction, beam elements in the Y-direction and connector elements, respectively).

For interpretation of the printed output, the numbering schemes for the different types of elements and nodal degrees of freedom are described in the following.

C.4.1 Element Numbering Scheme

Figure C.3 illustrates the element numbering scheme as generated by the progran for the finite element model of the general example diaphragm of Fig. 5.1. The scheme is described below.

(1) Plate Elements:

These are numbered from 1 to NMP, starting with element No. 1 at the lower left corner (corner B) and ending with element No. NMP at the top right corner (corner D). Elements are numbered in an increasing order in each row from left to right.

(2) Beam Elements in X-direction:

These are numbered from 1 to NMBX. End marginal members BC and AD are labelled "Beam No. 1" and "Beam No. 2" resepctively, if the diaphragm installation does not contain intermediate purlins (girts), i.e., NGIRT = 0. If NGIRT ≠ 0, steel members are labelled in order from bottom ("Beam No. 1" for BC) to top ("Beam No. (NGIRT+2) for AD). Numbering starts with beam elements comprising end purlin BC, with element No. 1 being assigned to that connected to corner B, and proceeds in increasing order from left to right, purlin by purlin, till it ends with beam element No. NMBX connected to the top corner D.

(3) Beam Elements in Y-direction:

These are numbered from 1 to NMBY. Numbering starts with beam elements comprising side member AB, with element No. 1 being assigned to that connected to corner B, and proceeds in increasing order from B to A and from C to D till it ends with beam element No. NMBY connected to the top corner D.

(4) Connector Elements:

These are numbered from 1 to NMC, in the following sequence:

(a) End fasteners, connecting the diaphragm panels to the end marginal members BC and AD. Numbering starts with the nearest fastener to corner B (connector element No. 1) and proceeds in an increasing order in the BC direction, followed by end connector elements extending from corner A to corner D.

(b) Side fasteners, connecting the exterior panels to the side marginal members AB and CD. Numbering continues with the first side fastener closest to corner B and proceeds in an increasing order in the BA direction, followed by side connector elements extending from corner C to corner D. If NSIDE = 0, numbering proceeds with the next existing type of connection, from the last connector element number reached in (a).

(c) Seam fasteners, connecting the diaphragm panels at the seam lines. Numbering picks up at the first seam line to the left side (closest to BA), the first seam connector being the one nearest to BC, and proceeds upwards in an increasing order. Connector elements for other seam lines from left to right are next numbered in the same manner. If NSEAM = 0, the seam connector elements numbering is bypassed.

(d) Sheet-to-purlins fasteners. These are numbered last, if NGIRT $\neq$ 0, in the same manner end connectors are numbered, i.e. from left to right, starting with the purlin closest to BC and ending with the purlin closest to AD.

C.4.2 Nodal DOF Numbering Scheme

The automatic generation of the nodal degrees of freedom was developed such that it would yield the minimum bandwidth for the overall diaphragm stiffness matrix, an essential feature for storage savings and speed of execution. A small band width is usually obtained simply by numbering the nodal points along the shorter dimension of a structure [54]. This criterion was adopted in the current program for DOF numbering as illustrated in Fig. C.4, the shorter dimension being the depth (AB) of the diaphragm. It should be emphasized that the word "shorter" does not imply that the diaphragm depth (AB) is necessarily numerically smaller than its width (BC), but it rather means that the number of nodal points in the depth direction are mostly less than that in the width direction.

The numbering scheme starts at the nodal point at corner B and assigns the numbers 1, 2 and 3 to represent two translational and one rotational degrees of freedom. Numbering proceeds in increasing order vertically assigning three DOF numbers to each nodal point of the beam elements simulating side marginal member BA. Numbered next are the DOF at the nodal points of the first vertical line of plate elements closest to BA also vertically from the nodal point near corner B. Only two DOF numbers are assigned to plate elements' nodal points. Numbering proceeds in the same manner where three DOF numbers are assigned to each beam element's nodal point aligned with the vertical lines of plate element's nodal points. Finally, as it started the numbering scheme assigns DOF numbers to nodal points of beam elements simulating the other side marginal member CD and terminates at the nodal point D, as illustrated in Fig. C.4.

C.5 SAMPLE PROBLEM INPUT AND OUTPUT

To demonstrate the use of the program, the input data needed to analyze the cavity deck diaphragm of Test C-2 is presented in Fig. C.5. The illustrations describing the finite element modelling of the actual diaphragm and indicating the sequential order in which the different types of elements are numbered; and the nodal degrees of freedom numbering, have been reported in Figures 5.5 and 5.6. The study is made for a Jack load of 1000 lbs (1 kip) so that the resulting diaphragm tip deflection in direction of load application would directly represent the diaphragm shear flexibility.

The program output as described in the previous section is presented following the program listing.

C.6 PROGRAM LISTING

A complete FORTRAN IV listing of the program SHEAR is documented below.

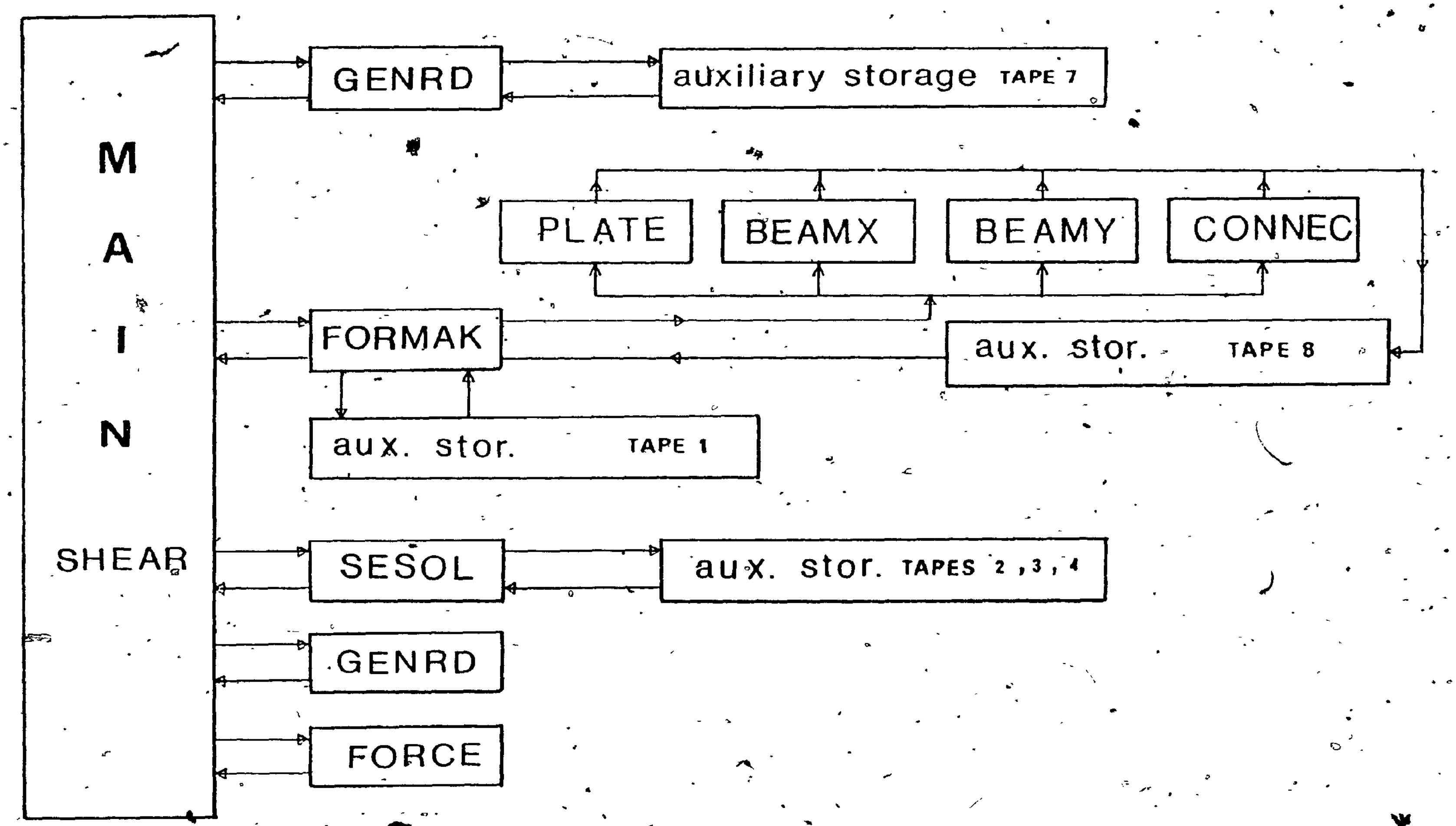

FIG. C.1 PROGRAM BLOCK DIAGRAM

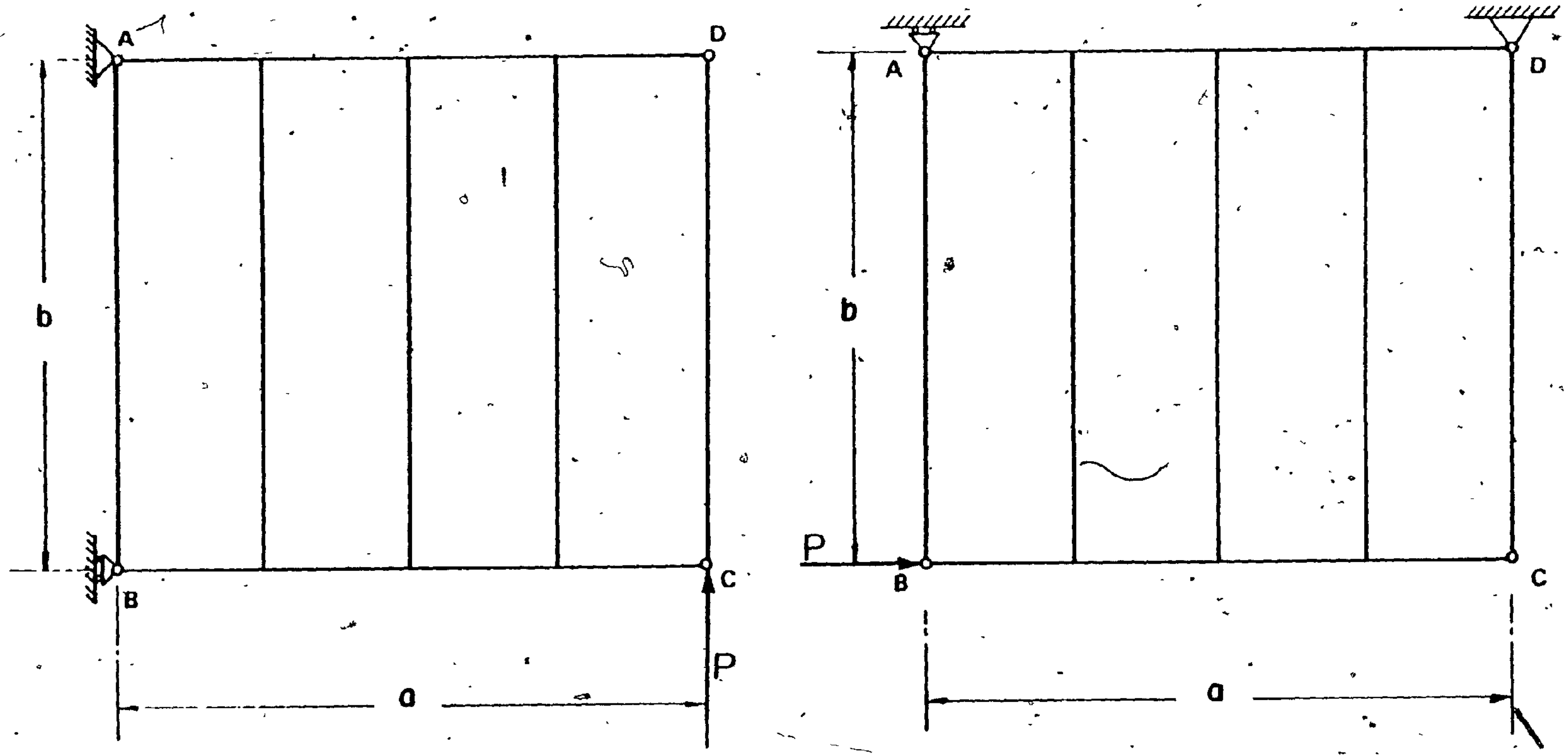

(a)

ICASE = 1

(b)

ICASE = 2

FIG. C.2 LOADING CONFIGURATIONS CONSIDERED IN PROGRAM

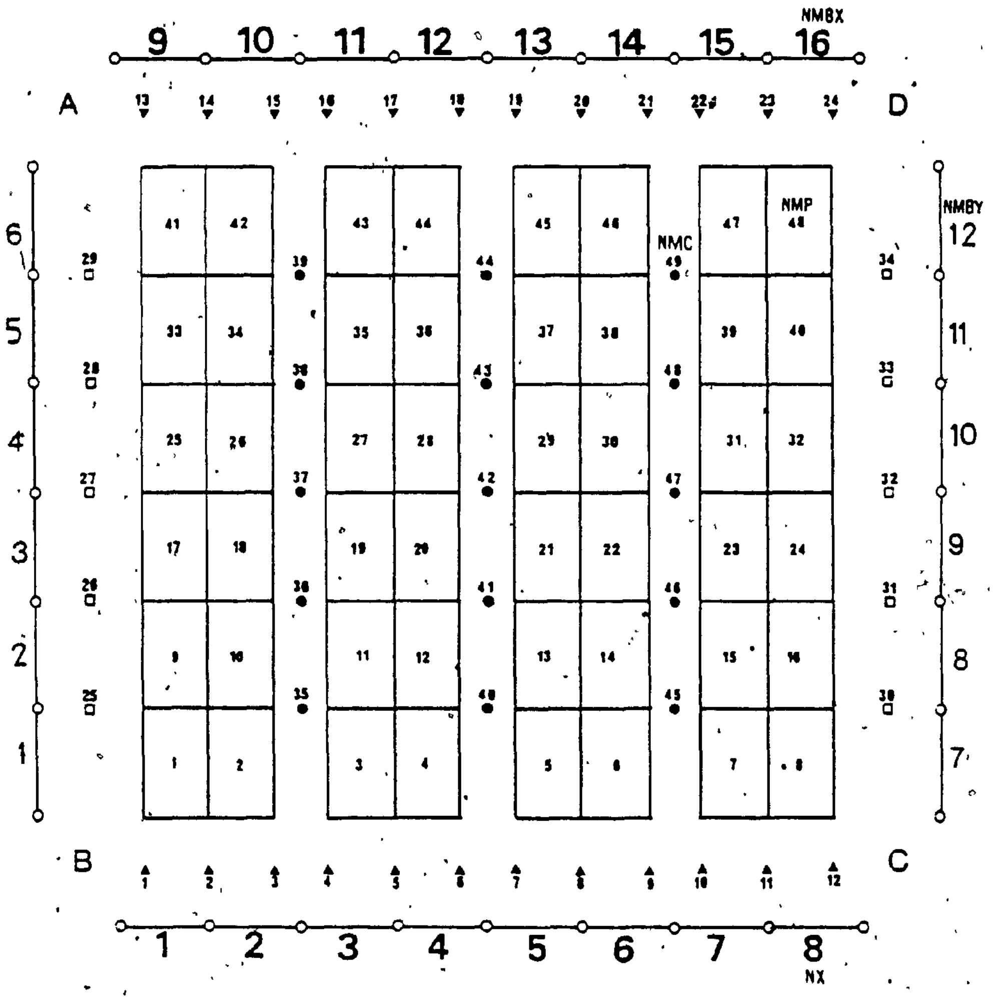

NMP = 48
NMBX = 16
NMBY = 12
NMC = 49

FIG. C.3 ELEMENT NUMBERING GENERATION SCHEME

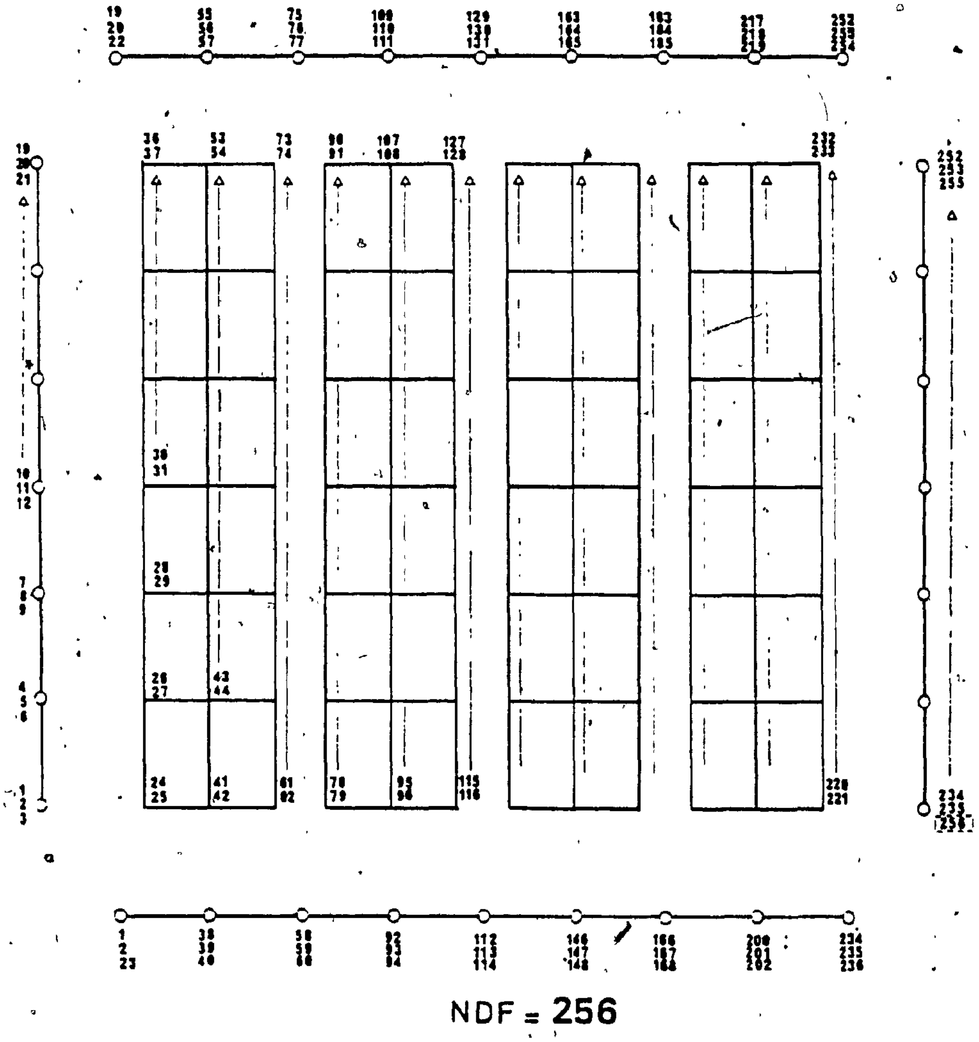

FIG. C.4 DEGREE OF FREEDOM NUMBERING GENERATION SCHEME

```
12345678901234567890123456789012345678901234567890123456789012345678901234567890
 SAMPLE EXAMPLE  :  ANALYSIS OF CAVITY DECK DIAPHRAGM OF TEST C-2
    1  108   36   12   64    1      1000.
    9    2    6    6   1[illegible]    0
    3   14   10   40    5    0
    3    5    7    9   11   13   15
    1    2    3    4    5
    1    2    3    4    5
   .15    .2  7.5      20.0     1700000.      2250000.       .375   900000.
        7.5           10.8            6.2     30000000.
        7.5           10.8            6.2     30000000.
       20.0           10.8            6.2     30000000.
    28000.         28000.
    28000.         28000.
     6720.          8400.
```

FIG. C.5 LISTING OF INPUT FOR SAMPLE PROBLEM

```
      PROGRAM SHEAR(INPUT,OUTPUT,TAPE5=INPUT,TAPE6=OUTPUT,TAPE1,TAPE2,
     *              TAPE3,TAPE4,TAPE7,TAPE8)
C
C  *********************************************************************
C  *                                                                   *
C  *      THIS FORTRAN PROGRAM PERFORMS LINEAR ELASTIC ANALYSIS BY     *
C  *  THE DIRECT STIFFNESS METHOD OF PLANE RECTANGULAR SHEAR DIAPHRAGMS*
C  *  COMPOSED OF LIGHT GAGE STEEL PANELS OR ASBESTOS-CEMENT PANELS ,  *
C  *  MARGINAL BEAMS AND PURLINS .                                     *
C  *                                                                   *
C  *      GIVEN THE LOADING AND SUPPORT CONDITIONS ( TO CONSTITUTE A   *
C  *  HORIZONTAL CANTILEVER ) , IT CALCULATES DISPLACEMENTS AT ALL     *
C  *  NODAL POINTS AND INTERNAL FORCES THROUGHOUT THE DIAPHRAGM .      *
C  *                                                                   *
C  *      THE PROGRAM DOES NO CONVERSION OF UNITS                      *
C  *      ANY SELF-CONSISTENT SET OF UNITS  CAN BE USED .              *
C  *                                                                   *
C  *********************************************************************
C
      DIMENSION TITLE (10)
C
      DIMENSION AK(11000)
C
      MTOT=11000
C
C     [ MTOT-N ] IS THE REQUIRED HIGH SPEED STORAGE LOCATIONS
C
C     THIS CARD MAY BE CHANGED TOGETHER WITH PREVIOUS CARD
C     [ DIMENSION AK(N) ]  DEPENDING UPON THE SIZE OF PROBLEM
C
      NSTIF=1
      NRED=2
      NL=3
      NR=4
      ND=7
      NS=8
C
      WRITE (6,5)
    5 FORMAT('1',1X,'FINITE ELEMENT PROGRAM FOR THE LINEAR ELASTIC ANALY
     *SIS'/1X,' OF PLANE RECTANGULAR SHEAR DIAPHRAGMS .....'//)
C
C     READ AND PRINT OUT PROBLEM IDENTIFICATION AND DISCRIPTION TITLE
C
      READ (5,10) (TITLE(I),I=1,10)
   10 FORMAT (10A8)
      WRITE(6,20) (TITLE(I),I=1,10)
   20 FORMAT (//1X,10A8//)
C
C     READ AND PRINT OUT THE BASIC DATA REQUIRED FOR THE PROGRAM :
C     -------- LOAD ORIENTATION RELATIVE TO DIAPHRAGM PANELS ,
C     -------- DESIRED F.E. IDEALISATION (NO. OF ELEMENTS FOR EACH TYPE)
C     -------- APPLIED JACK SHEAR LOAD .
C
      READ (5,30) ICASE,NMP,NMBX,NMBY,NMC,NLC,P
   30 FORMAT (6I5,F15.5)
C
      IF (ICASE.EQ.1) WRITE (6,40)
      IF (ICASE.EQ.2) WRITE (6,50)
C
   40 FORMAT (//2X,'LOAD IS APPLIED IN DIRECTION PARALLEL TO THE CORRUGA
     *TIONS')
   50 FORMAT (//2X,'LOAD IS APPLIED IN DIRECTION PERPENDICULAR TO THE
     *CORRUGATIONS')
C
      WRITE (6,60) NMP,NMBX,NMBY,NMC,NLC,P
   60 FORMAT(////5X,'INPUT  DATA ....... BASIC  PARAMETERS............'//
     1         5X,'TOTAL NUMBER OF PLATE ELEMENTS ......................',I5/
     2         5X,'TOTAL NUMBER OF BEAM ELEMENTS IN X-DIRECTION ........',I5/
     3         5X,'TOTAL NUMBER OF BEAM ELEMENTS IN Y-DIRECTION ........',I5/
     4         5X,'TOTAL NUMBER OF CONNECTOR ELEMENTS ..................',I5/
     5         5X,'NUMBER  OF  LOAD  CASES .............................',I5/
     6         5X,'APPLIED JACK LOAD AT DIAPHRAGM END ..............',F13.5)
C
      M1=1
      M2=(NMP*8)+M1
      M3=(NMBX*6)+M2
      M4=(NMBY*6)+M3
      M5=(NMC*4)+M4
```

```
C
C     CALL F.E. GRID GENERATIN ROUTINE
C
      CALL GENRD (AK(M1),AK(M2),AK(M3),AK(M4),NMP,NMBX,NMBY,NMC,ND,
     1               NDF,MA,NDFP,ICASE,1)
C
C     CALCULATE THE DIMENSIONS OF THE ARRAYS A , B , MAXA . NEEDED
C     FOR SOLUTION SUBROUTINE SESOL
C
      NU=NLC
      NEQ=NDF
      N1=NEQ*(MA+NU)
      N2=NU*NEQ*((MA-2)/NEQ+2)
      N3=NEQ+MA-1
      IF (MTOT.GE.(N1+N2+N3)) GO TO 130
      N4=(MTOT-MA)/(2*(MA+NU)+1)
      N5=(MTOT-MA-NU*(MA-2))/(3*NU+MA+1)
      IF (N5-N4) 70,70,80
   70 NEQB=N5
      GO TO 90
   80 NEQB=N4
   90 NBLOCK=(NEQ-1)/NEQB+1
      NVA1=NEQB*(MA+NU)
      N6=NEQB*(MA+NU)
      N7=NU*NEQB*((MA-2)/NEQB+2)
      IF (N7-N6) 100,100,110
  100 NVA2=N6
      GO TO 120
  110 NVA2=N7
  120 MI=NEQB+MA-1
      GO TO 140
C
  130 NEQB=NEQ
      NBLOCK=1
      NVA1=N1
      NVA2=N2
      MI=NEQ+MA-1
C
  140 NAV=NEQB*(MA+NU)
C
C     CHECK STORAGE REQUIREMENTS
C
      NN2=1
      NN3=NN2+NVA2
      IF ((NVA2+MI).GT.(M5-1))  NN1=NN3+MI
      IF ((NVA2+MI).LT.(M5-1))  NN1=M5
      IF ((NN1+NVA1).GT.MTOT) STOP
C
C     CALL DIAPHRAGM STIFFNESS MATRIX ASSEMBLY ROUTINE
C
      CALL FORMAK (NBLOCK,NEQB,MA,NDFP,P,NSTIF,AK(NN1),NVA1,AK(M1),
     *             AK(M2),AK(M3),AK(M4),NMP,NMBX,NMBY,NMC,N5)
C
C     CALL SOLUTION ROUTINE
C
      CALL SESOL (AK(NN1),AK(NN2),AK(NN3),NEQ,MA,NU,NBLOCK,NEQB,NAV,
     *            MI,NSTIF,NRED,NL,NR)
C
      REWIND NL
C
      NTOT=NEQB*NBLOCK
      DO 160 J=1,NBLOCK
      READ (NL) (AK(KJ),KJ=1,NEQB)
      L1=NEQB*J
      L3=NTOT-L1+1
      DO 150 K=1,NEQB
      AK(L3)=AK(K)
      L3=L3+1
  150 CONTINUE
  160 CONTINUE
C
C     PRINT OUT DISPLACEMENTS
C
      WRITE (6,170)
  170 FORMAT ('1',35X,'DISPLACEMENTS AT EACH CORRESPONDING D.O.F.'//
      WRITE (6,180) (II,AK(II),II=1,NDF)
  180 FORMAT (5(6H   DOF,I4,2X,E12.6))
 C
      M1=NDF+1
      M2=(NMP*8)+M1
      M3=(NMBX*6)+M2
      M4=(NMBY*6)+M3
 C
 C    RETRIEVE ELEMENT DATA
 C
      CALL GENRD (AK(M1),AK(M2),AK(M3),AK(M4),NMP,NMBX,NMBY,NMC,ND,
     *            NDF,MA,NDFP,ICASE,2)
 C
 C    CALL FORCE CALCULATION ROUTINE
 C
      CALL FORCE (NDF,NMP,NMBX,NMBY,NMC,AK(1),AK(M1),AK(M2),
     *            AK(M3),AK(M4),NS)
 C
      STOP
      END
 C
```

```
C
      SUBROUTINE GENRD (IVCP,IVCBX,IVCBY,IVCC,NMP,NMBX,NMBY,NMC,ND,
     1                  NDF,MA,NDFP,ICASE,IOPT)
C
C   **************************************************************
C   *                                                            *
C   *     SUBROUTINE GENRD GENERATES AND STORES CONNECTIVITY MATRICES *
C   *  OF ALL DIAPHRAGM ELEMENTS                                 *
C   *                                                            *
C   *     THE PROGRAM DOES NOT REQUIRE ANY D.O.F. OR ELEMENT NUMBERING*
C   *  INPUT . THESE ARE AUTOMATICALLY NUMBERED IN THE MANNER EXPLAINED *
C   *  IN THE TEXT . THE USER HAS TO KEEP TRACK OF THE NUMBERING ORDER  *
C   *  OF THE DIFFERENT TYPES OF ELEMENTS ( PLATE , BEAM , CONNECTORS ) *
C   *  IN ORDER TO BE ABLE , LATER ON , TO INTERPRET THE PRINTED OUTPUT.*
C   *                                                            *
C   **************************************************************
C
      COMMON/BLK1/ NEND,NSIDE,NSEAM,NCTS,NGIRT,NX,NDF1,NDF2,NDF3
C
      DIMENSION IVCP(NMP,8),IVCBX(NMBX,6),IVCBY(NMBY,6),IVCC(NMC,4)
      DIMENSION X(100),XGC(100),Y(100),YS(100)
C
      INTEGER X,Y,YS,XGC
C
      IF (IOPT.EQ.2) GO TO 300
C
      LX=LY=LBX=LBY=1
C
C     READ IN VARIABLES NEEDED FOR THE AUTOMATIC F.E. GRID GENERATION
C     ( DEGREES OF FREEDOM AND ELEMENT NUMBERING )
C
C     DATA RELEVANT TO PLATE AND BEAM ELEMENTS GENERATION
C
      READ  (5,510) NPANEL,NMPPX,NMPPY,NY,NX,NGIRT
C
C     DATA RELEVANT TO CONNECTOR ELEMENTS GENERATION
C
      READ  (5,510) NCTS,NEND,NSIDE,NSEAM,NCPS,NCGIRT
C
  510 FORMAT (16I5)
C
      WRITE (6,520)
  520 FORMAT(////5X,'INPUT VARIABLES FOR THE AUTOMATIC F.E. GRID GENERAT
     *ION'//)
C
      WRITE (6,530) NPANEL,NMPPX,NMPPY,NY,NX,NGIRT
  530 FORMAT(5X,'NPANEL  =',I5/5X,'NMPPX    =',I5/5X,'NMPPY    =',I5/5X,'N
     +Y        =',I5/,5X,'NX        =',I5/5X,'NGIRT    =',I5/)
C
      WRITE (6,540) NCTS,NEND,NSIDE,NSEAM,NCPS,NCGIRT
C
  540 FORMAT(/5X,'NCTS     =',I5/5X,'NEND     =',I5/5X,'NSIDE    =',I5/5X,'
     +NSEAM    =',I5/5X,'NCPS     =',I5/5X,'NCGIRT  =',I5////)
C
C     COMPUTE TOTAL NUMBER OF DEGREES OF FREEDOM
C
      NDF= (NMPPX+1)*NPANEL*(NMPPY+1)*2+(NX+1)*(2+NGIRT)*3
     1    +((NMBY+2)-(NGIRT+2)*2)*3+NGIRT*2+4
```

```
C
C  ****************** BASIC VARIABLES DEFINITIONS *******************
C  *                                                                *
C  *     NPANEL= NUMBER OF DIAPHRAGM PANELS                         *
C  *                                                                *
C  *     NMP   = TOTAL NUMBER OF PLATE ELEMENTS                     *
C  *                                                                *
C  *     NMPPX = NUMBER OF PLATE ELEMENTS PER PANEL IN THE X-DIRECTION*
C  *                                                                *
C  *     NMPPY = NUMBER OF PLATE ELEMENTS PER PANEL IN THE Y-DIRECTION*
C  *                                                                *
C  *     NMBY  = NUMBER OF BEAM ELEMENTS IN THE Y-DIRECTION         *
C  *                                                                *
C  *     NY    = NUMBER OF PLATE ELEMENTS IN THE Y-DIRECTION BETWEEN *
C  *             TWO PURLINS                                        *
C  *                                                                *
C  *     NMBX  = NUMBER OF BEAM ELEMENTS IN THE X-DIRECTION         *
C  *                                                                *
C  *     NX    = NUMBER OF BEAM ELEMENTS IN THE X-DIRECTION FOR A   *
C  *             MARGINAL MEMBER OR PURLIN IN THE X-DIRECTION       *
C  *                                                                *
C  *     NGIRT = NUMBER OF GIRTS ( PURLINS )                        *
C  *                                                                *
C  *     NDF   = NUMBER OF DEGREES OF FREEDOM FOR THE WHOLE SYSTEM  *
C  *                                                                *
C  *                                                                *
C  *     LX    = LENGTH OF PLATE ELEMENT SIDE IN THE X-DIRECTION    *
C  *                                                                *
C  *     LY    = LENGTH OF PLATE ELEMENT SIDE IN THE Y-DIRECTION    *
C  *                                                                *
C  *     LBX   = LENGTH OF BEAM ELEMENT IN THE X-DIRECTION          *
C  *                                                                *
C  *     LBY   = LENGTH OF BEAM ELEMENT IN THE Y-DIRECTION          *
C  *                                                                *
C  *     NEND  = NUMBER OF END CONNECTIONS                          *
C  *                                                                *
C  *     NSIDE = NUMBER OF SIDE CONNECTIONS                         *
C  *                                                                *
C  *     NSEAM = NUMBER OF SEAM CONNECTIONS                         *
C  *                                                                *
C  *     NCGIRT= NUMBER OF SHEET-GIRT CONNECTORS PER GIRT           *
C  *                                                                *
C  *     NMC   = TOTAL NUMBER OF CONNECTOR ELEMENTS                 *
C  *                                                                *
C  *     NCPS  = NUMBER OF SEAM CONNECTORS PER SEAM                 *
C  *                                                                *
C  *     NCTS  = NUMBER OF CONNECTION TYPES                         *
C  *             1  END                                             *
C  *             2  END + SIDE                                      *
C  *             3  END + SIDE + SEAM                               *
C  *             4  END + SIDE + SEAM + SHEET-GIRT                  *
C  *                                                                *
C  *     X , Y , YS , AND XGC  ARE VECTORS CONTAINING INTEGER NUMBERS *
C  *     DEFINING THE RELATIVE LOCATIONS OF END , SIDE , SEAM , AND *
C  *     SHEET-TO-PURLINS FASTENERS , RESPECTIVELY .                *
C  *     NOTE THAT LX,LY,LBX,AND LBY ARE SET EQUAL TO 1             *
C  *     THE INTEGER NUMBERS OF THE ABOVE VECTORS ARE DEFINED       *
C  *     DEPENDING ON THE LOCATION OF THE FASTENER RELATIVE TO THE  *
C  *     PLATE AND BEAM ELEMENTS .                                  *
C  *                                                                *
C  *                                                                *
C  *     IVCP , IVCBX , IVCBY , AND IVCC ARE ELEMENTS' CONNECTIVITY *
C  *     MATRICES GENERATED BY THE ROUTINE FOR :                    *
C  *               -  PLATE ELEMENTS ,                              *
C  *               -  BEAM  ELEMENTS IN THE X-DIRECTION ,           *
C  *               -  BEAM  ELEMENTS IN THE Y-DIRECTION ,AND        *
C  *               -  CONNECTOR ELEMENTS , RESPECTIVELY  .          *
C  *                                                                *
C  ******************************************************************
C
      NCON=NEND+NSIDE
      NEND2=NEND/2
      N20=NEND2+1
      NSIDE2=NSIDE/2
      NEND1=NEND+1
      NCO=NSIDE2+NEND
      NCO1=NCO+1
      M1=NEND+NSIDE+1
      M2=NEND+NSIDE+NCPS
      M3=NEND+NSIDE+NSEAM-NCPS+1
      M4=NEND+NSIDE+NSEAM
      M9=NEND+NSIDE+NSEAM
      NG=NGIRT
```

```
C
C     READ IN RELATIVE LOCATIONS OF DIFFERENT TYPES OF FASTENERS
C     BETWEEN THE DIAPHRAGM PANELS AND THE STEEL FRAME MEMBERS
C
      READ (5,510) (X(IN),IN=1,NEND2)
C
      IF (NSIDE.NE.0) READ (5,510) (Y(IU),IU=1,NSIDE2)
C
      IF (NSEAM.NE.0) READ (5,510) (YS(IU),IU=1,NCPS)
C
      IF (NCGIRT.NE.0)READ (5,510) (XGC(IN),IN=1,NCGIRT)
C
      N2=NX
      N1=NY
      KN=0
      NN=1
      NMBY2=NMBY/2
C
C     GENERATE CONNECTIVITY OF BEAM ELEMENTS OF MARGINAL MEMBER [AB]
C     IN THE Y-DIRECTION
C
      DO 20 I=1,NMBY2
      KN=KN+1
      IF ((KN.GT.NY).AND.(KN.EQ.(N1-NY+1))) NN=NN-1
      IUCBY(I,1)=NN
      IUCBY(I,2)=NN+1
      IUCBY(I,3)=NN+2
      IF ((KN.GT.NY).AND.(KN.EQ.(N1-NY+1))) NN=NN+1
      IUCBY(I,4)=NN+2
      IUCBY(I,4)=NN+3
      IUCBY(I,5)=NN+4
      IUCBY(I,6)=NN+5
      NN=NN+3
      IF ((KN.EQ.N1).AND.(KN.LT.NMBY2)) GO TO 11
      GO TO 20
   11 N4=N1+NY
      II=N2+1
      N2=N2+NX
      IUCBX(II,1)=IUCBY(I,4)
      IUCBX(II,2)=IUCBY(I,5)
      IUCBX(II,3)=NN+3
      NN=NN+1
   20 CONTINUE
C
      NN=NN+5
      IUCBX(1,1)=IUCBY(1,1)
      IUCBX(1,2)=IUCBY(1,2)
      IUCBX(1,3)=NN-1
      II=N2+1
      IUCBX(II,1)=IUCBY(NMBY2,4)
      IUCBX(II,2)=IUCBY(NMBY2,5)
      IUCBX(II,3)=NN-2
C
      NDD=1
      N1=NY
      NO=NN
      NA=NN
      NER=NPANEL*NMPPX
      NB=NGIRT+2
C
C     GENERATE CONNECTIVITY OF PLATE ELEMENTS
C
    1 K=K+1
C
      IF (K.GT.NMPPY) GO TO 50
      L=0
C
      DO 40 I=1,NPANEL
      DO 30 J=1,NMPPX
      L=L+1
      KK=K*NER
      II=KK-NER+L
      IF ((K.EQ.(N1+1)).AND.(J.GT.1)) NO=NO-3
      IUCP(II,1)=NO
      IUCP(II,2)=NO+1
      IF ((K.EQ.(N1+1)).AND.(J.GT.1)) NO=NO+3
      IVCP(II,7)=NO+2
      IVCP(II,8)=NO+3
      NI=J*(NMPPY+1)*2
      NJ=NA+NI
      NK=NJ+((J-1)*NB*3)+3*NDD
      NO=NK
      IF ((I.EQ.NPANEL).AND.(J.EQ.NMPPX)) NO=NO-3*NDD
      IVCP(II,3)=NO
      IVCP(II,4)=NO+1
      IF (K.EQ.(N1+1)) NK=NK+3
      NO=NK
      IF ((I.EQ.NPANEL).AND.(J.EQ.NMPPX)) NO=NO-3*NDD
      IF ((K.EQ.(N1+1)).AND.(I.EQ.NPANEL).AND.(J.EQ.NMPPX)) NO=NO-3
      IVCP(II,5)=NO+2
      IVCP(II,6)=NO+3
   30 CONTINUE
      NO=NO+((NMPPY+1)*2)+((NGIRT+1)*3)
      NA=NO
      IF (K.EQ.(N1+1)) NO=NO-3
      IF (K.EQ.(N1+1)) NA=NA-3
   40 CONTINUE.
      NN=NN+2
      NO=NN
      NA=NN
      IF (K.EQ.(N1+1)) NDD=NDD+1
      IF (K.EQ.(N1+1)) NGIRT=NGIRT-1
      IF (K.EQ.(N1+1)) N1=N1+NY
C
      GO TO 1
C
C
C     GENERATE CONNECTIVITY OF BEAM ELEMENTS OF ALL MARGINAL MEMBERS
C     IN THE X-DIRECTION
C
   50 NN=NN+2
      N7=0
      NR=NN
      NC=NMPPX
      KN=0
      IKK=0
      NIN=((NMPPY+1)*2)+(NB*3)
C
      DO 110 I=1,NB
      KK=KN*NX
      IF (I.GT.2) NN=NN-2*(I-2)
      DO 1200 J=1,NX
      K=KK+J
      IF (J.EQ.1) GO TO 130
      GO TO 140
  130 IVCBX(K,4)=NN
      IVCBX(K,5)=NN+1
      IVCBX(K,6)=NN+2
      GO TO 1200
  140 IVCBX(K,1)=NN
      IVCBX(K,2)=NN+1
      IVCBX(K,3)=NN+2
      IF (J.EQ.(NC+1)) GO TO 123
      NN=NN+NIN
      GO TO 124
  123 NN=NN+NIN+((NMPPY+1)*2)
      NC=NC+NMPPX
  124 IF (K.EQ.NX) GO TO 150
      IF (K.EQ.NMBX) GO TO 180
      IF ((I.GT.1).AND.(I.LT.NB)) GO TO 160
  190 IVCBX(K,4)=NN
      IVCBX(K,5)=NN+1
      IVCBX(K,6)=NN+2
      GO TO 1200
  160 IF (J.EQ.NX) GO TO 170
      GO TO 190
  170 N7=N7+NY
      IKK=IKK+1
      IVCBX(K,4)=IVCBX(NX,6)+((N7-1)*3)+IKK
      IVCBX(K,5)=IVCBX(K,4)+1
      IVCBX(K,6)=IVCBX(K,5)+2
      GO TO 1200
  150 IUCBX(K,4)=NN+((NMPPY+1)*2)
      IUCBX(K,5)=IUCBX(K,4)+1
      IUCBX(K,6)=IUCBX(K,5)+1
      GO TO 1200
  180 IUCBX(K,4)=NDF-4
      IUCBX(K,5)=NDF-3
      IUCBX(K,6)=NDF-2
 1200 CONTINUE
      NN=NR+((NY+1)*2)+3
      NR=NN
      KN=KN+1
      NC=NMPPX
  110 CONTINUE
C
C     GENERATE CONNECTIVITY OF BEAM ELEMENTS OF MARGINAL MEMBER [CD]
C     IN THE Y-DIRECTION
C
      KN=0
      N1=NY
      MM=IUCBX(NX,6)+1
      NF=NMBY2+1
C
      DO 603 I=NF,NMBY
      KN=KN+1
      IF (I.EQ.NF) GO TO 601
      IF (I.EQ.NMBY) GO TO 602
      IUCBY(I,1)=MM
      IUCBY(I,2)=MM+1
      IUCBY(I,3)=MM+2
      IF (KN.EQ.(N1+1)) MM=MM+1
      IF (KN.EQ.(N1+1)) N1=N1+NY
      IUCBY(I,4)=MM+3
      IUCBY(I,5)=MM+4
      IUCBY(I.6)=MM+5
     MM=MM+3
      GO TO 603
  601 IUCBY(I,1)=MM-3
      IUCBY(I,2)=MM-2
      IUCBY(I,3)=NDF
      IUCBY(I,4)=MM
      IUCBY(I,5)=MM+1
      IUCBY(I,6)=MM+2
      GO TO 603
  602 IUCBY(I,1)=MM
      IUCBY(I,2)=MM+1
      IUCBY(I,3)=MM+2
      IUCBY(I,4)=MM+3
      IUCBY(I,5)=MM+4
      IUCBY(I,6)=NDF-1
  603 CONTINUE
C
C     GENERATE CONNECTIVITY OF CONNECTOR ELEMENTS
C     ( END FASTENERS )
C
      NGIRT=NG
      KN=0
      NGC=0
C
      DO 724 I=1,NB
      LXX1=0
      KK=KN*NX
      DO 725 J=1,NX
      LXX1=LXX1+LBX
      K=KK+J
      IF ((K.LE.NX).OR.(K.GE.(NMBX-NX+1))) GO TO 31
      GO TO 32
   31 IF (K.GE.(NMBX-NX+1)) GO TO 33
C
C     END  FASTENERS TO MEMBER [BC] .... D'S.O.F. 1 & 3
C
      DO 115 LO=1,NEND2
      IF ((X(LO).EQ.0).AND.(LXX1.EQ.LBX)) GO TO 81
      IF (X(LO).EQ.LXX1) GO TO 82
      GO TO 115
   81 IVCC(L0,1)=IVCBX(K,1)
      IVCC(L0,3)=IVCBX(K,2)
      GO TO 115
   82 IVCC(L0,1)=IVCBX(K,4)
      IVCC(L0,3)=IVCBX(K,5)
  115 CONTINUE
      GO TO 32
   33 L1=0
C
C     END  FASTENERS TO MEMBER [AD] .... D'S.O.F. 1 & 3
C
      DO 116 L00=N20,NEND
      L1=L1+1
      IF ((X(L1).EQ.0).AND.(LXX1.EQ.LBX)) GO TO 83
      IF (X(L1).EQ.LXX1) GO TO 84
      GO TO 116
   83 IVCC(L00,1)=IVCBX(K,1)
      IVCC(L00,3)=IVCBX(K,2)
      GO TO 116
   84 IVCC(L00,1)=IVCBX(K,4)
      IVCC(L00,3)=IVCBX(K,5)
  116 CONTINUE
C
      IF (NGIRT.EQ.0) GO TO 725
C
C     GENERATE CONNECTIVITY OF CONNECTOR ELEMENTS
C     ( SHEET-TO-PURLINS FASTENERS ) .... D'S.O.F. 1 & 3
C
   32 IF((K.GE.(KK+1)).AND.(K.GT.1)) GO TO 205
      GO TO 725
  205 IF (K.GE.(NMBX-NX+1)) GO TO 725
      KKC=NGC-NCGIRT+1
      N10=M9+KKC
      N11=M9+NGC
      L3=0
      DO 208 L06=N10,N11
      L3=L3+1
      IF ((XGC(L3).EQ.0).AND.(LXX1.EQ.LBX)) GO TO 206
      IF (XGC(L3).EQ.LXX1) GO TO 207
      GO TO 208
  206 IVCC(L06,1)=IVCBX(K,1)
      IVCC(L06,3)=IVCBX(K,2)
      GO TO 208
  207 IVCC(L06,1)=IVCBX(K,4)
      IVCC(L06,3)=IVCBX(K,5)
  208 CONTINUE
  725 CONTINUE
      NGC=NGC+NCGIRT
      KN=KN+1
  724 CONTINUE
C
      LYY=0
      K=0
      N7=NY
      NGC=0
C
      IF (NSIDE.EQ.0) GO TO 726
C
C
C     GENERATE CONNECTIVITY OF CONNECTOR ELEMENTS
C     ( SIDE FASTENERS )
C
      LYY1=0
      DO 722 I=1,NMBY2
      LYY1=LYY1+LBY
      L6=0
C
C     SIDE FASTENERS TO M[illegible]AB] .... D'S.O.F. 1 & 3
C
      DO 135 J3=NEND1,NCO
      L6=L6+1
      IF ((Y(L6).EQ.0).AND.(LYY1.EQ.LBY)) GO TO 85
      IF (Y(L6).EQ.LYY1) GO TO 86
      GO TO 135
   85 IVCC(J3,1)=IVCBY(I,1)
      IVCC(J3,3)=IVCBY(I,2)
      GO TO 135
   86 IVCC(J3,1)=IVCBY(I,4)
      IVCC(J3,3)=IVCBY(I,5)
  135 CONTINUE
   22 CONTINUE
      LYY2=0
      DO 723 I=NF,NMBY
      LYY2=LYY2+LBY
      L7=0
C
C     SIDE FASTENERS TO MEMBER [CD] .... D'S.O.F. 1 & 3
C
      DO 136 J4=NCO1,NCON
      L7=L7+1
      IF ((Y(L7).EQ.0).AND.(LYY2.EQ.LBY)) GO TO 87
      IF (Y(L7).EQ.LYY2) GO TO 88
      GO TO 136
   87 IVCC(J4,1)=IVCBY(I,1)
      IVCC(J4,3)=IVCBY(I,2)
      GO TO 136
   88 IVCC(J4,1)=IVCBY(I,4)
      IVCC(J4,3)=IVCBY(I,5)
  136 CONTINUE
  723 CONTINUE
C
  726 K=K+1
      IF (K.GT.NMPPY) GO TO 727
      L=0
      LYY=LYY+LY
      LXX=0
C
      DO 720 I=1,NPANEL
      DO 721 J=1,NMPPX
      LXX=LXX+LX
      L=L+1
      KK=K*NER
      KKK=KK-NER+L
      IF ((KKK.LE.NER).OR.(KKK.GE.(NMP-NER+1))) GO TO 21
      GO TO 22
   21 IF (KKK.GE.(NMP-NER+1)) GO TO 23
C
C     END  FASTENERS TO MEMBER [BC] .... D'S.O.F. 2 & 4
C
      DO 105 LO=1,NEND2
      IF ((X(LO).EQ.0).AND.(LXX.EQ.LX)) GO TO 91
      IF (X(LO).EQ.LXX) GO TO 92
      GO TO 105
   91 IVCC(LO,2)=IVCP(KKK,1)
      IVCC(LO,4)=IVCP(KKK,2)
      GO TO 105
   92 IF(X(LO).EQ.X(LO-1)) GO TO 999
      IVCC(LO,2)=IVCP(KKK,3)
      IVCC(LO,4)=IVCP(KKK,4)
      GO TO 105
  999 KS=KKK+1
      IVCC(LO,2)=IVCP(KS,1)
      IVCC(LO,4)=IVCP(KS,2)
  105 CONTINUE
C
      GO TO 22
   23 LL=0
C
C     END  FASTENERS TO MEMBER [AD] .... D'S.O.F. 2 & 4
C
      DO 106 LOO=N20,NEND
      LL=LL+1
      IF ((X(LL).EQ.0).AND.(LXX.EQ.LX)) GO TO 93
      IF (X(LL).EQ.LXX) GO TO 94
      GO TO 106
   93 IVCC(LOO,2)=IVCP(KKK,7)
```

```
      IVCC(LOO,4)=IVCP(KKK,8)
      GO TO 106
   94 IF(X(LL).EQ.X(LL-1)) GO TO 998
      IVCC(LOO,2)=IVCP(KKK,5)
      IVCC(LOO,4)=IVCP(KKK,6)
      GO TO 106
  998 KS=KKK+1
      IVCC(LOO,2)=IVCP(KS,7)
      IVCC(LOO,4)=IVCP(KS,8)
  106 CONTINUE
C
   22 CONTINUE
C
      IF (NSIDE.EQ.0) GO TO 222
C
      L5=0
C
C     SIDE FASTENERS TO MEMBER [AB] .... D'S.O.F. 2 & 4
C
      IF ((I.EQ.1).AND.(J.EQ.1)) GO TO 41
      IF ((I.EQ.NPANEL).AND.(J.EQ.NMPPX)) GO TO 42
      GO TO 222
   41 DO 125 J1=NEND1,NCO
      L5=L5+1
      IF ((Y(L5).EQ.0).AND.(LYY.EQ.LY)) GO TO 95
      IF (Y(L5).EQ.LYY) GO TO 96
      GO TO 125
   95 IVCC(J1,2)=IVCP(KKK,1)
      IVCC(J1,4)=IVCP(KKK,2)
      GO TO 125
   96 IVCC(J1,2)=IVCP(KKK,7)
      IVCC(J1,4)=IVCP(KKK,8)
  125 CONTINUE
C
      ~~GO TO 222~~
   42 L2=0
C
C     SIDE FASTENERS TO MEMBER [CD] .... D'S.O.F. 2 & 4
C
      DO 126 J2=NCO1,NCON
      L2=L2+1
      IF ((Y(L2).EQ.0).AND.(LYY.EQ.LY)) GO TO 97
      IF (Y(L2).EQ.LYY) GO TO 98
      GO TO 126
   97 IVCC(J2,2)=IVCP(KKK,1)
      IVCC(J2,4)=IVCP(KKK,2)
      GO TO 126
   98 IVCC(J2,2)=IVCP(KKK,5)
      IVCC(J2,4)=IVCP(KKK,6)
  126 CONTINUE
C
  222 CONTINUE
C
      IF (NSEAM.EQ.0) GO TO 2222
C
C     GENERATE CONNECTIVITY OF CONNECTOR ELEMENTS
C     ( SEAM FASTENERS )
C
      IF ((I.EQ.1).AND.(J.EQ.NMPPX)) GO TO 51
      IF ((I.EQ.NPANEL).AND.(J.EQ.1)) GO TO 52
      IF ((I.GT.1).AND.(I.LT.NPANEL)) GO TO 53
      GO TO 2222
   51 LYY3=0
C
C     EXTERIOR LEFT SEAM ( FIRST SEAM )
C
      DO 145 J5=M1,M2
      LYY3=LYY3+1
      IF (YS(LYY3).EQ.LYY ) GO TO 54
      GO TO 145
   54 IVCC(J5,1)=IVCP(KKK,5)
      IVCC(J5,3)=IVCP(KKK,6)
  145 CONTINUE
      GO TO 2222
   52 LYY4=0
C
C     EXTERIOR RIGHT SEAM ( LAST SEAM )
C
```

```
      DO 155 J6=M3,M4
      LYY4=LYY4+1
      IF (YS(LYY4).EQ.LYY ) GO TO 55
      GO TO 155
   55 IUCC(J6,2)=IUCP(KKK,7)
      IUCC(J6,4)=IUCP(KKK,8)
  155 CONTINUE
      GO TO 2222
   53 IF (J.EQ.1) GO TO 56
      IF(J.EQ.NMPPX) GO TO 57
      GO TO 2222
   56 LYY5=0
      M6=NEND+NSIDE+(I-1)*NCPS
      M5=M6-NCPS+1
C
C     INTERIOR SEAMS
C
      DO 165 J7=M5,M6
      LYY5=LYY5+1
      IF (YS(LYY5).EQ.LYY ) GO TO 58
      GO TO 165
   58 IUCC(J7,2)=IUCP(KKK,7)
      IUCC(J7,4)=IUCP(KKK,8)
  165 CONTINUE
      GO TO 2222
   57 LYY6=0
      M8=NEND+NSIDE+I*NCPS
      M7=M8-NCPS+1
      DO 175 J8=M7,M8
      LYY6=LYY6+1
      IF (YS(LYY6).EQ.LYY ) GO TO 59
      GO TO 175
   59 IUCC(J8,1)=IUCP(KKK,5)
      IUCC(J8,3)=IUCP(KKK,6)
  175 CONTINUE
C
 2222 CONTINUE
C
      IF (NGIRT.EQ.0) GO TO 22222
C
C     GENERATE CONNECTIVITY OF CONNECTOR ELEMENTS
C     ( SHEET-TO-PURLINS FASTENERS ) .... D'S.O.F. 2 & 4
C
      N8=(N7*NMPPX*NPANEL)+1
      IF((KKK.GE.N8).AND.(KKK.LT.(NMP-NER+1))) GO TO 215
      GO TO 22222
  215 IF ((I.GT.1).OR.(J.GT.1)) GO TO 227
      NGC=NGC+NCGIRT
      KKC=NGC-NCGIRT+1
      M10=M9+KKC
      M11=M9+NGC
  227 L4=0
      DO 211 L07=M10,M11
      L4=L4+1
      IF ((XGC(L4).EQ.0).AND.(LXX.EQ.LX)) GO TO 209
      IF (XGC(L4).EQ.LXX) GO TO 212
      GO TO 211
  209 IUCC(L07,2)=IUCP(KKK,1)
      IUCC(L07,4)=IUCP(KKK,2)
      GO TO 211
  212 IF (XGC(L4).EQ.XGC(L4-1)) GO TO 997
      IUCC(L07,2)=IUCP(KKK,3)
      IUCC(L07,4)=IUCP(KKK,4)
      GO TO 211
  997 KS=KKK+1
      IUCC(L07,2)=IUCP(KS,1)
      IUCC(L07,4)=IUCP(KS,2)
  211 CONTINUE
C
22222 CONTINUE
C
  721 CONTINUE
  720 CONTINUE
      IF(K.EQ.(N7+1)) N7=N7+NY
      GO TO 726
  727 CONTINUE
C
```

```
      WRITE (6,7)
    7 FORMAT('1',35X,'GENERATED  CONNECTIVITY  MATRIX  (PLATE ELEMENTS)
     1(IVCP)')
C
      WRITE (6,70)
   70 FORMAT('0',15X,'ELEMENT NO',4X,'U1  (1)',4X,'V1  (2)',4X,'U2  (3)'
     1,4X,'V2  (4)',4X,'U3  (5)',4X,'V3  (6)',4X,'U4  (7)',4X,'V4  (8)')
C
      DO 700 J=1,NMP
  700 WRITE (6,7000) J,(IVCP(J,K),K=1,8)
 7000 FORMAT ('0',17X,I3,11X,8(I4,7X))
      WRITE (6,8)
    8 FORMAT('1',30X,'GENERATED  CONNECTIVITY MATRIX (BEAM ELEMENTS IN X
     1)  (IVCBX)')
C
      WRITE (6,80)
   80 FORMAT('0',25X,'ELEMENT NO',4X,'U1  (1)',4X,'V1  (2)',4X,'O1  (3)'
     1,4X,'U2  (4)',4X,'V2  (5)',4X,'O2  (6)')
C
      DO 800 J=1,NMBX
  800 WRITE (6,8000) J,(IVCBX(J,K),K=1,6)
 8000 FORMAT('0',27X,I3,11X,6(I4,7X))
C
      WRITE (6,9)
    9 FORMAT('1',30X,'GENERATED  CONNECTIVITY MATRIX (BEAM ELEMENTS IN Y
     1)  (IVCBY)')
C
      WRITE (6,80)
C
      DO 900 J=1,NMBY
  900 WRITE (6,8000) J,((IVCBY(J,K),K=1,6))
C
      WRITE (6,10)
   10 FORMAT('1',27X,'GENERATED  CONNECTIVITY MATRIX (CONNECTOR  ELEMENT
     1S)  (IVCC)')
C
      WRITE (6,100)
  100 FORMAT('0',30X,'ELEMENT NO',4X,'U1  (1)',4X,'U2  (2)',4X,'V1  (3)'
     1,4X,'V2  (4)')
C
      N1=NEND+1
      N2=N1+NSIDE
      N3=N2+NSEAM
      DO 101 J=1,NMC
C
      IF (J.EQ.1 ) WRITE (6,5)
      IF (J.EQ.N1) WRITE (6,6)
      IF (J.EQ.N2) WRITE (6,12)
      IF (J.EQ.N3) WRITE (6,13)
C
    5 FORMAT (///45X,'*****  END  CONNECTIONS  *****'///)
    6 FORMAT (///45X,'*****  SIDE CONNECTIONS  *****'///)
   12 FORMAT (///45X,'*****  SEAM CONNECTIONS  *****'///)
   13 FORMAT (///38X,'****  SHEET-TO-PURLINS  CONNECTIONS  ****'///)
C
  101 WRITE (6,102) J,(IVCC(J,K),K=1,4)
  102 FORMAT('0',32X,I3,11X,4(I4,7X))
C
C     COMPUTE MAXIMUM HALF-BANDWIDTH OF ASSEMBLY STIFFNESS MATRIX
C     ( INCLUDING DIAGONAL )
C
      MAXDIF=0
      DO 4 I=1,NMBX
      DO 3 J=1,6
      IF ( IVCBX(I,J).EQ.0) GO TO 3
      DO 2 K=1,6
      IF ( IVCBX(I,K).EQ.0) GO TO 2
      LHBW=IABS(IVCBX(I,J)-IVCBX(I,K))
      IF (LHBW.GT.MAXDIF) MAXDIF=LHBW
    2 CONTINUE
    3 CONTINUE
    4 CONTINUE
      MA=MAXDIF+1
C
```

```
C     DEFINE CONSTRAINED DISPLACEMENT DEGREES OF FREEDOM
C     DEPENDING UPON DIAPHRAGM ORIENTATION  RELATIVE  TO
C     LOAD ( I.E. LOCATIONS OF SUPPORTS )
C
C     NDF1 ......................... FOR ROLLER SUPPORT
C     NDF2 & NDF3 .................. FOR HINGE  SUPPORT
C
      IF ( ICASE.EQ.1 ) GO TO 606
C
      NDF1=IVCBY(NMBY2,5)
      NDF2=IVCBY(NMBY,4)
      NDF3=IVCBY(NMBY,5)
      NDFP=IVCBX(1,1)
      NDFTIP=IVCBX(NX,4)
      GO TO 707
C
  606 NDF1=IVCBX(1,1)
      NDF2=IVCBY(NMBY2,4)
      NDF3=IVCBY(NMBY2,5)
      NDFP=IVCBX(NX,5)
      NDFTIP=IVCBY(NMBY,5)
  707 CONTINUE
C
      WRITE (6,60) NDF1,NDF2,NDF3,NDFP,NDFTIP,NDF,MA
C
   60 FORMAT(////36X,'CONSTRAINED  DISPLACEMENT  DEGREES  OF  FREEDOM'//
     142X,'D.O.F.',3X,I4,3X,'FOR ROLLER SUPPORT'//42X,'D.O.F.',3X,I4,3X,
     2'FOR HINGE  SUPPORT'//42X,'D.O.F.'.3X,I4,3X,'FOR HINGE  SUPPORT'//
     3/36X,'D.O.F. AT WHICH THE JACK LOAD IS APPLIED',I6//36X,'D.O.F. AT
     4 DIAPHRAGM TIP IN LOAD DIRECTION',I5//36X,'TOTAL  NUMBER  OF DEGRE
     5ES  OF  FREEDOM',I8//36X,'MAXIMUM HALF-BANDWIDTH  (INCL. DIAGONAL)
     6',I6//)
C
C     STORE ELEMENTS CONNECTIVITY MATRICES ON TAPE7 [.ND ]
C     FOR LATER USE IN CALCULATION OF ELEMENTS NODAL FORCES
C
      REWIND ND
      WRITE (ND) ((IVCP(I,J),J=1,8),I=1,NMP)
      WRITE (ND) ((IVCBX(I,J),J=1,6),I=1,NMBX)
      WRITE (ND) ((IVCBY(I,J),J=1,6),I=1,NMBY)
      WRITE (ND) ((IVCC(I,J),J=1,4),I=1,NMC)
      GO TO 200
C
C     RETRIEVE ELEMENTS' CONNECTIVITY MATRICES
C
  300 REWIND ND
      READ  (ND) ((IVCP(I,J),J=1,8),I=1,NMP)
      READ  (ND) ((IVCBX(I,J),J=1,6),I=1,NMBX)
      READ  (ND) ((IVCBY(I,J),J=1,6),I=1,NMBY)
      READ  (ND) ((IVCC(I,J),J=1,4),I=1,NMC)
  200 CONTINUE
C
      RETURN
      END
C
```

```
C
      SUBROUTINE BEAMY
C
C    ******************************************************************
C    *                                                                *
C    *     SUBROUTINE BEAMY GENERATES THE STIFFNESS MATRIX FOR MARGINAL*
C    *  MEMBERS POSITIONED PARALLEL TO THE Y-DIRECTION , ACCOUNTING FOR *
C    *  AXIAL DEFORMATION AND BENDING ABOUT A SINGLE AXIS ( FIG. 5.2B ) .*
C    *                                                                *
C    *     IT GIVES DIRECTLY THE TRANSFORMED STIFFNESS MATRIX FROM      *
C    *  LOCAL TO SYSTEM COORDINATES ACCORDING TO EQUATION 5.2 .         *
C    *                                                                *
C    ******************************************************************
C
      COMMON/BLK4/ BYK(6,6)
      REAL  LBY
C
C    ******************************************************************
C    *                                                                *
C    *    THE FOLLOWING STATEMENT READS IN THE GEOMETRIC AND ELASTIC    *
C    *  PROPERTIES REQUIRED TO GENERATE THE BEAM ELEMENT STIFFNESS MATRIX*
C    *  ( IN THE Y-DIRECTION ). THE VARIABLES READ IN ARE :             *
C    *      LBY  = LENGTH OF THE BEAM ELEMENT                           *
C    *      ZIBY = MOMENT OF INERTIA ABOUT THE AXIS OF BENDING          *
C    *             ( PERPENDICULAR TO DIAPHRAGM PLANE )                 *
C    *      ABY  = CROSS SECTIONAL AREA OF THE BEAM                     *
C    *      EBY  = ELASTIC MODULUS OF THE BEAM MATERIAL                 *
C    *                                                                *
C    ******************************************************************
C
      READ (5,10) LBY,ZIBY,ABY,EBY
   10 FORMAT (4F15.5)
C
      WRITE (6,20) LBY,ZIBY,ABY,EBY
   20 FORMAT('-',5X,'PROPERTIES OF BEAM ELEMENTS IN THE Y-DIRECTION..'//
     1        5X,'LENGTH  OF  THE  BEAM  ELEMENT................',F10.4/
     2        5X,'MOMENT  OF  INERTIA  ABOUT THE AXIS OF BENDING.',F10.4/
     3        5X,'CROSS  SECTIONAL  AREA  OF  THE  BEAM..........',F10.4/
     4        5X,'ELASTIC  MODULUS  OF  THE  BEAM  MATERIAL......',F15.5)
C
C     INITIALIZE ELEMENT STIFFNESS MATRIX  .. BYK ..
C
      DO 40  I=1,6
      DO 30  J=1,6
      BYK(I,J)=0.0
   30 CONTINUE
   40 CONTINUE
C
      BYK(1,1)= (12.0*EBY*ZIBY)/(LBY**3)
      BYK(1,4)=-BYK(1,1)
      BYK(2,2)= (ABY*EBY)/LBY
      BYK(1,3)= (-6.0*EBY*ZIBY)/(LBY**2)
      BYK(2,5)=-BYK(2,2)
      BYK(1,6)= BYK(1,3)
      BYK(3,3)= ( 4.0*EBY*ZIBY)/ LBY
      BYK(3,4)=-BYK(1,3)
      BYK(3,6)= ( 2.0*EBY*ZIBY)/ LBY
      BYK(4,4)= BYK(1,1)
      BYK(5,5)= BYK(2,2)
      BYK(4,6)= BYK(3,4)
      BYK(6,6)= BYK(3,3)
C
      DO 50  I=2,6
      DO 50  J=1,5
      IF (I.LE.J) GO TO 50
      BYK(I,J)=BYK(J,I)
   50 CONTINUE
C
      RETURN
      END
```

```
C
      SUBROUTINE BEAMX (IB)
C
C   ***********************************************************************
C   *                                                                     *
C   *      SUBROUTINE BEAMX GENERATES THE STIFFNESS MATRIX FOR MARGINAL*
C   *  MEMBERS OR PURLINS POSITIONED PARALLEL TO THE X-AXIS , ACCOUNTING*
C   *  FOR AXIAL DEFORMATION AND BENDING ABOUT A SINGLE AXIS .           *
C   *                                                                     *
C   *      FOR THE DERIVATION OF THE STIFFNESS MATRIX SEE ANY TEXT ON   *
C   *  MATRIX METHODS . THE POSITIVE DIRECTIONS OF FORCES AND DISPLACE- *
C   *  MENTS ARE SHOWN IN FIGURE 5.2A  .                                  *
C   *                                                                     *
C   *      THE STIFFNESS COEFFICIENTS ARE DIRECTLY CALCULATED FROM       *
C   *  EXPLICIT EXPRESSIONS OF EQUATION 5.1  .                            *
C   *                                                                     *
C   ***********************************************************************
C
      COMMON/BLK3/ BXK(6,6)
      REAL  LBX
C
C   ***********************************************************************
C   *                                                                     *
C   *     THE FOLLOWING STATEMENT READS IN THE GEOMETRIC AND ELASTIC     *
C   *  PROPERTIES REQUIRED TO GENERATE THE BEAM ELEMENT STIFFNESS MATRIX*
C   *  ( IN THE X-DIRECTION ). THE VARIABLES READ IN ARE :               *
C   *     LBX  = LENGTH OF THE BEAM ELEMENT                               *
C   *     ZIBX = MOMENT OF INERTIA ABOUT THE AXIS OF BENDING              *
C   *            ( PERPENDICULAR TO DIAPHRAGM PLANE )                     *
C   *     ABX  = CROSS SECTIONAL AREA OF THE BEAM                         *
C   *     EBX  = ELASTIC MODULUS OF THE BEAM MATERIAL                     *
C   *                                                                     *
C   ***********************************************************************
C
      READ (5,10) LBX,ZIBX,ABX,EBX
   10 FORMAT (4F15.5)
C
      WRITE (6,20) IB,LBX,ZIBX,ABX,EBX
   20 FORMAT('-',5X,'PROPERTIES OF BEAM ELEMENTS IN THE X-DIRECTION..'//
     *        5X,'FOR MEMBER NO. *************',I5,4X,'************   -'//
     1        5X,'LENGTH  OF  THE  BEAM  ELEMENT.................',F10.4/
     2        5X,'MOMENT .OF  INERTIA  ABOUT THE AXIS OF BENDING.',F10.4/
     3        5X,'CROSS  SECTIONAL  AREA  OF  THE  BEAM..........',F10.4/
     4        5X,'ELASTIC  MODULUS  OF  THE  BEAM  MATERIAL......',F15.5)
C
C     INITIALIZE ELEMENT STIFFNESS MATRIX  .. BXK ..
C
      DO 40  I=1,6
      DO 30 J=1,6
      BXK(I,J)=0.0
   30 CONTINUE
   40 CONTINUE
C
      BXK(1,1)= (ABX*EBX)/LBX
      BXK(1,4)=-BXK(1,1)
      BXK(2,2)= (12.0*EBX*ZIBX)/(LBX**3)
      BXK(2,3)= (-6.0*EBX*ZIBX)/(LBX**2)
      BXK(2,5)=-BXK(2,2)
      BXK(2,6)= BXK(2,3)
      BXK(3,3)= ( 4.0*EBX*ZIBX)/ LBX
      BXK(3,5)=-BXK(2,3)
      BXK(3,6)= ( 2.0*EBX*ZIBX)/ LBX
      BXK(4,4)= BXK(1,1)
      BXK(5,5)= BXK(2,2)
      BXK(5,6)= BXK(3,5)
      BXK(6,6)= BXK(3,3)
C
      DO 50  I=2,6
      DO 50  J=1,5
      IF (I.LE.J) GO TO 50
      BXK(I,J)=BXK(J,I)
   50 CONTINUE
C
      RETURN
      END
```

```
C
      SUBROUTINE CONNEC (IT) .
C
C  *******************************************************************
C  *                                                                 *
C  *     SUBROUTINE CONNEC GENERATES THE STIFFNESS MATRIX OF A       *
C  *  CONNECTOR ELEMENT , USED TO SIMULATE ANY OF THE FOUR TYPES OF  *
C  *  CONNECTIONS IN THE DIAPHRAGM INSTALLATION ( END , SIDE , SEAM , *
C  *  AND GIRT-SHEET FASTENERS ) .                                   *
C  *                                                                 *
C  *     THE CONNECTIONS ARE MODELLED IN THE FORM OF TWO MUTUALLY    *
C  *  PERPENDICULAR SPRINGS OF STIFFNESSES KX AND KY RESPECTIVELY    *
C  *  DETERMINED EXPERIMENTALLY .  ( EQ. 5.5 , FIG. 5.4 )            *
C  *                                                                 *
C  *******************************************************************
C
      COMMON/BLK5/ CONK(4,4)
      REAL  KX,KY
C
C  *******************************************************************
C  *                                                                 *
C  *     READ IN THE CONNECTOR ELEMENT'S SPRING COEFFICINTS IN THE X *
C  *  AND Y DIRECTIONS .                                             *
C  *                                                                 *
C  *******************************************************************
C
      READ (5,10) KX,KY
   10 FORMAT(2F15.5)
C
      WRITE (6,20) IT,KX,KY
   20 FORMAT('-',5X,'SPRING  COEFFICENTS  OF  CONNECTOR  ELEMENTS....'//
     *      5X,'TYPE NO. ********************',I5,4X,'**************  '//
     1      5X,'SPRING  COEFFICENT   IN  THE  X-DIRECTION......',F15.5/
     2      5X,'SPRING  COEFFICENT   IN  THE  Y-DIRECTION......',F15.5)
C
      DO 100 I=1,4
      DO 101 J=1,4
      CONK(I,J)=0.0
101   CONTINUE
100   CONTINUE
C
      CONK(1,1)= KX
      CONK(1,2)=-KX
      CONK(2,2)= KX
      CONK(3,3)= KY
      CONK(3,4)=-KY
      CONK(4,4)= KY
C
      DO 109 I=2,4
      DO 109 J=1,3
      IF (I.LE.J) GO TO 109
      CONK(I,J)=CONK(J,I)
109   CONTINUE
C
      RETURN
      END
```

```
C
      SUBROUTINE PLATE
C
C  *********************************************************************
C  *                                                                   *
C  *     SUBROUTINE PLATE CALCULATES THE ELEMENT STIFFNESS MATRIX FOR  *
C  *  AN ORTHOTROPIC PLANE STRESS RECTANGULAR ELEMENT WITH TWO DEGREES *
C  *  OF FREEDOM AT EACH CORNER .                                      *
C  *                                                                   *
C  *     THE STIFFNESS MATRIX DERIVATION IS OUTLINED IN REF.    . AND  *
C  *  THE D.O.F. NUMBERS AND COORDINATES ARE SHOWN IN FIGURE 5.3  .    *
C  *                                                                   *
C  *     THE ELEMENTS OF THE STIFFNESS MATRIX ARE CALCULATED DIRECTLY  *
C  *  USING THE EXPRESSIONS GIVEN BE EQUATIONS 5.3 & 5.4  .            *
C  *                                                                   *
C  *********************************************************************
C
      COMMON/BLK2/ PLK(8,8)
      REAL   NUXY,NUYX,LX,LY
C
C  *********************************************************************
C  *                                                                   *
C  *      THE FOLLOWING STATEMENT READS IN THE GEOMETRIC AND ELASTIC   *
C  *  PROPERTIES REQUIRED TO GENERATE THE ORTHOTROPIC PLANE STRESS     *
C  *  ELEMENT STIFFNESS MATRIX . THE VARIABLES READ IN ARE :           *
C  *        NUXY = THE POISSON'S RATIO RELATING STRAINS IN THE Y       *
C  *               DIRECTION TO STRESSES IN THE X DIRECTION            *
C  *        NUYX = THE POISSON'S RATIO RELATING STRAINS IN THE X       *
C  *               DIRECTION TO STRESSES IN THE Y DIRECTION            *
C  *       LX   = LENGTH OF THE ELEMENT SIDE IN THE X DIRECTION        *
C  *       LY   = LENGTH OF THE ELEMENT SIDE IN THE Y DIRECTION        *
C  *       EX   = ELASTIC MODULUS IN THE X DIRECTION                   *
C  *       EY   = ELASTIC MODULUS IN THE Y DIRECTION                   *
C  *       T    = ELEMENT THICKNESS                                    *
C  *       G    = SHEAR MODULUS OF THE ELEMENT                         *
C  *                                                                   *
C  *********************************************************************
C
      READ (5,10) NUXY,NUYX,LX,LY,EX,EY,T,G
   10 FORMAT(2F6.4,2F9.5,2F15.5,F5.3,F15.5)
C
      WRITE (6,20) NUXY,NUYX,LX,LY,EX,EY,T,G
   20 FORMAT('1',5X,'PROPERTIES  OF  PLATE  ELEMENTS  .............   '//
     1      5X,'POISSONS  RATIO  (NUXY)......................... ',F9.5/
     2      5X,'POISSONS  RATIO  (NUYX)......................... ',F9.5/
     3      5X,'LENGTH  OF  ELEMENT  SIDE   IN THE X-DIRECTION..',F10.4/
     4      5X,'LENGTH  OF  ELEMENT  SIDE   IN THE Y-DIRECTION..',F10.4/
     5      5X,'ELASTIC  MODULUS  IN THE X-DIRECTION............',F15.5/
     6      5X,'ELASTIC  MODULUS  IN THE Y-DIRECTION............',F15.5/
     7      5X,'THICKNESS  OF  THE  ELEMENT..................... ',F9.5/
     8      5X,'SHEAR  MODULUS  OF  THE  ELEMENT................',F15.5)
C
      A= EX/(1.0-NUXY*NUYX)
      B= EY/(1.0-NUXY*NUYX)
      C= EX*NUYX/(1.0-NUXY*NUYX)
      D= LY/LX
C
      DO 30  I=1,7,2
      PLK(I,I)= T*((A*D/3.0)+(G/(3.0*D)))
      PLK(I+1,I+1)= T*((B/(3.0*D))+(G*D/3.0))
   30 CONTINUE
```

```
C
      PLK(2,1)=  T*(C+G)/4.0
      PLK(4,3)= -PLK(2,1)
      PLK(6,5)=  PLK(2,1)
      PLK(8,7)= -PLK(2,1)
      PLK(3,2)=  T*(-C+G)/4.0
      PLK(5,4)=  PLK(3,2)
      PLK(7,6)=  PLK(3,2)
      PLK(4,1)= -PLK(3,2)
      PLK(6,3)=  PLK(4,1)
      PLK(8,5)=  PLK(4,1)
      PLK(5,2)= -PLK(2,1)
      PLK(7,4)=  PLK(2,1)
      PLK(6,1)= -PLK(2,1)
      PLK(8,3)=  PLK(2,1)
      PLK(7,2)= -PLK(3,2)
      PLK(8,1)= -PLK(7,2)
      PLK(3,1)=  T*((-A*D/3.0)+G/(6.0*D))
      PLK(4,2)=-T*((-B/(6.0*D))+(G*D/3.0))
      PLK(5,3)=  T*((A*D/6.0)-(G/(3.0*D)))
      PLK(6,4)=  T*((-B/(3.0*D))+(G*D/6.0))
      PLK(7,5)=  PLK(3,1)
      PLK(8,6)=  PLK(4,2)
      PLK(5,1)= -PLK(1,1)/2.0
      PLK(6,2)= -PLK(2,2)/2.0
      PLK(7,3)=  PLK(5,1)
      PLK(8,4)=  PLK(6,2)
      PLK(7,1)=  PLK(5,3)
      PLK(8,2)=  PLK(6,4)
C
      DO 50  I=2,8
      DO 40  J=1,7
      IF (I.LE.J) GO TO 50
      PLK(J,I)=PLK(I,J)
   40 CONTINUE
   50 CONTINUE
C
      RETURN
      END
```

```
C
      SUBROUTINE FORMAK (NBLOCK,NEQB,MA,NDFP,P,NSTIF,AK,NVA1,IVCP,IVCBX,
     *                   IVCBY,IVCC,NMP,NMBX,NMBY,NMC,NS)
C
C  ***************************************************************
C  *                                                             *
C  *      SUBROUTINE FORMAK CONSTRUCTS THE DIAPHRAGM STIFFNESS MATRIX.*
C  *  IT GOES THROUGH EACH ELEMENT ONE BY ONE , ADDING THE STIFFNESS  *
C  *  CONTRIBUTION OF EACH TO ( AK ) , AND AT THE SAME TIME INTRODUCING*
C  *  THE KINEMATIC CONSTRAINTS ( GEOMETRIC BOUNDARY CONDITIONS , AT  *
C  *  THE SUPPORTS ) .                                               *
C  *      A BLOCK STORAGE ROW-WISE SCHEME OF THE ASSEMBELED BANDED    *
C  *  STIFFNESS MATRIX AND LOAD VECTORS , ON TAPE ( NSTIF ) , IS      *
C  *  PERFORMED , AS REQUIRED BY THE SOLUTION ROUTINE ( SESOL ) .     *
C  *                                                                 *
C  ***************************************************************
C
      COMMON/BLK1/ NEND,NSIDE,NSEAM,NCTS,NGIRT,NX,NDF1,NDF2,NDF3
      COMMON/BLK2/ PLK(8,8)
      COMMON/BLK3/ BXK(6,6)
      COMMON/BLK4/ BYK(6,6)
      COMMON/BLK5/ CONK(4,4)
      DIMENSION IVCP(NMP,8),IVCBX(NMBX,6),IVCBY(NMBY,6),IVCC(NMC,4)
      DIMENSION AK(NVA1)
C
      NB=NGIRT+2
      N1=NEND+1
      N2=NEND+NSIDE+1
      N3=NEND+NSIDE+NSEAM+1
C
      REWIND NS
C
C     STORE DIFFERENT ELEMENTS STIFFNESS MATRICES IN AUXILARY
C     STORAGE TAPE8 [ NS ]
C
      CALL PLATE
      WRITE (NS) ((PLK(I,J),J=1,8),I=1,8)
C
      DO 10 IB=1,NB
      CALL BEAMX (IB)
      WRITE (NS) ((BXK(I,J),J=1,6),I=1,6)
   10 CONTINUE
C
      CALL BEAMY
      WRITE (NS) ((BYK(I,J),J=1,6),I=1,6)
C
      DO 20 IT=1,NCTS
      CALL CONNEC (IT)
      WRITE (NS) ((CONK(I,J),J=1,4),I=1,4)
   20 CONTINUE
C
      REWIND NSTIF
C
C     MAIN LOOP OVER ALL BLOCKS
C
      DO 1000 LL=1,NBLOCK
C
      REWIND NS
C
C     INITIALIZE STRUCTURE STIFFNESS MATRIX ( AK ) .. EACH BLOCK
C
      DO 30 I=1,NVA1
   30 AK(I)=0.0
      L1=NEQB*LL
      L2=L1-NEQB+1
C
      READ  (NS) ((PLK(I,J),J=1,8),I=1,8)
C
C     LOOP OVER PLATE ELEMENTS
C
      DO 60  I=1,NMP
      DO 50 J=1,8
      M=IVCP(I,J)
      IF ((M.GT.L1).OR.(M.LT.L2)) GO TO 50
      DO 40 K=1,8
      N=IVCP(I,K)
      IF (N.LT.M) GO TO 40
      L=N-M+1
      KK=NEQB*L-(L1-M)
      AK(KK)=AK(KK)+PLK(J,K)
```

```
C
C     INTRODUCE KINEMATIC CONSTRAINTS (SUPPORTS BOUNDARY CONDITIONS)
C
      IF  ((N.EQ.NDF1).OR.(M.EQ.NDF1))    AK(KK)=0.0
      IF  ((N.EQ.NDF1).AND.(M.EQ.NDF1))   AK(KK)=1.0
      IF  ((N.EQ.NDF2).OR.(M.EQ.NDF2))    AK(KK)=0.0
      IF  ((N.EQ.NDF2).AND.(M.EQ.NDF2))   AK(KK)=1.0
      IF  ((N.EQ.NDF3).OR.(M.EQ.NDF3))    AK(KK)=0.0
      IF  ((N.EQ.NDF3).AND.(M.EQ.NDF3))   AK(KK)=1.0
C
   40 CONTINUE
   50 CONTINUE
   60 CONTINUE
C
C     LOOP OVER BEAM ELEMENTS IN THE X-DIRECTION
C
      KN=0
      DO 100 II=1,NB
      READ (NS) ((BXK(IO,JO),JO=1,6),IO=1,6)
      K1=KN*NX
      DO 90  JJ=1,NX
      I=K1+JJ
      DO 80 J=1,6
      M=IVCBX(I,J)
      IF ((M.GT.L1).OR.(M.LT.L2)) GO TO 80
      DO 70 K=1,6
      N=IVCBX(I,K)
      IF (N.LT.M) GO TO 70
      L=N-M+1
      KK=NEQB*L-(L1-M)
      AK(KK)=AK(KK)+BXK(J,K)
C
C     INTRODUCE KINEMATIC CONSTRAINTS (SUPPORTS BOUNDARY CONDITIONS)
C
      IF  ((N.EQ.NDF1).OR.(M.EQ.NDF1))   AK(KK)=0.0
      IF  ((N.EQ.NDF1).AND.(M.EQ.NDF1))  AK(KK)=1.0
      IF  ((N.EQ.NDF2).OR.(M.EQ.NDF2))   AK(KK)=0.0
      IF  ((N.EQ.NDF2).AND.(M.EQ.NDF2))  AK(KK)=1.0
      IF  ((N.EQ.NDF3).OR.(M.EQ.NDF3))   AK(KK)=0.0
      IF  ((N.EQ.NDF3).AND.(M.EQ.NDF3))  AK(KK)=1.0
C
   70 CONTINUE
   80 CONTINUE
   90 CONTINUE
      KN=KN+1
  100 CONTINUE
C
C     LOOP OVER BEAM ELEMENTS IN THE Y-DIRECTION
C
      READ  (NS) ((BYK(I,J),J=1,6),I=1,6)
      DO 130 I=1,NMBY
      DO 120 J=1,6
      M=IVCBY(I,J)
      IF ((M.GT.L1).OR.(M.LT.L2)) GO TO 120
      DO 110 K=1,6
      N=IVCBY(I,K)
      IF (N.LT.M) GO TO 110
      L=N-M+1
      KK=NEQB*L-(L1-M)
      AK(KK)=AK(KK)+BYK(J,K)
C
C     INTRODUCE KINEMATIC CONSTRAINTS (SUPPORTS BOUNDARY CONDITIONS)
C
      IF  ((N.EQ.NDF1).OR.(M.EQ.NDF1))   AK(KK)=0.0
      IF  ((N.EQ.NDF1).AND.(M.EQ.NDF1))  AK(KK)=1.0
      IF  ((N.EQ.NDF2).OR.(M.EQ.NDF2))   AK(KK)=0.0
      IF  ((N.EQ.NDF2).AND.(M.EQ.NDF2))  AK(KK)=1.0
      IF  ((N.EQ.NDF3).OR.(M.EQ.NDF3))   AK(KK)=0.0
      IF  ((N.EQ.NDF3).AND.(M.EQ.NDF3))  AK(KK)=1.0
C
  110 CONTINUE
  120 CONTINUE
  130 CONTINUE
C
```

```
C
C     LOOP OVER CONNECTOR ELEMENTS
C
      DO 160 I=1,NMC
      IF (I.EQ.1)  READ (NS) ((CONK(I1,J1),J1=1,4),I1=1,4)
C
      IF (I.EQ.N1) READ (NS) ((CONK(I1,J1),J1=1,4),I1=1,4)
      IF (I.EQ.N2) READ (NS) ((CONK(I1,J1),J1=1,4),I1=1,4)
      IF (I.EQ.N3) READ (NS) ((CONK(I1,J1),J1=1,4),I1=1,4)
C
      DO 150 J=1,4
      M=IVCC(I,J)
      IF ((M.GT.L1).OR.(M.LT.L2)) GO TO 150
      DO 140 K=1,4
      N=IVCC(I,K)
      IF (N.LT.M) GO TO 140
      L=N-M+1
      KK=NEQB*L-(L1-M)
      AK(KK)=AK(KK)+CONK(J,K)
C
C     INTRODUCE KINEMATIC CONSTRAINTS (SUPPORTS BOUNDARY CONDITIONS)
C
      IF  ((N.EQ.NDF3).OR.(M.EQ.NDF3))   AK(KK)=0.0
      IF  ((N.EQ.NDF3).AND.(M.EQ.NDF3))  AK(KK)=1.0
      IF  ((N.EQ.NDF2).OR.(M.EQ.NDF2))   AK(KK)=0.0
      IF  ((N.EQ.NDF2).AND.(M.EQ.NDF2))  AK(KK)=1.0
      IF  ((N.EQ.NDF1).OR.(M.EQ.NDF1))   AK(KK)=0.0
      IF  ((N.EQ.NDF1).AND.(M.EQ.NDF1))  AK(KK)=1.0
C
  140 CONTINUE
  150 CONTINUE
  160 CONTINUE
C
      IF ((NDFP.LE.L1).AND.(NDFP.GE.L2)) GO TO 170
      GO TO 180
  170 LLL=MA+1
      KKK=NEQB*LLL-(L1-NDFP)
      AK(KKK)= P
C
C     STORE ASSEMBELED STIFFNESS MATRIX AND LOAD VECTORS IN TAPE NSTIF
C
  180 WRITE (NSTIF) (AK(IJ),IJ=1,NVA1)
C
 1000 CONTINUE
C
      RETURN
      END
```

```
C
      SUBROUTINE SESOL (A,B,MAXA,NEQ,MA,NV,NBLOCK,NEQB,NAV,MI,NSTIF,
     1                  NRED,NL,NR)
C
C ****************************************************************
C *                                                              *
C *      SESOL IS AN EFFICIENT SUBROUTINE FOR THE SOLUTION OF    *
C *   LARGE NUMBERS OF SIMULTANEOUS LINEAR EQUATIONS ( K X = R ) .*
C *                                                              *
C *   WHERE :                                                    *
C *                                                              *
C *        K = POSITIVE DEFINITE MATRIX                          *
C *        R = SUPPLIED RIGHT HAND SIDE VECTORS                  *
C *        X = CALCULATED SOLUTION VECTORS                       *
C *                                                              *
C *   BASICALLY THE PROGRAM USES GAUSS ELEMINATION ON POSITIVE - *
C *   DEFINITE SYMMETRICAL SYSTEMS . THE SPECIFIC FEATURES ARE THAT*
C *   SYSTEMS OF VERY LARGE SIZES AND BANDWIDTH CAN BE SOLVED AND *
C *   THAT ALL OPERATIONS ON ZERO ELEMENTS ARE ELEMINATED .      *
C *                                                              *
C *        SESOL IS FULLY DESCRIBED AND DOCUMENTED IN REF.       *
C *                                                              *
C *   THE MATRIX [ K ] AND THE RIGHT HAND SIDE VECTORS ( R ) ARE *
C *   READ IN BLOCKS FROM TAPE .. NSTIF ..                       *
C *   THE SOLUTION VECTORS ( X ) ARE STORED IN BLOCKS IN REVERSE *
C *   ORDER ON TAPE .. NL ..                                     *
C *                                                              *
C ***************************  INPUTS  ***************************
C *                                                              *
C *     NEQ    =  NUMBER OF EQUATIONS                            *
C *                                                              *
C *     MA     =  MAXIMUM HALF BANDWIDTH OF [ K ] (INCLUDING DIAGONAL)*
C *                                                              *
C *     NV     =  NUMBER OF LOAD CASES                           *
C *                                                              *
C *     NBLOCK =  NUMBER OF BLOCKS                               *
C *                                                              *
C *     NEQB   =  NUMBER OF EQUATIONS IN EACH BLOCK              *
C *                                                              *
C *     NAV    =  NEQB*(MA+NV)                                   *
C *                                                              *
C *     MI     =  MA+NEQB-1                                      *
C *                                                              *
C *     NSTIF  =  TAPE ON WHICH THE STIFFNESS MATRIX IS STORED IN *
C *               BLOCKS                                         *
C *                                                              *
C *     NRED   =  TAPE ON WHICH THE DECOMPOSED STIFFNESS MATRIX AND *
C *               REDUCED LOAD VECTORS ARE STORED IN BLOCK FORM  *
C *                                                              *
C *     NL     =  TAPE ON WHICH THE SOLUTION OF EQUATIONS , I.E. *
C *               DISPLACEMENT VECTORS , STORED BLOCK-BY-BLOCK IN *
C *               IN SUCCESSION WITH THE LAST BLOCK FIRST        *
C *                                                              *
C *     NR     =  WORKING TAPE                                   *
C *                                                              *
C *     A,B,MAXA = HIGH_SPEED_STORAGE_ARRAYS                     *
C *                                                              *
C ****************************************************************
C
      DIMENSION A(NAV),B(NAV),MAXA(MI)
C
      MM=1
      MA2=MA-2
      IF (MA2.EQ.0) MA2=1
      INC=NEQB-1
      NVA=NEQB*MA
      NTB=(MA-2)/NEQB+1
      NEB=NTB*NEQB
      NEBT=NEB+NEQB
      NVV=NEQB*NV
      NVVV=NEBT*NV
C
      N1=NL
      N2=NR
      REWIND NSTIF
      REWIND NRED
      REWIND N1
      REWIND N2
```

```
C
C     *************************
C     MAIN LOOP OVER ALL BLOCKS
C     *************************
C
      DO 600 NJ=1,NBLOCK
      IF (NJ.NE.1) GO TO 10
      READ (NSTIF) A
      IF (NEQ.GT.1) GO TO 100
      MAXA(1)=1
      WRITE (NRED) A,MAXA
      IF (A(1)) 1,174,3
    1 KK=1
      WRITE (6,1010) KK,A(1)
    3 DO 5 L=1,NV
    5 A(1+L)=A(1+L)/A(1)
      KR=1+NV
      WRITE (NL) (A(KK),KK=2,KR)
      RETURN
   10 IF (NTB.EQ.1) GO TO 100
      REWIND N1
      REWIND N2
      READ (N1) A
C
C     ********************
C     FIND COLUMN HEIGHTS
C     ********************
C
  100 KU=1
      IF (MA-NEQB) 30,30,40
   30 KM=MA
      GO TO 50
   40 KM=NEQB
50    MAXA(1)=1
      DO 110 N=2,MI
      IF (N-MA) 120,120,130
  120 KU=KU+NEQB
      KK=KU
      IF (N-KM) 31,31,41
   31 MM=N
      GO TO 51
   41 MM=KM
   51 CONTINUE
      GO TO 140
  130 KU=KU+1
      KK=KU
      IF (N-NEQB) 140,140,136
  136 MM=MM-1
  140 DO 160 K=1,MM
      IF (A(KK)) 110,160,110
  160 KK=KK-INC
  110 MAXA(N)=KK
C
      IF (A(1)) 172,174,176
  174 KK=(NJ-1)*NEQB+1
      IF (KK.GT.NEQ) GO TO 590
      WRITE (6,1000) KK
      STOP
  172 KK=(NJ-1)*NEQB+1
      WRITE (6,1010) KK,A(1)
C
C     ************************
C     FACTORIZE LEADING BLOCK
C     ************************
C
  176 DO 200 N=2,NEQB
      NH=MAXA(N)
      IF (NH-N) 200,200,210
  210 KL=N+INC
      K=N
      D=0.0
      DO 220 KK=KL,NH,INC
      K=K-1
      C=A(KK)/A(K)
      D=D+C*A(KK)
  220 A(KK)=C
      A(N)=A(N)-D
C
      IF (A(N)) 222,224,230
  224 KK=(NJ-1)*NEQB+N
      IF (KK.GT.NEQ) GO TO 590
      WRITE (6,1000) KK
      STOP
  222 KK=(NJ-1)*NEQB+N
      WRITE (6,1010) KK,A(N)
C
  230 IC=NEQB
      DO 240 J=1,MA2
      MJ=MAXA(N+J)-IC
      IF (MJ-N) 240,240,280
  280 IF (MJ-NH) 32,32,42
   32 KU=MJ
      GO TO 52
   42 KU=NH
   52 KN=N+IC
      C=0.0
      DO 300 KK=KL,KU,INC
  300 C=C+A(KK)*A(KK+IC)
      A(KN)=A(KN)-C
  240 IC=IC+NEQB
C
      K=N+NUA
      DO 430 L=1,NU
      KJ=K
      C=0.0
      DO 440 KK=KL,NH,INC
      KJ=KJ-1
  440 C=C+A(KK)*A(KJ)
      A(K)=A(K)-C
  430 K=K+NEQB
C
  200 CONTINUE
C
C     *******************************
C     CARRY OVER INTO TRAILING BLOCKS
C     *******************************
C
      DO 400 NK=1,NTB
      IF ((NK+NJ).GT.NBLOCK) GO TO 400
      NI=N1
      IF ((NJ.EQ.1).OR.(NK.EQ.NTB)) NI=NSTIF
      READ (NI) B
      ML=NK*NEQB+1
      IF (((NK+1)*NEQB)-MI) 33,33,43
   33 MR=(NK+1)*NEQB
      GO TO 53
   43 MR=MI
   53 IF (MA.EQ.1) ML=MR
      MD=MI-ML
      KL=NEQB+(NK-1)*NEQB*NEQB
      N=1
C
      DO 500 M=ML,MR
      NH=MAXA(M)
      KL=KL+NEQB
      IF (NH-KL) 505,510,510
  510 K=NEQB
      D=0.0
      DO 520 KK=KL,NH,INC
      C=A(KK)/A(K)
      D=D+C*A(KK)
      A(KK)=C
  520 K=K-1
      B(N)=B(N)-D
      IF (MD) 580,580,530
  530 IC=NEQB
      DO 540 J=1,MD
      MJ=MAXA(M+J)-IC
      IF (MJ-KL) 540,550,550
 550  IF (MJ-NH) 34,34,44
   34 KU=MJ
      GO TO 54
   44 KU=NH
   54 KN=N+IC
      C=0.0
      DO 575 KK=KL,KU,INC
  575 C=C+A(KK)*A(KK+IC)
      B(KN)=B(KN)-C
  540 IC=IC+NEQB
```

```
C
  580 KN=N+NUA
      K=NEQB+NUA
      DO 610 L=1,NU
      KJ=K
      C=0.0
      DO 620 KK=KL,NH,INC
      C=C+A(KK)*A(KJ)
  620 KJ=KJ-1
      B(KN)=B(KN)-C
      KN=KN+NEQB
  610 K=K+NEQB
C
  505 MD=MD-1
  500 N=N+1
C
      IF (NTB.NE.1) GO TO 560
      WRITE (NRED) A,MAXA
      DO 570 I=1,NAV
  570 A(I)=B(I)
      GO TO 600
  560 WRITE (N2) B
C
  400 CONTINUE
C
      M=N1
      N1=N2
      N2=M
  590 WRITE (NRED) A,MAXA
C
  600 CONTINUE
C
C     ***********************
C     VECTOR BACKSUBSTITUTION
C     ***********************
C
      DO 700 K=1,NUUV
  700 B(K)=0.0
      REWIND NL
C
      DO 800 NJ=1,NBLOCK
      BACKSPACE NRED
      READ (NRED) A,MAXA
      BACKSPACE NRED
      K=NEBT
      DO 810 L=1,NU
      DO 820 I=1,NEB
      B(K)=B(K-NEQB)
  820 K=K-1
  810 K=K+NEBT+NEB
      KN=0
      KK=NUA
      NDIF=NEQB
      IF (NJ.EQ.1) NDIF=NEQB-(NBLOCK*NEQB-NEQ)
      DO 855 L=1,NU
      DO 850 K=1,NDIF
  850 B(KN+K)=A(KK+K)/A(K)
      KK=KK+NEQB
  855 KN=KN+NEBT
      IF (MA.EQ.1) GO TO 915
      ML=NEQB+1
      KL=NEQB
      DO 860 M=ML,MI
      KL=KL+NEQB
      KU=MAXA(M)
      IF (KU-KL) 860,870,870
  870 K=NEQB
      KM=M
      DO 880 L=1,NU
      KJ=K
      DO 890 KK=KL,KU,INC
      B(KJ)=B(KJ)-A(KK)*B(KM)
  890 KJ=KJ-1
      KM=KM+NEBT
  880 K=K+NEBT
  860 CONTINUE
```

```
      N=NEQB
      DO 910 I=2,NEQB
      KL=N+INC
      KU=MAXA(N)
      IF (KU-KL) 910,920,920
  920 K=N
      DO 930 L=1,NV
      KJ=K
      DO 940 KK=KL,KU,INC
      KJ=KJ-1
  940 B(KJ)=B(KJ)-A(KK)*B(K)
  930 K=K+NEBT
  910 N=N-1
C
  915 KK=0
      KN=0
      DO 950 L=1,NV
      DO 960 K=1,NEQB
      KK=KK+1
  960 A(KK)=B(KN+K)
  950 KN=KN+NEBT
C
      WRITE (NL) (A(K),K=1,NWV)
  800 CONTINUE.
C
 1000 FORMAT (// 46H   STOP  ***  ZERO DIAGONAL ENCOUNTERED DURING,
     1              18H EQUATION SOLUTION, /
     2          13X,18H EQUATION NUMBER =, I6 )
 1010 FORMAT (/  50H WARNING ***  NEGATIVE DIAGONAL ENCOUNTERED DURING,
     1              18H EQUATION SOLUTION, /
     2          13X,18H EQUATION NUMBER =, I6, 5X, 7HVALUE =,E20.8)
C
      RETURN
      END
C
```

```
C
      SUBROUTINE FORCE(NDF,NMP,NMBX,NMBY,NMC,U,IVCP,IVCBX,IVCBY,IVCC,NS)
C
C  *********************************************************************
C  *                                                                   *
C  *     SUBROUTINE FORCE CALCULATES ELEMENT'S NODAL FORCES . FIRST    *
C  *  ELEMENT'S NODAL DISPLACEMENTS VECTOR IS EXTRACTED FROM THE GLOBAL*
C  *  DISPLACEMENT VECTOR ( SOLUTION OF EQUILIBRIUM EQUATIONS ) . THEN *
C  *  MULTIPLIED BY THE ELEMENT'S STIFFNESS MATRIX GIVES NODAL FORCES .*
C  *                                                                   *
C  *********************************************************************
C
      COMMON/BLK1/ NEND,NSIDE,NSEAM,NCTS,NGIRT,NX,NDF1,NDF2,NDF3
      COMMON/BLK2/PLK(8,8)
      COMMON/BLK3/BXK(6,6)
      COMMON/BLK4/BYK(6,6)
      COMMON/BLK5/CONK(4,4)
      DIMENSION IVCP(NMP,8),IVCBX(NMBX,6),IVCBY(NMBY,6),IVCC(NMC,4)
      DIMENSION U(NDF)
      DIMENSION UP(8),UBX(6),UBY(6),UC(4),FP(8),FBX(6),FBY(6),FC(4)
C
      NB=NGIRT+2
      N1=NEND+1
      N2=NEND+NSIDE+1
      N3=NEND+NSIDE+NSEAM+1
C
      REWIND NS
C
      WRITE (6,10)
   10 FORMAT('1',5X,'NODAL  FORCES  OF  PLATE  ELEMENTS..............'//
     15X,'ELEMENT NO',6X,'U1  (1)',6X,'V1  (2)',6X,'U2  (3)',6X,'V2  (4)
     2',6X,'U3  (5)',6X,'V3  (6)',6X,'U4  (7)',6X,'V4  (8)')
C
      READ  (NS) ((PLK(I,J),J=1,8),I=1,8)
C
C     LOOP OVER PLATE ELEMENTS
C
      DO 50 I=1,NMP
      DO 20 J=1,8
      M=IVCP(I,J)
      UP(J)=U(M)
   20 CONTINUE
      DO 30 J=1,8
      FP(J)=0.0
      DO 30 K=1,8
   30 FP(J)=FP(J)+PLK(J,K)*UP(K)
      WRITE (6,40) I,(FP(J),J=1,8)
   40 FORMAT('0',7X,I3,8F14.5)
   50 CONTINUE
C
      WRITE (6,60)
   60 FORMAT('1',5X,'NODAL FORCES OF BEAM ELEMENTS IN THE X-DIRECTION'//
     15X,'ELEMENT NO',6X,'U1  (1)',6X,'V1  (2)',6X,'01  (3)',6X,'U2  (4)
     2',6X,'V2  (5)',6X,'02  (6)')
C
C     LOOP OVER BEAM ELEMENTS IN THE X-DIRECTION
C
      KN=0
      DO 110 II=1,NB
C
      WRITE (6,65) II
   65 FORMAT(///34X,'*****  BEAM  NO.  ',I2,2X,'*****'///)
      READ (NS) ((BXK(IO,JO),JO=1,6),IO=1,6)
      KK=KN*NX
      DO 100 JJ=1,NX
      I=KK+JJ
      DO 70 J=1,6
      M=IVCBX(I,J)
      UBX(J)=U(M)
   70 CONTINUE
      DO 80 J=1,6
      FBX(J)=0.0
      DO 80 K=1,6
   80 FBX(J)=FBX(J)+BXK(J,K)*UBX(K)
      WRITE (6,90) I,(FBX(J),J=1,6)
   90 FORMAT('0',7X,I3,6F14.5)
  100 CONTINUE
      KN=KN+1
  110 CONTINUE
```

```
C
      WRITE (6,120)
  120 FORMAT('1',5X,'NODAL FORCES OF BEAM ELEMENTS IN THE Y-DIRECTION'//
     15X,'ELEMENT NO',6X,'U1  (1)',6X,'V1  (2)',6X,'01  (3)',6X,'U2  (4)
     2',6X,'V2  (5)',6X,'02  (6)')
C
C     LOOP OVER BEAM ELEMENTS IN THE Y-DIRECTION
C
      READ  (NS) ((BYK(I,J),J=1,6),I=1,6)
      DO 150 I=1,NMBY
      DO 130 J=1,6
      M=IVCBY(I,J)
      UBY(J)=U(M)
  130 CONTINUE
      DO 140 J=1,6
      FBY(J)=0.0
      DO 140 K=1,6
  140 FBY(J)=FBY(J)+BYK(J,K)*UBY(K)
      WRITE (6,90) I,(FBY(J),J=1,6)
  150 CONTINUE
C
      WRITE (6,160)
  160 FORMAT('1',5X,'NODAL FORCES OF CONNECTION ELEMENTS.............'//
     15X,'ELEMENT NO',6X,'U1  (1)',6X,'U2  (2)',6X,'V1  (3)',6X,'V2  (4)
     2')
C
C     LOOP OVER CONNECTOR ELEMENTS
C
      DO 240 I=1,NMC
C
      IF (I.EQ.1 ) WRITE (6,170)
      IF (I.EQ.N1) WRITE (6,180)
      IF (I.EQ.N2) WRITE (6,190)
      IF (I.EQ.N3) WRITE (6,200)
C
  170 FORMAT (///18X,'*****  END  CONNECTIONS  *****'///)
  180 FORMAT (///18X,'*****  SIDE CONNECTIONS  *****'///)
  190 FORMAT (///18X,'*****  SEAM CONNECTIONS  *****'///)
  200 FORMAT (///11X,'****  SHEET-TO-PURLINS  CONNECTIONS  ****'///)
C
      IF (I.EQ.1)  READ (NS) ((CONK(I1,J1),J1=1,4),I1=1,4)
      IF (I.EQ.N1) READ (NS) ((CONK(I1,J1),J1=1,4),I1=1,4)
      IF (I.EQ.N2) READ (NS) ((CONK(I1,J1),J1=1,4),I1=1,4)
      IF (I.EQ.N3) READ (NS) ((CONK(I1,J1),J1=1,4),I1=1,4)
C
      DO 210 J=1,4
      M=IVCC(I,J)
      UC(J)=U(M)
  210 CONTINUE
C
      DO 220 J=1,4
      FC(J)=0.0
      DO 220 K=1,4
      FC(J)=FC(J)+CONK(J,K)*UC(K)
  220 CONTINUE
      WRITE (6,230) I,(FC(J),J=1,4)
  230 FORMAT('0',7X,I3,4F14.5)
  240 CONTINUE
C
      RETURN
      END
```

```
1 FINITE ELEMENT PROGRAM FOR THE LINEAR ELASTIC ANALYSIS
  OF PLANE RECTANGULAR SHEAR DIAPHRAGMS ....


  SAMPLE EXAMPLE  :  ANALYSIS OF CAVITY DECK DIAPHRAGM OF TEST C-2


  LOAD IS APPLIED IN DIRECTION PARALLEL TO THE CORRUGATIONS


     INPUT  DATA ....... BASIC  PARAMETERS .........

     TOTAL NUMBER OF PLATE ELEMENTS...................   108
     TOTAL NUMBER OF BEAM ELEMENTS IN X-DIRECTION .....    36
     TOTAL NUMBER OF BEAM ELEMENTS IN Y-DIRECTION .....    12
     TOTAL NUMBER OF CONNECTOR ELEMENTS ...............    64
     NUMBER  OF  LOAD  CASES ..........................     1
     APPLIED JACK LOAD AT DIAPHRAGM END ............   1000.00000


     INPUT VARIABLES FOR THE AUTOMATIC F.E. GRID GENERATION


     NPANEL  =    9
     NMPPX   =    2
     NMPPY   =    6
     NY      =    6
     NX      =   18
     NGIRT   =    0

     NCTS    =    3
     NEND    =   14
     NSIDE   =   10
     NSEAM   =   40
     NCPS    =    5
     NCGIRT  =    0
```

```
1                            GENERATED  CONNECTIVITY  MATRIX  (PLATE ELEMENTS) (IUCP)
0           ELEMENT NO    U1   (1)     V1   (2)     U2   (3)     V2   (4)     U3   (5)     V3   (6)     U4   (7)     V4   (8)
0                1             24           25           41           42           43           44           26           27
0                2             41           42           61           62           63           64           43           44
0                3             78           79           95           96           97           98           80           81
0                4             95           96          115          116          117          118           97           98
0                5            132          133          149          150          151          152          134          135
0                6            149          150          169          170          171          172          151          152
0                7            186          187          203          204          205          206          188          189
0                8            203          204          223          224          225          226          205          206
0                9            240          241          257          258          259          260          242          243
0               10            257          258          277          278          279          280          259          260
0               11            294          295          311          312          313          314          296          297
0               12            311          312          331          332          333          334          313          314
0               13            348          349          365          366          367          368          350          351
0               14            365          366          385          386          387          388          367          368
0               15            402          403          419          420          421          422          404          405
0               16            419          420          439          440          441          442          421          422
0               17            456          457          473          474          475          476          458          459
0               18            473          474          490          491          492          493          475          476
0               19             26           27           43           44           45           46           28           29
0               20             43           44           63           64           65           66           45           46
0               21             80           81           97           98           99          100           82           83
0               22             97           98          117          118          119          120           99          100
0               23            134          135          151          152          153          154          136          137
0               24            151          152          171          172          173          174          153          154
0               25            188          189          205          206          207          208          190          191
0               26            205          206          225          226          227          228          207          208
0               27            242          243          259          260          261          262          244          245
0               28            259          260          279          280          281          282          261          262
0               29            296          297          313          314          315          316          298          299
0               30            313          314          333          334          335          336          315          316
0               31            350          351          367          368          369          370          352          353
0               32            367          368          387          388          389          390          369          370
0               33            404          405          421          422          423          424          406          407
0               34            421          422          441          442          443          444          423          424
0               35            458          459          475          476          477          478          460          461
0               36            475          476          492          493          494          495          477          478
0               37             28           29           45           46           47           48           30           31
0               38             45           46           65           66           67           68           47           48
0               39             82           83           99          100          101          102           84           85
0               40             99          100          119          120          121          122          101          102
0               41            136          137          153          154          155          156          138          139
0               42            153          154          173          174          175          176          155          156
0               43            190          191          207          208          209          210          192          193
0               44            207          208          227          228          229          230          209          210
0               45            244          245          261          262          263          264          246          247
0               46            261          262          281          282          283          284          263          264
0               47            298          299          315          316          317          318          300          301
0               48            315          316          335          336          337          338          317          318
0               49            352          353          369          370          371          372          354          355
0               50            369          370          389          390          301          392          371          372
0               51            406          407          423          424          425          426          408          409
0               52            423          424          443          444          445          446          425          426
0               53            460          461          477          478          479          480          462          463
0               54            477          478          494          495          496          497          479          480
0               55             30           31           47           48           49           50           32           33
0               56             47           48           67           68           69           70           49           50
```

```
0      57     84    85   101   102   103   104    86    87
0      58    101   102   121   122   123   124   103   104
0      59    138   139   155   156   157   158   140   141
0      60    155   156   175   176   177   178   157   158
0      61    192   193   209   210   211   212   194   195
0      62    209   210   229   230   231   232   211   212
0      63    246   247   263   264   265   266   248   249
0      64    263   264   283   284   285   286   265   266
0      65    300   301   317   318   319   320   302   303
0      66    317   318   337   338   339   340   319   320
0      67    354   355   371   372   373   374   356   357
0      68    371   372   391   392   393   394   373   374
0      69    408   409   425   426   427   428   410   411
0      70    425   426   445   446   447   448   427   428
0      71    462   463   479   480   481   482   464   465
0      72    479   480   496   497   498   499   481   482
0      73     32    33    49    50    51    52    34    35
0      74     49    50    69    70    71    72    51    52
0      75     86    87   103   104   105   106    88    89
0      76    103   104   123   124   125   126   105   106
0      77    140   141   157   158   159   160   142   143
0      78    157   158   177   178   179   180   159   160
0      79    194   195   211   212   213   214   196   197
0      80    211   212   231   232   233   234   213   214
0      81    248   249   265   266   267   268   250   251
0      82    265   266   285   286   287   288   267   268
0      83    302   303   319   320   321   322   304   305
0      84    319   320   339   340   341   342   321   322
0      85    356   357   373   374   375   376   358   359
0      86    373   374   393   394   395   396   375   376
0      87    410   411   427   428   429   430   412   413
0      88    427   428   447   448   449   450   429   430
0      89    464   465   481   482   483   484   466   467
0      90    481   482   498   499   500   501   483   484
0      91     34    35    51    52    53    54    36    37
0      92     51    52    71    72    73    74    53    54
0      93     88    89   105   106   107   108    90    91
0      94    105   106   125   126   127   128   107   108
0      95    142   143   159   160   161   162   144   145
0      96    159   160   179   180   181   182   161   162
0      97    196   197   213   214   215   216   198   199
0      98    213   214   233   234   235   236   215   216
0      99    250   251   267   268   269   270   252   253
0     100    267   268   287   288   289   290   269   270
0     101    304   305   321   322   323   324   306   307
0     102    321   322   341   342   343   344   323   324
0     103    358   359   375   376   377   378   360   361
0     104    375   376   395   396   397   398   377   378
0     105    412   413   429   430   431   432   414   415
0     106    429   430   449   450   451   452   431   432
0     107    466   467   483   484   485   486   468   469
0     108    483   484   500   501   502   503   485   486
```

```
1         GENERATED  CONNECTIVITY MATRIX (BEAM ELEMENTS IN X)  (IVCBX)
0       ELEMENT NO    U1  (1)     V1  (2)    01  (3)    U2  (4)    V2  (5)    02  (6)
0            1             1          2         23         38         39         40
0            2            38         39         40         58         59         60
0            3            58         59         60         92         93         94
0            4            92         93         94        112        113        114
0            5           112        113        114        146        147        148
0            6           146        147        148        166        167        168
0            7           166        167        168        200        201        202
0            8           200        201        202        220        221        222
0            9           220        221        222        254        255        256
0           10           254        255        256        274        275        276
0           11           274        275        276        308        309        310
0           12           308        309        310        328        329        330
0           13           328        329        330        362        363        364
0           14           362        363        364        382        383        384
0           15           382        383        384        416        417        418
0           16           416        417        418        436        437        438
0           17           436        437        438        470        471        472
0           18           470        471        472        504        505        506
0           19            19         20         22         55         56         57
0           20            55         56         57         75         76         77
0           21            75         76         77        109        110        111
0           22           109        110        111        129        130        131
0           23           129        130        131        163        164        165
0           24           163        164        165        183        184        185
0           25           183        184        185        217        218        219
0           26           217        218        219        237        238        239
0           27           237        238        239        271        272        273
0           28           271        272        273        291        292        293
0           29           291        292        293        325        326        327
0           30           325        326        327        345        346        347
0           31           345        346        347        379        380        381
0           32           379        380        381        399        400        401
0           33           399        400        401        433        434        435
0           34           433        434        435        453        454        455
0           35           453        454        455        487        488        489
0           36           487        488        489        522        523        524
```

```
1              GENERATED  CONNECTIVITY MATRIX (BEAM ELEMENTS IN Y)  (IVCBY)
0           ELEMENT NO    U1   (1)    V1   (2)    01   (3)    U2   (4)    V2   (5)    02   (6)
0                1             1             2             3             4             5             6
0                2             4             5             6             7             8             9
0                3             7             8             9            10            11            12
0                4            10            11            12            13            14            15
0                5            13            14            15            16            17            18
0                6            16            17            18            19            20            21
0                7           504           505           526           507           508           509
0                8           507           508           509           510           511           512
0                9           510           511           512           513           514           515
0               10           513           514           515           516           517           518
0               11           516           517           518           519           520           521
0               12           519           520           521           522           523           525
```

```
GENERATED  CONNECTIVITY MATRIX (CONNECTOR  ELEMENTS)  (IVCC)
   ELEMENT NO     U1  (1)     U2  (2)     V1  (3)     U2  (4)


                 *****  END  CONNECTIONS  *****

        1          92          95          93          96
        2         146         149         147         150
        3         200         203         201         204
        4         254         257         255         258
        5         308         311         309         312
        6         362         365         363         366
        7         416         419         417         420
        8         109         107         110         108
        9         163         161         164         162
       10         217         215         218         216
       11         271         269         272         270
       12         325         323         326         324
       13         379         377         380         378
       14         433         431         434         432


                 *****  SIDE CONNECTIONS  *****

       15           4          26           5          27
       16           7          28           8          29
       17          10          30          11          31
       18          13          32          14          33
       19          16          34          17          35
       20         507         492         508         493
       21         510         494         511         495
       22         513         496         514         497
       23         516         498         517         499
       24         519         500         520         501


                 *****  SEAM CONNECTIONS  *****

       25          63          80          64          81
       26          65          82          66          83
       27          67          84          68          85
       28          69          86          70          87
       29          71          88          72          89
       30         117         134         118         135
       31         119  [illegible]         120         137
       32         121         138         122         139
       33         123         140         124         141
       34         125         142         126         143
       35         171         188         172         189
       36         173         190         174         191
       37         175         192         176         193
       38         177         194         178         195
       39         179         196         180         197
```

```
0                40       225    242    226    243
0                41       227    244    228    245
0                42       229    246    230    247
0                43       231    248    232    249
0                44       233    250    234    251
0                45       279    296    280    297
0                46       281    298    282    299
0                47       283    300    284    301
0                48       285    302    286    303
0                49       287    304    288    305
0                50       333    350    334    351
0                51       335    352    336    353
0                52       337    354    338    355
0                53       339    356    340    357
0                54       341    358    342    359
0                55       387    404    388    405
0                56       389    406    390    407
0                57       391    408    392    409
0                58       393    410    394    411
0                59       395    412    396    413
0                60       441    458    442    459
0                61       443    460    4[illegible]    461
0                62       445    462    446    463
0                63       447    464    448    465
0                64       449    466    450    467

         CONSTRAINED  DISPLACEMENT  DEGREES  OF  FREEDOM

               D.O.F.      1   FOR ROLLER SUPPORT

               D.O.F.     19   FOR HINGE  SUPPORT

               D.O.F.     20   FOR HINGE  SUPPORT

         D.O.F. AT WHICH THE JACK LOAD IS APPLIED   505

         D.O.F. AT DIAPHRAGM TIP IN LOAD DIRECTION  523

         TOTAL  NUMBER  OF DEGREES  OF  FREEDOM     526

         MAXIMUM HALF-BANDWIDTH  (INCL. DIAGONAL)    40
```

```
1     PROPERTIES  OF  PLATE  ELEMENTS  .............

     POISSONS  RATIO  (NUXY)........................     .15000
     POISSONS  RATIO  (NUYX)........................     .20000
     LENGTH  OF  ELEMENT  SIDE  IN THE X-DIRECTION..     7.5000
     LENGTH  OF  ELEMENT  SIDE  IN THE Y-DIRECTION..    20.0000
     ELASTIC  MODULUS  IN THE X-DIRECTION...........  1700000.00000
     ELASTIC  MODULUS  IN THE Y-DIRECTION...........  2250000.00000
     THICKNESS  OF  THE  ELEMENT....................     .37500
     SHEAR  MODULUS  OF  THE  ELEMENT...............   900000.00000
-     PROPERTIES OF BEAM ELEMENTS IN THE X-DIRECTION..

     FOR MEMBER NO. *************    1    ************

     LENGTH  OF  THE  BEAM  ELEMENT.................     7.5000
     MOMENT  OF  INERTIA  ABOUT THE AXIS OF BENDING.    10.8000
     CROSS  SECTIONAL  AREA  OF  THE  BEAM..........     6.2000
     ELASTIC  MODULUS  OF  THE  BEAM  MATERIAL...... 30000000.00000
-     PROPERTIES OF BEAM ELEMENTS IN THE X-DIRECTION..

     FOR MEMBER NO. *************    2    ************

     LENGTH  OF  THE  BEAM  ELEMENT.................     7.5000
     MOMENT  OF  INERTIA  ABOUT THE AXIS OF BENDING.    10.8000
     CROSS  SECTIONAL  AREA  OF  THE  BEAM..........     6.2000
     ELASTIC  MODULUS  OF  THE  BEAM  MATERIAL...... 30000000.00000
-     PROPERTIES OF BEAM ELEMENTS IN THE Y-DIRECTION..

     LENGTH  OF  THE  BEAM  ELEMENT.................    20.0000
     MOMENT  OF  INERTIA  ABOUT THE AXIS OF BENDING.    10.8000
     CROSS  SECTIONAL  AREA  OF  THE  BEAM..........     6.2000
     ELASTIC  MODULUS  OF  THE  BEAM  MATERIAL...... 30000000.00000
-     SPRING  COEFFICENTS  OF  CONNECTOR  ELEMENTS....

     TYPE NO. ******************    1    *************

     SPRING  COEFFICENT   IN  THE  X-DIRECTION......    28000.00000
     SPRING  COEFFICENT   IN  THE  Y-DIRECTION......    28000.00000
-     SPRING  COEFFICENTS  OF  CONNECTOR  ELEMENTS....

     TYPE NO. ******************    2    *************

     SPRING  COEFFICENT   IN  THE  X-DIRECTION......    28000.00000
     SPRING  COEFFICENT   IN  THE  Y-DIRECTION......    28000.00000
-     SPRING  COEFFICENTS  OF  CONNECTOR  ELEMENTS....

     TYPE NO. ******************    3    *************

     SPRING  COEFFICENT   IN  THE  X-DIRECTION......     6720.00000
     SPRING  COEFFICENT   IN  THE  Y-DIRECTION......     8400.00000
```

```
1                                   DISPLACEMENTS AT EACH CORRESPONDING D.O.F.

DOF   1  0.            DOF   2   .320402E-03   DOF   3  -.124279E-03   DOF   4   .202094E-02   DOF   5   .322027E-03
DOF   6  -.945829E-04  DOF   7   .187260E-02   DOF   8   .302673E-03   DOF   9   .617204E-04   DOF  10   .156063E-04
DOF  11   .260959E-03  DOF  12   .108502E-03   DOF  13  -.184739E-02   DOF  14   .196209E-03   DOF  15   .622708E-04
DOF  16  -.200883E-02  DOF  17   .108851E-03   DOF  18  -.539190E-04   DOF  19  0.            DOF  20  0.
DOF  21  -.123703E-03  DOF  22  -.164754E-02   DOF  23  -.163791E-02   DOF  24   .130373E-01   DOF  25   .728680E-02
DOF  26   .738928E-02  DOF  27   .729022E-02   DOF  28   .322315E-02   DOF  29   .772973E-02   DOF  30   .241658E-04
DOF  31   .791167E-02  DOF  32  -.318977E-02   DOF  33   .770559E-02   DOF  34  -.739896E-02   DOF  35   .724757E-02
DOF  36  -.131073E-01  DOF  37   .724537E-02   DOF  38   .408102E-04   DOF  39   .126080E-01   DOF  40  -.163922E-02
DOF  41   .129970E-01  DOF  42   .938600E-02   DOF  43   .748005E-02   DOF  44   .936591E-02   DOF  45   .320905E-02
DOF  46   .933630E-02  DOF  47   .249311E-04   DOF  48   .933031E-02   DOF  49  -.317441E-02   DOF  50   .932508E-02
DOF  51  -.748962E-02  DOF  52   .934771E-02   DOF  53  -.130669E-01   DOF  54   .936650E-02   DOF  55  -.408044E-04
DOF  56   .123592E-01  DOF  57  -.164861E-02   DOF  58   .816203E-04   DOF  59   .249152E-01   DOF  60  -.164316E-02
DOF  61   .129853E-01  DOF  62   .114384E-01   DOF  63   .750973E-02   DOF  64   .114477E-01   DOF  65   .322843E-02
DOF  66   .109573E-01  DOF  67   .251284E-04   DOF  68   .107390E-01   DOF  69  -.319366E-02   DOF  70   .109581E-01
DOF  71  -.751917E-02  DOF  72   .114502E-01   DOF  73  -.130550E-01   DOF  74   .114422E-01   DOF  75  -.816088E-04
DOF  76   .247345E-01  DOF  77  -.165182E-02   DOF  78   .512628E-02   DOF  79   .363503E-01   DOF  80   .441431E-02
DOF  81   .358274E-01  DOF  82   .252835E-02   DOF  83   .354521E-01   DOF  84   .807881E-05   DOF  85   .353239E-01
DOF  86  -.251452E-02  DOF  87   .354463E-01   DOF  88  -.440690E-02   DOF  89   .358161E-01   DOF  90  -.512464E-02
DOF  91   .363357E-01  DOF  92   .122430E-03   DOF  93   .372619E-01   DOF  94  -.164972E-02   DOF  95   .508638E-02
DOF  96   .365757E-01  DOF  97   .443613E-02   DOF  98   .365391E-01   DOF  99   .253397E-02   DOF 100   .365192E-01
DOF 101   .823735E-05  DOF 102   .365075E-01   DOF 103  -.251995E-02   DOF 104   .365149E-01   DOF 105  -.442800E-02
DOF 106   .365306E-01  DOF 107  -.508485E-02   DOF 108   .365610E-01   DOF 109  -.122413E-03   DOF 110   .371418E-01
DOF 111  -.165716E-02  DOF 112   .157636E-03   DOF 113   .496634E-01   DOF 114  -.165724E-02   DOF 115   .513535E-02
DOF 116   .367758E-01  DOF 117   .440800E-02   DOF 118   .372560E-01   DOF 119   .252866E-02   DOF 120   .375776E-01
DOF 121   .835482E-05  DOF 122   .376856E-01   DOF 123  -.251449E-02   DOF 124   .375749E-01   DOF 125  -.439126E-02
DOF 126   .372494E-01  DOF 127  -.513385E-02   DOF 128   .367661E-01   DOF 129  -.157615E-03   DOF 130   .495937E-01
DOF 131  -.166323E-02  DOF 132   .473084E-02   DOF 133   .617314E-01   DOF 134   .394634E-02   DOF 135   .612721E-01
DOF 136   .222670E-02  DOF 137   .609951E-01   DOF 138   .420617E-05   DOF 139   .609045E-01   DOF 140  -.221923E-02
DOF 141   .600332E-01  DOF 142  -.394160E-02   DOF 143   .6[illegible]5E-01   DOF 144  -.472945E-02   DOF 145   .617269E-01
DOF 146   .192842E-03  DOF 147   .621186E-01   DOF 148  -.166404E-02   DOF 149   .469002E-02   DOF 150   .619750E-01
DOF 151   .397429E-02  DOF 152   .619674E-01   DOF 153   .222899E-02   DOF 154   .619646E-01   DOF 155   .425370E-05
DOF 156   .619633E-01  DOF 157  -.222145E-02   DOF 158   .619635E-01   DOF 159  -.396939E-02   DOF 160   .619651E-01
DOF 161  -.468866E-02  DOF 162   .619712E-01   DOF 163  -.192817E-03   DOF 164   .620886E-01   DOF 165  -.166862E-02
DOF 166   .222970E-03  DOF 167   .746214E-01   DOF 168  -.166979E-02   DOF 169   .473197E-02   DOF 170   .622130E-01
DOF 171   .394490E-02  DOF 172   .626629E-01   DOF 173   .222552E-02   DOF 174   .629332E-01   DOF 175   .427767E-05
DOF 176   .630214E-01  DOF 177  -.221797E-02   DOF 178   .629327E-01   DOF 179  -.393987E-02   DOF 180   .626617E-01
DOF 181  -.473060E-02  DOF 182   .622111E-01   DOF 183  -.222942E-03   DOF 184   .746206E-01   DOF 185  -.167303E-02
DOF 186   .470348E-02  DOF 187   .869049E-01   DOF 188   .389103E-02   DOF 189   .864589E-01   DOF 190   .218221E-02
DOF 191   .861985E-01  DOF 192   .191981E-05   DOF 193   .861154E-01   DOF 194  -.217881E-02   DOF 195   .861989E-01
DOF 196  -.388974E-02  DOF 197   .864598E-01   DOF 198  -.470286E-02   DOF 199   .869062E-01   DOF 200   .253098E-03
DOF 201   .871620E-01  DOF 202  -.167413E-02   DOF 203   .466280E-02   DOF 204   .871567E-01   DOF 205   .391936E-02
DOF 206   .871565E-01  DOF 207   .218481E-02   DOF 208   .871566E-01   DOF 209   .188689E-05   DOF 210   .871569E-01
DOF 211  -.218146E-02  DOF 212   .871573E-01   DOF 213  -.391717E-02   DOF 214   .871579E-01   DOF 215  -.466218E-02
DOF 216   .871591E-01  DOF 217  -.253068E-03   DOF 218   .871809E-01   DOF 219  -.167619E-02   DOF 220   .278246E-03
DOF 221   .997298E-01  DOF 222  -.167705E-02   DOF 223   .470356E-02   DOF 224   .874084E-01   DOF 225   .389068E-02
DOF 226   .878540E-01  DOF 227   .218201E-02   DOF 228   .881147E-01   DOF 229   .184316E-05   DOF 230   .881984E-01
DOF 231  -.217872E-02  DOF 232   .881157E-01   DOF 233  -.388880E-02   DOF 234   .878560E-01   DOF 235  -.470292E-02
DOF 236   .874110E-01  DOF 237  -.278216E-03   DOF 238   .997602E-01   DOF 239  -.167804E-02   DOF 240   .474052E-02
DOF 241   .112068E+00  DOF 242   .390920E-02   DOF 243   .111624E+00   DOF 244   .218776E-02   DOF 245   .111366E+00
DOF 246   .786976E-07  DOF 247   .111284E+00   DOF 248  -.218764E-02   DOF 249   .111367E+00   DOF 250  -.390898E-02
DOF 251   .111627E+00  DOF 252  -.474051E-02   DOF 253   .112071E+00   DOF 254   .303397E-03   DOF 255   .112314E+00
DOF 256  -.167853E-02  DOF 257   .469984E-02   DOF 258   .112327E+00   DOF 259   .393766E-02   DOF 260   .112327E+00
DOF 261   .219045E-02  DOF 262   .112328E+00   DOF 263   .169624E-07   DOF 264   .112328E+00   DOF 265  -.219841E-02
DOF 266   .112329E+00  DOF 267  -.393763E-02   DOF 268   .112330E+00   DOF 269  -.469980E-02   DOF 270   .112331E+00
DOF 271  -.303363E-03  DOF 272   .112348E+00   DOF 273  -.167853E-02   DOF 274   .323503E-03   DOF 275   .124704E+00
DOF 276  -.167860E-02  DOF 277   .474039E-02   DOF 278   .112586E+00   DOF 279   .390939E-02   DOF 280   .113031E+00
DOF 281   .218778E-02  DOF 282   .113290E+00   DOF 283  -.447727E-07   DOF 284   .113373E+00   DOF 285  -.218783E-02
DOF 286   .113291E+00  DOF 287  -.390953E-02   DOF 288   .113033E+00   DOF 289  -.474034E-02   DOF 290   .112589E+00
DOF 291  -.323547E-03  DOF 292   .124935E+00   DOF 293  -.167761E-02   DOF 294   .479248E-02   DOF 295   .137243E+00
DOF 296   .394782E-02   DOF 297   .136798E+00   DOF 298   .220826E-02   DOF 299   .136538E+00   DOF 300  -.180924E-05
DOF 301   .136455E+00   DOF 302  -.221148E-02   DOF 303   .136539E+00   DOF 304  -.394983E-02   DOF 305   .136800E+00
DOF 306  -.479305E-02   DOF 307   .137245E+00   DOF 308   .343769E-03   DOF 309   .137490E+00   DOF 310  -.167730E-02
DOF 311   .475160E-02   DOF 312   .137506E+00   DOF 313   .397656E-02   DOF 314   .137507E+00   DOF 315   .221110E-02
DOF 316   .137507E+00   DOF 317  -.185297E-05   DOF 318   .137508E+00   DOF 319  -.221439E-02   DOF 320   .137508E+00
DOF 321  -.397868E-02   DOF 322   .137508E+00   DOF 323  -.475215E-02   DOF 324   .137509E+00   DOF 325  -.343731E-03
DOF 326   .137509E+00   DOF 327  -.167524E-02   DOF 328   .358978E-03   DOF 329   .150060E+00   DOF 330  -.167467E-02
DOF 331   .479212E-02   DOF 332   .137770E+00   DOF 333   .394850E-02   DOF 334   .138216E+00   DOF 335   .220856E-02
DOF 336   .138477E+00   DOF 337  -.188589E-05   DOF 338   .138560E+00   DOF 339  -.221188E-02   DOF 340   .138477E+00
DOF 341  -.395072E-02   DOF 342   .138217E+00   DOF 343  -.479267E-02   DOF 344   .137772E+00   DOF 345  -.358938E-03
DOF 346   .150060E+00   DOF 347  -.167143E-02   DOF 348   .490938E-02   DOF 349   .162455E+00   DOF 350   .405813E-02
DOF 351   .162084E+00   DOF 352   .227706E-02   DOF 353   .161733E+00   DOF 354  -.424375E-05   DOF 355   .161644E+00
DOF 356  -.228455E-02   DOF 357   .161733E+00   DOF 358  -.406309E-02   DOF 359   .162003E+00   DOF 360  -.491069E-02
DOF 361   .162453E+00   DOF 362   .374187E-03   DOF 363   .162607E+00   DOF 364  -.167075E-02   DOF 365   .486731E-02
DOF 366   .162717E+00   DOF 367   .408801E-02   DOF 368   .162723E+00   DOF 369   .228065E-02   DOF 370   .162724E+00
DOF 371  -.421377E-05   DOF 372   .162724E+00   DOF 373  -.228811E-02   DOF 374   .162723E+00   DOF 375  -.409284E-02
DOF 376   .162721E+00   DOF 377  -.486860E-02   DOF 378   .162714E+00   DOF 379  -.374145E-03   DOF 380   .162576E+00
DOF 381  -.166617E-02   DOF 382   .384324E-03   DOF 383   .175119E+00   DOF 384  -.166580E-02   DOF 385   .490792E-02
DOF 386   .162984E+00   DOF 387   .406061E-02   DOF 388   .163442E+00   DOF 389   .227853E-02   DOF 390   .163717E+00
DOF 391  -.417225E-05   DOF 392   .163805E+00   DOF 393  -.228593E-02   DOF 394   .163715E+00   DOF 395  -.486529E-02
DOF 396   .163438E+00   DOF 397  -.490924E-02   DOF 398   .162979E+00   DOF 399  -.384277E-03   DOF 400   .175049E+00
DOF 401  -.165980E-02   DOF 402   .540184E-02   DOF 403   .187925E+00   DOF 404   .456885E-02   DOF 405   .187442E+00
DOF 406   .260324E-02   DOF 407   .187116E+00   DOF 408  -.832089E-05   DOF 409   .187005E+00   DOF 410  -.261734E-02
DOF 411   .187113E+00   DOF 412  -.457752E-02   DOF 413   .187435E+00   DOF 414  -.540327E-02   DOF 415   .187915E+00
DOF 416   .394460E-03   DOF 417   .187592E+00   DOF 418  -.166009E-02   DOF 419   .535272E-02   DOF 420   .188164E+00
DOF 421   .460595E-02   DOF 422   .188194E+00   DOF 423   .260880E-02   DOF 424   .188209E+00   DOF 425  -.820343E-05
DOF 426   .188216E+00   DOF 427  -.262275E-02   DOF 428   .188205E+00   DOF 429  -.461401E-02   DOF 430   .188185E+00
DOF 431  -.535418E-02   DOF 432   .188149E+00   DOF 433  -.394409E-03   DOF 434   .187472E+00   DOF 435  -.165265E-02
DOF 436   .398998E-03   DOF 437   .200022E+00   DOF 438  -.165502E-02   DOF 439   .539231E-02   DOF 440   .188423E+00
DOF 441   .458527E-02   DOF 442   .188942E+00   DOF 443   .260349E-02   DOF 444   .189311E+00   DOF 445  -.804488E-05
DOF 446   .189433E+00   DOF 447  -.261725E-02   DOF 448   .189305E+00   DOF 449  -.459261E-02   DOF 450   .188930E+00
DOF 451  -.539388E-02   DOF 452   .188408E+00   DOF 453  -.398942E-03   DOF 454   .199841E+00   DOF 455  -.164636E-02
DOF 456   .134122E-01   DOF 457   .213285E+00   DOF 458   .775810E-02   DOF 459   .213277E+00   DOF 460   .331371E-02
DOF 461   .213769E+00   DOF 462  -.250945E-04   DOF 463   .213988E+00   DOF 464  -.334841E-02   DOF 465   .213770E+00
DOF 466  -.774860E-02   DOF 467   .213280E+00   DOF 468  -.133424E-01   DOF 469   .213289E+00   DOF 470   .403537E-03
DOF 471   .212422E+00   DOF 472  -.165198E-02   DOF 473   .134239E-01   DOF 474   .215405E+00   DOF 475   .772897E-02
DOF 476   .215424E+00   DOF 477   .329457E-02   DOF 478   .215446E+00   DOF 479  -.248971E-04   DOF 480   .215441E+00
DOF 481  -.332914E-02   DOF 482   .215435E+00   DOF 483  -.771934E-02   DOF 484   .215406E+00   DOF 485  -.133540E-01
DOF 486   .215386E+00   DOF 487  -.403475E-03   DOF 488   .212173E+00   DOF 489  -.164259E-02   DOF 490   .134641E-01
DOF 491   .217570E+00   DOF 492   .763884E-02   DOF 493   .217568E+00   DOF 494   .330998E-02   DOF 495   .217110E+00
DOF 496  -.241319E-04   DOF 497   .216905E+00   DOF 498  -.334328E-02   DOF 499   .217086E+00   DOF 500  -.762909E-02
DOF 501   .217525E+00   DOF 502  -.133941E-01   DOF 503   .217529E+00   DOF 504   .408075E-03   DOF 505   .224807E+00
DOF 506  -.165097E-02   DOF 507   .227182E-02   DOF 508   .224698E+00   DOF 509  -.468701E-04   DOF 510   .197496E-02
DOF 511   .224611E+00   DOF 512   .687931E-04   DOF 513  -.155724E-04   DOF 514   .224546E+00   DOF 515   .114806E-03
DOF 516  -.200011E-02   DOF 517   .224504E+00   DOF 518   .682426E-04   DOF 519  -.228386E-02   DOF 520   .224485E+00
DOF 521  -.475340E-04   DOF 522  -.408007E-03   DOF 523   .224486E+00   DOF 524  -.164133E-02   DOF 525  -.116922E-03
DOF 526  -.116346E-03   DOF
```

```
1     NODAL  FORCES  OF  PLATE  ELEMENTS..............

      ELEMENT NO      U1  (1)      V1  (2)      U2  (3)      V2  (4)      U3  (5)      V3  (6)      U4  (7)      V4  (8)
0          1         -.00000      -.00000      2.02462      -.59382     41.06553     -4.80517    -43.09015      5.39900
0          2        -2.02462       .59382       .00000       .00000     14.99931      5.39900    -12.97468     -5.99282
0          3         -.00000      -.00000    -71.93082     92.42569     19.32757     99.38984     52.60326   -191.81553
0          4       -67.05986    -73.21175      -.00000       .00000     40.40964    178.82629     26.65922   -105.61455
0          5          .00000      -.00000    -63.49830     76.99539     21.53562     92.33342     41.96268   -169.32881
0          6       -62.42272    -72.97261       .00000       .00000     40.07783    166.46060     22.34489    -93.48799
0          7         -.00000      -.00000    -61.76211     73.59356     21.61357     91.10540     40.14854   -164.69896
0          8       -61.70951    -73.44575      -.00000       .00000     40.02355    164.55870     21.68596    -91.11295
0          9         -.00000      -.00000    -61.50927     73.12281     21.65612     90.90190     39.85314   -164.02471
0         10       -61.59106    -73.47254       .00000       .00000     40.03533    164.24284     21.55573    -90.77030
0         11         -.00000      -.00000    -61.64305     73.25609     21.80202     91.12539     39.84104   -164.38148
0         12       -61.77617    -73.72091      -.00000       .00000     40.29895    164.73647     21.47722    -91.01556
0         13         -.00000      -.00000    -62.46011     73.36508     22.53319     93.19521     39.92692   -166.56029
0         14       -63.34722    -76.46776      -.00000       .00000     42.04540    168.92592     21.30182    -92.45816
0         15         -.00000      -.00000    -67.32365     74.71101     27.00198    104.81873     40.32167   -179.52974
0         16       -71.50764    -90.73856      -.00000       .00000     52.63369    190.68705     18.87396    -99.94849
0         17         -.00000      -.00000     -1.81872      -.59300    -12.77845      5.44291     14.59717     -4.84992
0         18         1.81872       .59300      -.00000       .00000    -42.64900     -4.84992     40.83028      4.25692
0         19      -107.22314   -200.50841     19.75337    128.61485     74.38090    104.63786     13.08887    -32.74431
0         20       -47.84422   -117.81686    -35.80054    199.39091     44.61732     23.66176     39.02743   -105.23581
0         21       -31.80203    -12.97438    -28.65490     75.61653     26.72761     85.60193     33.72931   -148.24408
0         22       -17.32289    -69.39182    -43.45818     22.90866     26.97513    139.17420     33.80594    -92.69103
0         23       -38.91414    -32.40615    -22.77371     76.05042     30.87706     88.45050     30.81079   -132.09478
0         24       -21.10680    -24.89586    -40.43981     33.42558     29.22742    130.69872     32.31919    -89.22844
0         25       -39.78656    -35.18722    -21.72211     75.59652     31.72942     88.42661     29.77925   -128.83591
0         26       -21.57742    -75.58897    -39.90042     35.10780     29.61960    128.83313     31.85825    -88.35196
0         27       -39.97627    -35.64178    -21.51936     75.55883     31.99384     88.42951     29.59229   -128.34656
0         28       -21.69250    -75.69043    -39.77702     35.40209     29.71839    128.51662     31.75713    -88.22829
0         29       -40.09935    -35.26345    -21.37631     75.51443     31.99082     88.42066     29.48484   -128.67163
0         30       -21.90293    -75.62426    -39.56222     35.08080     29.89122    128.82626     31.57393    -88.28281
0         31       -40.66365    -33.25698    -20.83385     75.04954     32.43019     88.94380     29.06731   -130.73636
0         32       -23.00116    -75.78659    -38.63002     32.67326     30.91905    131.67654     30.71213    -88.56321
0         33       -43.73706    -22.06944    -16.87509     69.88341     33.86090     91.74897     26.75125   -139.56295
0         34       -29.00085    -74.75365    -31.31226     13.73225     33.81130    147.10273     26.50182    -86.08133
0         35       -35.91859   -199.56938    -47.56204    118.90672     39.04777    103.70829     44.43286    -23.04563
0         36        19.51021   -128.60655   -107.62759    204.48623     13.54553     30.49344     74.57185   -106.37311
0         37       -50.90407   -175.21328    -55.67073    147.39219     55.55703    136.80727     51.01777   -108.98618
0         38       -57.73761   -146.79424    -49.32187    182.09469     51.73092    103.39727     55.32857   -138.69772
0         39       -29.02476    -57.51237    -31.45659     79.96902     27.31529     81.31456     33.16505   -103.77121
0         40       -29.07697    -72.87992    -29.00425     57.53261     30.77658     97.35065     27.30464    -82.00334
0         41       -28.78167    -64.61203    -32.07748     79.44744     28.08108     82.84361     32.77806    -97.67991
0         42       -31.11878    -78.66950    -29.51849     64.72997     32.21146     96.96940     28.42580    -83.02987
0         43       -29.48818    -66.59278    -31.84729     79.92361     28.66180     83.63763     32.67367    -96.96847
0         44       -31.74039    -79.99827    -29.58091     66.47819     32.60598     97.04528     28.71532    -83.52520
0         45       -29.63097    -66.96476    -31.80294     80.02281     28.77061     83.80096     32.66330    -96.85900
0         46       -31.85753    -80.22403    -29.57474     66.77035     32.67447     97.04904     28.75780    -83.59537
0         47       -29.62249    -66.61534    -31.68180     79.87377     28.71828     83.60434     32.58601    -96.86276
0         48       -31.88295    -80.01163    -29.43088     66.52446     32.67113     96.97907     28.64270    -83.49190
0         49       -29.52765    -64.61437    -31.06954     78.82537     28.41172     82.76713     32.18547    -96.97813
0         50       -32.07278    -79.20595    -28.73698     64.97833     32.75100     97.28102     28.05876    -82.95340
0         51       -28.93332    -56.99192    -29.04217     73.47439     27.22778     81.12692     30.74771    -97.60939
0         52       -31.32055    -79.14203    -29.03860     58.34326     33.03560    102.61447     27.32355    -81.81579
0         53       -49.20556   -182.40036    -57.81524    148.79379     55.26128    136.59499     51.75951   -102.98842
0         54       -55.80438   -146.12897    -50.92602    179.51108     51.21843    105.10333     55.51198   -138.48544
0         55       -51.25744   -105.23373    -55.58692    138.63926     55.02793    146.27932     51.01643   -179.68454
0         56       -55.29068   -136.74881    -51.84549    103.11599     49.20843    182.60179     57.93574   -148.95897
0         57       -33.05148   -102.74204    -27.38456     81.91097     31.30249     79.25179     29.13354    -58.42072
0         58       -27.23537    -81.22219    -30.80446     97.68857     28.90844     57.08432     29.13140    -73.55070
0         59       -32.75018    -97.36021    -28.10238     83.00611     32.03980     79.26738     28.81275    -64.91328
```

```
0     60    -28.40451   -82.81984   -32.22731    97.02047    29.48937    64.66438    31.14245   -78.86500
0     61    -32.65782   -97.02140   -28.67594    83.51557    31.83809    80.04113    29.49567   -66.53529
0     62    -28.70118   -83.62800   -32.61784    96.87599    29.57437    66.64138    31.74464   -79.88938
0     63    -32.65145   -97.06227   -28.78293    83.59537    31.80329    80.22962    29.63108   -66.76272
0     64    -28.74548   -83.80096   -32.68633    96.84577    29.57463    66.97240    31.85718   -80.01721
0     65    -32.57415   -97.03205   -28.73242    83.50153    31.67755    79.98266    29.62903   -66.45215
0     66    -28.62856   -83.61397   -32.68697    96.92613    29.42338    66.58195    31.89214   -79.89411
0     67    -32.16962   -96.92707   -28.43301    82.97716    31.04586    78.62987    29.55677   -64.67996
0     68    -28.03747   -82.79090   -32.77887    97.59983    28.70589    64.57708    32.11045   -79.38602
0     69    -30.71983   -97.27147   -27.29705    81.90807    28.98774    72.80361    29.02914   -57.44021
0     70    -27.25428   -81.21929   -33.15017   103.64364    28.92982    57.43491    31.47464   -79.85926
0     71    -51.64494  -103.26970   -55.29117   138.54390    57.61711   146.61906    49.31900  -181.89326
0     72    -55.48209  -136.65345   -50.97876   108.85578    50.81367   175.03981    55.64718  -147.24214
0     73    -13.42965   -30.57809   -74.82424   106.53610   -19.77363   128.80761   108.02752  -204.76562
0     74    -38.93942  -103.84615   -44.64460    23.09888    35.71289   199.79185    47.87113  -119.04458
0     75    -33.69737  -147.27995   -26.69790    86.15656    28.78948    74.89750    31.60579   -13.77411
0     76    -33.73599   -91.85765   -26.92433   139.62960    43.53121    22.13124    17.12911   -69.90319
0     77    -30.79687  -131.80064   -30.88833    88.60737    22.78788    75.88649    38.89732   -32.69322
0     78    -32.29392   -89.00975   -29.22627   130.77155    40.44624    33.28229    21.07395   -75.04409
0     79    -29.75877  -128.90064   -31.73860    88.30113    21.68383    75.69185    39.81354   -35.09235
0     80    -31.84413   -88.45288   -29.63434   128.67224    39.87058    35.27036    21.60790   -75.48971
0     81    -29.57111  -128.55091   -31.91278    88.22269    21.46741    75.73435    40.01648   -35.40613
0     82    -31.74769   -88.43510   -29.73357   128.31227    39.73681    35.63775    21.74444   -75.51492
0     83    -29.47009  -128.83252   -32.00494    88.31974    21.34584    75.61368    40.12919   -35.10089
0     84    -31.56475   -88.40829   -29.91170   128.76154    39.53524    35.17567    21.94121   -75.52892
0     85    -29.06845  -130.66352   -32.45547    89.16249    20.86671    74.98130    40.65721   -33.40027
0     86    -30.70085   -88.40634   -30.93297   131.97067    38.6[illegible]683    32.38619    22.98699   -75.95051
0     87    -26.80206  -139.10754   -33.93085    92.58236    17.06887    69.37205    43.66403   -22.84687
0     88    -26.53153   -85.52670   -33.84324   148.06686    31.50850    12.93252    28.86627   -75.47268
0     89    -44.40558   -23.60852   -39.13578   105.09796    47.53512   117.67900    36.00624  -199.16845
0     90    -74.12851  -104.47487   -13.20474    32.65966   106.82321   200.22901   -19.48996  -128.41380
0     91     42.89597     4.88152   -41.06540    -4.28755    -1.83057    -.59396      .00000    -.00000
0     92     12.96789    -5.47548   -14.79846     4.88152     -.00000    -.00000     1.83057     .59396
0     93    -52.52022  -190.89925   -19.06700    99.97281    71.58722    90.92644      .00000    -.00000
0     94    -26.85159  -104.96713   -40.50947   179.62950      .00000      .00000    67.36106   -74.66237
0     95    -41.91905  -169.06751   -21.48126    92.46170    63.40032    76.60581      .00000    -.00000
0     96    -22.38057   -93.30410   -40.10263   166.62185     0.00000    -.00000    62.48319   -73.31775
0     97    -40.15716  -164.81179   -21.64726    90.99586    61.80442    73.81593      .00000    -.00000
0     98    -21.64446   -91.19800   -40.00620   164.40176      .00000      .00000    61.65066   -73.20377
0     99    -39.88086  -164.26599   -21.71889    90.72638    61.59975    73.53961      .00000    -.00000
0    100    -21.49296   -90.94581   -40.00762   164.00155     -.00000     0.00000    61.50058   -73.05574
0    101    -39.85839  -164.53841   -21.84352    91.04034    61.70190    73.49807      .00000    -.00000
0    102    -21.44353   -91.12510   -40.29033   164.62363      .00000      .00000    61.73386   -73.49854
0    103    -39.90212  -166.39904   -22.49751    93.37909    62.39964    73.01994      .00000    -.00000
0    104    -21.35618   -92.32988   -42.08903   169.18722      .00000      .00000    63.44521   -76.85734
0    105    -40.22184  -178.72654   -26.80061   105.46615    67.02245    73.26039      .00000    -.00000
0    106    -19.13453   -99.36552   -52.71672   191.60332      .00000      .00000    71.85125   -92.23780
0    107    -14.79802    -5.36740    12.78524     5.96025     2.01277    -.59286      .00000    -.00000
0    108    -40.83041     4.77454    42.84318    -5.36740     -.00000      .00000    -2.01277     .59286
```

```
1     NODAL FORCES OF BEAM ELEMENTS IN THE X-DIRECTION

      ELEMENT NO      U1  (1)       V1  (2).      01  (3)       U2  (4)       V2  (5)       02  (6)

                                   *****  BEAM  NO.   1  *****

0           1     -1012.09179    15.11854        .00000    1012.09179    -15.11854    -113.38903
0           2     -1012.09179    15.11854     113.38903    1012.09179    -15.11854    -226.77806
0           3     -1012.09179    15.11854     226.77806    1012.09179    -15.11854    -340.16708
0           4      -873.10111    -4.09540     340.16708     873.10111      4.09540    -309.45155
0           5      -873.10111    -4.09540     309.45155     873.10111      4.09540    -278.73602
0           6      -747.18008    -8.11818     278.73602     747.18008      8.11818    -217.84968
0           7      -747.18008    -8.11818     217.84968     747.18008      8.11818    -156.96335
0           8      -623.70846    -8.26599     156.96335     623.70846      8.26599     -94.96846
0           9      -623.70846    -8.26599      94.96846     623.70846      8.26599     -32.97357
0          10      -500.60813    -7.91625      32.97357     500.60813      7.91625      26.39832
0          11      -500.60813    -7.91625     -26.39832     500.60813      7.91625      85.77021
0          12      -377.18890    -7.45143     -85.77021     377.18890      7.45143     141.65595
0          13      -377.18890    -7.45143    -141.65595     377.18890      7.45143     197.54169
0          14      -251.38157    -4.34875    -197.54169     251.38157      4.34875     230.15730
0          15      -251.38157    -4.34875    -230.15730     251.38157      4.34875     262.77291
0          16      -112.55028    11.67880    -262.77291     112.55028    -11.67880     175.18194
0          17      -112.55028    11.67880    -175.18194     112.55028    -11.67880      87.59097
0          18      -112.55028    11.67880     -87.59097     112.55028    -11.67880        .00000

                                   *****  BEAM  NO.   2  *****

0          19      1011.94969    12.31511        .00000   -1011.94969    -12.31511     -92.36331
0          20      1011.94969    12.31511      92.36331   -1011.94969    -12.31511    -184.72663
0          21      1011.94969    12.31511     184.72663   -1011.94969    -12.31511    -277.08994
0          22       873.00141    -3.94896     277.08994    -873.00141      3.94896    -247.47271
0          23       873.00141    -3.94896     247.47271    -873.00141      3.94896    -217.85548
0          24       747.11790    -7.23702     217.85548    -747.11790      7.23702    -163.57782
0          25       747.11790    -7.23702     163.57782    -747.11790      7.23702    -109.30016
0          26       623.66282    -7.84918     109.30016    -623.66282      7.84918     -50.43127
0          27       623.66282    -7.84918      50.43127    -623.66282      7.84918       8.43761
0          28       500.56249    -8.33305      -8.43761    -500.56249      8.33305      70.93551
0          29       500.56249    -8.33305     -70.93551    -500.56249      8.33305     133.43340
0          30       377.12672    -8.33259    -133.43340    -377.12672      8.33259     195.92782
0          31       377.12672    -8.33259    -195.92782    -377.12672      8.33259     258.42223
0          32       251.28188    -4.49519    -258.42223    -251.28188      4.49519     292.13614
0          33       251.28188    -4.49519    -292.13614    -251.28188      4.49519     325.85006
0          34       112.40818    14.48222    -325.85006    -112.40818    -14.48222     217.23337
0          35       112.40818    14.48222    -217.23337    -112.40818    -14.48222     108.61669
0          36       112.40818    14.48222    -108.61668    -112.40818    -14.48222        .00000
```

```
1     NODAL FORCES OF BEAM ELEMENTS IN THE Y-DIRECTION
      ELEMENT NO        U1  (1)        V1  (2)        01  (3)        U2  (4)        V2  (5)        02  (6)
0          1         -112.90821      -15.11854         .00000     112.90821       15.11854    2258.16412
0          2           37.40509      179.99087    -2258.16412     -37.40509     -179.99087    1510.06242
0          3           75.22029      387.94846    -1510.06242     -75.22029     -387.94846       5.65662
0          4           75.45995      602.16837       -5.65662     -75.45995     -602.16837   -1503.54247
0          5           37.87318      812.43100     1503.54247     -37.87318     -812.43100   -2261.00609
0          6         -113.05030     1012.31511     2261.00609     113.05030    -1012.31511       -.00000
0          7         -112.55028     1011.67880         .00000     112.55028    -1011.67880    2251.00555
0          8           37.72631      812.04249    -2251.00555     -37.72631     -812.04249    1496.47942
0          9           75.10680      602.03797    -1496.47942     -75.10680     -602.03797      -5.65662
0         10           74.86714      388.07886        5.65662     -74.86714     -388.07886   -1502.99936
0         11           37.25821      180.37939     1502.99936     -37.25821     -180.37939   -2248.16358
0         12         -112.40818      -14.48222     2248.16358     112.40818       14.48222       -.00000
```

```
1     NODAL FORCES OF CONNECTION ELEMENTS.............

      ELEMENT NO      U1  (1)       U2  (2)       V1  (3)       V2  (4)


                  *****  END  CONNECTIONS  *****


            1      -138.99068    138.99068     19.21394     -19.21394
            2      -125.92103    125.92103      4.02277      -4.02277
            3      -123.47162    123.47162       .14781      -.14781
            4      -123.10033    123.10033      -.34973       .34973
            5      -123.41923    123.41923      -.46482       .46482
            6      -125.80733    125.80733     -3.10268      3.10268
            7      -138.83130    138.83130    -16.02754     16.02754
            8       138.94828   -138.94828     16.26407    -16.26407
            9       125.88351   -125.88351      3.28806     -3.28806
           10       123.45508   -123.45508       .61216      -.61216
           11       123.10033   -123.10033       .48387      -.48387
           12       123.43577   -123.43577      -.00046       .00046
           13       125.84485   -125.84485     -3.83740      3.83740
           14       138.87370   -138.87370    -18.97741     18.97741


                  *****  SIDE CONNECTIONS  *****


           15      -150.31329    150.31329   -195.10941    195.10941
           16       -37.81520     37.81520   -207.95758    207.95758
           17         -.23966       .23966   -214.21991    214.21991
           18        37.58677    -37.58677   -210.26263    210.26263
           19       150.92349   -150.92349   -199.88411    199.88411
           20      -150.27658    150.27658    199.63631   -199.63631
           21       -37.38050     37.38050    210.00452   -210.00452
           22          .23966      -.23966    213.95911   -213.95911
           23        37.60893    -37.60893    207.69947   -207.69947
           24       149.66639   -149.66639    194.86161   -194.86161


                  *****  SEAM CONNECTIONS  *****


           25        20.80123    -20.80123   -204.78991    204.78991
           26         4.70455     -4.70455   -205.75645    205.75645
           27          .11457      -.11457   -206.51325    206.51325
           28        -4.56383      4.56383   -205.70067    205.70067
           29       -20.91443     20.91443   -204.67336    204.67336
           30         3.04854     -3.04854   -201.73495    201.73495
           31         2.02912     -2.02912   -196.70680    196.70680
           32          .02788      -.02788   -195.03922    195.03922
           33        -1.98411      1.98411   -196.71392    196.71392
           34        -3.02174      3.02174   -201.76073    201.76073
           35          .36197      -.36197   -199.88617    199.88617
           36          .29107      -.29107   -195.42869    195.42869
           37          .01584      -.01584   -193.98987    193.98987
           38         -.26309       .26309   -195.43593    195.43593
```

```
●    39      -.34362      .34362   -199.90414   199.90414
●    40      -.12313      .12313   -199.66649   199.66649
●    41      -.03868      .03868   -195.31132   195.31132
●    42       .01186     -.01186   -193.92127   193.92127
●    43       .05997     -.05997   -195.31362   195.31362
●    44       .13562     -.13562   -199.67212   199.67212
●    45      -.25831      .25831   -199.64493   199.64493
●    46      -.13765      .13765   -195.28698   195.28698
●    47       .01186     -.01186   -193.89481   193.89481
●    48       .15893     -.15893   -195.28467   195.28467
●    49       .27081     -.27081   -199.63930   199.63930
●    50      -.73673      .73673   -199.81727   199.81727
●    51      -.46034      .46034   -195.35072   195.35072
●    52       .01584     -.01584   -193.90520   193.90520
●    53       .48832     -.48832   -195.34348   195.34348
●    54       .75509     -.75509   -199.79931   199.79931
●    55     -3.41539     3.41539   -201.59919   201.59919
●    56     -2.18207     2.18207   -196.55486   196.55486
●    57       .02788     -.02788   -194.88086   194.88086
●    58      2.22708    -2.22708   -196.54775   196.54775
●    59      3.44219    -3.44219   -201.57341   201.57341
●    60    -21.32142    21.32142   -204.41930   204.41930
●    61     -4.77269     4.77269   -205.44599   205.44599
●    62       .11457     -.11457   -206.25812   206.25812
●    63      4.91342    -4.91342   -205.50177   205.50177
●    64     21,20822   -21.20822   -204.53584   204.53584
```